Modélisation mathématique et simulation numérique avancée des phénomènes de propagation d'ondes dans les médias élastiques sans limite.

Eduardo Godoy

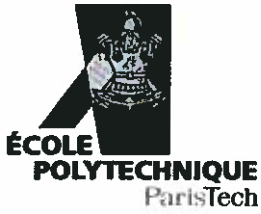

Thèse présentée pour obtenir le grade de

Docteur de l'École Polytechnique

Spécialité:

Mathématiques Appliquées

par

Eduardo Ignacio GODOY RIVEROS

MATHEMATICAL MODELING AND ADVANCED NUMERICAL SIMULATION OF WAVE PROPAGATION PHENOMENA IN UNBOUNDED ELASTIC MEDIA

Soutenue le 17 May 2010 devant le jury composé de:

Jean-Claude NÉDÉLEC	Directeur de thèse
Mario DURÁN	Co-directeur de thèse
Rafael BENGURIA	Examinateur et rapporteur
Sergio GUTIÉRREZ	Examinateur et rapporteur
Jaime H. ORTEGA	Examinateur et rapporteur
Cristián VIAL	Président du jury

A mis padres, por su apoyo incondicional

ACKNOWLEDGEMENTS

The work presented in this doctoral thesis has been carried out under the joint supervision of the *Pontificia Universidad Católica de Chile* and the *École Polytechnique de Paris.*

I would like to acknowledge my gratitude to both of my supervisors, Professor Mario Durán and Professor Jean-Claude Nédélec, without whose guidance and support the accomplishment of this work would not have been possible. I owe to Professor Mario Durán my interest in applied mathematics and numerical methods. His passionate enthusiasm tremendously encouraged me to pursue this research. I am deeply grateful to Professor Jean-Claude Nédélec, who generously shared with me his expert knowledge and vast experience. He was always available to answer questions and give helpful advice.

I also wish to sincerely thank Professor Rafael Benguria, Professor Sergio Gutiérrez, Professor Jaime H. Ortega and Professor Cristián Vial, for kindly accepting to be members of the Examining Committee and spending their valuable time in reviewing this work.

I am indebted to the people in the CMAP of the *École Polytechnique*, for their warm reception and useful assistance in overcoming the difficulties I encountered as an inexperienced foreigner in France. Particularly, I thank Jeanne Bailleul, Nasséra Naar and Anna Johnsson. I also wish to express my sincere gratitude to my colleagues in the PUC and in the CMAP. I am especially grateful to Ignacio Muga for beneficial discussions and useful contributions to this work, to Ricardo Hein for his constant willingness to explain any questions I may have, and to Carlos Pérez for the numerous references he provided me. I extend my thanks to Sebastián Ossandón, Joaquín Mura, Carlos Jerez, José Arturo Infante, Juan Cristóbal García-Huidobro, Valeria Boccardo, Pedro Ramaciotti, Jean-Baptiste Bellet and Meisam Sharify for their encouragement and support.

Finally, I thank the organizations that funded this work: The PUC and CONICYT grants for doctoral students and the *Proyecto Anillo de Investigación* ADI30 *del Programa Bicentenario en Ciencia y Tecnología de* CONICYT/*World Bank.* I also thank the PUC grant for joint supervision abroad, which partially funded my stay in France.

CONTENTS

LIST OF FIGURES

LIST OF TABLES

RÉSUMÉ

Motivée par des applications en géophysique et ingénierie sismique, cette thèse cherche à contribuer à l'étude de phénomènes de propagation d'ondes en milieux élastiques non bornés. Nous développons des techniques mathématiques et numériques pour résoudre des problèmes de diffraction en régime harmonique, dans des domaines infinis extérieurs et demi-infinis localement perturbés. En plus, nous introduisons une nouvelle condition aux limites du type impédance en élasticité, laquelle généralise la condition de frontière libre utilisée d'habitude pour décrire la surface de la terre en problèmes géophysiques. Les ondes de surface qui apparaissent avec cette condition aux limites sont étudiées. Nous montrons l'existence de l'onde de Rayleigh et comment elle dépend de l'impédance. En plus, nous prouvons qu'il apparaît une onde de surface additionnelle dans un cas particulière.

Pour traiter numériquement les domaines non bornés, nous considérons des approches basées sur des conditions aux limites exactes et des méthodes d'équations intégrales de frontière. Les premières s'appliquent à des domaines extérieurs, pendant que les deuxièmes s'emploient pour les deux types de domaine. Un accent particulier est mis sur les équations intégrales et les méthodes d'éléments de frontière pour résoudre des problèmes de diffraction dans des demi-plans localement perturbés. Nous calculons de manière efficace et précise la fonction de Green d'un demi-plan élastique avec des conditions aux limites d'impédance, à l'aide d'une méthode de calcul qui combine de façon appropriée des techniques analytiques et numériques. Nous proposons aussi une méthode d'équations intégrales de frontière basée sur la fonction de Green calculée. Finalement, les procédures numériques sont validées en utilisant des problèmes benchmark appropriés.

Mots clés: Élasticité en régime harmonique, ondes élastiques, domaines non bornés, conditions aux limites d'impédance, ondes de surface, diffraction élastique, conditions aux limites exactes, équations intégrales de frontière, méthode d'éléments de frontière, fonction de Green.

ABSTRACT

Motivated by applications in geophysics and seismic engineering, this thesis seeks to contribute to the study of wave propagation phenomena in unbounded elastic media. Mathematical and numerical techniques are developed to solve time-harmonic scattering problems in exterior infinite and locally perturbed semi-infinite domains. In addition, we introduce a novel impedance boundary condition in elasticity, which generalizes the traction-free boundary condition usually considered to describe the ground surface in geophysical problems. The surface waves appearing with this boundary condition are investigated. We show the existence of the Rayleigh wave and how it depends on impedance. Moreover, we prove that an additional surface wave appears in a particular case.

To deal numerically with unbounded domains, we consider approaches based upon exact boundary conditions and boundary integral equation methods. The former is applied to exterior domains, while the latter is employed in both types of unbounded domains. Special emphasis is placed on integral equations and boundary element methods to solve scattering problems in locally perturbed half-planes. The Green's function of the elastic half-plane with impedance boundary conditions is computed in an effective and accurate way, by employing a method of calculation that combines appropriately analytical and numerical techniques. A boundary integral equation method based on the calculated Green's function is then proposed. Finally, the numerical procedures are validated by employing appropriate benchmark problems.

Keywords: Time-harmonic elasticity, elastic waves, unbounded domains, impedance boundary conditions, surface waves, elastic scattering, exact boundary conditions, boundary integral equations, boundary element methods, Green's function.

RESUMEN

Motivada por aplicaciones en geofísica e ingeniería sísmica, esta tesis busca contribuir al estudio de fenómenos de propagación de ondas en medios elásticos no acotados. Se desarrollan técnicas matemáticas y numéricas para resolver problemas de difracción en régimen armónico, en dominios infinitos exteriores y semi-infinitos localmente perturbados. Además, se introduce una nueva condición de borde de tipo impedancia, la cual generaliza la condición de frontera libre normalmente considerada para describir la superficie de la tierra en problemas geofísicos. Las ondas de superficie que aparecen con esta condición de borde son estudiadas. Se muestra la existencia de la onda de Rayleigh y cómo ésta depende de la impedancia. Además, se prueba que aparece una onda de superficie adicional en un caso particular.

Para tratar numéricamente los dominios no acotados, se consideran procedimientos basados en condiciones de borde exactas y ecuaciones integrales de frontera. Los primeros se aplican a dominios exteriores, mientras que los segundos se emplean para ambos tipos de dominios. Se pone especial énfasis en ecuaciones integrales y métodos de elementos de frontera para resolver problemas de difracción en semiplanos localmente perturbados. Se calcula de manera eficiente y precisa la función de Green de un semiplano elástico con condiciones de borde de impedancia, utilizando un método que combina apropiadamente técnicas analíticas y numéricas. Se propone también un método de ecuaciones integrales basado en la función de Green calculada. Finalmente, los procedimientos numéricos son validados usando problemas benchmark apropiados.

Palabras claves: Elasticidad en régimen armónico, ondas elasticas, dominios no acotados, condiciones de borde de impedancia, ondas de superficie, difracción elástica, condiciones de borde exactas, ecuaciones integrales de frontera, método de elementos de frontera, función de Green.

I. INTRODUCTION

1.1 Motivation

This thesis deals with mathematical modeling and numerical simulation of linear wave propagation phenomena in unbounded elastic media. Motivation for this study is provided by a class of problems arising in geosciences and engineering, where for practical purposes, the soil can be regarded as an elastic continuum. We are mainly referring to propagation of seismic waves, and the way they affect and are affected by natural and man-made structures. Such events are treated as elastic scattering phenomena.

Several numerical studies on the seismic response of local geological and topographical irregularities, such as, for example, alluvial valleys, sedimentary basins and canyons, have demonstrated that such natural structures are generally exposed to significant amplification of surface motion during earthquakes (cf., e.g., Sánchez-Sesma & Luzón 1995, Reinoso, Wrobel & Power 1997, Zheng & Dravinski 2000), sometimes giving rise to locally generated surface or Rayleigh waves (cf. Savage 2004). Surface waves are usually the most destructive type of seismic wave, because of their long duration and strong amplitude at the ground surface.

In addition, elastic waves are important in induced seismicity, where the seismic events are caused by human activity. A typical example of this arises in mining, where the mineral resources are extracted from the ground by excavating surface pits (open-pit mining) or subterranean passages (underground mining). Most of such excavations are constructed by rock blasting, that is, the controlled use of explosives to break up a rock formation. However, when an explosion occurs, a shock elastic wave is produced, inducing seismic activity in the mine and the surrounding area (cf. García-Huidobro 2009). This could eventually cause serious damage to the mine infrastructure and equipment.

It is therefore of interest to develop adequate mathematical models and numerical methods of simulation, capable of predicting the behavior of different structures, located either on the ground surface or underground, when excited by seismic waves.

1.2 Overview

From the point of view of mathematical modeling, the problems to be studied herein involve two kinds of domains. If the structure under consideration is located deeply underground, the influence of the surface could be eventually neglected. The soil is then modeled as an infinite elastic medium containing a bounded obstacle or inclusion. This type of geometry is called an exterior domain. On the contrary, if we are dealing with a structure that lies near or at the ground surface, the effect of the surface must be taken into account. In that case, the soil is modeled as a semi-infinite elastic medium with a free surface, and the structure is regarded as a geometrical perturbation of finite size. We call this geometry a locally perturbed half-space. In both cases, the domain is of infinite extent, so it cannot be

discretized and stored within a computer in a trivial manner. It is therefore necessary to devise special numerical procedures, capable of dealing with such domains.

A possible idea to overcome this difficulty of unboundedness is to restrict the computation to a finite domain by introducing artificial boundaries. The discretization is then performed in this domain, and the problem can be solved by using finite difference methods (FDM) or finite element methods (FEM). Nevertheless, adequate boundary conditions must be prescribed on the artificial boundaries in order to be accurate. For this, the Dirichlet-to-Neumann (DtN) map is often considered, which is a mathematical tool that provides exact nonreflecting boundary conditions. This approach has been used in two-dimensional elastostatics, both for exterior domains (cf. Han & Wu 1992), and for semi-infinite domains (cf. Givoli & Vigdergauz 1993, Han, Bao & Wang 1997). The application to elastodynamics, however, has been limited to exterior domains. Nonreflecting boundary conditions for two-dimensional time-harmonic elastic waves have been introduced by Givoli & Keller (1990). A further study of their mathematical properties has been provided by Harari & Shohet (1998). The numerical implementation in FEM has been performed by Harari & Haham (1998). In the three-dimensional case, nonreflecting boundary conditions have been given by Grote & Keller (2000) and Gächter & Grote (2003), for transient and time-harmonic elastic waves, respectively.

A less evident approach to deal with unbounded domains is the technique of boundary integral equations, together with its discrete counterpart, the boundary element method (BEM). The basic idea comes from potential theory (cf. Helms 1969), which basically states that a harmonic function can be represented as a sum of certain boundary integrals. This result can be further extended to vector functions satisfying the equations of linear elasticity (cf. Kupradze 1965, Rizzo 1967). The main merit of this technique is to transform a problem in a whole domain into one on its boundary, reducing the dimensionality by one. Thus, a considerable amount of computer resources can be saved. Nevertheless, a major drawback is the requirement of knowing a fundamental solution or Green's function, that is, the response of the system to a unit point source. Depending on the particular problem under study, a fundamental solution could be far from easy to obtain.

Boundary integral equation methods that deal with exterior domains use Kelvin or full-space fundamental solutions, which are known explicitly for isotropic media. Bonnet (1995) provides Kelvin fundamental solutions for elastostatics and elastodynamics in two and three dimensions. Integral equations are then stated on the boundary of the obstacle, which can be easily discretized, since it is of finite extent. Some authors that have employed this procedure to solve various elastodynamic problems are Shibahara & Taniguchi (1983), Antes (1985), Rizzo, Shippy & Rezayat (1985), Martin (1990) and Tadeu, Kausel & Vrettos (1996). In the case of non-isotropic media, special calculation methods need to be devised in order to calculate the appropriate fundamental solutions (cf., e.g., Wang & Achenbach 1994, Liu & Lam 1996, Dravinski & Zheng 2000).

A locally perturbed half-space can be also treated by boundary integral equation methods based upon a Kelvin fundamental solution. However, one encounters the difficulty that

not only the boundary of the perturbation, but also the half-space free surface must be discretized. As the latter is of infinite extent, it is often approximated by a truncated surface, which needs to be large enough in order to yield accurate solutions. This approach has been adopted by Karabalis & Beskos (1986) and Niwa, Hirose & Kitahara (1986) for transient scattering. More recently, Arias & Achenbach (2004) have used the far-field asymptotic behavior of the Rayleigh waves to correct the error introduced by the truncation.

The problem of truncation can be avoided if instead of using a Kelvin solution, a half-space fundamental solution is considered in the boundary integral approach. In that case, only the boundary of the local perturbation requires discretization, since the half-space fundamental solution contains the influence of the infinite free surface. Half-space fundamental solutions for elastostatics can often be determined in explicit form. In the two-dimensional case, the fundamental solution for an isotropic half-plane has been introduced by Telles & Brebbia (1981) and improved by Huang & Yin (1987). The extension to an orthotropic half-plane has been performed by Dumir & Mehta (1987). These works also include BEM approaches based upon the respective fundamental solutions applied to solve some classical problems in elastostatics. In the three-dimensional case, the fundamental solution for an isotropic half-space has been provided by Okada (1992).

Nevertheless, half-space fundamental solution or Green's function for elastodynamics rarely can be expressed in analytical form. The standard procedure to obtain a half-space Green's function consists in applying integral transforms (Fourier, Laplace, or others) in time and space to the partial differential equations of motion fulfilled by the Green's function. These equations are then solved analytically in the frequency-wavenumber domain, and the Green's function is expressed in terms of inverse integral transforms, which are not simple to evaluate since the integrands are often singular. The effective and accurate evaluation of these infinite integrals has been the object of many studies, giving rise to several methods for this purpose, either analytical, numerical, or a combination of both. In most cases, these methods are very complex and only provide approximate solutions.

A pioneering work in the analysis of elastic wave propagation in semi-infinite domains was done by Lamb (1904). He considered the surface displacement generated by periodic and transient line sources situated at the free surface, using Fourier transforms in space and time. Since his publication, the problem of determining the dynamic response of an elastic half-space subjected to different force sources (not necessarily applied on the surface), either transient or time-harmonic, is usually referred as the Lamb's problem. The calculation of a Green's function can then be regarded as a particular case of the Lamb's problem, where the source corresponds to a unit point force.

The Lamb's problem has been studied by so many authors that it is impossible to give an exhaustive list. An important contribution was made by Johnson (1974), who obtained the transient Green's function of the isotropic elastic half-space. For this, he applied Laplace transforms in space and time, and the inversion was performed by employing the Cagniard-de Hoop method. In the two-dimensional case, a expression for the Green's function of the isotropic half-plane has been given by Buchen (1978), using a displacement potential decomposition and the Pekeris-Cagniard-de Hoop method. The time-harmonic

Green's function of an orthotropic half-plane has been obtained by Rajapakse & Wang (1990) by applying a Fourier transform in the horizontal space variable. A method to evaluate the infinite integrals based on contour integration was proposed. More recently, Chen & Dravinski (2007*a*,*b*) have treated the case of triclinic half-planes and half-spaces, expressing the Green's function as double Fourier integrals. The first integral was evaluated by contour integration, while the second one was calculated by quadrature formulae.

Even though the half-space Green's functions provided by different authors can be evaluated numerically, they are not always well-suited for BEM applications, since a large amount of successive evaluations at different points is required, so the method to evaluate the Green's function needs to be fast and accurate. If this issue is resolved, BEM approaches based upon half-space Green's functions have proven to be far more efficient than their counterparts using Kelvin fundamental solutions. For a detailed discussion about this subject, see Pan, Rizzo & Martin (1998). Time-domain BEM approaches employing half-space Green's functions have been developed and applied by Triantafyllidis (1991) and Richter & Schmid (1999), for the two and the three-dimensional case, respectively.

A third approach to treat unbounded domains is a hybrid technique that combines the two methods mentioned above. Basically, a finite computational domain is defined by introducing an artificial boundary, and integral equations are stated on that boundary. Then, the finite domain is discretized by FEM and its boundary is discretized by BEM. Such a method is called a coupled FEM/BEM approach. Some authors that have applied this method to problems of foundations and soil-structure interaction are, e.g., Karabalis & Beskos (1985), Gaitanaros & Karabalis (1987), and Von Estorff & Kausel (1989).

1.3 Contributions

The main contribution of this thesis is a novel boundary condition in elastodynamics, which is of the impedance-type and generalizes the usual one of free surface assumed in most literature dealing with semi-infinite elastic media. Similar boundary conditions have been previously studied in acoustics. The Helmholtz equation in a half-plane with impedance boundary conditions has been investigated by Chandler-Wilde (1997) and Durán, Muga & Nédélec (2005*a*, 2006). Extensions to the half-space have been carried out by Durán, Muga & Nédélec (2005*b*, 2009*a*). Boundary integral equation methods for locally perturbed half-planes have been established by Peplow & Chandler-Wilde (1999), Chandler-Wilde & Peplow (2005) and Durán, Hein & Nédélec (2007), based upon half-plane Green's functions appropriately calculated. Moreover, the impedance boundary condition to be considered herein has some similar features with certain transmission conditions that describe an imperfect interface between two elastic solids, where slipping is allowed to occur (cf. Martin 1992, Durán & Nédélec 2000). In this thesis, we provide some results on the existence of surface waves when this novel boundary condition holds on the surface of the half-plane. Specifically, it is proven that the Rayleigh wave exists for all impedance and there is a particular case where an additional surface wave appears, completing that presented by Durán, Godoy & Nédélec (2006, 2010).

Another contribution is the calculation of the half-plane Green's function of time-harmonic elastodynamics with impedance boundary conditions. The calculation is performed by employing an effective and accurate method that appropriately combines analytical and numerical techniques. An analogous method has been previously used by Durán, Hein & Nédélec (2007) to calculate the half-plane Green's function of acoustics with impedance boundary conditions. Nevertheless, the extension to elastodynamics is not immediate, due to the vector nature of the involved equations, besides the coexistence of two types of volume elastic waves (longitudinal and transverse) and the appearance of surface waves. Furthermore, a boundary integral equation approach based on this Green's function is implemented and successfully validated for suitable benchmark problems.

1.4 Outline

This thesis involves eight chapters and two appendices. Chapter I is an introductory chapter that mentions some applied problems that motivate this study and gives an overview of the most important mathematical and numerical approaches to treat unbounded media. Chapter II presents the mathematical models to be considered throughout the thesis. These are models of boundary-value problems governing elastic scattering phenomena in both exterior domains and locally perturbed half-planes. Chapter III gives some methods based upon infinite series to treat scattering in exterior domains. Boundary-value problems are solved analytically for the exterior of a circle, and the DtN map is calculated explicitly, allowing obtention of exact boundary conditions for elastic waves in two-dimensions. In Chapter IV, integral representation formulae and integral equations to solve the boundary-value problems stated in Chapter II are developed. The discretization of these integral equations by a BEM approach is detailed in Chapter V, including the obtention of the variational formulations and their approximation by a Galerkin scheme. The semi-analytical computation of singular integrals involved in the BEM formulation is also presented. Chapter VI describes the effective calculation of the half-plane Green's function with impedance boundary conditions. Roughly speaking, a Fourier transform is applied in the horizontal space variable, the problem is solved in the wavenumber domain, and the evaluation of the inverse integral is performed by removing the singularities in the integrand. The normal derivative of the Green's function is also calculated, since it is required for the BEM formulation. In Chapter VII, the appearance of surface waves with impedance boundary conditions is investigated, providing a theoretical basis and some numerical results. Chapter VIII presents validation of the numerical procedures established above, including the approaches based upon exact boundary conditions and FEM, and upon boundary integral equations and BEM, both for exterior and semi-infinite domains. Adequate benchmark problems are used in each case and numerical results are given. In Appendix A, an analysis of elastic plane waves is performed, both for the full-plane and the half-plane. Appendix B shows some properties of Bessel and Hankel functions to be used throughout the thesis.

II. MATHEMATICAL MODELING OF ELASTIC SCATTERING PHENOMENA

2.1 Introduction

In this chapter, we present the mathematical models of elastic scattering phenomena, in exterior domains and in locally perturbed half-planes. Most concepts introduced herein can be found in general texts on elastic waves such as Achenbach (1973), Graff (1991) and Harris (2001), or in books specialized on seismic waves such as Aki & Richards (2002), Pujol (2003) and Chapman (2004). The propagation of elastic waves in an homogeneous isotropic medium is first approached in the time-domain. Next, we suppose harmonic dependence in time, leading to the elastic wave equation in the frequency domain, which is assumed for the rest of this work. By using the well-known decomposition into longitudinal and transverse waves, we show that elastic waves in the full-plane can be studied by means of two scalar potentials satisfying Helmholtz equations. This result will be useful tool in subsequent applications. The mathematical models for time-harmonic scattering phenomena are first presented for an exterior domain. We give the basic notion of scattering, that is, an incident field that encounters an obstacle, which generates a new field of scattered waves. This field has to fulfill radiation conditions at infinity, in order to avoid nonphysical solutions, and we write these conditions in two different forms. The boundary conditions considered in the obstacle are of the Dirichlet and Neumann-type, and each associated boundary-value problem governing the scattering phenomenon is introduced. In the case of a locally perturbed half-plane, we give the basic idea of scattering, where an incident field is reflected by the infinite flat boundary and local perturbation generates the scattered field. Impedance boundary conditions are introduced as a generalization of the usual free boundary conditions considered in geophysical applications, where the elastic half-plane represents the ground. An important related issue is the propagation of surface waves. We exhibit the radiation conditions obtained recently by Durán, Muga & Nédélec (2009*b*) for a half-plane with free boundary. The impedance boundary-value problem governing scattering in a locally perturbed half-plane is finally introduced.

2.2 The elastic wave equation

2.2.1 Time-dependent waves

Let us consider an elastic medium that fills the full-plane $\mathbb{R}^2$. An arbitrary position in the plane is denoted by $\boldsymbol{x} = (x_1, x_2)$ and a given instant of time is denoted by t. Let $\boldsymbol{U} = (U_1, U_2)$ be the field of displacements of each point, and let $\boldsymbol{F} = (F_1, F_2)$ be a source term representing external volume forces that act on the medium. Both $\boldsymbol{U}$ and $\boldsymbol{F}$ are vectorial fields depending on position and time. In a general context, the law of momentum conservation, or Newton's second law, can be mathematically expressed by means of the equation:

$$\rho(\boldsymbol{x})\,\ddot{\boldsymbol{U}}(\boldsymbol{x},t) = \operatorname{div}\Sigma(\boldsymbol{x},t) + \boldsymbol{F}(\boldsymbol{x},t), \tag{2.1}$$

where the scalar field ρ is the density of the medium, and Σ denotes Cauchy's stress tensor. The divergence operator is applied to each row of the tensor. In elasticity theory, it is assumed that the stress tensor is a function of the displacement field, that is,

$$\Sigma(\boldsymbol{x}, t) = \Sigma(\boldsymbol{U}(\boldsymbol{x}, t)). \tag{2.2}$$

Such a dependence is called a constitutive law, which describes the elastic response of the medium when subjected to forces. If large deformations are involved, the constitutive law is often a non-linear relation. Nevertheless, deformations associated with propagation of elastic waves are usually small, so it is reasonable to suppose a linear law. In addition, we assume that the elastic medium is homogeneous, that is, physical properties are unchanged at different positions. In particular the density ρ is constant. Moreover, the models of scattering phenomena studied in this work do not consider volume forces, so we set $\boldsymbol{F} = \boldsymbol{0}$. Taking into account these assumptions, (2.1) is restated as

$$\rho\, \ddot{\boldsymbol{U}}(\boldsymbol{x}, t) - \operatorname{div} \Sigma(\boldsymbol{U}(\boldsymbol{x}, t)) = \boldsymbol{0}. \tag{2.3}$$

Furthermore, the medium is assumed isotropic, that is, physical properties are the same in all directions. Therefore, the elastic medium is linear, homogeneous and isotropic. Such a medium is described by Hooke's isotropic law:

$$\Sigma(\boldsymbol{U}(\boldsymbol{x}, t)) = \lambda \operatorname{div} \boldsymbol{U}(\boldsymbol{x}, t) + \mu\big(\nabla \boldsymbol{U}(\boldsymbol{x}, t) + \nabla \boldsymbol{U}(\boldsymbol{x}, t)^T\big), \tag{2.4}$$

where λ and μ are the Lamé's parameters, which are positive quantities. Replacing (2.4) in (2.3), and rearranging, we obtain

$$\rho\, \ddot{\boldsymbol{U}}(\boldsymbol{x}, t) - \mu\, \triangle \boldsymbol{U}(\boldsymbol{x}, t) - (\lambda + \mu) \nabla \operatorname{div} \boldsymbol{U}(\boldsymbol{x}, t) = \boldsymbol{0}, \tag{2.5}$$

where $\triangle(\cdot)$ stands for the Laplacian or Laplace operator. Combining with the relation

$$\triangle \boldsymbol{U} = \nabla \operatorname{div} \boldsymbol{U} - \nabla^{\perp} \operatorname{div}^{\perp} \boldsymbol{U}, \tag{2.6}$$

we obtain that (2.5) can be alternatively written as

$$\rho\, \ddot{\boldsymbol{U}}(\boldsymbol{x}, t) - (\lambda + 2\mu) \nabla \operatorname{div} \boldsymbol{U}(\boldsymbol{x}, t) + \mu \nabla^{\perp} \operatorname{div}^{\perp} \boldsymbol{U}(\boldsymbol{x}, t) = \boldsymbol{0}, \tag{2.7}$$

where $\nabla^{\perp}(\cdot)$ denotes the orthogonal gradient and $\operatorname{div}^{\perp}(\cdot)$ the orthogonal divergence. Both equations (2.5) and (2.7) are alternative ways of expressing the time-dependent elastic wave equation, which describes the propagation of waves through an homogeneous isotropic elastic medium in the time-domain. Let us rewrite (2.7) as

$$\ddot{\boldsymbol{U}}(\boldsymbol{x}, t) - c_L^2 \nabla \operatorname{div} \boldsymbol{U}(\boldsymbol{x}, t) + c_T^2 \nabla^{\perp} \operatorname{div}^{\perp} \boldsymbol{U}(\boldsymbol{x}, t) = \boldsymbol{0}, \tag{2.8}$$

where

$$c_L = \sqrt{\frac{\lambda + 2\mu}{\rho}}, \qquad c_T = \sqrt{\frac{\mu}{\rho}}, \tag{2.9}$$

and we decompose the field of displacements $\boldsymbol{U}$ as follows:

$$\boldsymbol{U}(\boldsymbol{x}, t) = \boldsymbol{U}^{(L)}(\boldsymbol{x}, t) + \boldsymbol{U}^{(T)}(\boldsymbol{x}, t), \tag{2.10}$$

where $\boldsymbol{U}^{(L)}$ and $\boldsymbol{U}^{(T)}$ are two vectorial fields satisfying

$$\operatorname{div}^{\perp} \boldsymbol{U}^{(L)}(\boldsymbol{x}, t) = 0, \tag{2.11a}$$

$$\operatorname{div} \boldsymbol{U}^{(T)}(\boldsymbol{x}, t) = 0. \tag{2.11b}$$

From the vectorial analysis, it is well-known that this kind of decomposition is possible under reasonable hypothesis on $\boldsymbol{U}$. Substituting (2.10) in (2.8), combining with (2.11), and rearranging, we obtain that (2.8) holds if $\boldsymbol{U}^{(L)}$ and $\boldsymbol{U}^{(T)}$ satisfy the following equations:

$$\ddot{\boldsymbol{U}}^{(L)}(\boldsymbol{x}, t) - c_L^2 \nabla \operatorname{div} \boldsymbol{U}^{(L)}(\boldsymbol{x}, t) = \boldsymbol{0}, \tag{2.12a}$$

$$\ddot{\boldsymbol{U}}^{(T)}(\boldsymbol{x}, t) + c_T^2 \nabla^{\perp} \operatorname{div}^{\perp} \boldsymbol{U}^{(T)}(\boldsymbol{x}, t) = \boldsymbol{0}. \tag{2.12b}$$

Using identity (2.6) and combining with (2.11), we reexpress (2.12a)-(2.12b) as follows:

$$\ddot{\boldsymbol{U}}^{(L)}(\boldsymbol{x}, t) - c_L^2 \triangle \boldsymbol{U}^{(L)}(\boldsymbol{x}, t) = \boldsymbol{0}, \tag{2.13a}$$

$$\ddot{\boldsymbol{U}}^{(T)}(\boldsymbol{x}, t) - c_T^2 \triangle \boldsymbol{U}^{(T)}(\boldsymbol{x}, t) = \boldsymbol{0}. \tag{2.13b}$$

Equations (2.13a) and (2.13b) correspond to classical vector wave equations, where the respective velocities of propagation c_L and c_T are given in (2.9) and satisfy $c_L > c_T$. This analysis yields the well-known fact that an elastic wave has two kind of components, namely the compressional or longitudinal wave (L) and the shear or transverse wave (T).

2.2.2 Time-harmonic waves

Let us go back to the time-dependent elastic wave equation (2.3). When dealing with wave phenomena, it is often reasonable to suppose that the dependence on time is of the harmonic-type. We thus assume that the displacement field $\boldsymbol{U}$ has the form:

$$\boldsymbol{U}(\boldsymbol{x}, t) = \mathfrak{Re}\{\boldsymbol{u}(\boldsymbol{x})\, e^{-\mathrm{i}\omega t}\}, \tag{2.14}$$

where $\boldsymbol{u} = (u_1, u_2)$ only depends on position and ω is the angular frequency or pulsation, assumed to be given. Replacing (2.14) in (2.3) and rearranging terms yields

$$\operatorname{div} \sigma(\boldsymbol{u}(\boldsymbol{x})) + \rho \omega^2 \boldsymbol{u}(\boldsymbol{x}) = \boldsymbol{0}, \tag{2.15}$$

where the stress tensor σ can be easily expressed in terms of $\boldsymbol{u}$ by substituting (2.14) in (2.4). The following Hooke's time-independent law is obtained:

$$\sigma(\boldsymbol{u}(\boldsymbol{x})) = \lambda \operatorname{div} \boldsymbol{u}(\boldsymbol{x}) I + \mu\big(\nabla \boldsymbol{u}(\boldsymbol{x}) + \nabla \boldsymbol{u}(\boldsymbol{x})^T\big). \tag{2.16}$$

Replacing (2.16) in (2.15) gives

$$\mu \triangle \boldsymbol{u}(\boldsymbol{x}) + (\lambda + \mu) \nabla \operatorname{div} \boldsymbol{u}(\boldsymbol{x}) + \rho \omega^2 \boldsymbol{u}(\boldsymbol{x}) = \boldsymbol{0}, \tag{2.17}$$

and combining with (2.6), we obtain that (2.17) can be rewritten as

$$(\lambda + 2\mu) \nabla \operatorname{div} \boldsymbol{u}(\boldsymbol{x}) - \mu \nabla^{\perp} \operatorname{div}^{\perp} \boldsymbol{u}(\boldsymbol{x}) + \rho \omega^2 \boldsymbol{u}(\boldsymbol{x}) = \boldsymbol{0}. \tag{2.18}$$

Equations (2.17) and (2.18) are two alternative ways of expressing the time-harmonic elastic wave equation. This equation governs the propagation of elastic waves through an homogeneous isotropic elastic medium in the frequency-domain. The assumption of time-harmonic dependence on time is made from here on. Let us restate (2.18) as follows:

$$\frac{1}{k_L^2} \nabla \operatorname{div} \boldsymbol{u}(\boldsymbol{x}) - \frac{1}{k_T^2} \nabla^{\perp} \operatorname{div}^{\perp} \boldsymbol{u}(\boldsymbol{x}) + \boldsymbol{u}(\boldsymbol{x}) = \boldsymbol{0}, \tag{2.19}$$

where k_L and k_T are the wave numbers associated with the longitudinal and the transverse wave, defined respectively as

$$k_L = \frac{\omega}{c_L}, \qquad k_T = \frac{\omega}{c_T}, \tag{2.20}$$

or alternatively,

$$k_L = \omega\sqrt{\frac{\rho}{\lambda + 2\mu}}, \qquad k_T = \omega\sqrt{\frac{\rho}{\mu}}. \tag{2.21}$$

In analogy with the time-dependent case, the displacement field $\boldsymbol{u}$ is decomposed as

$$\boldsymbol{u}(\boldsymbol{x}) = \boldsymbol{u}^{(L)}(\boldsymbol{x}) + \boldsymbol{u}^{(T)}(\boldsymbol{x}), \tag{2.22}$$

with $\boldsymbol{u}^{(L)}$ and $\boldsymbol{u}^{(T)}$ satisfying

$$\operatorname{div}^{\perp}\boldsymbol{u}^{(L)}(\boldsymbol{x}) = 0, \tag{2.23a}$$

$$\operatorname{div}\boldsymbol{u}^{(T)}(\boldsymbol{x}) = 0. \tag{2.23b}$$

Hence, replacing (2.22) in (2.19) and combining with (2.6) and (2.23), we obtain that $\boldsymbol{u}^{(L)}$ and $\boldsymbol{u}^{(T)}$ fulfill two vector Helmholtz equations:

$$\triangle\boldsymbol{u}^{(L)}(\boldsymbol{x}) + k_L^2\,\boldsymbol{u}^{(L)}(\boldsymbol{x}) = \boldsymbol{0}, \tag{2.24a}$$

$$\triangle\boldsymbol{u}^{(T)}(\boldsymbol{x}) + k_T^2\,\boldsymbol{u}^{(T)}(\boldsymbol{x}) = \boldsymbol{0}. \tag{2.24b}$$

These equations govern the dynamics of the longitudinal and the transverse wave in the frequency-domain. Furthermore, the relations (2.23a) and (2.23b) give the existence of two scalar potentials $\psi^{(L)}$ and $\psi^{(T)}$ such that $\boldsymbol{u}^{(L)}$ and $\boldsymbol{u}^{(T)}$ can be expressed as

$$\boldsymbol{u}^{(L)}(\boldsymbol{x}) = \nabla\psi^{(L)}(\boldsymbol{x}), \tag{2.25a}$$

$$\boldsymbol{u}^{(T)}(\boldsymbol{x}) = \nabla^{\perp}\psi^{(T)}(\boldsymbol{x}). \tag{2.25b}$$

Substituting (2.25) in (2.24a) and (2.24b), we obtain that these two equations hold if $\psi^{(L)}$ and $\psi^{(T)}$ satisfy two scalar Helmholtz equations:

$$\triangle\psi^{(L)}(\boldsymbol{x}) + k_L^2\,\psi^{(L)}(\boldsymbol{x}) = 0, \tag{2.26a}$$

$$\triangle\psi^{(T)}(\boldsymbol{x}) + k_T^2\,\psi^{(T)}(\boldsymbol{x}) = 0. \tag{2.26b}$$

From the above analysis, it follows that it is possible to calculate a solution of the time-harmonic elastic wave equation (2.19) (or (2.17) and (2.18)) if we know explicit expressions for $\psi^{(L)}$ and $\psi^{(T)}$. Substituting the two potentials in (2.25) and combining with (2.22) yields an expression for the desired solution, given by

$$\boldsymbol{u}(\boldsymbol{x}) = \nabla\psi^{(L)}(\boldsymbol{x}) + \nabla^{\perp}\psi^{(T)}(\boldsymbol{x}). \tag{2.27}$$

REMARK II.1. *We have obtained that both the longitudinal and the transverse wave can be described by scalar potentials. This result is only valid in* $\mathbb{R}^2$. *In three dimensions, only the longitudinal wave can be represented by a scalar potential. On the contrary, a vector potential is required for a complete representation of the transverse wave.*

REMARK II.2. *It is natural to wonder if there may be other solutions to the time-harmonic elastic wave equation* (2.19) *that are not of the form* (2.27). *The answer is no.*

It is possible to prove that, under reasonable hypothesis, the solution given in (2.27) *is complete, that is, any solution to* (2.19) *can be expressed in terms of potentials. The proof of completeness can be found in Achenbach (1973).*

2.3 Scattering phenomena in exterior domains

2.3.1 Basic principle

In the case where the homogeneous isotropic elastic medium fills the full-plane $\mathbb{R}^2$, there exist fields of displacements satisfying the elastic wave equation that correspond to plane waves, that is, waves whose phase is constant along straight lines, perpendicular to the direction of propagation. Such waves usually have constant amplitude and they can propagate unalterably through the infinite medium. Let us suppose now that a bounded obstacle or inclusion is introduced somewhere in the medium, perturbing the full-plane geometrically. The interior of the obstacle is denoted by Ω^{int} and its boundary is denoted by Γ, which is assumed to be sufficiently regular (at least of the Lipschitz-type). The exterior domain is defined as $\Omega^{\text{ext}} = \mathbb{R}^2 \backslash \overline{\Omega^{\text{int}}}$. Both domains Ω^{int} and Ω^{ext} are assumed to be open sets. Fig. 2.1 presents a scheme of the obstacle and the exterior domain. The presence

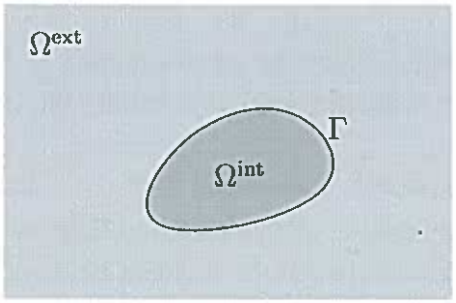

FIGURE 2.1. Obstacle inside an infinite elastic medium.

of this obstacle obviously modifies the nature of the plane waves that propagate through the non-perturbed full-plane. This phenomenon is modeled by separating the whole field of displacements into an incident field, which is constituted by the plane waves that exist in the absence of the obstacle, and a scattered field, that includes any new wave generated due to the obstacle. The incident field is denoted by $\boldsymbol{u}^{\text{inc}}$ and the scattered field is denoted by $\boldsymbol{u}^{\text{sca}}$. Fig. 2.2 shows schematically this physical phenomenon. The incident field thus fulfills the elastic wave equation on the full-plane, which is written as

$$\operatorname{div} \sigma(\boldsymbol{u}^{\text{inc}}(\boldsymbol{x})) + \rho\omega^2 \boldsymbol{u}^{\text{inc}}(\boldsymbol{x}) = \mathbf{0} \qquad \text{in } \mathbb{R}^2, \tag{2.28}$$

where the Cauchy's stress tensor σ is given in terms of the displacement in (2.16). The incident field can be determined explicitly in terms of plane waves. The corresponding analytical expressions are obtained in Appendix A.1. For the time being, we assume $\boldsymbol{u}^{\text{inc}}$

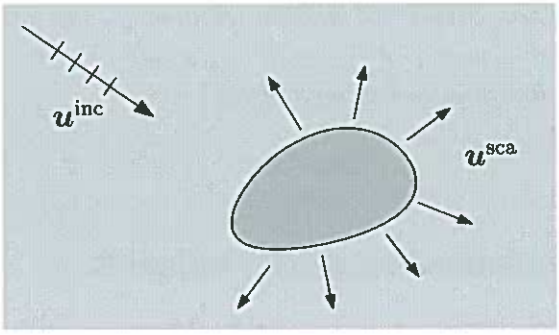

FIGURE 2.2. Incident field and scattered field from an obstacle.

to be given. The total field, denoted by $\boldsymbol{u}^{\text{tot}}$, is the sum of the other two fields, that is,

$$\boldsymbol{u}^{\text{tot}}(\boldsymbol{x}) = \boldsymbol{u}^{\text{inc}}(\boldsymbol{x}) + \boldsymbol{u}^{\text{sca}}(\boldsymbol{x}). \tag{2.29}$$

This field satisfies the elastic wave equation in the exterior domain, that is,

$$\operatorname{div} \sigma(\boldsymbol{u}^{\text{tot}}(\boldsymbol{x})) + \rho\omega^2 \boldsymbol{u}^{\text{tot}}(\boldsymbol{x}) = \boldsymbol{0} \qquad \text{in } \Omega^{\text{ext}}. \tag{2.30}$$

Notice that as the incident field is given, the true unknown of our problem is $\boldsymbol{u}^{\text{sca}}$.

2.3.2 Scattered field and radiation conditions at infinity

Henceforth, in order to simplify the notation, we denote the scattered field simply by $\boldsymbol{u}$. As the total field defined in (2.29) satisfies the elastic wave equation (2.30) in the exterior domain, and the incident field satisfies the same equation (2.28) but in the full-plane, we deduce from (2.29) that the scattered field also fulfills the elastic wave equation in the exterior domain:

$$\operatorname{div} \sigma(\boldsymbol{u}(\boldsymbol{x})) + \rho\omega^2 \boldsymbol{u}(\boldsymbol{x}) = \boldsymbol{0} \qquad \text{in } \Omega^{\text{ext}}. \tag{2.31}$$

This equation governs the dynamics of the scattered field, which is composed by waves generated due to the interaction between the incident field and the obstacle. These waves are outgoing, that is, they are moving away from the obstacle towards infinity, which characterizes an outward energy flux. Nevertheless, the mathematical model may allow the existence of incoming waves, that is, those that come from infinity towards the obstacle. Such waves are not physically admissible, because they have infinite energy. Therefore, it is necessary to eliminate them, and this is done by imposing adequate radiation conditions at infinity. These conditions prescribe an asymptotic behavior to the scattered field, permitting only outgoing waves, which are physically admissible since they have finite energy. We present two alternative forms of expressing the outgoing radiation conditions at infinity. Both forms consider terms evaluated at a circumference whose radius goes to infinity, so we use standard polar coordinates (r, θ), where $r = |\boldsymbol{x}|$. The unit vectors associated with r and θ are $\hat{\boldsymbol{r}} = (\cos\theta, \sin\theta)$ and $\hat{\boldsymbol{\theta}} = (-\sin\theta, \cos\theta)$, respectively. The first form of the radiation conditions can be found in Bonnet (1995) and Ammari (2008), and uses the

following explicit expressions for the fields $\boldsymbol{u}^{(L)}$ and $\boldsymbol{u}^{(T)}$ of the decomposition (2.22):

$$\boldsymbol{u}^{(L)}(\boldsymbol{x}) = -\big(k_L^2 - k_T^2\big)^{-1}\big(\triangle \boldsymbol{u}(\boldsymbol{x}) + k_T^2\, \boldsymbol{u}(\boldsymbol{x})\big), \tag{2.32a}$$

$$\boldsymbol{u}^{(T)}(\boldsymbol{x}) = \big(k_L^2 - k_T^2\big)^{-1}\big(\triangle \boldsymbol{u}(\boldsymbol{x}) + k_L^2\, \boldsymbol{u}(\boldsymbol{x})\big). \tag{2.32b}$$

It can be easily verified that (2.32a) and (2.32b) satisfy (2.22). On the other hand, applying orthogonal divergence to (2.19), using vectorial calculus and rearranging, yields the identity

$$\operatorname{div}^{\perp}\big(\triangle \boldsymbol{u}(\boldsymbol{x}) + k_T^2\, \boldsymbol{u}(\boldsymbol{x})\big) = 0, \tag{2.33}$$

which proves that $\boldsymbol{u}^{(L)}$ defined in (2.32a) satisfies (2.23a). Analogously, applying divergence to (2.19) and proceeding as above gives the relation

$$\operatorname{div}\big(\triangle \boldsymbol{u}(\boldsymbol{x}) + k_L^2\, \boldsymbol{u}(\boldsymbol{x})\big) = 0, \tag{2.34}$$

which proves that $\boldsymbol{u}^{(T)}$ given in (2.32b) satisfies (2.23b). From the previous analysis we already know that the two fields satisfy the vector Helmholtz equations (2.24a) and (2.24b). Therefore, we impose outgoing Sommerfeld radiation conditions (cf. Nédélec 2001, Lenoir 2005) to both fields:

$$\begin{aligned} \big|\partial_r \boldsymbol{u}^{(L)}(\boldsymbol{x}) - \mathrm{i}k_L \boldsymbol{u}^{(L)}(\boldsymbol{x})\big| &= O(r^{-1}) \\ \big|\partial_r \boldsymbol{u}^{(T)}(\boldsymbol{x}) - \mathrm{i}k_T \boldsymbol{u}^{(T)}(\boldsymbol{x})\big| &= O(r^{-1}) \end{aligned} \qquad \text{as } r \to +\infty, \tag{2.35}$$

where ∂_r stands for the radial derivative. We thus say that $\boldsymbol{u}$ satisfies the radiation conditions if it admits the decomposition (2.22), with $\boldsymbol{u}^{(L)}$ and $\boldsymbol{u}^{(T)}$ satisfying (2.23), (2.24) and (2.35) (cf. Ammari 2008). The second form of the outgoing radiation conditions at infinity is given by the following asymptotic relations (cf. Harris 2001):

$$\begin{aligned} \big|\big(\sigma(\boldsymbol{u}(\boldsymbol{x}))\hat{\boldsymbol{r}} - \mathrm{i}k_L(\lambda + 2\mu)\, \boldsymbol{u}(\boldsymbol{x})\big) \cdot \hat{\boldsymbol{r}}\,\big| &= O(r^{-1}) \\ \big|\big(\sigma(\boldsymbol{u}(\boldsymbol{x}))\hat{\boldsymbol{r}} - \mathrm{i}k_T \mu\, \boldsymbol{u}(\boldsymbol{x})\big) \cdot \hat{\boldsymbol{\theta}}\,\big| &= O(r^{-1}) \end{aligned} \qquad \text{as } r \to +\infty. \tag{2.36}$$

It should be observed that this second form of radiation conditions at infinity involves directly the field of displacements $\boldsymbol{u}$ and not its decomposition in terms of $\boldsymbol{u}^{(L)}$ and $\boldsymbol{u}^{(T)}$.

2.3.3 Dirichlet and Neumann boundary-value problems

We now deduce the boundary-value problems that model the elastic scattering by an obstacle. A well-posed model in an exterior domain includes the differential equation, the boundary conditions and the outgoing radiation conditions at infinity. We use the second form of the radiations conditions, since it has the advantage of being expressed in terms of $\boldsymbol{u}$ directly. Two kinds of obstacles are considered, namely a rigid body and a cavity. In the first case, as a rigid body cannot be deformed, the total field of displacements is null in $\overline{\Omega^{\mathrm{int}}}$. The situation is illustrated in Fig. 2.3. In particular, the total field vanishes on the boundary, that is,

$$\boldsymbol{u}^{\mathrm{tot}}(\boldsymbol{x}) = 0 \qquad \text{on } \Gamma, \tag{2.37}$$

and combining with (2.29) yields the next boundary condition for the scattered field:

$$\boldsymbol{u}(\boldsymbol{x}) = -\boldsymbol{u}^{\mathrm{inc}}(\boldsymbol{x}) \qquad \text{on } \Gamma, \tag{2.38}$$

which is a non-homogeneous Dirichlet boundary condition. Thus, putting (2.31), (2.38)

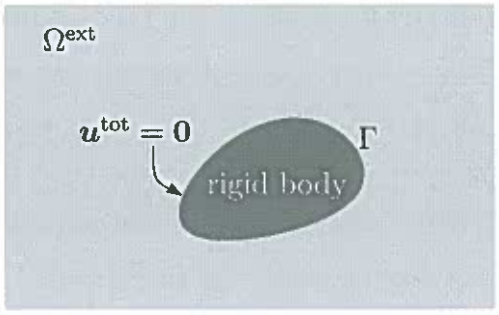

FIGURE 2.3. Rigid body within an infinite elastic medium.

and (2.36) together, we obtain the boundary-value problem: Find $\boldsymbol{u} : \Omega^{\text{ext}} \to \mathbb{C}^2$ such that

$$\operatorname{div} \sigma(\boldsymbol{u}(\boldsymbol{x})) + \rho\omega^2 \boldsymbol{u}(\boldsymbol{x}) = \mathbf{0} \qquad \text{in } \Omega^{\text{ext}}, \tag{2.39a}$$

$$\boldsymbol{u}(\boldsymbol{x}) = -\boldsymbol{u}^{\text{inc}}(\boldsymbol{x}) \qquad \text{on } \Gamma, \tag{2.39b}$$

$$\begin{aligned} \left| \left(\sigma(\boldsymbol{u}(\boldsymbol{x}))\hat{\boldsymbol{r}} - \mathrm{i}k_L(\lambda + 2\mu)\,\boldsymbol{u}(\boldsymbol{x})\right) \cdot \hat{\boldsymbol{r}} \right| &= O(r^{-1}) \\ \left| \left(\sigma(\boldsymbol{u}(\boldsymbol{x}))\hat{\boldsymbol{r}} - \mathrm{i}k_T\mu\,\boldsymbol{u}(\boldsymbol{x})\right) \cdot \hat{\boldsymbol{\theta}} \right| &= O(r^{-1}) \end{aligned} \qquad \text{as } r \to +\infty. \tag{2.39c}$$

In the case where the obstacle is an cavity, the displacement is not defined at Ω^{int}. However, it is possible to make appropriate assumptions on Γ. As there is vacuum at the interior, the points of the elastic solid that are just on the surface are not being forced. This fact can be expressed by means of a traction-free boundary condition:

$$\sigma(\boldsymbol{u}^{\text{tot}}(\boldsymbol{x}))\boldsymbol{n} = \mathbf{0} \qquad \text{on } \Gamma, \tag{2.40}$$

where $\boldsymbol{n}$ denotes the unit normal vector on Γ, which points towards the interior of the obstacle (exterior to Ω^{ext}). The situation is shown in Fig. 2.4. Hence, combining (2.40)

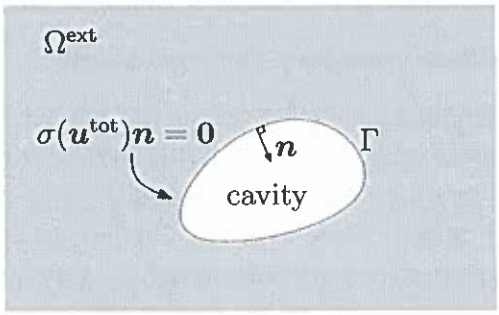

FIGURE 2.4. Cavity within an infinite elastic medium.

with (2.29) and using linearity of σ in $\boldsymbol{u}$ gives the following boundary condition for $\boldsymbol{u}$:

$$\sigma(\boldsymbol{u}(\boldsymbol{x}))\boldsymbol{n} = -\sigma(\boldsymbol{u}^{\text{inc}}(\boldsymbol{x}))\boldsymbol{n} \qquad \text{on } \Gamma, \tag{2.41}$$

which corresponds to a non-homogeneous Neumann boundary condition. Consequently, putting (2.31), (2.41) and (2.36) together, we obtain the desired boundary-value problem:

Find $\boldsymbol{u} : \Omega^{\text{ext}} \to \mathbb{C}^2$ such that

$$\begin{aligned} \operatorname{div}\sigma(\boldsymbol{u}(\boldsymbol{x})) + \rho\omega^2\boldsymbol{u}(\boldsymbol{x}) &= \boldsymbol{0} && \text{in } \Omega^{\text{ext}}, && (2.42a)\\ \sigma(\boldsymbol{u}(\boldsymbol{x}))\boldsymbol{n} &= -\sigma(\boldsymbol{u}^{\text{inc}}(\boldsymbol{x}))\boldsymbol{n} && \text{on } \Gamma, && (2.42b)\\ \left|\left(\sigma(\boldsymbol{u}(\boldsymbol{x}))\hat{\boldsymbol{r}} - \mathrm{i}k_L(\lambda+2\mu)\,\boldsymbol{u}(\boldsymbol{x})\right)\cdot\hat{\boldsymbol{r}}\right| &= O(r^{-1}) && && \\ \left|\left(\sigma(\boldsymbol{u}(\boldsymbol{x}))\hat{\boldsymbol{r}} - \mathrm{i}k_T\mu\,\boldsymbol{u}(\boldsymbol{x})\right)\cdot\hat{\boldsymbol{\theta}}\right| &= O(r^{-1}) && \text{as } r\to+\infty. && (2.42c) \end{aligned}$$

Boundary-value problems (2.39) and (2.42) are mathematical models for the exterior elastic elastic scattering by a rigid body and a cavity, respectively.

2.4 Scattering phenomena in locally perturbed half-planes

2.4.1 Basic principle

We study now the scattering of waves propagating in semi-infinite domains. Throughout this section, we deal with the upper half-plane, denoted by $\mathbb{R}^2_+$ and defined as

$$\mathbb{R}^2_+ = \left\{(x_1, x_2) \in \mathbb{R}^2 \,:\, x_2 > 0\right\}. \tag{2.43}$$

The boundary of $\mathbb{R}^2_+$ is simply denoted by $\{x_2 = 0\}$. Let us assume that $\mathbb{R}^2_+$ is filled with an homogeneous isotropic elastic medium. As in the full-plane case, there are plane waves propagating through $\mathbb{R}^2_+$, but this time the phenomenon looks slightly different. The same kind of plane waves of $\mathbb{R}^2$ can propagate here, but only if they are coming from the interior of the half-plane. In that case, when such waves encounter the infinite boundary, they are reflected, generating new plane waves that go towards the interior of the half-plane. Consequently, there are two fields, namely an incident field, denoted by $\boldsymbol{u}^{\text{inc}}$, and a reflected field, denoted by $\boldsymbol{u}^{\text{ref}}$. The physical situation is illustrated in Fig. 2.5. Each one

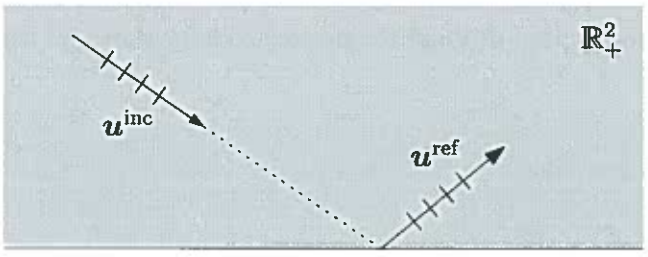

FIGURE 2.5. Incident and reflected field in a non-perturbed half-plane.

of these fields satisfies the elastic wave equation in the half-plane, that is,

$$\begin{aligned} \operatorname{div}\sigma(\boldsymbol{u}^{\text{inc}}(\boldsymbol{x})) + \rho\omega^2\boldsymbol{u}^{\text{inc}}(\boldsymbol{x}) &= \boldsymbol{0} && \text{in } \mathbb{R}^2_+, && (2.44a)\\ \operatorname{div}\sigma(\boldsymbol{u}^{\text{ref}}(\boldsymbol{x})) + \rho\omega^2\boldsymbol{u}^{\text{ref}}(\boldsymbol{x}) &= \boldsymbol{0} && \text{in } \mathbb{R}^2_+. && (2.44b) \end{aligned}$$

If the semi-infinite domain remains unchanged, both the incident and the reflected field propagate indefinitely through it. The incident field $\boldsymbol{u}^{\text{inc}}$ can be determined in an analogous way to that of the full-plane. However, in order to calculate explicitly the reflected field

$\boldsymbol{u}^{\text{ref}}$, boundary conditions on $\{x_2 = 0\}$ are necessary, which are introduced in the next subsection. The obtention of expressions for $\boldsymbol{u}^{\text{inc}}$ and $\boldsymbol{u}^{\text{ref}}$ as plane waves is presented in Appendix A.2. In analogy with the case of an exterior domain, we introduce a local perturbation situated on the flat boundary. The resulting perturbed half-plane is denoted by Ω_+^{ext}, and its boundary is denoted by Γ. Notice that Γ is composed of two parts, namely a perturbed part Γ_p (assumed sufficiently regular) and a flat part Γ_∞, which extends to infinity on both sides. The geometry of Ω_+^{ext} is shown in Fig. 2.6. The perturbed part of the boundary obviously modifies the field of displacements existing in the non-perturbed half-plane. A scattered field arises, which is constituted by the new waves generated from

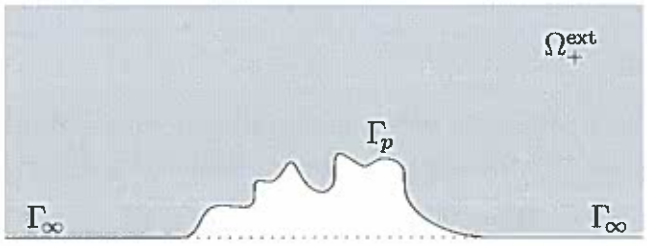

FIGURE 2.6. Half-plane with a local perturbation on the boundary.

the perturbed part. We denote this field by $\boldsymbol{u}^{\text{sca}}$. Consequently, the total field $\boldsymbol{u}^{\text{tot}}$ in Ω_+^{ext} corresponds to the sum of the incident, the reflected, and the scattered field, that is,

$$\boldsymbol{u}^{\text{tot}}(\boldsymbol{x}) = \boldsymbol{u}^{\text{inc}}(\boldsymbol{x}) + \boldsymbol{u}^{\text{ref}}(\boldsymbol{x}) + \boldsymbol{u}^{\text{sca}}(\boldsymbol{x}), \tag{2.45}$$

which fulfills the elastic wave equation in the perturbed half-plane:

$$\operatorname{div} \sigma(\boldsymbol{u}^{\text{tot}}(\boldsymbol{x})) + \rho\omega^2 \boldsymbol{u}^{\text{tot}}(\boldsymbol{x}) = \boldsymbol{0} \qquad \text{in } \Omega_+^{\text{ext}}. \tag{2.46}$$

These three fields propagating through the perturbed half-plane are illustrated in Fig. 2.7.

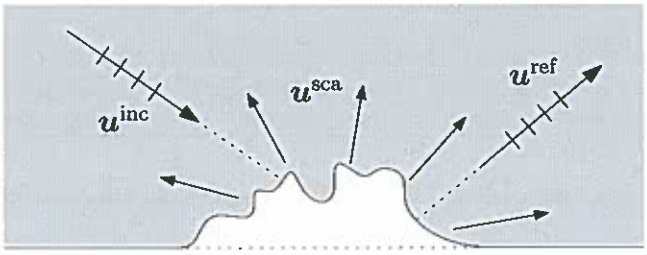

FIGURE 2.7. Incident, reflected and scattered field from a perturbation in a half-plane.

REMARK II.3. *In order to avoid future complications in establishing integral equations to solve scattering phenomena, we will only deal with perturbations of the flat boundary that enter into the upper half-plane, as the one displayed in Figs.2.6 and 2.7. Perturbations that cross the flat boundary towards the lower half-plane will be not permitted.*

REMARK II.4. *An embedded obstacle or inclusion, such as the rigid body or the cavity previously considered, is also allowed as a local perturbation of the half-plane.*

2.4.2 Impedance boundary conditions

One of the main differences of a semi-infinite domain with respect to an infinite exterior domain is that the former is delimited by infinite boundaries, whereas the latter is not. Consequently, the boundary conditions are a fundamental issue in the study of a scattering phenomenon in a perturbed half-plane. As the motivation of the present work comes from geosciences, the elastic half-plane is actually supposed to represent the ground. Therefore, in order to introduce the boundary conditions, we assume for a moment our perturbed half-plane to be located at the lower half of $\mathbb{R}^2$, as indicated in Fig. 2.8. The unit outward normal and tangent vectors on Γ are denoted by $\boldsymbol{n}$ and $\boldsymbol{\tau}$, respectively. Next, we concen-

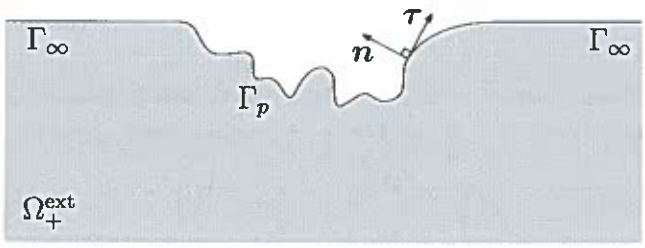

FIGURE 2.8. Locally perturbed half-plane representing the ground.

trate our attention on the boundary conditions for the model, and specially on those that will hold on Γ_∞. In applications to geophysics, Dirichlet boundary conditions are not usually considered, since prescribing the displacements of the ground surface does not make physical sense. Actually, most geophysical models consider a traction-free condition on the ground surface, that is, the boundary is not being forced. This assumption corresponds to homogeneous Neumann boundary conditions, that is, the total field satisfies

$$\sigma(\boldsymbol{u}^{\text{tot}}(\boldsymbol{x}))\boldsymbol{n} = \boldsymbol{0} \qquad \text{on } \Gamma. \tag{2.47}$$

In the present work, we consider special impedance boundary conditions that generalize (2.47) and are of interest from a mathematical point of view. In a simplified geophysical model of the ground, we can suppose that the normal stresses on the surface are equal to the atmospheric pressure exerted by tiny particles of air. As in practice this pressure has no significant influence on the elastic waves that occur in the ground, it can be neglected, so we assume the normal stresses to vanish, that is,

$$\sigma(\boldsymbol{u}^{\text{tot}}(\boldsymbol{x}))\boldsymbol{n} \cdot \boldsymbol{n} = 0 \qquad \text{on } \Gamma. \tag{2.48}$$

In addition, we may suppose shear stresses to be zero, retrieving the usual traction-free boundary condition (2.47). Instead of this, we make a more general assumption: The shear stresses are assumed to be proportional to the tangential displacements as follows:

$$\sigma(\boldsymbol{u}^{\text{tot}}(\boldsymbol{x}))\boldsymbol{n} \cdot \boldsymbol{\tau} = \omega Z(\boldsymbol{x})\, \boldsymbol{u}^{\text{tot}}(\boldsymbol{x}) \cdot \boldsymbol{\tau} \qquad \text{on } \Gamma, \tag{2.49}$$

where the function $Z(\cdot)$ is the surface impedance, which in general could have complex values, but we only treat the case where Z is a real function of the form

$$Z(\boldsymbol{x}) = \begin{cases} Z_p(\boldsymbol{x}) & \text{if } \boldsymbol{x} \in \Gamma_p, \\ Z_\infty & \text{if } \boldsymbol{x} \in \Gamma_\infty, \end{cases} \tag{2.50}$$

where $Z_p : \Gamma_p \to \mathbb{R}$ is a bounded function and $Z_\infty \in \mathbb{R}$ is a given constant. From a physical point of view, as (2.49) states a linear relation between stresses and displacements, Z can be assimilated to a shear stiffness modulus. Notice that $Z = 0$ corresponds to the traction-free case mentioned above. Both relations (2.48) and (2.49) can be written together by means of the following single vector identity:

$$-\sigma(\boldsymbol{u}^{\text{tot}}(\boldsymbol{x}))\boldsymbol{n} + \omega Z(\boldsymbol{x}) u_\tau^{\text{tot}}(\boldsymbol{x})\boldsymbol{\tau} = \boldsymbol{0} \qquad \text{on } \Gamma, \tag{2.51}$$

where $u_\tau^{\text{tot}} = \boldsymbol{u}^{\text{tot}} \cdot \boldsymbol{\tau}$. Relation (2.51) expresses mathematically the impedance boundary conditions to be considered throughout this work in any application to elastic half-planes, either perturbed or not. In the non-perturbed case, we assume that there is no scattered field, so the total field is the sum of the incident and the reflected field. In this case, the surface impedance reduces to $Z = Z_\infty$. Furthermore, the normal and tangent unit vectors are constants and given by $\boldsymbol{n} = -\hat{\boldsymbol{e}}_2$ and $\boldsymbol{\tau} = \hat{\boldsymbol{e}}_1$, respectively, and (2.51) is restated as

$$\sigma(\boldsymbol{u}^{\text{inc}}(\boldsymbol{x}) + \boldsymbol{u}^{\text{ref}}(\boldsymbol{x}))\hat{\boldsymbol{e}}_2 + \omega Z_\infty (u_1^{\text{inc}}(\boldsymbol{x}) + u_1^{\text{ref}}(\boldsymbol{x}))\hat{\boldsymbol{e}}_1 = \boldsymbol{0} \qquad \text{on } \{x_2 = 0\}. \tag{2.52}$$

2.4.3 Scattered field and radiation conditions in the free boundary case

As it was done in the case of an exterior domain, we denote the scattered field by $\boldsymbol{u}$ instead of $\boldsymbol{u}^{\text{sca}}$. We already know that both the incident and the reflected field satisfy the elastic wave equation (2.44) in the non-perturbed half-plane, and the total field defined in (2.45) satisfies the same equation (2.46) in the perturbed half-plane. Consequently, the scattered field also fulfills the elastic wave equation in the perturbed half-plane:

$$\operatorname{div} \sigma(\boldsymbol{u}(\boldsymbol{x})) + \rho\omega^2 \boldsymbol{u}(\boldsymbol{x}) = \boldsymbol{0} \qquad \text{in } \Omega_+^{\text{ext}}. \tag{2.53}$$

On the other hand, there is an important phenomenon that arises in the case of an elastic half-plane: The existence of surface waves, which behave oscillatorily along the infinite flat surface and decay exponentially towards the half-plane interior. Such waves usually appear as a part of the scattered field from the local perturbation, but they could also exist in the non-perturbed half-plane (see Appendix B). In the case of a traction-free boundary, it is well-known that there always exist a surface wave called the Rayleigh wave. The wave number associated with this wave, denoted by k_R, satisfies $k_R > k_T > k_L$. The Rayleigh wave has been widely studied due to its importance in practical applications (cf., e.g., Achenbach 1973, Graff 1991, Harris 2001). On the contrary, in the case of the impedance boundary conditions introduced above, it is not known what the surface waves are like, and this matter will be subsequently studied in Chapter VII. The existence of surface waves makes it difficult to establish radiation conditions at infinity, because it is necessary to ensure that both the volume and the surface waves are physically admissible, that is, they correspond to outgoing waves. The radiation conditions for a non-perturbed half-plane with traction-free boundary have been recently determined by Durán et al. (2009*b*). In that

work, the effect of the surface wave is separated from that of the volume waves by dividing the half-plane into two different regions. Given a parameter α such that $0 < \alpha < 1/2$, these regions are defined as

$$\mathbb{R}^2_+(\alpha+) := \{(x_1, x_2) \in \mathbb{R}^2_+ \,:\, x_2 > r^\alpha\}, \tag{2.54a}$$

$$\mathbb{R}^2_+(\alpha-) := \{(x_1, x_2) \in \mathbb{R}^2_+ \,:\, x_2 < r^\alpha\}, \tag{2.54b}$$

and it is assumed that the volume waves occur mainly in the region $\mathbb{R}^2_+(\alpha+)$, while the Rayleigh wave is almost completely contained within the region $\mathbb{R}^2_+(\alpha-)$. Therefore, radiation conditions analogous to those for an exterior domain are imposed in $\mathbb{R}^2_+(\alpha+)$:

$$\begin{aligned} \left|\left(\sigma(\boldsymbol{u}(\boldsymbol{x}))\hat{\boldsymbol{r}} - \mathrm{i}k_L(\lambda+2\mu)\,\boldsymbol{u}(\boldsymbol{x})\right)\cdot\hat{\boldsymbol{r}}\right| &= O(r^{-1}) \\ \left|\left(\sigma(\boldsymbol{u}(\boldsymbol{x}))\hat{\boldsymbol{r}} - \mathrm{i}k_T\mu\,\boldsymbol{u}(\boldsymbol{x})\right)\cdot\hat{\boldsymbol{\theta}}\right| &= O(r^{-1}) \end{aligned} \quad \text{in } \mathbb{R}^2_+(\alpha+),\ \text{as } r \to +\infty, \tag{2.55}$$

and a new radiation condition is considered in $\mathbb{R}^2_+(\alpha-)$ in order to avoid incoming surface waves:

$$\left|\sigma(\boldsymbol{u}(\boldsymbol{x})\hat{\boldsymbol{r}} - \mathrm{i}M\boldsymbol{u}(\boldsymbol{x})\right| = o(r^{-1/2}) \qquad \text{in } \mathbb{R}^2_+(\alpha-),\ \text{as } r \to +\infty, \tag{2.56}$$

where M is the following matrix:

$$\begin{aligned} M = 2\mu k_R I + \frac{\mu \operatorname{sign} x_1}{k_R^2 - \sqrt{k_R^2 - k_L^2}\sqrt{k_R^2 - k_T^2}} \begin{pmatrix} k_T^2 - 2k_L^2 & 0 \\ 0 & k_T^2 \end{pmatrix} \\ \times \begin{pmatrix} \operatorname{sign} x_1\, k_R & \mathrm{i}\sqrt{k_R^2 - k_T^2} \\ \mathrm{i}\sqrt{k_R^2 - k_L^2} & -\operatorname{sign} x_1\, k_R \end{pmatrix}. \end{aligned} \tag{2.57}$$

The radiation conditions introduced by Durán et al. (2009*b*) (given in (2.55) and (2.56)) are valid for an elastic half-plane with free boundary. In the case of a half-plane with impedance, the radiation conditions have not been obtained yet, and the main difficulty lies in the lack of a mathematically precise description of the surface waves that appear in this case. The determination of explicit forms to express the radiation conditions constitutes a complex matter, and it is beyond the scope of the present work.

REMARK II.5. *Notice that as a first approach to the radiation conditions for the case with impedance, one could think of considering the same division of* $\mathbb{R}^2_+$ *into the regions* $\mathbb{R}^2_+(\alpha+)$ *and* $\mathbb{R}^2_+(\alpha-)$. *As the asymptotic behavior of the volume waves when* x_2 *goes to infinity is not dramatically influenced by the boundary conditions on* $\{x_2 = 0\}$, *it makes sense to impose* (2.55) *in* $\mathbb{R}^2_+(\alpha+)$. *After that, it would be necessary to study mathematically the surface waves appearing with impedance boundary conditions, in order to find an adequate radiation condition to impose in* $\mathbb{R}^2_+(\alpha-)$.

2.4.4 Impedance boundary-value problem

Next, we write the boundary-value problem that describes the scattering phenomenon in a locally perturbed half-plane with impedance boundary conditions. The case of traction-free boundary conditions is mentioned as a particular case. In order to determine precisely the right-hand side of the impedance boundary conditions satisfied by the scattered field, it is necessary to distinguish between the infinite flat part Γ_∞ and the finite perturbed part

Γ_p. In the first case, the impedance is constant and given by $Z = Z_\infty$. Additionally, as $\Gamma_\infty \subset \{x_2 = 0\}$, it holds that $\boldsymbol{n} = -\hat{\boldsymbol{e}}_2$, $\boldsymbol{\tau} = \hat{\boldsymbol{e}}_1$ and the boundary conditions (2.51) for the total field $\boldsymbol{u}^{\text{tot}}$ can be written as

$$\sigma(\boldsymbol{u}^{\text{tot}}(\boldsymbol{x}))\hat{\boldsymbol{e}}_2 + \omega Z_\infty u_1^{\text{tot}}(\boldsymbol{x})\hat{\boldsymbol{e}}_1 = \boldsymbol{0} \qquad \text{on } \Gamma_\infty. \tag{2.58}$$

Substituting (2.45) in (2.58) and combining with (2.52), we obtain that the scattered field $\boldsymbol{u}$ satisfies homogeneous boundary conditions in the flat part of the boundary, that is

$$\sigma(\boldsymbol{u}(\boldsymbol{x}))\hat{\boldsymbol{e}}_2 + \omega Z_\infty u_1(\boldsymbol{x})\hat{\boldsymbol{e}}_1 = \boldsymbol{0} \qquad \text{on } \Gamma_\infty. \tag{2.59}$$

In the perturbed part of the boundary, the impedance depends on the position and is given by $Z = Z_p$. Replacing (2.45) in (2.51) yields

$$\begin{aligned} -\sigma(\boldsymbol{u}(\boldsymbol{x}))\boldsymbol{n} + \omega Z_p(\boldsymbol{x})u_\tau(\boldsymbol{x})\boldsymbol{\tau} = \sigma(\boldsymbol{u}^{\text{inc}}(\boldsymbol{x}) + \boldsymbol{u}^{\text{ref}}(\boldsymbol{x}))\boldsymbol{n} \\ - \omega Z_p(\boldsymbol{x})(u_\tau^{\text{inc}}(\boldsymbol{x}) + u_\tau^{\text{ref}}(\boldsymbol{x}))\boldsymbol{\tau} \qquad \text{on } \Gamma_p, \end{aligned} \tag{2.60}$$

that is, the scattered field $\boldsymbol{u}$ satisfies inhomogeneous impedance boundary conditions in the perturbed part Γ_p. Hence, putting (2.53), (2.59) and (2.60) together yields the impedance boundary-value problem in the locally perturbed half-plane: Find $\boldsymbol{u} : \Omega_+^{\text{ext}} \to \mathbb{C}^2$ such that

$$\operatorname{div}\sigma(\boldsymbol{u}(\boldsymbol{x})) + \rho\omega^2\boldsymbol{u}(\boldsymbol{x}) = \boldsymbol{0} \qquad \text{in } \Omega_+^{\text{ext}}, \tag{2.61a}$$

$$-\sigma(\boldsymbol{u}(\boldsymbol{x}))\boldsymbol{n} + \omega Z_p(\boldsymbol{x})u_\tau(\boldsymbol{x})\boldsymbol{\tau} = \boldsymbol{f}(\boldsymbol{x}) \qquad \text{on } \Gamma_p, \tag{2.61b}$$

$$\sigma(\boldsymbol{u}(\boldsymbol{x}))\hat{\boldsymbol{e}}_2 + \omega Z_\infty u_1(\boldsymbol{x})\hat{\boldsymbol{e}}_1 = \boldsymbol{0} \qquad \text{on } \Gamma_\infty, \tag{2.61c}$$

$$+ \text{ Outgoing radiation conditions} \qquad \text{as } r = |\boldsymbol{x}| \to +\infty, \tag{2.61d}$$

where the right-hand side of (2.61b) is given by

$$\boldsymbol{f}(\boldsymbol{x}) = \sigma(\boldsymbol{u}^{\text{inc}}(\boldsymbol{x}) + \boldsymbol{u}^{\text{ref}}(\boldsymbol{x}))\boldsymbol{n} - \omega Z_p(\boldsymbol{x})(u_\tau^{\text{inc}}(\boldsymbol{x}) + u_\tau^{\text{ref}}(\boldsymbol{x}))\boldsymbol{\tau}, \tag{2.62}$$

and as the radiation conditions are not known in this case, they have been expressed in words. If $Z = 0$ in Γ, we obtain a Neumann boundary-value problem describing scattering in a locally perturbed half-plane with free boundary. Although the radiation conditions mentioned above have been obtained for a non-perturbed half-plane, they can be incorporated into this problem, since the considered perturbation is local. We obtain the next boundary-value problem in the perturbed half-plane: Find $\boldsymbol{u} : \Omega_+^{\text{ext}} \to \mathbb{C}^2$ such that

$$\operatorname{div}\sigma(\boldsymbol{u}(\boldsymbol{x})) + \rho\omega^2\boldsymbol{u}(\boldsymbol{x}) = \boldsymbol{0} \qquad \text{in } \Omega_+^{\text{ext}}, \tag{2.63a}$$

$$-\sigma(\boldsymbol{u}(\boldsymbol{x}))\boldsymbol{n} = \boldsymbol{f}(\boldsymbol{x}) \qquad \text{on } \Gamma_p, \tag{2.63b}$$

$$\sigma(\boldsymbol{u}(\boldsymbol{x}))\hat{\boldsymbol{e}}_2 = \boldsymbol{0} \qquad \text{on } \Gamma_\infty, \tag{2.63c}$$

$$\begin{aligned} \left|\left(\sigma(\boldsymbol{u}(\boldsymbol{x}))\hat{\boldsymbol{r}} - \mathrm{i}k_L(\lambda + 2\mu)\,\boldsymbol{u}(\boldsymbol{x})\right)\cdot\hat{\boldsymbol{r}}\right| &= O(r^{-1}) \\ \left|\left(\sigma(\boldsymbol{u}(\boldsymbol{x}))\hat{\boldsymbol{r}} - \mathrm{i}k_T\mu\,\boldsymbol{u}(\boldsymbol{x})\right)\cdot\hat{\boldsymbol{\theta}}\right| &= O(r^{-1}) \end{aligned} \qquad \text{as } r \to +\infty, r^\alpha < x_2, \tag{2.63d}$$

$$\left|\sigma(\boldsymbol{u}(\boldsymbol{x})\hat{\boldsymbol{r}} - \mathrm{i}M\boldsymbol{u}(\boldsymbol{x})\right| = o(r^{-1/2}) \qquad \text{as } r \to +\infty, r^\alpha > x_2, \tag{2.63e}$$

where the right-hand side of (2.63b) is obtained by setting $Z_p = 0$ in (2.62), that is,

$$\boldsymbol{f}(\boldsymbol{x}) = \sigma(\boldsymbol{u}^{\text{inc}}(\boldsymbol{x}) + \boldsymbol{u}^{\text{ref}}(\boldsymbol{x}))\boldsymbol{n}, \tag{2.64}$$

and M is the matrix defined in (2.57).

III. METHODS INVOLVING INFINITE SERIES FOR EXTERIOR SCATTERING

3.1 Introduction

This chapter introduces two methods for solving the exterior scattering problems mentioned in Section 2.3, where the incident field is assumed to consist of pure longitudinal or transverse plane waves. Both of these methods employ analytical techniques and yield explicit expressions as infinite series. The first method is restricted to the particular case where the obstacle is a circle. The respective Dirichlet and Neumann boundary-value problems are analytically solved by separation of variables in polar coordinates, yielding analytical formulae for the scattered field that involve infinite series. These solutions are of practical interest, because they can be used as benchmarks to validate numerical solutions. The second method is closely related to the first one and involves the so-called Dirichlet-to-Neumann (or Steklov-Poincaré) map, which is a powerful tool to solve exterior boundary-value problems where the bounded domain is arbitrarily shaped. A detailed description of this technique applied to exterior acoustic scattering can be found in Ihlenburg (1998). The DtN map for two-dimensional time-harmonic elastic waves has been obtained by Givoli & Keller (1990) and its mathematical properties have been further studied by Harari & Shohet (1998). A circular artificial boundary surrounding the obstacle is introduced, and an auxiliary boundary-value problem is stated at the exterior of the circle, which is analytically solved by proceeding as above. The DtN map is then defined as the normal derivative of the solution of this problem on the circumference. We provide an explicit formula for the DtN map in terms of an infinite series. This procedure naturally leads to restate the scattering problem within the bounded domain that lies between the circumference and the boundary of the obstacle. Exact nonreflecting boundary conditions are then specified on the circumference in terms of the DtN map. The new boundary-value problem is posed in variational form and approximated by a Galerkin-type method. The emphasis is placed on the approximation of the term involving the DtN map.

3.2 Explicit solutions for the exterior of a circle

3.2.1 General solution to the elastic wave equation

We start by defining the mathematical domain to be considered throughout this section. The obstacle is the ball B_a of radius $a > 0$ centered at the origin. The exterior domain corresponds to the complement of the closed ball, defined as $\Omega_a^{\text{ext}} := \mathbb{R}^2 \backslash \overline{B_a}$. The boundary is the circumference of radius a, denoted by $S_a := \partial B_a$. The domain is illustrated in Fig. 3.1. The polar coordinates appear as the natural way to describe this domain. It can be defined as

$$\Omega_a^{\text{ext}} = \big\{(r\cos\theta, r\sin\theta) \;:\; a < r < +\infty,\; 0 \le \theta < 2\pi\big\}, \tag{3.1}$$

and we desire to compute a solution to the elastic wave equation in Ω_a^{ext}, that is,

$$\operatorname{div}\sigma(\boldsymbol{u}(r,\theta)) + \rho\omega^2\boldsymbol{u}(r,\theta) = \mathbf{0} \qquad (r,\theta) \in]a, +\infty[\times[0, 2\pi[. \tag{3.2}$$

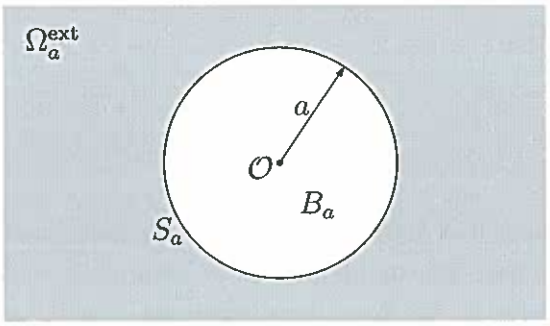

FIGURE 3.1. Circular obstacle in an infinite elastic medium.

The calculation is made using the decomposition (2.27) for the solution $\boldsymbol{u}$:

$$\boldsymbol{u}(r,\theta) = \nabla\psi^{(L)}(r,\theta) + \nabla^{\perp}\psi^{(T)}(r,\theta). \tag{3.3}$$

From Section 2.2, we know that $\psi^{(L)}$ and $\psi^{(T)}$ satisfy (2.26a) and (2.26b), respectively. We write these Helmholtz equations in a single way as follows:

$$\triangle\psi^{(\alpha)}(r,\theta) + k_\alpha^2\psi^{(\alpha)}(r,\theta) = 0, \qquad \alpha = L, T, \tag{3.4}$$

and we look for solutions to (3.4) fulfilling the Sommerfeld radiation conditions at infinity:

$$\left|\partial_r\psi^{(\alpha)}(r,\theta) - \mathrm{i}k_\alpha\psi^{(\alpha)}(r,\theta)\right| = o\left(r^{-1/2}\right) \qquad \text{as } r \longrightarrow +\infty. \tag{3.5}$$

Let us expand the Laplacian in polar coordinates. The Helmholtz equation (3.4) becomes

$$\frac{\partial^2\psi^{(\alpha)}}{\partial r^2}(r,\theta) + \frac{1}{r}\frac{\partial\psi^{(\alpha)}}{\partial r}(r,\theta) + \frac{1}{r^2}\frac{\partial^2\psi^{(\alpha)}}{\partial\theta^2}(r,\theta) + k_\alpha^2\psi^{(\alpha)}(r,\theta) = 0. \tag{3.6}$$

To solve (3.6), we apply separation of variables on $\psi^{(\alpha)}$ in the form

$$\psi^{(\alpha)}(r,\theta) = \eta(r)\chi(\theta), \tag{3.7}$$

where η and χ are unknown functions to be determined later. Replacing (3.7) in (3.6) yields

$$\eta''(r)\,\chi(\theta) + \frac{1}{r}\,\eta'(r)\,\chi(\theta) + \frac{1}{r^2}\,\eta(r)\,\chi''(\theta) + k_\alpha^2\eta(r)\,\chi(\theta) = 0, \tag{3.8}$$

and rearranging appropriately, we obtain the equation

$$r^2\frac{\eta''(r)}{\eta(r)} + r\,\frac{\eta'(r)}{\eta(r)} + k_\alpha^2 r^2 = -\frac{\chi''(\theta)}{\chi(\theta)}. \tag{3.9}$$

As the left-hand side of (3.9) only depends on r and the right-hand side only depends on θ, this equations holds on condition that both sides are equal to a constant. Let us denote this constant by ν. On one hand, we obtain from (3.9) that the pair (ν,χ) is a solution to the spectral problem

$$-\chi''(\theta) = \nu\,\chi(\theta), \qquad 0 \le \theta \le 2\pi, \tag{3.10}$$

which has a countable number of nonzero periodic solutions $\{(\nu_n,\chi_n)\}_{n\in\mathbb{Z}}$, given by

$$\nu_n = n^2, \qquad \chi_n(\theta) = e^{\mathrm{i}n\theta}, \tag{3.11}$$

where the eigenfunctions χ_n are actually defined up to a multiplicative constant. Moreover, the set $\{\chi_n\}_{n\in\mathbb{Z}}$ is an orthogonal basis of $L^2(S_a)$ that satisfies

$$\big(\chi_n, \chi_m\big)_{0,S_a} = 2\pi a\, \delta_{nm}, \qquad n,\, m \in \mathbb{Z}, \tag{3.12}$$

where $(\,\cdot\,,\cdot\,)_{0,S_a}$ stands for the inner product in $L^2(S_a)$. Therefore, if $v : S_a \to \mathbb{C}$ is any square integrable function, then it can be expressed as a Fourier series as follows:

$$v(\theta) = \frac{1}{2\pi} \sum_{n=-\infty}^{+\infty} \int_0^{2\pi} v(\phi)\, e^{-\mathrm{i}n\phi} \mathrm{d}\phi\; e^{\mathrm{i}n\theta}. \tag{3.13}$$

On the other hand, we obtain from (3.9), (3.10) and (3.11) that η is a solution of the equation

$$r^2\eta_n''(r) + r\,\eta_n'(r) + (k_\alpha^2 r^2 - n^2)\,\eta_n(r) = 0. \tag{3.14}$$

Performing the change of variable $z = k_\alpha r$ and defining $v_n(z) \equiv \eta_n(r)$, we obtain the following ordinary differential equation:

$$z^2 v_n''(z) + z\, v_n'(z) + (z^2 - n^2)\, v_n(z) = 0, \qquad n \in \mathbb{Z}, \tag{3.15}$$

which corresponds to the Bessel equation of order n. Its solution is written in terms of the Hankel functions of order n (See Appendix B):

$$v_n(z) = A_n^{(1)} H_n^{(1)}(z) + A_n^{(2)} H_n^{(2)}(z), \tag{3.16}$$

where $A_n^{(1)}$ and $A_n^{(2)}$ are generic coefficients. Hence, the solution to (3.14) is

$$\eta_n(r) = A_n^{(1)} H_n^{(1)}(k_\alpha r) + A_n^{(2)} H_n^{(2)}(k_\alpha r), \qquad n \in \mathbb{Z}, \tag{3.17}$$

and the general solution to (3.4) is expressed as a series of products of functions $\eta_n(r)\chi_n(\theta)$ over $n \in \mathbb{Z}$, that is,

$$\psi^{(\alpha)}(r,\theta) = \sum_{n=-\infty}^{+\infty} \big(A_n^{(1)} H_n^{(1)}(k_\alpha r) + A_n^{(2)} H_n^{(2)}(k_\alpha r)\big) e^{\mathrm{i}n\theta}. \tag{3.18}$$

In addition, the Hankel functions fulfill the recurrence formulae (B.12) and the asymptotic expansions (B.14). Using these relations, it is possible to prove that the next relations hold for large enough r:

$$\left|\frac{\mathrm{d}}{\mathrm{d}r} H_n^{(1)}(k_\alpha r) - \mathrm{i}k_\alpha H_n^{(1)}(k_\alpha r)\right| = O(r^{-3/2}), \tag{3.19a}$$

$$\left|\frac{\mathrm{d}}{\mathrm{d}r} H_n^{(2)}(k_\alpha r) - \mathrm{i}k_\alpha H_n^{(2)}(k_\alpha r)\right| = O(r^{-1/2}). \tag{3.19b}$$

From (3.19a)-(3.19b), it follows that only the Hankel functions $H_n^{(1)}$ satisfy the outgoing radiation conditions at infinity (3.5). Consequently, functions $H_n^{(2)}$ are eliminated from the solution by setting $A_n^{(2)} = 0$ in (3.18) for all $n \in \mathbb{Z}$. We then write the scalar potentials separately for $\alpha = L, T$:

$$\psi^{(L)}(r,\theta) = \frac{1}{2\pi} \sum_{n=-\infty}^{+\infty} A_n H_n^{(1)}(k_L r)\, e^{\mathrm{i}n\theta}, \tag{3.20a}$$

$$\psi^{(T)}(r,\theta) = \frac{1}{2\pi}\sum_{n=-\infty}^{+\infty} B_n H_n^{(1)}(k_T r)\, e^{in\theta} \tag{3.20b}$$

where coefficients A_n and B_n are general. The factor $1/2\pi$ is added in order to simplify subsequent calculations. Computing $\nabla\psi^{(L)}$ and $\nabla^\perp\psi^{(T)}$ gives

$$\nabla\psi^{(L)}(r,\theta) = \frac{1}{2\pi}\sum_{n=-\infty}^{+\infty} A_n\Big(k_L H_n^{(1)\prime}(k_L r)\,\hat{\boldsymbol{r}} + \frac{in}{r} H_n^{(1)}(k_L r)\,\hat{\boldsymbol{\theta}}\Big)e^{in\theta}, \tag{3.21a}$$

$$\nabla^\perp\psi^{(T)}(r,\theta) = \frac{1}{2\pi}\sum_{n=-\infty}^{+\infty} B_n\Big(\frac{in}{r} H_n^{(1)}(k_T r)\,\hat{\boldsymbol{r}} - k_T H_n^{(1)\prime}(k_T r)\,\hat{\boldsymbol{\theta}}\Big)e^{in\theta}. \tag{3.21b}$$

Substitution of (3.21a) and (3.21b) in (3.3) yields a general expression for the solution of (3.2) in polar coordinates:

$$\boldsymbol{u}(r,\theta) = u_r(r,\theta)\,\hat{\boldsymbol{r}} + u_\theta(r,\theta)\,\hat{\boldsymbol{\theta}}, \tag{3.22}$$

where

$$u_r(r,\theta) = \frac{1}{2\pi}\sum_{n=-\infty}^{+\infty}\Big(A_n k_L H_n^{(1)\prime}(k_L r) + B_n\frac{in}{r} H_n^{(1)}(k_T r)\Big)e^{in\theta}, \tag{3.23a}$$

$$u_\theta(r,\theta) = \frac{1}{2\pi}\sum_{n=-\infty}^{+\infty}\Big(A_n\frac{in}{r} H_n^{(1)}(k_L r) - B_n k_T H_n^{(1)\prime}(k_T r)\Big)e^{in\theta}. \tag{3.23b}$$

Coefficients A_n and B_n can be obtained explicitly from particular boundary conditions specified on S_a. In the subsequent subsections, we determine the scattered fields for Dirichlet and Neumann boundary conditions, by solving analytically the corresponding boundary-value problems.

3.2.2 Scattered field by a rigid circular body

Next, we determine the field scattered by the circle when it corresponds to a rigid body. The Dirichlet boundary-value problem (2.39) is then reexpressed in polar coordinates: Find $\boldsymbol{u} : \Omega_a^{\text{ext}} \to \mathbb{C}^2$ such that

$$\operatorname{div}\sigma(\boldsymbol{u}(r,\theta) + \rho\omega^2\boldsymbol{u}(r,\theta) = \boldsymbol{0} \qquad \text{in } \Omega_a^{\text{ext}}, \tag{3.24a}$$

$$\boldsymbol{u}(a,\theta) = -\boldsymbol{u}^{\text{inc}}(a,\theta) \qquad \theta\in[0,2\pi], \tag{3.24b}$$

$$\begin{aligned}\big|\big(\sigma(\boldsymbol{u}(r,\theta)\hat{\boldsymbol{r}} - ik_L(\lambda+2\mu)\,\boldsymbol{u}(r,\theta)\big)\cdot\hat{\boldsymbol{r}}\,\big| &= O(r^{-1})\\ \big|\big(\sigma(\boldsymbol{u}(r,\theta)\hat{\boldsymbol{r}} - ik_T\mu\,\boldsymbol{u}(r,\theta)\big)\cdot\hat{\boldsymbol{\theta}}\,\big| &= O(r^{-1})\end{aligned} \qquad \text{as } r\to+\infty. \tag{3.24c}$$

The incident field $\boldsymbol{u}^{\text{inc}}$ is expressed by components in polar coordinates as

$$\boldsymbol{u}^{\text{inc}}(r,\theta) = u_r^{\text{inc}}(r,\theta)\,\hat{\boldsymbol{r}} + u_\theta^{\text{inc}}(r,\theta)\,\hat{\boldsymbol{\theta}}, \tag{3.25}$$

We assume that this field consists of either pure longitudinal or transverse plane waves, as indicated in Fig. 3.2. The direction of propagation is defined by the angle α_0, measured downwards with respect to the horizontal. A general incident field in terms of plane waves can be obtained as a linear combination of these two elementary fields, which are denoted by $\boldsymbol{u}^{\text{inc}(L)}$ and $\boldsymbol{u}^{\text{inc}(T)}$, respectively. Explicit expressions for a longitudinal and a transverse

elastic plane wave in cartesian coordinates are determined in Appendix A.1. These expressions are given in (A.10a) and (A.10b), respectively, as functions of α_0. As we are using

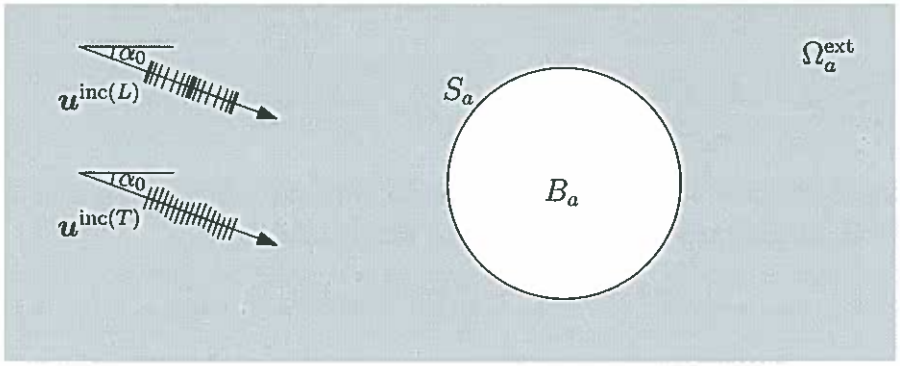

FIGURE 3.2. Longitudinal and transverse incident waves with angle α_0.

polar coordinates, we attempt to express the incident fields $\boldsymbol{u}^{\mathrm{inc}(L)}$ and $\boldsymbol{u}^{\mathrm{inc}(T)}$ in terms of their radial and angular components, that is,

$$\boldsymbol{u}^{\mathrm{inc}(L)}(r,\theta) = u_r^{\mathrm{inc}(L)}(r,\theta)\,\hat{\boldsymbol{r}} + u_\theta^{\mathrm{inc}(L)}(r,\theta)\,\hat{\boldsymbol{\theta}}, \tag{3.26a}$$

$$\boldsymbol{u}^{\mathrm{inc}(T)}(r,\theta) = u_r^{\mathrm{inc}(T)}(r,\theta)\,\hat{\boldsymbol{r}} + u_\theta^{\mathrm{inc}(T)}(r,\theta)\,\hat{\boldsymbol{\theta}}. \tag{3.26b}$$

Performing a change of coordinates, we obtain that the components of $\boldsymbol{u}^{\mathrm{inc}(L)}$ are

$$u_r^{\mathrm{inc}(L)}(r,\theta) = \cos(\alpha_0+\theta)\, e^{ik_L r\cos(\alpha_0+\theta)}, \tag{3.27a}$$

$$u_\theta^{\mathrm{inc}(L)}(r,\theta) = -\sin(\alpha_0+\theta)\, e^{ik_L r\cos(\alpha_0+\theta)}, \tag{3.27b}$$

while the components of $\boldsymbol{u}^{\mathrm{inc}(T)}$ are

$$u_r^{\mathrm{inc}(T)}(r,\theta) = \sin(\alpha_0+\theta)\, e^{ik_T r\cos(\alpha_0+\theta)}, \tag{3.28a}$$

$$u_\theta^{\mathrm{inc}(T)}(r,\theta) = \cos(\alpha_0+\theta)\, e^{ik_T r\cos(\alpha_0+\theta)}. \tag{3.28b}$$

To simplify the notation, we consider the general incident field $\boldsymbol{u}^{\mathrm{inc}}$ given in (3.25), and we go back to the distinction between longitudinal and transverse waves later. In order to solve (3.24), the incident field is evaluated at $r = a$ and its components are expanded as Fourier series, as given in (3.13):

$$u_r^{\mathrm{inc}}(a,\theta) = \frac{1}{2\pi}\sum_{n=-\infty}^{+\infty}\int_0^{2\pi} u_r^{\mathrm{inc}}(a,\phi)\, e^{-in\phi}\mathrm{d}\phi\; e^{in\theta}, \tag{3.29a}$$

$$u_\theta^{\mathrm{inc}}(a,\theta) = \frac{1}{2\pi}\sum_{n=-\infty}^{+\infty}\int_0^{2\pi} u_\theta^{\mathrm{inc}}(a,\phi)\, e^{-in\phi}\mathrm{d}\phi\; e^{in\theta}. \tag{3.29b}$$

On the other hand, the components of the general solution to (3.24a) given in (3.23) are evaluated at $r = a$, obtaining

$$u_r(a,\theta) = \frac{1}{2\pi}\sum_{n=-\infty}^{+\infty}\Big(A_n k_L H_n^{(1)\prime}(k_L a) + B_n \frac{\mathrm{i}n}{a} H_n^{(1)}(k_T a)\Big)e^{\mathrm{i}n\theta}, \tag{3.30a}$$

$$u_\theta(a,\theta) = \frac{1}{2\pi}\sum_{n=-\infty}^{+\infty}\Big(A_n \frac{\mathrm{i}n}{a} H_n^{(1)}(k_L a) - B_n k_T H_n^{(1)\prime}(k_T a)\Big)e^{\mathrm{i}n\theta}. \tag{3.30b}$$

Substituting (3.29) and (3.30) in (3.24b) and separating into radial and angular components yields the following system of linear equations for A_n and B_n:

$$k_L H_n^{(1)\prime}(k_L a)A_n + \frac{\mathrm{i}n}{a} H_n^{(1)}(k_T a)B_n = -I_{n,r}, \tag{3.31a}$$

$$\frac{\mathrm{i}n}{a} H_n^{(1)}(k_L a)A_n - k_T H_n^{(1)\prime}(k_T a)B_n = -I_{n,\theta}, \tag{3.31b}$$

where

$$I_{n,r} = \int_0^{2\pi} u_r^{\mathrm{inc}}(a,\phi)e^{-\mathrm{i}n\phi}\mathrm{d}\phi, \tag{3.32a}$$

$$I_{n,\theta} = \int_0^{2\pi} u_\theta^{\mathrm{inc}}(a,\phi)e^{-\mathrm{i}n\phi}\mathrm{d}\phi. \tag{3.32b}$$

By solving this system, we obtain the next expressions for the coefficients A_n and B_n:

$$A_n = \frac{1}{\delta_n}\Big(k_T H_n^{(1)\prime}(k_T a)\, I_{n,r} + \frac{\mathrm{i}n}{a} H_n^{(1)}(k_T a)\, I_{n,\theta}\Big), \tag{3.33a}$$

$$B_n = \frac{1}{\delta_n}\Big(\frac{\mathrm{i}n}{a} H_n^{(1)}(k_L a)\, I_{n,r} - k_L H_n^{(1)\prime}(k_L a)\, I_{n,\theta}\Big), \tag{3.33b}$$

where

$$\delta_n = \frac{n^2}{a^2} H_n^{(1)}(k_L a)H_n^{(1)}(k_T a) - k_L k_T H_n^{(1)\prime}(k_L a)H_n^{(1)\prime}(k_T a). \tag{3.34}$$

If $\boldsymbol{u}^{\mathrm{inc}} = \boldsymbol{u}^{\mathrm{inc}(L)}$, we can reexpress integrals $I_{n,r}$ and $I_{n,\theta}$ by replacing (3.27) in (3.32):

$$I_{n,r} = \int_0^{2\pi} \cos(\alpha_0 + \phi)e^{\mathrm{i}(k_L a\cos(\alpha_0+\phi)-n\phi)}\mathrm{d}\phi, \tag{3.35a}$$

$$I_{n,\theta} = -\int_0^{2\pi} \sin(\alpha_0 + \phi)e^{\mathrm{i}(k_L a\cos(\alpha_0+\phi)-n\phi)}\mathrm{d}\phi, \tag{3.35b}$$

Analogously, if $\boldsymbol{u}^{\mathrm{inc}} = \boldsymbol{u}^{\mathrm{inc}(T)}$, we reexpress $I_{n,r}$ and $I_{n,\theta}$ by replacing (3.28) in (3.32):

$$I_{n,r} = \int_0^{2\pi} \sin(\alpha_0 + \phi)e^{\mathrm{i}(k_T a\cos(\alpha_0+\phi)-n\phi)}\mathrm{d}\phi, \tag{3.36a}$$

$$I_{n,\theta} = \int_0^{2\pi} \cos(\alpha_0 + \phi)e^{\mathrm{i}(k_T a\cos(\alpha_0+\phi)-n\phi)}\mathrm{d}\phi. \tag{3.36b}$$

Consequently, substituting A_n and B_n from (3.33) in the general solution $\boldsymbol{u}$ given in (3.22)-(3.23), we obtain the explicit solution to the Dirichlet boundary-value problem (3.24).

3.2.3 Scattered field by a circular cavity

We determine now the scattered field in the case where the circle is an empty cavity. This problem has been previously treated by Perrey-Debain et al. (2003) for a transverse incident wave. As the boundary of the obstacle corresponds to a circumference, it holds that $\boldsymbol{n} = -\hat{\boldsymbol{r}}$, and the Neumann boundary-value problem (2.42) is reexpressed in polar coordinates as: Find $\boldsymbol{u} : \Omega_a^{\text{ext}} \to \mathbb{C}^2$ such that

$$\operatorname{div} \sigma(\boldsymbol{u}(r,\theta)) + \rho\omega^2 \boldsymbol{u}(r,\theta) = \boldsymbol{0} \qquad \text{in } \Omega_a^{\text{ext}}, \tag{3.37a}$$

$$\boldsymbol{t}(\theta) = -\boldsymbol{t}^{\text{inc}}(\theta) \qquad \theta \in [0, 2\pi], \tag{3.37b}$$

$$\begin{aligned} \left|\left(\sigma(\boldsymbol{u}(r,\theta))\hat{\boldsymbol{r}} - \mathrm{i}k_L(\lambda+2\mu)\,\boldsymbol{u}(r,\theta)\right)\cdot\hat{\boldsymbol{r}}\right| &= O(r^{-1}) \\ \left|\left(\sigma(\boldsymbol{u}(r,\theta))\hat{\boldsymbol{r}} - \mathrm{i}k_T\mu\,\boldsymbol{u}(r,\theta)\right)\cdot\hat{\boldsymbol{\theta}}\right| &= O(r^{-1}) \end{aligned} \qquad \text{as } r \to +\infty, \tag{3.37c}$$

where $\boldsymbol{t}$ and $\boldsymbol{t}^{\text{inc}}$ are the surface traction vectors associated with the scattered and the incident field on S_a, respectively. These vectors are defined as

$$\boldsymbol{t}(\theta) = -\sigma(\boldsymbol{u}(a,\theta))\hat{\boldsymbol{r}}, \tag{3.38a}$$

$$\boldsymbol{t}^{\text{inc}}(\theta) = -\sigma(\boldsymbol{u}^{\text{inc}}(a,\theta))\hat{\boldsymbol{r}}, \tag{3.38b}$$

and they can be written by components in polar coordinates as

$$\boldsymbol{t}(\theta) = t_r(\theta)\,\hat{\boldsymbol{r}} + t_\theta(\theta)\,\hat{\boldsymbol{\theta}}, \tag{3.39a}$$

$$\boldsymbol{t}^{\text{inc}}(\theta) = t_r^{\text{inc}}(\theta)\,\hat{\boldsymbol{r}} + t_\theta^{\text{inc}}(\theta)\,\hat{\boldsymbol{\theta}}. \tag{3.39b}$$

Substituting (3.22) in (2.16) and combining with (3.38a), we obtain explicit formulae for t_r and t_θ expressed in terms of u_r, u_θ and their derivatives:

$$t_r(\theta) = -(\lambda+2\mu)\frac{\partial u_r}{\partial r}(a,\theta) - \frac{\lambda}{a}\Big(\frac{\partial u_\theta}{\partial\theta}(a,\theta) + u_r(a,\theta)\Big), \tag{3.40a}$$

$$t_\theta(\theta) = -\mu\,\frac{\partial u_\theta}{\partial r}(a,\theta) - \frac{\mu}{a}\Big(\frac{\partial u_r}{\partial\theta}(a,\theta) - u_\theta(a,\theta)\Big). \tag{3.40b}$$

It should be observed that the formulae that express t_r^{inc} and t_θ^{inc} in function of u_r^{inc}, u_θ^{inc} and their derivatives are completely analogous. If $\boldsymbol{u}^{\text{inc}} = \boldsymbol{u}^{\text{inc}(L)}$, we obtain a surface traction vector which we denote by $\boldsymbol{t}^{\text{inc}(L)}$. Its components can be obtained by replacing (3.27) in (3.40) for $\boldsymbol{u} = \boldsymbol{u}^{\text{inc}(L)}$:

$$t_r^{\text{inc}(L)}(\theta) = -\mathrm{i}k_L\big(\lambda+\mu+\mu\cos 2(\alpha_0+\theta)\big)\,e^{\mathrm{i}k_L a\cos(\alpha_0+\theta)}, \tag{3.41a}$$

$$t_\theta^{\text{inc}(L)}(\theta) = \mathrm{i}k_L\mu\sin 2(\alpha_0+\theta)\,e^{\mathrm{i}k_L a\cos(\alpha_0+\theta)}. \tag{3.41b}$$

In analogous way, if $\boldsymbol{u}^{\text{inc}} = \boldsymbol{u}^{\text{inc}(T)}$, we obtain another surface traction vector, denoted by $\boldsymbol{t}^{\text{inc}(T)}$, whose components are obtained by replacing (3.28) in (3.40) for $\boldsymbol{u} = \boldsymbol{u}^{\text{inc}(T)}$:

$$t_r^{\text{inc}(T)}(\theta) = -\mathrm{i}k_T\mu\sin 2(\alpha_0+\theta)\,e^{\mathrm{i}k_T a\cos(\alpha_0+\theta)}, \tag{3.42a}$$

$$t_\theta^{\text{inc}(T)}(\theta) = -\mathrm{i}k_T\mu\cos 2(\alpha_0+\theta)\,e^{\mathrm{i}k_T a\cos(\alpha_0+\theta)}. \tag{3.42b}$$

In what follows, we consider a generic surface traction vector $\boldsymbol{t}^{\text{inc}}$ as the one given in (3.39b), and we make subsequently the distinction between longitudinal and transverse waves. In order to solve (3.37), the components of $\boldsymbol{t}^{\text{inc}}$ are expanded as the Fourier series

given in (3.13):

$$t_r^{\text{inc}}(\theta) = \frac{1}{2\pi}\sum_{n=-\infty}^{+\infty}\int_0^{2\pi} t_r^{\text{inc}}(\phi)\, e^{-in\phi}\mathrm{d}\phi\, e^{in\theta}, \tag{3.43a}$$

$$t_\theta^{\text{inc}}(\theta) = \frac{1}{2\pi}\sum_{n=-\infty}^{+\infty}\int_0^{2\pi} t_\theta^{\text{inc}}(\phi)\, e^{-in\phi}\mathrm{d}\phi\, e^{in\theta}. \tag{3.43b}$$

On the other hand, replacing u_r and u_θ from (3.23) in (3.40) yields the next expressions for t_r and t_θ:

$$\begin{aligned} t_r(\theta) = -\frac{\mu}{\pi}\sum_{n=-\infty}^{+\infty}\Big(&A_n k_L^2\Big(H_n^{(1)\prime\prime}(k_L a) - \frac{\lambda}{2\mu}H_n^{(1)}(k_L a)\Big) \\ &+ B_n\frac{in}{a}\Big(k_T H_n^{(1)\prime}(k_T a) - \frac{1}{a}H_n^{(1)}(k_T a)\Big)\Big)e^{in\theta}, \end{aligned} \tag{3.44a}$$

$$\begin{aligned} t_\theta(\theta) = -\frac{\mu}{\pi}\sum_{n=-\infty}^{+\infty}\Big(&A_n\frac{in}{a}\Big(k_L H_n^{(1)\prime}(k_L a) - \frac{1}{a}H_n^{(1)}(k_L a)\Big) \\ &- B_n k_T^2\Big(H_n^{(1)\prime\prime}(k_T a) + \frac{1}{2}H_n^{(1)}(k_T a)\Big)\Big)e^{in\theta}. \end{aligned} \tag{3.44b}$$

Replacing (3.43) and (3.44) in (3.37b) and separating into radial and angular components, we obtain a system of linear equations for A_n and B_n:

$$\begin{aligned} &k_L^2\Big(H_n^{(1)\prime\prime}(k_L a) - \frac{\lambda}{2\mu}H_n^{(1)}(k_L a)\Big)A_n \\ &\quad+\frac{in}{a}\Big(k_T H_n^{(1)\prime}(k_T a) - \frac{1}{a}H_n^{(1)}(k_T a)\Big)B_n = -J_{r,n}, \end{aligned} \tag{3.45a}$$

$$\begin{aligned} &\frac{in}{a}\Big(k_L H_n^{(1)\prime}(k_L a) - \frac{1}{a}H_n^{(1)}(k_L a)\Big)A_n \\ &\quad-k_T^2\Big(H_n^{(1)\prime\prime}(k_T a) + \frac{1}{2}H_n^{(1)}(k_T a)\Big)B_n = -J_{\theta,n}, \end{aligned} \tag{3.45b}$$

where

$$J_{r,n} = \frac{1}{2\mu}\int_0^{2\pi} t_r^{\text{inc}}(\phi)\, e^{-in\phi}\mathrm{d}\phi, \tag{3.46a}$$

$$J_{\theta,n} = \frac{1}{2\mu}\int_0^{2\pi} t_\theta^{\text{inc}}(\phi)\, e^{-in\phi}\mathrm{d}\phi. \tag{3.46b}$$

By solving this system, we obtain the coefficients A_n and B_n:

$$\begin{aligned} A_n = \frac{1}{2\mu\epsilon_n}\Big(&k_T^2\Big(H_n^{(1)\prime\prime}(k_T a) + \frac{1}{2}H_n^{(1)}(k_T a)\Big)J_{r,n} \\ &+ \frac{in}{a}\Big(k_T H_n^{(1)\prime}(k_T a) - \frac{1}{a}H_n^{(1)}(k_T a)\Big)J_{\theta,n}\Big), \end{aligned} \tag{3.47a}$$

$$B_n = \frac{1}{2\mu\epsilon_n}\Big(\Big(k_L H_n^{(1)\prime}(k_L a) - \frac{1}{a}H_n^{(1)}(k_L a)\Big)J_{r,n} - k_L^2\Big(H_n^{(1)\prime\prime}(k_L a) - \frac{\lambda}{2\mu}H_n^{(1)}(k_L a)\Big)J_{\theta,n}\Big). \tag{3.47b}$$

where

$$\begin{aligned}\epsilon_n = &- k_L^2 k_T^2\Big(H_n^{(1)\prime\prime}(k_L a) - \frac{\lambda}{2\mu}H_n^{(1)}(k_L a)\Big)\Big(H_n^{(1)\prime\prime}(k_T a) + \frac{1}{2}H_n^{(1)}(k_T a)\Big)\\ &+ \frac{n^2}{a^2}\Big(k_L H_n^{(1)\prime}(k_L a) - \frac{1}{a}H_n^{(1)}(k_L a)\Big)\Big(k_T H_n^{(1)\prime}(k_T a) - \frac{1}{a}H_n^{(1)}(k_T a)\Big).\end{aligned} \tag{3.48}$$

If $\boldsymbol{u}^{\text{inc}} = \boldsymbol{u}^{\text{inc}(L)}$, it is possible to make these integrals explicit by replacing (3.41) in (3.46):

$$J_{r,n} = -\frac{\mathrm{i}k_L}{2}\int_0^{2\pi}\big(1 + \lambda/\mu + \cos 2(\alpha_0 + \phi)\big)\, e^{\mathrm{i}(k_L a\cos(\alpha_0+\phi) - n\phi)}\mathrm{d}\phi, \tag{3.49a}$$

$$J_{\theta,n} = \frac{\mathrm{i}k_L}{2}\int_0^{2\pi}\sin 2(\alpha_0 + \phi)\, e^{\mathrm{i}(k_L a\cos(\alpha_0+\phi) - n\phi)}\mathrm{d}\phi. \tag{3.49b}$$

Analogously, if $\boldsymbol{u}^{\text{inc}} = \boldsymbol{u}^{\text{inc}(T)}$, we reexpress explicitly $I_n^{(T)}$ and $I_n^{(L)}$ by replacing (3.42) in (3.46):

$$J_{r,n} = -\frac{\mathrm{i}k_T}{2}\int_0^{2\pi}\sin 2(\alpha_0 + \phi)\, e^{\mathrm{i}(k_T a\cos(\alpha_0+\phi) - n\phi)}\mathrm{d}\phi, \tag{3.50a}$$

$$J_{\theta,n} = -\frac{\mathrm{i}k_T}{2}\int_0^{2\pi}\cos 2(\alpha_0 + \phi)\, e^{\mathrm{i}(k_T a\cos(\alpha_0+\phi) - n\phi)}\mathrm{d}\phi. \tag{3.50b}$$

Therefore, substituting A_n and B_n from (3.47) in the general solution $\boldsymbol{u}$ given in (3.22)-(3.23) yields an explicit solution to the Neumann boundary-value problem (3.37).

3.3 Dirichlet-to-Neumann (DtN) map for an exterior domain

3.3.1 Artificial boundary and definition of the DtN map

Next, we introduce the Dirichlet-to-Neumann (DtN) map as a mathematical tool that yields exact nonreflecting boundary conditions for time-harmonic elastic waves, thus providing a numerical approach to solve scattering problems in exterior domains. Let us suppose that we desire to find the scattered field from a bounded obstacle Ω^{int} with arbitrary shape. The corresponding exterior domain is defined as $\Omega^{\text{ext}} = \mathbb{R}^2\backslash\overline{\Omega^{\text{int}}}$. Moreover, we denote by Γ the boundary and by $\boldsymbol{n}$ the unit normal vector, as indicated in Fig. 3.3. The boundary-value problem describing this phenomenon is written as: Find $\boldsymbol{u} : \Omega^{\text{ext}} \to \mathbb{C}^2$ such that

$$\operatorname{div}\sigma(\boldsymbol{u})(\boldsymbol{x}) + \rho\omega^2\boldsymbol{u}(\boldsymbol{x}) = \boldsymbol{0} \qquad \text{in } \Omega^{\text{ext}}, \tag{3.51a}$$

$$\sigma(\boldsymbol{u}(\boldsymbol{x}))\boldsymbol{n} = \boldsymbol{f}(\boldsymbol{x}) \qquad \text{on } \Gamma, \tag{3.51b}$$

$$\begin{aligned}\big|\big(\sigma(\boldsymbol{u}(\boldsymbol{x}))\hat{\boldsymbol{r}} - \mathrm{i}k_L(\lambda + 2\mu)\,\boldsymbol{u}(\boldsymbol{x})\big)\cdot\hat{\boldsymbol{r}}\,\big| &= O(r^{-1})\\ \big|\big(\sigma(\boldsymbol{u}(\boldsymbol{x}))\hat{\boldsymbol{r}} - \mathrm{i}k_T\mu\,\boldsymbol{u}(\boldsymbol{x})\big)\cdot\hat{\boldsymbol{\theta}}\,\big| &= O(r^{-1})\end{aligned} \qquad \text{as } r \to +\infty, \tag{3.51c}$$

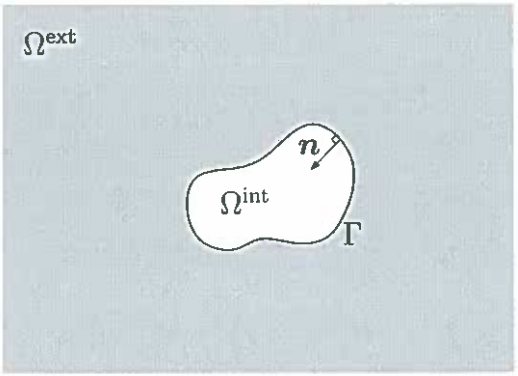

FIGURE 3.3. Arbitrarily shaped bounded obstacle in an infinite elastic medium.

where the right-hand side function $\boldsymbol{f}$ is related to the incident field, assumed to be given. Notice that the Neumann boundary conditions have been specified on Γ for the sake of simplicity, but Dirichlet boundary conditions could have been considered as well. In order to restrict the analysis to a finite domain, we introduce an artificial boundary that truncates the unbounded exterior domain. This boundary corresponds to the circumference S_R of radius R centered at the origin. The exterior domain Ω^{ext} is then divided into two subdomains, namely a bounded subdomain $\Omega_R^{\text{int}} = B_R \backslash \overline{\Omega^{\text{int}}}$ and an unbounded subdomain $\Omega_R^{\text{ext}} = \mathbb{R}^2 \backslash \overline{B_R}$. The radius R has to be chosen sufficiently large, in such a way that $\overline{\Omega^{\text{int}}} \subset B_R$, as indicated in Fig. 3.4. After that, we establish a bounded boundary-value

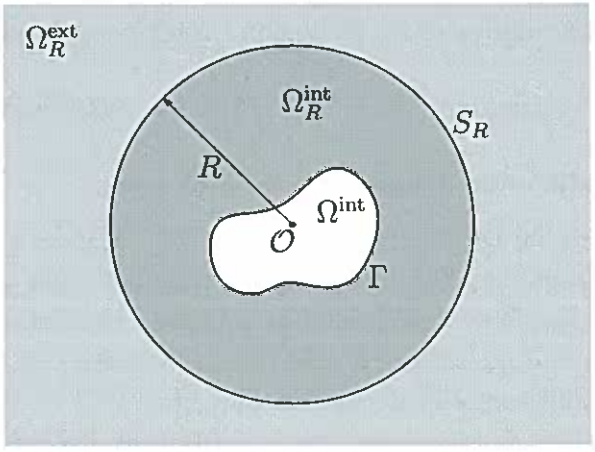

FIGURE 3.4. Infinite elastic domain truncated by a circumference of radius R.

problem: Find $\boldsymbol{u} : \Omega_R^{\text{int}} \to \mathbb{C}^2$ such that

$$\operatorname{div} \sigma(\boldsymbol{u}(\boldsymbol{x})) + \rho\omega^2 \boldsymbol{u}(\boldsymbol{x}) = \boldsymbol{0} \qquad \text{in } \Omega_R^{\text{int}}, \tag{3.52a}$$

$$\sigma(\boldsymbol{u}(\boldsymbol{x}))\boldsymbol{n} = \boldsymbol{f}(\boldsymbol{x}) \qquad \text{on } \Gamma, \tag{3.52b}$$

$$\sigma(\boldsymbol{u}(\boldsymbol{x}))\boldsymbol{n} = \sigma(\boldsymbol{U}(\boldsymbol{x}))\hat{\boldsymbol{r}} \qquad \text{on } S_R, \tag{3.52c}$$

and an unbounded boundary-value problem: Find $\boldsymbol{U} : \Omega_R^{\text{ext}} \to \mathbb{C}^2$ such that

$$\begin{aligned}
\operatorname{div}\sigma(\boldsymbol{U}(r,\theta)) + \rho\omega^2\boldsymbol{U}(r,\theta) &= \boldsymbol{0} && \text{in } \Omega_R^{\text{ext}}, && \text{(3.53a)}\\
\boldsymbol{U}(R,\theta) &= \boldsymbol{u}(R,\theta) && \theta \in [0,2\pi], && \text{(3.53b)}\\
\left|\left(\sigma(\boldsymbol{U}(r,\theta))\hat{\boldsymbol{r}} - \mathrm{i}k_L(\lambda+2\mu)\,\boldsymbol{U}(r,\theta)\right)\cdot\hat{\boldsymbol{r}}\right| &= O(r^{-1}) && \text{as } r \to +\infty, && \text{(3.53c)}\\
\left|\left(\sigma(\boldsymbol{U}(r,\theta))\hat{\boldsymbol{r}} - \mathrm{i}k_T\mu\,\boldsymbol{U}(r,\theta)\right)\cdot\hat{\boldsymbol{\theta}}\right| &= O(r^{-1}) && && \text{(3.53c)}
\end{aligned}$$

and the DtN map is defined as indicated next:

$$\begin{aligned}
\boldsymbol{\mathcal{T}}_\omega : [H^{1/2}(S_R)]^2 &\longrightarrow [H^{-1/2}(S_R)]^2\\
\boldsymbol{u} &\longrightarrow \boldsymbol{\mathcal{T}}_\omega\boldsymbol{u} = \sigma(\boldsymbol{U})\hat{\boldsymbol{r}}\big|_{S_R}.
\end{aligned} \tag{3.54}$$

In the next subsection, we determine an explicit formula for this map.

3.3.2 Explicit expression as an infinite series

In order to explicitly determine $\boldsymbol{\mathcal{T}}_\omega$, we solve (3.53) analytically. This is feasible, because the domain is the exterior of a circle. The components of the solution to (3.53a) in polar coordinates are computed as made in Section 3.2:

$$U_r(r,\theta) = \frac{1}{2\pi}\sum_{n=-\infty}^{+\infty}\left(k_L H_n^{(1)\prime}(k_L r)A_n + \frac{\mathrm{i}n}{r}H_n^{(1)}(k_T r)\,B_n\right)e^{\mathrm{i}n\theta}, \tag{3.55a}$$

$$U_\theta(r,\theta) = \frac{1}{2\pi}\sum_{n=-\infty}^{+\infty}\left(\frac{\mathrm{i}n}{r}H_n^{(1)}(k_L r)\,A_n - k_T H_n^{(1)\prime}(k_T r)B_n\right)e^{\mathrm{i}n\theta}. \tag{3.55b}$$

Evaluating this solution at $r = R$ yields

$$U_r(R,\theta) = \frac{1}{2\pi}\sum_{n=-\infty}^{+\infty}\left(k_L H_n^{(1)\prime}(k_L R)A_n + \frac{\mathrm{i}n}{R}H_n^{(1)}(k_T R)\,B_n\right)e^{\mathrm{i}n\theta}, \tag{3.56a}$$

$$U_\theta(R,\theta) = \frac{1}{2\pi}\sum_{n=-\infty}^{+\infty}\left(\frac{\mathrm{i}n}{R}H_n^{(1)}(k_L R)\,A_n - k_T H_n^{(1)\prime}(k_T R)B_n\right)e^{\mathrm{i}n\theta}. \tag{3.56b}$$

On the other hand, the components of the solution $\boldsymbol{u}$ to (3.52) are evaluated at $r = R$ and expanded as Fourier series, as given in (3.13):

$$u_r(R,\theta) = \frac{1}{2\pi}\sum_{n=-\infty}^{+\infty}\int_0^{2\pi} u_r(R,\phi)\,e^{-\mathrm{i}n\phi}\mathrm{d}\phi\; e^{\mathrm{i}n\theta} \tag{3.57a}$$

$$u_\theta(R,\theta) = \frac{1}{2\pi}\sum_{n=-\infty}^{+\infty}\int_0^{2\pi} u_\theta(R,\phi)\,e^{-\mathrm{i}n\phi}\mathrm{d}\phi\; e^{\mathrm{i}n\theta} \tag{3.57b}$$

Therefore, replacing (3.56) and (3.57) in (3.53b) and separating into components, we obtain a system of linear equations for A_n and B_n:

$$k_L H_n^{(1)\prime}(k_L R)A_n + \frac{\mathrm{i}n}{R}H_n^{(1)}(k_T R)B_n = \int_0^{2\pi} u_r(R,\phi)\,e^{-\mathrm{i}n\phi}\mathrm{d}\phi, \tag{3.58a}$$

$$\frac{\mathrm{i}n}{R}H_n^{(1)}(k_L R)A_n - k_T H_n^{(1)\prime}(k_T R)B_n = \int_0^{2\pi} u_\theta(R,\phi)\,e^{-\mathrm{i}n\phi}\mathrm{d}\phi. \tag{3.58b}$$

The solution is given by

$$A_n = -\frac{1}{\delta_n}\Big(k_T H_n^{(1)\prime}(k_T R)\int_0^{2\pi} u_r(R,\phi)\,e^{-in\phi}\mathrm{d}\phi + \frac{in}{R}H_n^{(1)}(k_T R)\int_0^{2\pi} u_\theta(R,\phi)\,e^{-in\phi}\mathrm{d}\phi\Big), \tag{3.59a}$$

$$B_n = -\frac{1}{\delta_n}\Big(\frac{in}{R}H_n^{(1)}(k_L R)\int_0^{2\pi} u_r(R,\phi)\,e^{-in\phi}\mathrm{d}\phi - k_L H_n^{(1)\prime}(k_L R)\int_0^{2\pi} u_\theta(R,\phi)\,e^{-in\phi}\mathrm{d}\phi\Big). \tag{3.59b}$$

where

$$\delta_n = \frac{n^2}{R^2}H_n^{(1)}(k_L R)H_n^{(1)}(k_T R) - k_L k_T H_n^{(1)\prime}(k_L R)H_n^{(1)\prime}(k_T R). \tag{3.60}$$

Consequently, substitution of A_n and B_n from (3.59) in (3.55) yields the solution of (3.53). From the definition of the DtN map given in (3.54), it is immediate that its components in polar coordinates are obtained from formulae analogous to (3.40):

$$\big(\boldsymbol{\mathcal{T}}_\omega \boldsymbol{u}\big)_r(\theta) = (\lambda+2\mu)\frac{\partial U_r}{\partial r}(R,\theta) + \frac{\lambda}{R}\Big(\frac{\partial U_\theta}{\partial\theta}(R,\theta) + U_r(R,\theta)\Big), \tag{3.61a}$$

$$\big(\boldsymbol{\mathcal{T}}_\omega \boldsymbol{u}\big)_\theta(\theta) = \mu\frac{\partial U_\theta}{\partial r}(R,\theta) + \frac{\mu}{R}\Big(\frac{\partial U_r}{\partial\theta}(R,\theta) - U_\theta(R,\theta)\Big). \tag{3.61b}$$

Replacing (3.55) in (3.61), we have that the components of the DtN map are

$$\big(\boldsymbol{\mathcal{T}}_\omega \boldsymbol{u}\big)_r(\theta) = \frac{\mu}{\pi}\sum_{n=-\infty}^{+\infty}\Big(k_L^2\Big(H_n^{(1)\prime\prime}(k_L R) - \frac{\lambda}{2\mu}H_n^{(1)}(k_L R)\Big)A_n + \frac{in}{R}\Big(k_T H_n^{(1)\prime}(k_T R) - \frac{1}{R}H_n^{(1)}(k_T R)\Big)B_n\Big)e^{in\theta}, \tag{3.62a}$$

$$\big(\boldsymbol{\mathcal{T}}_\omega \boldsymbol{u}\big)_\theta(\theta) = \frac{\mu}{\pi}\sum_{n=-\infty}^{+\infty}\Big(\frac{in}{R}\Big(k_L H_n^{(1)\prime}(k_L R) - \frac{1}{R}H_n^{(1)}(k_L R)\Big)A_n - k_T^2\Big(H_n^{(1)\prime\prime}(k_T R) + \frac{1}{2}H_n^{(1)}(k_T R)\Big)B_n\Big)e^{in\theta}, \tag{3.62b}$$

and to make explicit the dependance of $\boldsymbol{\mathcal{T}}_\omega$ on $\boldsymbol{u}$, we substitute A_n and B_n from (3.59):

$$\big(\boldsymbol{\mathcal{T}}_\omega \boldsymbol{u}\big)_r(\theta) = -\frac{\mu}{\pi}\sum_{n=-\infty}^{+\infty}\frac{1}{\delta_n}\int_0^{2\pi}\big(q_n^{rr}u_r(R,\phi) + q_n^{r\theta}u_\theta(R,\phi)\big)e^{-in(\phi-\theta)}\mathrm{d}\phi, \tag{3.63a}$$

$$\big(\boldsymbol{\mathcal{T}}_\omega \boldsymbol{u}\big)_\theta(\theta) = \frac{\mu}{\pi}\sum_{n=-\infty}^{+\infty}\frac{1}{\delta_n}\int_0^{2\pi}\big(q_n^{r\theta}u_r(R,\phi) - q_n^{\theta\theta}u_\theta(R,\phi)\big)e^{-in(\phi-\theta)}\mathrm{d}\phi, \tag{3.63b}$$

where

$$q_n^{rr} = k_T R H_n^{(1)\prime}(k_T R)\Big(k_L^2 H_n^{(1)\prime\prime}(k_L R) - \Big(\frac{k_T^2}{2} - k_L^2 + \frac{n^2}{R^2}\Big)H_n^{(1)}(k_L R)\Big) + \frac{n^2}{R^2}H_n^{(1)}(k_L R)H_n^{(1)}(k_T R), \tag{3.64a}$$

$$q_n^{r\theta} = ink_T\Big(k_T\Big(H_n^{(1)\prime\prime}(k_TR) + \frac{1}{2}H_n^{(1)}(k_TR)\Big) - H_n^{(1)\prime}(k_TR)\Big(k_LH_n^{(1)\prime}(k_LR) - \frac{1}{R}H_n^{(1)}(k_LR)\Big)\Big), \tag{3.64b}$$

$$q_n^{\theta\theta} = k_LRH_n^{(1)\prime}(k_LR)\Big(k_T^2H_n^{(1)\prime\prime}(k_TR) - \Big(\frac{n^2}{R^2} - \frac{k_T^2}{2}\Big)H_n^{(1)}(k_TR)\Big) + \frac{n^2}{R^2}H_n^{(1)}(k_LR)H_n^{(1)}(k_TR). \tag{3.64c}$$

Expression (3.63) corresponds to an explicit formula for the DtN map, represented as an infinite series of integral terms. Employing the DtN map, the boundary-value problem (3.51) can be conveniently restated as: Find $\boldsymbol{u} : \Omega_R^{\text{int}} \to \mathbb{C}^2$ such that

$$\operatorname{div}\sigma(\boldsymbol{u}(\boldsymbol{x})) + \rho\omega^2\boldsymbol{u}(\boldsymbol{x}) = \boldsymbol{0} \qquad \text{in } \Omega_R^{\text{int}}, \tag{3.65a}$$

$$\sigma(\boldsymbol{u}(\boldsymbol{x}))\boldsymbol{n} = \boldsymbol{f}(\boldsymbol{x}) \qquad \text{on } \Gamma, \tag{3.65b}$$

$$\sigma(\boldsymbol{u}(\boldsymbol{x}))\boldsymbol{n} = \boldsymbol{\mathcal{T}}_\omega\boldsymbol{u}(\boldsymbol{x}) \qquad \text{on } S_R. \tag{3.65c}$$

This is a Neumann boundary-value problem posed in a bounded domain, where the influence of the exterior is stored within the DtN map. Therefore, (3.65c) corresponds to an exact nonreflecting boundary condition for elastic waves. From a mathematical point of view, this is a non-local boundary condition of the Neumann-type, with the difficulty that the right-hand side is not a known function but involves the solution $\boldsymbol{u}$.

3.3.3 Galerkin approximation of the DtN term

In order to obtain a Galerkin approximation of (3.65), we state the following variational formulation: Find $\boldsymbol{u} \in [H^1(\Omega_R^{\text{int}})]^2$ such that

$$\int_{\Omega_R^{\text{int}}}\sigma(\boldsymbol{u}(\boldsymbol{x})) : \varepsilon(\boldsymbol{v}(\boldsymbol{x}))\mathrm{d}\boldsymbol{x} - \rho\omega^2\int_{\Omega_R^{\text{int}}}\boldsymbol{u}(\boldsymbol{x})\cdot\boldsymbol{v}(\boldsymbol{x})\mathrm{d}\boldsymbol{x} - \int_{S_R}\boldsymbol{\mathcal{T}}_\omega\boldsymbol{u}(\boldsymbol{x})\cdot\boldsymbol{v}(\boldsymbol{x})\mathrm{d}s(\boldsymbol{x}) = \int_\Gamma\boldsymbol{f}(\boldsymbol{x})\cdot\boldsymbol{v}(\boldsymbol{x})\mathrm{d}s(\boldsymbol{x}), \qquad \forall\boldsymbol{v} \in [H^1(\Omega_R^{\text{int}})]^2. \tag{3.66}$$

The approximation of the two volume integrals and the right-hand side is standard. It can be found, e.g., in Ciarlet (1978), Raviart & Thomas (1983), or Zienkiewicz (2000), in the context of finite element methods. However, the approximation of the integral containing the DtN map is not commonly found in books of this type, so we concentrate our attention on this term. An expression in polar coordinates for the DtN map as (3.63), even though it is right, is not very useful for practical purposes. If one desires to make numerical calculations, an expression in cartesian coordinates is necessary, because it can be directly implemented in a computational code. Thus, we make a conversion of coordinates in (3.63). If the displacement $\boldsymbol{u}$ is expressed in cartesian coordinates as

$$\boldsymbol{u}(\boldsymbol{x}) = u_1(\boldsymbol{x})\,\hat{\boldsymbol{e}}_1 + u_2(\boldsymbol{x})\,\hat{\boldsymbol{e}}_2, \tag{3.67}$$

then the polar components u_r and u_θ can be obtained from the cartesian coordinates u_1 and u_2 by means of the relations

$$u_r(r,\theta) = u_1(x_1,x_2)\cos\theta + u_2(x_1,x_2)\sin\theta, \tag{3.68a}$$

$$u_\theta(r,\theta) = -u_1(x_1,x_2)\sin\theta + u_2(x_1,x_2)\cos\theta. \tag{3.68b}$$

Moreover, let us recall that the unit vectors $\hat{\boldsymbol{r}}$ and $\hat{\boldsymbol{\theta}}$ are defined as

$$\hat{\boldsymbol{r}} = \cos\theta\,\hat{\boldsymbol{e}}_1 + \sin\theta\,\hat{\boldsymbol{e}}_2, \qquad \hat{\boldsymbol{\theta}} = -\sin\theta\,\hat{\boldsymbol{e}}_1 + \cos\theta\,\hat{\boldsymbol{e}}_2. \tag{3.69}$$

Replacing (3.68) and (3.69) in (3.63) and expanding in an appropriate way, we obtain that the DtN map can be written as follows:

$$\boldsymbol{\mathcal{T}}_\omega \boldsymbol{u}(\theta) = \frac{\mu}{\pi R}\sum_{n=-\infty}^{+\infty}\frac{1}{\delta_n}\int_0^{2\pi} Q_n(\theta,\phi)\boldsymbol{u}(R,\phi)\,e^{-\mathrm{i}n(\phi-\theta)}\,\mathrm{d}\phi, \tag{3.70}$$

where Q_n is the matrix defined by

$$Q_n(\theta,\phi) = \begin{bmatrix} \cos\theta & -\sin\theta \\ \sin\theta & \cos\theta \end{bmatrix}\begin{bmatrix} q_n^{rr} & q_n^{r\theta} \\ -q_n^{r\theta} & q_n^{\theta\theta} \end{bmatrix}\begin{bmatrix} \cos\phi & \sin\phi \\ -\sin\phi & \cos\phi \end{bmatrix}, \tag{3.71}$$

and the coefficients q_n^{rr}, $q_n^{r\theta}$, and $q_n^{\theta\theta}$ are given in (3.64). Consequently, the term appearing in (3.66) and involving the DtN map corresponds to the following series of double integrals:

$$\int_{S_R}\boldsymbol{\mathcal{T}}_\omega\boldsymbol{u}(\boldsymbol{x})\cdot\boldsymbol{v}(\boldsymbol{x})\mathrm{d}s(\boldsymbol{x}) = \frac{\mu}{\pi}\sum_{n=-\infty}^{+\infty}\frac{1}{\delta_n}\int_0^{2\pi}\int_0^{2\pi} Q_n(\theta,\phi)\boldsymbol{u}(R,\phi)\cdot\boldsymbol{v}(R,\theta)\,e^{-\mathrm{i}n(\phi-\theta)}\,\mathrm{d}\phi\,\mathrm{d}\theta. \tag{3.72}$$

Let us consider a Galerkin approximation of (3.66), for which we define a vector subspace $V_h \subset H^1(\Omega_R^{\mathrm{int}})$ of finite dimension N_h and an orthogonal basis of V_h, denoted by $\{\varphi_j\}_{j=1}^{N_h}$. The space $[H^1(\Omega_R^{\mathrm{int}})]^2$ is thus approximated by V_h^2, whose basis is given by $\{\varphi_j\hat{\boldsymbol{e}}_1, \varphi_j\hat{\boldsymbol{e}}_2\}_{j=1}^{N_h}$. Furthermore, in order to implement the DtN map, the series in (3.72) is truncated at some sufficiently large positive number $N_t \in \mathbb{N}$. The term of the DtN map has an associated matrix which we call the matrix of transparency, defined by blocks as

$$T = \begin{bmatrix} T_{11} & T_{12} \\ T_{21} & T_{22} \end{bmatrix}, \tag{3.73}$$

where

$$\big[T_{k\ell}\big]_{ij} = \int_{S_R}\varphi_i\hat{\boldsymbol{e}}_k\cdot\boldsymbol{\mathcal{T}}_\omega\varphi_j\hat{\boldsymbol{e}}_\ell\,\mathrm{d}s, \qquad k,\ell = 1,2. \tag{3.74}$$

Combining this expression with (3.72) yields

$$\big[T_{k\ell}\big]_{ij} = \frac{\mu}{\pi R^2}\sum_{n=-N_t}^{N_t}\frac{1}{\delta_n}\int_0^{2\pi}\int_0^{2\pi} Q_n(\theta,\phi)\hat{\boldsymbol{e}}_\ell\cdot\hat{\boldsymbol{e}}_k\,\varphi_i(R,\theta)\varphi_j(R,\phi)e^{-\mathrm{i}n(\phi-\theta)}\,\mathrm{d}\phi\,\mathrm{d}\theta. \tag{3.75}$$

Hence, replacing Q_n from (3.71) and expanding the matrix product gives the following expressions for each block:

$$\left[T_{11}\right]_{ij} = \frac{\mu}{\pi} \sum_{n=-N_t}^{N_t} \frac{1}{\delta_n} \Big(q_n^{rr} I_{i,n} I_{j,-n} - q_n^{r\theta} \big(I_{i,n} J_{j,-n} - J_{i,n} I_{j,-n} \big) + q_n^{\theta\theta} J_{i,n} J_{j,-n} \Big), \quad (3.76a)$$

$$\left[T_{12}\right]_{ij} = \frac{\mu}{\pi} \sum_{n=-N_t}^{N_t} \frac{1}{\delta_n} \Big(q_n^{rr} I_{i,n} J_{j,-n} + q_n^{r\theta} \big(I_{i,n} I_{j,-n} + J_{i,n} J_{j,-n} \big) - q_n^{\theta\theta} J_{i,n} I_{j,-n} \Big), \quad (3.76b)$$

$$\left[T_{21}\right]_{ij} = \frac{\mu}{\pi} \sum_{n=-N_t}^{N_t} \frac{1}{\delta_n} \Big(q_n^{rr} J_{i,n} I_{j,-n} - q_n^{r\theta} \big(I_{i,n} I_{j,-n} + J_{i,n} J_{j,-n} \big) - q_n^{\theta\theta} I_{i,n} J_{j,-n} \Big), \quad (3.76c)$$

$$\left[T_{22}\right]_{ij} = \frac{\mu}{\pi} \sum_{n=-N_t}^{N_t} \frac{1}{\delta_n} \Big(q_n^{rr} J_{i,n} J_{j,-n} - q_n^{r\theta} \big(I_{i,n} J_{j,-n} - J_{i,n} I_{j,-n} \big) + q_n^{\theta\theta} I_{i,n} I_{j,-n} \Big), \quad (3.76d)$$

where for each $i = 1, \ldots, N_h$ and $n \in \mathbb{Z}$, $I_{i,n}$ and $J_{i,n}$ are the following integrals:

$$I_{i,n} = \int_0^{2\pi} \varphi_i(R, \theta) \cos\theta \, e^{in\theta} \mathrm{d}\theta, \quad (3.77a)$$

$$J_{i,n} = \int_0^{2\pi} \varphi_i(R, \theta) \sin\theta \, e^{in\theta} \mathrm{d}\theta. \quad (3.77b)$$

IV. INTEGRAL REPRESENTATIONS AND INTEGRAL EQUATIONS

4.1 Introduction

This chapter is concerned with the integral representation formulae and integral equations to solve the scattering problems introduced in Chapter II. The cases of an exterior domain and a locally perturbed half-plane are separately considered. The integral representations are developed for a transmission problem, which is defined in the entire domain (that is, either the full-plane $\mathbb{R}^2$ or the half-plane $\mathbb{R}^2_+$), and jump conditions are specified on the boundary that separates the unbounded part from the bounded part of the domain. A detailed study of analogous representations for acoustic waves can be found in Nédélec (2001) or Abboud & Terrasse (2006), where integral representation theorems are stated for the solution of the Helmholtz equation at the exterior and the interior of a closed and bounded surface in $\mathbb{R}^3$. An essential issue of the integral representations and equations is the Green's function. In the case of an exterior domain, we obtain the explicit expression of the elastodynamic fundamental solution, and we prove that it satisfies the radiation conditions introduced in Section 2.3. This fundamental solution provides directly the full-plane Green's function, which is exhaustively used while obtaining the integral representations. In the case of a perturbed half-plane, we do not have the explicit form of the half-plane Green's function, but it is well-known that it can be expressed as the sum of the full-plane Green's function and an additional regular term. This fact, together with some suitable assumptions, allows us to deduce the integral representations on the perturbed boundary, and the additional term of the half-plane Green's function is subsequently calculated in Chapter VI. The integral equations for each scattering problem are developed by extending appropriately the respective unbounded boundary-value problem to the bounded domain, which leads to retrieve a transmission problem, where the integral representation formulae are applicable. The boundary element method corresponds to the discrete version of the integral equation method, and it is studied in the next chapter. Throughout this chapter, the equations of elasticity are expressed in tensorial notation, rather than with vectors.

4.2 Exterior scattering

4.2.1 Fundamental solution and full-plane Green's function

Let us write the time-harmonic elastic wave equation (2.15) in tensor notation:

$$\sigma_{ij,j}(\boldsymbol{x}) + \rho\omega^2 u_i(\boldsymbol{x}) = 0, \tag{4.1}$$

where according to Einstein's summation convention, an index appearing twice on one side of the equation (as the case of j in (4.1)) is automatically summed over all of its possible values. The Hooke's law (2.16) is written in tensor notation as

$$\sigma_{ij}(\boldsymbol{x}) = \lambda u_{\ell,\ell}(\boldsymbol{x})\delta_{ij} + \mu(u_{i,j}(\boldsymbol{x}) + u_{j,i}(\boldsymbol{x})). \tag{4.2}$$

Any boundary integral method to solve an exterior boundary-value problem requires the knowledge of the fundamental solution associated with the underlying partial differential operator. In general, a fundamental solution satisfies the partial differential equation in the sense of distributions, with a Dirac's delta distribution applied at the origin as the right-hand side. In our case, as we are dealing with a vector partial differential equation, the fundamental solution corresponds to a second-order tensor, which takes into account that the Dirac's delta distribution can be applied in the horizontal and the vertical sense. Furthermore, because of the radial symmetry, we assume that the fundamental solution depends on $\boldsymbol{x}$ through $r = |\boldsymbol{x}|$. Let us denote the fundamental solution by U, which satisfies

$$-\big(\Sigma^k_{ij,j}(r) + \rho\omega^2 U^k_i(r)\big) = \delta_{ik}\delta_0(r), \tag{4.3}$$

where Σ is the third-order tensor defined as

$$\Sigma^k_{ij}(r) = \lambda U^k_{\ell,\ell}(r)\delta_{ij} + \mu\big(U^k_{i,j}(r) + U^k_{j,i}(r)\big), \tag{4.4}$$

and δ_0 denotes the Dirac's delta distribution applied at the origin. The notation δ_{ik} stands for the Kronecker's delta. Substitution of (4.4) in (4.3) yields

$$-\big(\mu U^k_{i,jj}(r) + (\lambda+\mu)U^k_{j,ij}(r) + \rho\omega^2 U^k_i(r)\big) = \delta_{ik}\delta_0(r). \tag{4.5}$$

To solve (4.5), we use Galerkin's vectors in order to express the fundamental solution U. A Galerkin's vector is a general displacement potential commonly used in static elasticity (cf. Brebbia & Domínguez 1989, Katsikadelis 2002). In our case, we adapt this technique to time-harmonic elasticity. Moreover, we have two Galerkin's vectors that constitute a second-order tensor denoted by V. The expression for U in terms of V is given by

$$U^k_i(r) = \frac{1}{\mu}\Big(V^k_{i,\ell\ell}(r) - \frac{\lambda+\mu}{\lambda+2\mu}V^k_{\ell,i\ell}(r) + \frac{\rho\omega^2}{\lambda+2\mu}V^k_i(r)\Big). \tag{4.6}$$

Replacing (4.6) in (4.5) and expanding yields the equation

$$-\Big(V^k_{i,jj\ell\ell}(r) + \frac{\rho\omega^2}{\lambda+2\mu}V^k_{i,jj}(r) + \frac{\rho\omega^2}{\mu}V^k_{i,\ell\ell}(r) + \frac{(\rho\omega^2)^2}{\mu(\lambda+2\mu)}V^k_i(r)\Big) = \delta_{ik}\delta_0(r),$$

which is a fourth-order partial differential equation in V. Notice that this equation can also be expressed in terms of Laplacian and wave numbers k_L and k_T defined in (2.21):

$$-\big(\triangle^2 V^k_i(r) + k_L^2\,\triangle V^k_i(r) + k_T^2\,\triangle V^k_i(r) + k_L^2 k_T^2\,V^k_i(r)\big) = \delta_{ik}\delta_0(r),$$

or equivalently,

$$-\big(\triangle + k_T^2\big)\big(\triangle + k_L^2\big)V^k_i(r) = \delta_{ik}\delta_0(r), \tag{4.7}$$

and we look for a tensor V in the form of a scalar function v, that is,

$$V^k_i(r) = v(r)\delta_{ik}. \tag{4.8}$$

Thus, replacing (4.8) in (4.7) gives

$$-\big(\triangle + k_T^2\big)\big(\triangle + k_L^2\big)v(r) = \delta_0(r), \tag{4.9}$$

and defining the scalar function w by

$$w(r) = \big(\triangle + k_L^2\big)v(r), \tag{4.10}$$

it is possible to restate (4.9) as

$$-\big(\triangle + k_T^2\big)w(r) = \delta_0(r).$$

Consequently, w corresponds to the outgoing fundamental solution of the two-dimensional Helmholtz operator associated with the transverse wave number k_T. This fundamental solution is well-known. It can be found, e.g., in Bonnet (1995), Nédélec (2001), Lenoir (2005) or Beer, Smith & Duenser (2008). The scalar function w is thus given by

$$w(r) = \frac{\mathrm{i}}{4}H_0^{(1)}(k_T r). \tag{4.11}$$

Substituting (4.11) in (4.10), we obtain that v is a solution to an inhomogeneous Helmholtz equation:

$$\big(\triangle + k_L^2\big)v(r) = \frac{\mathrm{i}}{4}H_0^{(1)}(k_T r),$$

which can be rewritten as an ordinary differential equation in v by expanding the Laplacian in the radial variable:

$$\frac{1}{r}\frac{\mathrm{d}}{\mathrm{d}r}\left(r\,\frac{\mathrm{d}v}{\mathrm{d}r}(r)\right) + k_L^2\,v(r) = \frac{\mathrm{i}}{4}H_0^{(1)}(k_T r). \tag{4.12}$$

On the other hand, it should be observed that the order of application of the Helmholtz operators in (4.9) was arbitrarily chosen, so it can be inverted. Hence, v also satisfies

$$-\big(\triangle + k_L^2\big)\big(\triangle + k_T^2\big)v(r) = \delta_0(r),$$

and proceeding analogously as before, we obtain that v is also a solution of the ordinary differential equation

$$\frac{1}{r}\frac{\mathrm{d}}{\mathrm{d}r}\left(r\,\frac{\mathrm{d}v}{\mathrm{d}r}(r)\right) + k_T^2\,v(r) = \frac{\mathrm{i}}{4}H_0^{(1)}(k_L r). \tag{4.13}$$

Hence, combining (4.12) and (4.13), it is possible to determine v without needing to solve any differential equation. It is given by

$$v(r) = \frac{\mathrm{i}}{4(k_L^2 - k_T^2)}\big(H_0^{(1)}(k_T r) - H_0^{(1)}(k_L r)\big). \tag{4.14}$$

Prior to using this explicit expression for v, we reexpress the fundamental solution U in terms of v by replacing (4.8) in (4.6) and combining with (2.21):

$$U_i^k(r) = \frac{1}{\mu}\Big(\big(v_{,\ell\ell}(r) + k_L^2 v(r)\big)\delta_{ik} - (1-\beta^2)v_{,ik}(r)\Big), \tag{4.15}$$

where $\beta = k_L/k_T$. Substituting (4.14) in (4.15), expanding and combining with the recurrence formulae (B.12a), (B.13a) and the identity $r_{,ik} = (\delta_{ik} - r_{,i}r_{,k})/r$, we obtain the following expression for the desired fundamental solution:

$$U_i^k(r) = \frac{\mathrm{i}}{4\mu}\big(A(r)\delta_{ik} + B(r)r_{,i}r_{,k}\big), \tag{4.16}$$

where $A(\cdot)$ and $B(\cdot)$ are the functions

$$A(r) = H_0^{(1)}(k_T r) - \frac{1}{k_T r}\big(H_1^{(1)}(k_T r) - \beta H_1^{(1)}(k_L r)\big), \tag{4.17a}$$

$$B(r) = H_0^{(1)}(k_T r) + \beta^2 H_0^{(1)}(k_L r) - 2A(r). \tag{4.17b}$$

Notice that U is a symmetric tensor in i and k. Expression (4.16) coincides with the two-dimensional time-harmonic elastodynamic fundamental solution for isotropic media given in Manolis & Beskos (1988) and Bonnet (1995). In addition, the third-order tensor Σ defined in (4.4) is regarded as part of the fundamental solution, since it plays an important role in subsequent applications. Hence, we obtain it explicitly by substituting (4.16) and (4.17) in (4.4). It is given by

$$\Sigma_{ij}^k(r) = \frac{\mathrm{i}}{4}\big(2C(r)r_{,i}r_{,j}r_{,k} + D(r)(\delta_{ik}r_{,j} + \delta_{jk}r_{,i}) + E(r)\delta_{ij}r_{,k}\big), \tag{4.18}$$

where $C(\cdot)$, $D(\cdot)$ and $E(\cdot)$ are the functions

$$C(r) = k_T\big(H_1^{(1)}(k_T r) - \beta^3 H_1^{(1)}(k_L r)\big) - \frac{4}{r}B(r), \tag{4.19a}$$

$$D(r) = -k_T H_1^{(1)}(k_T r) + \frac{2}{r}B(r), \tag{4.19b}$$

$$E(r) = -(1-2\beta^2)k_L H_1^{(1)}(k_L r) + \frac{2}{r}B(r). \tag{4.19c}$$

Due to the singular behavior of the Hankel functions at the origin, both tensors U and Σ are singular as $r \sim 0$. Moreover, U satisfies the outgoing radiation conditions at infinity defined in (2.36). To prove this result, we rewrite these conditions in tensor notation:

$$\begin{aligned} \big|\big(\Sigma_{ij}^k(r)\hat{r}_j - \mathrm{i}k_L(\lambda+2\mu)U_i^k(r)\big)\hat{r}_i\big| &= O(r^{-1}) \\ \big|\big(\Sigma_{ij}^k(r)\hat{r}_j - \mathrm{i}k_T\mu\, U_i^k(r)\big)\hat{\theta}_i\big| &= O(r^{-1}) \end{aligned} \qquad \text{as } r \to +\infty, \tag{4.20}$$

where we have posed $\hat{\boldsymbol{r}} = (\hat{r}_1, \hat{r}_2)$ and $\hat{\boldsymbol{\theta}} = (\hat{\theta}_1, \hat{\theta}_2)$. Notice that $\hat{\boldsymbol{r}}$ satisfies $\hat{r}_i = r_{,i}$ and $\hat{\boldsymbol{\theta}}$ can be defined by the orthogonality relation $\hat{r}_i\hat{\theta}_i = 0$. Taking into account this and combining with (4.16) and (4.18), we obtain the relations

$$\begin{aligned} \big(\Sigma_{ij}^k(r)\hat{r}_j - \mathrm{i}k_L(\lambda+2\mu)\,U_i^k(r)\big)\hat{r}_i = \frac{\mathrm{i}}{4}\big(&2C(r) + 2D(r) + E(r) \\ &- \mathrm{i}\beta^{-2}k_L(A(r)+B(r))\big)\hat{r}_k, \end{aligned} \tag{4.21a}$$

$$\big(\Sigma_{ij}^k(r)\hat{r}_j - \mathrm{i}k_T\mu\, U_i^k(r)\big)\hat{\theta}_i = \frac{\mathrm{i}}{4}\big(D(r) - \mathrm{i}k_T A(r)\big)\hat{\theta}_k. \tag{4.21b}$$

On the other hand, assuming r to be sufficiently large, we can use (B.14) to determine asymptotic approximations for functions $A(\cdot)$, $B(\cdot)$, $C(\cdot)$, $D(\cdot)$ and $E(\cdot)$:

$$A(r) = (1-\mathrm{i})(\pi k_T r)^{-1/2}e^{\mathrm{i}k_T r} + O(r^{-3/2}), \tag{4.22a}$$

$$B(r) = -(1-\mathrm{i})(\pi k_T r)^{-1/2}\big(e^{\mathrm{i}k_T r} - \beta^{3/2}\,e^{\mathrm{i}k_L r}\big) + O(r^{-3/2}), \tag{4.22b}$$

$$C(r) = -(1+\mathrm{i})(\pi k_T r)^{-1/2}\big(k_T\,e^{\mathrm{i}k_T r} - \beta^{3/2}k_L\,e^{\mathrm{i}k_L r}\big) + O(r^{-3/2}), \tag{4.22c}$$

$$D(r) = (1+\mathrm{i})\,k_T^{1/2}(\pi r)^{-1/2}e^{\mathrm{i}k_T r} + O(r^{-3/2}), \tag{4.22d}$$

$$E(r) = (1+\mathrm{i})(1-2\beta^2)\,k_L^{1/2}(\pi r)^{-1/2}e^{\mathrm{i}k_L r} + O(r^{-3/2}), \tag{4.22e}$$

and from these approximations, it is straightforward to obtain the asymptotic relations

$$2C(r) + 2D(r) + E(r) - \mathrm{i}\beta^{-2}k_L(A(r)+B(r)) = O(r^{-1}),$$

$$D(r) - \mathrm{i}k_T A(r) = O(r^{-1}),$$

which combined with (4.21) yield the desired result, since both vectors $\hat{\boldsymbol{r}}$ and $\hat{\boldsymbol{\theta}}$ have unit length. Consequently, the fundamental solution defined in (4.16), (4.17), (4.18) and (4.19) fulfills the outgoing radiation conditions at infinity (4.20). The full-plane Green's function, denoted by G, corresponds to a second-order tensor intimately related to the fundamental solution. Given two vector variables $\boldsymbol{x}$ and $\boldsymbol{y}$ in $\mathbb{R}^2$, G is defined as

$$G_i^k(\boldsymbol{x}, \boldsymbol{y}) = U_i^k(|\boldsymbol{y} - \boldsymbol{x}|). \tag{4.23}$$

It should be observed that the Green's function has a singular behavior as $\boldsymbol{y} \sim \boldsymbol{x}$.

4.2.2 Integral representation formulae

In order to deduce the integral representation formulae, we assume that the field of displacements is a solution of a transmission problem in the full-plane $\mathbb{R}^2$ stated next. Let us consider a bounded domain Ω^{int} with a regular boundary Γ. As usual, the corresponding exterior domain is defined as $\Omega^{\text{ext}} = \mathbb{R}^2 \backslash \overline{\Omega^{\text{int}}}$. The unit normal vector $\boldsymbol{n}$ on Γ is oriented from Ω^{ext} to Ω^{int}, as indicated in Fig. 4.1. The integral representations will then be de-

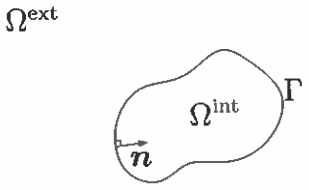

FIGURE 4.1. Exterior and interior domains in $\mathbb{R}^2$ separated by a boundary Γ.

fined on the boundary Γ. The transmission problem corresponds to an extension of the usual exterior boundary-value problem to the interior domain. This time, the elastic wave equation holds in $\Omega^{\text{ext}} \cup \Omega^{\text{int}}$, and jump conditions for the solution, rather than boundary conditions, are specified on Γ. Given the solution $\boldsymbol{u} = (u_1, u_2)$, we define the traction vector $\boldsymbol{t} = (t_1, t_2)$ in an analogous way to Section 3.2. In tensor notation, it is given by

$$t_i(\boldsymbol{x}) = \sigma_{ij}(\boldsymbol{x}) n_j(\boldsymbol{x}), \tag{4.24}$$

where the stress tensor σ was defined in (4.2) and $\boldsymbol{n} = (n_1, n_2)$ is the outward unit normal vector. The exterior and interior traces of $\boldsymbol{u}$ and $\boldsymbol{t}$ are defined as follows:

$$u_i^{\text{ext}}(\boldsymbol{x}) = \lim_{\hat{\boldsymbol{x}} \to \boldsymbol{x}} u_i(\hat{\boldsymbol{x}})\big|_{\Omega^{\text{ext}}} \qquad t_i^{\text{ext}}(\boldsymbol{x}) = \lim_{\hat{\boldsymbol{x}} \to \boldsymbol{x}} t_i(\hat{\boldsymbol{x}})\big|_{\Omega^{\text{ext}}} \qquad \boldsymbol{x} \in \Gamma, \tag{4.25a}$$

$$u_i^{\text{int}}(\boldsymbol{x}) = \lim_{\hat{\boldsymbol{x}} \to \boldsymbol{x}} u_i(\hat{\boldsymbol{x}})\big|_{\Omega^{\text{int}}} \qquad t_i^{\text{int}}(\boldsymbol{x}) = \lim_{\hat{\boldsymbol{x}} \to \boldsymbol{x}} t_i(\hat{\boldsymbol{x}})\big|_{\Omega^{\text{int}}} \qquad \boldsymbol{x} \in \Gamma. \tag{4.25b}$$

We then define the jumps of $\boldsymbol{u}$ and $\boldsymbol{t}$ through Γ as

$$[u_i](\boldsymbol{x}) = u_i^{\text{ext}}(\boldsymbol{x}) - u_i^{\text{int}}(\boldsymbol{x}), \qquad [t_i](\boldsymbol{x}) = t_i^{\text{ext}}(\boldsymbol{x}) - t_i^{\text{int}}(\boldsymbol{x}), \qquad \boldsymbol{x} \in \Gamma. \tag{4.26}$$

The transmission problem through Γ is defined as: Find $\boldsymbol{u} : \Omega^{\text{ext}} \cup \Omega^{\text{int}} \to \mathbb{C}^2$ such that

$$\sigma_{ij,j}(\boldsymbol{x}) + \rho\omega^2 u_i(\boldsymbol{x}) = 0 \qquad \text{in } \Omega^{\text{ext}} \cup \Omega^{\text{int}}, \tag{4.27a}$$

$$[u_i](\boldsymbol{x}) = p_i(\boldsymbol{x}) \qquad \text{on } \Gamma, \tag{4.27b}$$

$$[t_i](\boldsymbol{x}) = q_i(\boldsymbol{x}) \qquad \text{on } \Gamma, \tag{4.27c}$$

$$\begin{aligned} \left|\left(t_i(\boldsymbol{x}) - \mathrm{i}k_L(\lambda+2\mu)\,u_i(\boldsymbol{x})\right)\hat{r}_i(\boldsymbol{x})\right| &= O(r^{-1}) \\ \left|\left(t_i(\boldsymbol{x}) - \mathrm{i}k_T\mu\,u_i(\boldsymbol{x})\right)\hat{\theta}_i(\boldsymbol{x})\right| &= O(r^{-1}) \end{aligned} \qquad \text{as } r = |\boldsymbol{x}| \to +\infty, \tag{4.27d}$$

where $\boldsymbol{p} = (p_1, p_2)$ and $\boldsymbol{q} = (q_1, q_2)$ are vector functions defined on Γ, assumed to be known. Let us define two points in $\mathbb{R}^2$, namely a source point $\boldsymbol{x}$ and a receiver point $\boldsymbol{y}$. The point $\boldsymbol{x}$ is fixed at some location in $\Omega^{\text{ext}} \cup \Omega^{\text{int}}$, while $\boldsymbol{y}$ corresponds to a variable point in $\mathbb{R}^2$. Replacing (4.23) in (4.5), we obtain that the Green's function G satisfies

$$-\left(\mu G^k_{i,jj}(\boldsymbol{x},\boldsymbol{y}) + (\lambda+\mu)G^k_{j,ij}(\boldsymbol{x},\boldsymbol{y}) + \rho\omega^2 G^k_i(\boldsymbol{x},\boldsymbol{y})\right) = \delta_{ik}\delta_{\boldsymbol{x}}(\boldsymbol{y}), \tag{4.28}$$

where all the derivatives are taken with respect to the components of the receiver point $\boldsymbol{y}$. The notation $\delta_{\boldsymbol{x}}$ stands for the Dirac's delta distribution centered at $\boldsymbol{x}$. In addition, given any open set with regular boundary and outward unit normal vector $\boldsymbol{n} = (n_1, n_2)$, we define another second-order tensor depending on $\boldsymbol{x}$ and $\boldsymbol{y}$, denoted by H. We call this tensor the Green's function's normal derivative, by analogy with acoustics. It is defined as

$$H^k_i(\boldsymbol{x},\boldsymbol{y}) = \Sigma^k_{ij}(|\boldsymbol{y}-\boldsymbol{x}|)n_j(\boldsymbol{y}), \tag{4.29}$$

or alternatively

$$H^k_i(\boldsymbol{x},\boldsymbol{y}) = \lambda G^k_{\ell,\ell}(\boldsymbol{x},\boldsymbol{y})n_i(\boldsymbol{y}) + \mu\left(G^k_{i,j}(\boldsymbol{x},\boldsymbol{y}) + G^k_{j,i}(\boldsymbol{x},\boldsymbol{y})\right)n_j(\boldsymbol{y}). \tag{4.30}$$

where we have combined with (4.4) and (4.23) to obtain this last expression for H. In order to deduce appropriately the integral representation formulae for $\boldsymbol{u}$, we define the auxiliary domain $\Omega_{R,\varepsilon}$ as the open set $\Omega^{\text{ext}} \cup \Omega^{\text{int}}$ minus the ball B_ε of radius $\varepsilon > 0$ centered at $\boldsymbol{x}$, and truncated at infinity by the ball B_R of radius $R > 0$ centered at the origin. The boundaries of balls B_ε and B_R are denoted by S_ε and S_R, respectively. We assume the ball B_ε to be entirely contained either in Ω^{int} or Ω^{ext}, for which it is necessary that ε is small enough in such a way that $\overline{B_\varepsilon} \cap \Gamma = \emptyset$. Moreover, R has to be sufficiently large so that $\overline{\Omega^{\text{int}}} \cup \overline{B_\varepsilon} \subset B_R$. The domain $\Omega_{R,\varepsilon}$ is illustrated in Fig. 4.2. It is mathematically defined as

$$\Omega_{R,\varepsilon} = \left((\Omega^{\text{ext}} \cup \Omega^{\text{int}}) \cap B_R\right)\backslash\overline{B_\varepsilon},$$

and the idea behind it is to retrieve $\Omega^{\text{ext}} \cup \Omega^{\text{int}}$ at the end when we make $R \to +\infty$ and $\varepsilon \to 0^+$ in $\Omega_{R,\varepsilon}$. As $\boldsymbol{x} \notin \Omega_{R,\varepsilon}$, the Green's function G satisfies (4.28) with zero right-hand side in this domain, that is

$$\mu G^k_{i,jj}(\boldsymbol{x},\boldsymbol{y}) + (\lambda+\mu)G^k_{j,ij}(\boldsymbol{x},\boldsymbol{y}) + \rho\omega^2 G^k_i(\boldsymbol{x},\boldsymbol{y}) = 0 \qquad \text{in } \Omega_{R,\varepsilon},$$

and multiplying by the solution of (4.27) evaluated at $\boldsymbol{y}$ and integrating in $\Omega_{R,\varepsilon}$ yields

$$\int_{\Omega_{R,\varepsilon}} \left(\mu G^k_{i,jj}(\boldsymbol{x},\boldsymbol{y}) + (\lambda+\mu)G^k_{j,ij}(\boldsymbol{x},\boldsymbol{y}) + \rho\omega^2 G^k_i(\boldsymbol{x},\boldsymbol{y})\right)u_i(\boldsymbol{y})\mathrm{d}\boldsymbol{y} = 0. \tag{4.31}$$

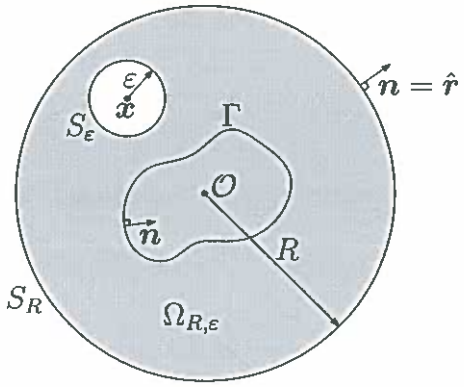

FIGURE 4.2. Truncated domain $\Omega_{R,\varepsilon}$ for a source point not located at Γ.

Since the boundary Γ actually divides $\Omega_{R,\varepsilon}$ into what is inside Ω^{int} and what is outside, we define the domain $\Omega^{\text{ext}}_{R,\varepsilon} = \Omega_{R,\varepsilon} \backslash \overline{\Omega^{\text{int}}}$, in such a way that $\Omega_{R,\varepsilon} = \Omega^{\text{ext}}_{R,\varepsilon} \cup \Omega^{\text{int}}$. Identity (4.31) is thus separated into two new identities:

$$\int_{\Omega^{\text{ext}}_{R,\varepsilon}} \big(\mu G^k_{i,jj}(\boldsymbol{x},\boldsymbol{y}) + (\lambda+\mu) G^k_{j,ij}(\boldsymbol{x},\boldsymbol{y}) + \rho\omega^2 G^k_i(\boldsymbol{x},\boldsymbol{y})\big) u_i(\boldsymbol{y}) \mathrm{d}\boldsymbol{y} = 0, \tag{4.32a}$$

$$\int_{\Omega^{\text{int}}} \big(\mu G^k_{i,jj}(\boldsymbol{x},\boldsymbol{y}) + (\lambda+\mu) G^k_{j,ij}(\boldsymbol{x},\boldsymbol{y}) + \rho\omega^2 G^k_i(\boldsymbol{x},\boldsymbol{y})\big) u_i(\boldsymbol{y}) \mathrm{d}\boldsymbol{y} = 0, \tag{4.32b}$$

and we start by analyzing (4.32a). Integrating by parts twice the first two terms, combining with (4.24) and (4.30), and regrouping terms, we obtain

$$\begin{aligned} &\int_{\Omega^{\text{ext}}_{R,\varepsilon}} G^k_i(\boldsymbol{x},\boldsymbol{y}) \big(\sigma_{ij,j}(\boldsymbol{y}) + \rho\omega^2 u_i(\boldsymbol{y})\big) \mathrm{d}\boldsymbol{y} \\ &= \int_{\partial\Omega^{\text{ext}}_{R,\varepsilon}} \big(G^k_i(\boldsymbol{x},\boldsymbol{y}) t_i(\boldsymbol{y}) - H^k_i(\boldsymbol{x},\boldsymbol{y}) u_i(\boldsymbol{y})\big) \mathrm{d}s(\boldsymbol{y}), \end{aligned} \tag{4.33}$$

and as $\boldsymbol{u}$ satisfies (4.27a), the left-hand side of (4.33) vanishes, giving

$$\int_{\partial\Omega^{\text{ext}}_{R,\varepsilon}} \big(G^k_i(\boldsymbol{x},\boldsymbol{y}) t_i(\boldsymbol{y}) - H^k_i(\boldsymbol{x},\boldsymbol{y}) u_i(\boldsymbol{y})\big) \mathrm{d}s(\boldsymbol{y}) = 0. \tag{4.34}$$

Let us suppose for a moment that $\overline{B_\varepsilon} \subset \Omega^{\text{ext}}_{R,\varepsilon}$, as shown in Fig. 4.2. In such a case, we have that the boundary of $\Omega^{\text{ext}}_{R,\varepsilon}$ can be decomposed as $\partial\Omega^{\text{ext}}_{R,\varepsilon} = S_R \cup S_\varepsilon \cup \Gamma$, which leads to restating (4.34) as a sum of integrals on each boundary:

$$\begin{aligned} &\int_{S_R} \big(G^k_i(\boldsymbol{x},\boldsymbol{y}) t_i(\boldsymbol{y}) - H^k_i(\boldsymbol{x},\boldsymbol{y}) u_i(\boldsymbol{y})\big) \mathrm{d}s(\boldsymbol{y}) \\ &+ \int_{S_\varepsilon} \big(G^k_i(\boldsymbol{x},\boldsymbol{y}) t_i(\boldsymbol{y}) - H^k_i(\boldsymbol{x},\boldsymbol{y}) u_i(\boldsymbol{y})\big) \mathrm{d}s(\boldsymbol{y}) \\ &+ \int_{\Gamma} \big(G^k_i(\boldsymbol{x},\boldsymbol{y}) t^{\text{ext}}_i(\boldsymbol{y}) - H^k_i(\boldsymbol{x},\boldsymbol{y}) u^{\text{ext}}_i(\boldsymbol{y})\big) \mathrm{d}s(\boldsymbol{y}) = 0, \end{aligned} \tag{4.35}$$

where we have used (4.25) to reexpress the last integral. Identity (4.32b) is treated in analogous way to (4.32a). As the boundary of Ω^{int} is given by $\partial\Omega^{\text{int}} = \Gamma$, we obtain

$$-\int_{\Gamma}\big(G_i^k(\boldsymbol{x},\boldsymbol{y})t_i^{\text{int}}(\boldsymbol{y}) - H_i^k(\boldsymbol{x},\boldsymbol{y})u_i^{\text{int}}(\boldsymbol{y})\big)\mathrm{d}s(\boldsymbol{y}) = 0. \tag{4.36}$$

Adding (4.36) with (4.35) and combining with (4.26), (4.27b) and (4.27c) yields

$$\begin{aligned}&\int_{S_R}\big(G_i^k(\boldsymbol{x},\boldsymbol{y})t_i(\boldsymbol{y}) - H_i^k(\boldsymbol{x},\boldsymbol{y})u_i(\boldsymbol{y})\big)\mathrm{d}s(\boldsymbol{y})\\ &+\int_{S_\varepsilon}\big(G_i^k(\boldsymbol{x},\boldsymbol{y})t_i(\boldsymbol{y}) - H_i^k(\boldsymbol{x},\boldsymbol{y})u_i(\boldsymbol{y})\big)\mathrm{d}s(\boldsymbol{y})\\ &+\int_{\Gamma}\big(G_i^k(\boldsymbol{x},\boldsymbol{y})q_i(\boldsymbol{y}) - H_i^k(\boldsymbol{x},\boldsymbol{y})p_i(\boldsymbol{y})\big)\mathrm{d}s(\boldsymbol{y}) = 0.\end{aligned} \tag{4.37}$$

On the contrary, if we had supposed that $\overline{B_\varepsilon} \subset \Omega^{\text{int}}$, then the integral on S_ε would have not appeared in (4.35) but in (4.36), and the result of the sum of the two identities would be the same. Consequently, formula (4.37) actually holds for any source point $\boldsymbol{x} \in \Omega_{R,\varepsilon}$. Next, we study the behavior of the first integral when $R \to +\infty$. In this case, the outward unit normal vector on S_R is $\boldsymbol{n} = \hat{\boldsymbol{r}}$. Let us express vectors $\boldsymbol{u}$ and $\boldsymbol{t}$ on S_R in their radial and angular components, that is,

$$u_i(\boldsymbol{y}) = u_\ell(\boldsymbol{y})\hat{r}_\ell(\boldsymbol{y})\,\hat{r}_i(\boldsymbol{y}) + u_\ell(\boldsymbol{y})\hat{\theta}_\ell(\boldsymbol{y})\,\hat{\theta}_i(\boldsymbol{y}), \tag{4.38a}$$

$$t_i(\boldsymbol{y}) = t_\ell(\boldsymbol{y})\hat{r}_\ell(\boldsymbol{y})\,\hat{r}_i(\boldsymbol{y}) + t_\ell(\boldsymbol{y})\hat{\theta}_\ell(\boldsymbol{y})\,\hat{\theta}_i(\boldsymbol{y}). \tag{4.38b}$$

Substituting (4.38) in the first integral of (4.37), adding and subtracting suitable terms, and rearranging, we obtain that this integral can be decomposed as the sum of four new integrals on S_R as follows:

$$\begin{aligned}&\int_{S_R}\big(G_i^k(\boldsymbol{x},\boldsymbol{y})t_i(\boldsymbol{y}) - H_i^k(\boldsymbol{x},\boldsymbol{y})u_i(\boldsymbol{y})\big)\mathrm{d}s(\boldsymbol{y})\\ &\quad=\int_{S_R}G_\ell^k(\boldsymbol{x},\boldsymbol{y})\hat{r}_\ell(\boldsymbol{y})\big(t_i(\boldsymbol{y}) - \mathrm{i}k_L(\lambda+2\mu)u_i(\boldsymbol{y})\big)\hat{r}_i(\boldsymbol{y})\mathrm{d}s(\boldsymbol{y})\\ &\quad+\int_{S_R}G_\ell^k(\boldsymbol{x},\boldsymbol{y})\hat{\theta}_\ell(\boldsymbol{y})\big(t_i(\boldsymbol{y}) - \mathrm{i}k_T\mu\,u_i(\boldsymbol{y})\big)\hat{\theta}_i(\boldsymbol{y})\mathrm{d}s(\boldsymbol{y})\\ &\quad-\int_{S_R}\big(H_i^k(\boldsymbol{x},\boldsymbol{y}) - \mathrm{i}k_L(\lambda+2\mu)G_i^k(\boldsymbol{x},\boldsymbol{y})\big)\hat{r}_i(\boldsymbol{y})u_\ell(\boldsymbol{y})\hat{r}_\ell(\boldsymbol{y})\mathrm{d}s(\boldsymbol{y})\\ &\quad-\int_{S_R}\big(H_i^k(\boldsymbol{x},\boldsymbol{y}) - \mathrm{i}k_T\mu\,G_i^k(\boldsymbol{x},\boldsymbol{y})\big)\hat{\theta}_i(\boldsymbol{y})u_\ell(\boldsymbol{y})\hat{\theta}_\ell(\boldsymbol{y})\mathrm{d}s(\boldsymbol{y}).\end{aligned} \tag{4.39}$$

Next, we assume $R \to +\infty$ and $\boldsymbol{y} \in S_R$. Each integral on the right-hand side of (4.39) is estimated separately. Replacing (4.22a) and (4.22b) in (4.16) and making the approximation $|\boldsymbol{y}-\boldsymbol{x}| \approx |\boldsymbol{y}| = R$, we obtain that

$$\big|G_\ell^k(\boldsymbol{x},\boldsymbol{y})\hat{r}_\ell(\boldsymbol{y})\big| \le \frac{C}{\sqrt{R}}, \qquad \big|G_\ell^k(\boldsymbol{x},\boldsymbol{y})\hat{\theta}_\ell(\boldsymbol{y})\big| \le \frac{C}{\sqrt{R}}, \tag{4.40}$$

for some constant $C > 0$. On the other hand, the radiation conditions (4.27d) for the transmission problem ensures the existence of a positive constant, which we also call C,

such that the following inequalities hold when $R \to +\infty$:

$$\left|\left(t_i(\boldsymbol{y}) - \mathrm{i}k_L(\lambda+2\mu)u_i(\boldsymbol{y})\right)\hat{r}_i(\boldsymbol{y})\right| \leq \frac{C}{R}, \tag{4.41a}$$

$$\left|\left(t_i(\boldsymbol{y}) - \mathrm{i}k_T\mu\, u_i(\boldsymbol{y})\right)\hat{\theta}_i(\boldsymbol{y})\right| \leq \frac{C}{R}. \tag{4.41b}$$

From (4.41) and (4.40), we obtain directly the bounds

$$\left|\int_{S_R} G_\ell^k(\boldsymbol{x},\boldsymbol{y})\hat{r}_\ell(\boldsymbol{y})\left(t_i(\boldsymbol{y}) - \mathrm{i}k_L(\lambda+2\mu)u_i(\boldsymbol{y})\right)\hat{r}_i(\boldsymbol{y})\mathrm{d}s(\boldsymbol{y})\right| \leq \frac{C}{\sqrt{R}}, \tag{4.42a}$$

$$\left|\int_{S_R} G_\ell^k(\boldsymbol{x},\boldsymbol{y})\hat{\theta}_\ell(\boldsymbol{y})\left(t_i(\boldsymbol{y}) - \mathrm{i}k_T\mu\, u_i(\boldsymbol{y})\right)\hat{\theta}_i(\boldsymbol{y})\mathrm{d}s(\boldsymbol{y})\right| \leq \frac{C}{\sqrt{R}}, \tag{4.42b}$$

which proves that these two integrals go to zero when R tends to infinity. Similarly, replacing (4.23) and (4.30) in the radiation conditions (4.20) for the fundamental solution, we deduce the existence of a another positive constant C such that the inequalities

$$\left|\left(H_i^k(\boldsymbol{x},\boldsymbol{y}) - \mathrm{i}k_L(\lambda+2\mu)G_i^k(\boldsymbol{x},\boldsymbol{y})\right)\hat{r}_i(\boldsymbol{y})\right| \leq \frac{C}{R}, \tag{4.43a}$$

$$\left|\left(H_i^k(\boldsymbol{x},\boldsymbol{y}) - \mathrm{i}k_T\mu\, G_i^k(\boldsymbol{x},\boldsymbol{y})\right)\hat{\theta}_i(\boldsymbol{y})\right| \leq \frac{C}{R}, \tag{4.43b}$$

are valid when $R \to +\infty$. In addition, we suppose that the solution of (4.27) decays as $R^{-1/2}$ at infinity, that is, there exists another constant C such that for R large enough it holds that

$$\left|u_\ell(\boldsymbol{y})\hat{r}_\ell(\boldsymbol{y})\right| \leq \frac{C}{\sqrt{R}}, \qquad \left|u_\ell(\boldsymbol{y})\hat{\theta}_\ell(\boldsymbol{y})\right| \leq \frac{C}{\sqrt{R}}. \tag{4.44}$$

From (4.43) and (4.44) it is not difficult to obtain the bounds

$$\left|\int_{S_R}\left(H_i^k(\boldsymbol{x},\boldsymbol{y}) - \mathrm{i}k_L(\lambda+2\mu)G_i^k(\boldsymbol{x},\boldsymbol{y})\right)\hat{r}_i(\boldsymbol{y})u_\ell(\boldsymbol{y})\hat{r}_\ell(\boldsymbol{y})\mathrm{d}s(\boldsymbol{y})\right| \leq \frac{C}{\sqrt{R}}, \tag{4.45a}$$

$$\left|\int_{S_R}\left(H_i^k(\boldsymbol{x},\boldsymbol{y}) - \mathrm{i}k_T\mu\, G_i^k(\boldsymbol{x},\boldsymbol{y})\right)\hat{\theta}_i(\boldsymbol{y})u_\ell(\boldsymbol{y})\hat{\theta}_\ell(\boldsymbol{y})\mathrm{d}s(\boldsymbol{y})\right| \leq \frac{C}{\sqrt{R}}, \tag{4.45b}$$

which implies that these two integrals vanish when R tends to infinity. Consequently, substitution of (4.42a), (4.42b), (4.45a) and (4.45b) in (4.39) leads us to conclude that

$$\lim_{R\to+\infty}\left|\int_{S_R}\left(H_i^k(\boldsymbol{x},\boldsymbol{y})u_i(\boldsymbol{y}) - G_i^k(\boldsymbol{x},\boldsymbol{y})t_i(\boldsymbol{y})\right)\mathrm{d}s(\boldsymbol{y})\right| = 0. \tag{4.46}$$

Let us study now the second integral in (4.37) when $\varepsilon \to 0^+$. This integral is separated as

$$\begin{aligned}&\int_{S_\varepsilon}\left(G_i^k(\boldsymbol{x},\boldsymbol{y})t_i(\boldsymbol{y}) - H_i^k(\boldsymbol{x},\boldsymbol{y})u_i(\boldsymbol{y})\right)\mathrm{d}s(\boldsymbol{y})\\ &\qquad = \int_{S_\varepsilon} G_i^k(\boldsymbol{x},\boldsymbol{y})t_i(\boldsymbol{y})\mathrm{d}s(\boldsymbol{y}) - \int_{S_\varepsilon} H_i^k(\boldsymbol{x},\boldsymbol{y})u_i(\boldsymbol{y})\mathrm{d}s(\boldsymbol{y}).\end{aligned} \tag{4.47}$$

Notice that the outward unit normal vector on S_ε is $\boldsymbol{n} = -\hat{\boldsymbol{r}}$, pointing towards $\boldsymbol{x}$. Moreover, as $\boldsymbol{y} \in S_\varepsilon$, we have that $|\boldsymbol{y}-\boldsymbol{x}| = \varepsilon$. Let us estimate the first integral on the right-hand

side of (4.47). Replacing (4.16) in (4.23) gives the next expression for G:

$$G_i^k(\boldsymbol{x},\boldsymbol{y}) = \frac{\mathrm{i}}{4\mu}\big(A(\varepsilon)\delta_{ik} + B(\varepsilon)\hat{r}_i(\boldsymbol{y})\hat{r}_k(\boldsymbol{y})\big), \tag{4.48}$$

and supposing ε to be small enough, expressions (B.16) for the Hankel functions of order 0 and 1 can be used to approximate functions $A(\cdot)$ and $B(\cdot)$, leading to restate (4.48) as

$$G_i^k(\boldsymbol{x},\boldsymbol{y}) = -\frac{1}{4\pi\mu}\big(\big((1+\beta^2)\ln\varepsilon + c_0\big)\delta_{ik} - (1-\beta^2)\hat{r}_i(\boldsymbol{y})\hat{r}_k(\boldsymbol{y})\big) + o(\varepsilon). \tag{4.49}$$

where $c_0 \in \mathbb{C}$ is some known constant. Assuming $\boldsymbol{t}$ to be sufficiently regular within the ball B_ε, we use (4.49) to bound the first integral in (4.47) when $\varepsilon \to 0^+$ as follows:

$$\left|\int_{S_\varepsilon} G_i^k(\boldsymbol{x},\boldsymbol{y})t_i(\boldsymbol{y})\mathrm{d}s(\boldsymbol{y})\right| \leq C\,\varepsilon\ln\varepsilon \sup_{\boldsymbol{y}\in B_\varepsilon}\big|t_k(\boldsymbol{y})\big|, \tag{4.50}$$

for some constant $C > 0$. This proves that this integral tends to zero when $\varepsilon \to 0^+$. We analyze now the second integral on the right-hand side of (4.47). Replacing (4.18) in (4.30), we obtain an expression for H:

$$H_i^k(\boldsymbol{x},\boldsymbol{y}) = -\frac{\mathrm{i}}{4}\big(D(\varepsilon)\delta_{ik} + \big(2C(\varepsilon) + D(\varepsilon) + E(\varepsilon)\big)\hat{r}_i(\boldsymbol{y})\hat{r}_k(\boldsymbol{y})\big), \tag{4.51}$$

and using (B.16) to approximate functions $C(\cdot)$, $D(\cdot)$ and $E(\cdot)$, we rewrite (4.51) as

$$H_i^k(\boldsymbol{x},\boldsymbol{y}) = \frac{1}{2\pi\varepsilon}\big(\beta^2\delta_{ik} + 2(1-\beta^2)\hat{r}_i(\boldsymbol{y})\hat{r}_k(\boldsymbol{y})\big) + o(1), \tag{4.52}$$

and if we combine with the tensor identity $\delta_{ik} = \hat{r}_i\hat{r}_k + \hat{\theta}_i\hat{\theta}_k$, (4.52) can be restated as

$$H_i^k(\boldsymbol{x},\boldsymbol{y}) = \frac{1}{2\pi\varepsilon}\big(\delta_{ik} + (1-\beta^2)\big(\hat{r}_i(\boldsymbol{y})\hat{r}_k(\boldsymbol{y}) - \hat{\theta}_i(\boldsymbol{y})\hat{\theta}_k(\boldsymbol{y})\big)\big) + o(1). \tag{4.53}$$

Integrating (4.53) in S_ε yields

$$\int_{S_\varepsilon} H_i^k(\boldsymbol{x},\boldsymbol{y})\mathrm{d}s(\boldsymbol{y}) = \delta_{ik} + \frac{1-\beta^2}{2\pi\varepsilon}\int_{S_\varepsilon}\big(\hat{r}_i(\boldsymbol{y})\hat{r}_k(\boldsymbol{y}) - \hat{\theta}_i(\boldsymbol{y})\hat{\theta}_k(\boldsymbol{y})\big)\mathrm{d}s(\boldsymbol{y}) + o(\varepsilon),$$

and using that $\hat{r}_1 = \hat{\theta}_2 = \cos\theta$ and $\hat{r}_2 = -\hat{\theta}_1 = \sin\theta$, it can be easily verified that

$$\int_{S_\varepsilon}\big(\hat{r}_i(\boldsymbol{y})\hat{r}_k(\boldsymbol{y}) - \hat{\theta}_i(\boldsymbol{y})\hat{\theta}_k(\boldsymbol{y})\big)\mathrm{d}s(\boldsymbol{y}) = 0,$$

for all $\varepsilon > 0$. Therefore, when $\varepsilon \to 0^+$ we have

$$\lim_{\varepsilon\to 0^+}\int_{S_\varepsilon} H_i^k(\boldsymbol{x},\boldsymbol{y})\mathrm{d}s(\boldsymbol{y}) = \delta_{ik}. \tag{4.54}$$

Let us separate the second integral on the right-hand side of (4.47) as

$$\begin{aligned}\int_{S_\varepsilon} H_i^k(\boldsymbol{x},\boldsymbol{y})u_i(\boldsymbol{y})\mathrm{d}s(\boldsymbol{y}) = &\int_{S_\varepsilon} H_i^k(\boldsymbol{x},\boldsymbol{y})\mathrm{d}s(\boldsymbol{y})u_i(\boldsymbol{x}) \\ &+ \int_{S_\varepsilon} H_i^k(\boldsymbol{x},\boldsymbol{y})(u_i(\boldsymbol{y}) - u_i(\boldsymbol{x}))\mathrm{d}s(\boldsymbol{y}).\end{aligned} \tag{4.55}$$

The value of the first integral on the right-hand side of (4.55) when $\varepsilon \to 0^+$ can be easily determined from (4.54), while the second integral is bounded by

$$\left| \int_{S_\varepsilon} H_i^k(\boldsymbol{x}, \boldsymbol{y})(u_i(\boldsymbol{y}) - u_i(\boldsymbol{x}))\mathrm{d}s(\boldsymbol{y}) \right| \leq \sup_{\boldsymbol{y} \in B_\varepsilon} |u_k(\boldsymbol{y}) - u_k(\boldsymbol{x})|, \tag{4.56}$$

and assuming that $\boldsymbol{u}$ is regular enough within the ball B_ε, it is immediate that this last term tends to zero when $\varepsilon \to 0^+$. Hence, replacing (4.54) in (4.55) and combining with (4.56) yields

$$\lim_{\varepsilon \to 0^+} \int_{S_\varepsilon} H_i^k(\boldsymbol{x}, \boldsymbol{y}) u_i(\boldsymbol{y}) \mathrm{d}s(\boldsymbol{y}) = u_k(\boldsymbol{x}). \tag{4.57}$$

Consequently, substituting (4.57) in (4.47) and using (4.50) gives

$$\lim_{\varepsilon \to 0^+} \int_{S_\varepsilon} \big(G_i^k(\boldsymbol{x}, \boldsymbol{y}) t_i(\boldsymbol{y}) - H_i^k(\boldsymbol{x}, \boldsymbol{y}) u_i(\boldsymbol{y})\big) \mathrm{d}s(\boldsymbol{y}) = -u_k(\boldsymbol{x}). \tag{4.58}$$

Finally, taking the limits $R \to +\infty$ and $\varepsilon \to 0^+$ in (4.37) and combining with (4.46) and (4.58), we obtain the following integral representation formula for the solution $\boldsymbol{u}$ of (4.27):

$$u_k(\boldsymbol{x}) = \int_\Gamma G_i^k(\boldsymbol{x}, \boldsymbol{y}) q_i(\boldsymbol{y}) \mathrm{d}s(\boldsymbol{y}) - \int_\Gamma H_i^k(\boldsymbol{x}, \boldsymbol{y}) p_i(\boldsymbol{y}) \mathrm{d}s(\boldsymbol{y}) \qquad \boldsymbol{x} \in \Omega^{\text{ext}} \cup \Omega^{\text{int}}. \tag{4.59}$$

In the case where the source point $\boldsymbol{x}$ is located on Γ, it is necessary to slightly modify the above analysis. The domain $\Omega_{R,\varepsilon}$ is defined in an analogous way to the case $\boldsymbol{x} \in \Omega^{\text{ext}} \cup \Omega^{\text{int}}$, but this time the ball B_ε is partially contained in Ω^{ext} and in Ω^{int}, as indicated in Fig. 4.3. Its

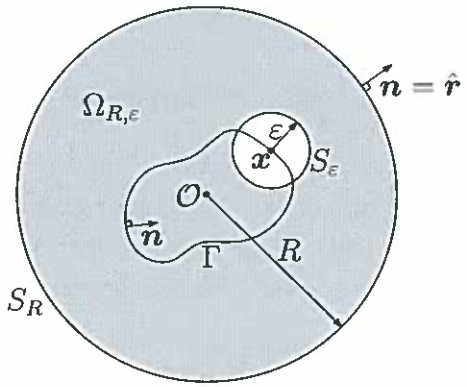

FIGURE 4.3. Truncated domain $\Omega_{R,\varepsilon}$ for a source point located at Γ.

boundary is thus separated as $S_\varepsilon = S_\varepsilon^{\text{ext}} \cup S_\varepsilon^{\text{int}}$, where $S_\varepsilon^{\text{ext}} = S_\varepsilon \cap \Omega^{\text{ext}}$ and $S_\varepsilon^{\text{int}} = S_\varepsilon \cap \Omega^{\text{int}}$. We also define $\Gamma_\varepsilon = \Gamma \backslash B_\varepsilon$. Identity (4.31) is obtained in the same way as above, but this time we have that $\Omega_{R,\varepsilon} = (\Omega_{R,\varepsilon}^{\text{ext}} \backslash \overline{B_\varepsilon}) \cup (\Omega^{\text{int}} \backslash \overline{B_\varepsilon})$, so it is decomposed as

$$\int_{\Omega_{R,\varepsilon}^{\text{ext}} \backslash B_\varepsilon} \big(\mu G_{i,jj}^k(\boldsymbol{x}, \boldsymbol{y}) + (\lambda + \mu) G_{j,ij}^k(\boldsymbol{x}, \boldsymbol{y}) + \rho\omega^2 G_i^k(\boldsymbol{x}, \boldsymbol{y})\big) u_i(\boldsymbol{y}) \mathrm{d}\boldsymbol{y} = 0, \tag{4.60a}$$

$$\int_{\Omega^{\text{int}} \backslash B_\varepsilon} \big(\mu G_{i,jj}^k(\boldsymbol{x}, \boldsymbol{y}) + (\lambda + \mu) G_{j,ij}^k(\boldsymbol{x}, \boldsymbol{y}) + \rho\omega^2 G_i^k(\boldsymbol{x}, \boldsymbol{y})\big) u_i(\boldsymbol{y}) \mathrm{d}\boldsymbol{y} = 0. \tag{4.60b}$$

These two identities are treated as above. Taking into account that the boundaries of the corresponding subdomains are $\partial(\Omega^{\text{ext}}_{R,\varepsilon}\backslash B_\varepsilon) = S_R \cup S^{\text{ext}}_\varepsilon \cup \Gamma_\varepsilon$ and $\partial(\Omega^{\text{int}}\backslash B_\varepsilon) = S^{\text{int}}_\varepsilon \cup \Gamma_\varepsilon$, respectively, it is possible to restate (4.60a) and (4.60b) as

$$\begin{aligned}
&\int_{S_R} \big(G_i^k(\boldsymbol{x},\boldsymbol{y})t_i(\boldsymbol{y}) - H_i^k(\boldsymbol{x},\boldsymbol{y})u_i(\boldsymbol{y})\big)\mathrm{d}s(\boldsymbol{y}) \\
&+ \int_{S^{\text{ext}}_\varepsilon} \big(G_i^k(\boldsymbol{x},\boldsymbol{y})t_i(\boldsymbol{y}) - H_i^k(\boldsymbol{x},\boldsymbol{y})u_i(\boldsymbol{y})\big)\mathrm{d}s(\boldsymbol{y}) \\
&+ \int_{\Gamma_\varepsilon} \big(G_i^k(\boldsymbol{x},\boldsymbol{y})t_i^{\text{ext}}(\boldsymbol{y}) - H_i^k(\boldsymbol{x},\boldsymbol{y})u_i^{\text{ext}}(\boldsymbol{y})\big)\mathrm{d}s(\boldsymbol{y}) = 0,
\end{aligned} \tag{4.61}$$

and

$$\begin{aligned}
&\int_{S^{\text{int}}_\varepsilon} \big(G_i^k(\boldsymbol{x},\boldsymbol{y})t_i(\boldsymbol{y}) - H_i^k(\boldsymbol{x},\boldsymbol{y})u_i(\boldsymbol{y})\big)\mathrm{d}s(\boldsymbol{y}) \\
&- \int_{\Gamma_\varepsilon} \big(G_i^k(\boldsymbol{x},\boldsymbol{y})t_i^{\text{int}}(\boldsymbol{y}) - H_i^k(\boldsymbol{x},\boldsymbol{y})u_i^{\text{int}}(\boldsymbol{y})\big)\mathrm{d}s(\boldsymbol{y}) = 0.
\end{aligned} \tag{4.62}$$

Adding (4.61) and (4.62) gives the identity

$$\begin{aligned}
&\int_{S_R} \big(G_i^k(\boldsymbol{x},\boldsymbol{y})t_i(\boldsymbol{y}) - H_i^k(\boldsymbol{x},\boldsymbol{y})u_i(\boldsymbol{y})\big)\mathrm{d}s(\boldsymbol{y}) \\
&+ \int_{S^{\text{ext}}_\varepsilon} \big(G_i^k(\boldsymbol{x},\boldsymbol{y})t_i(\boldsymbol{y}) - H_i^k(\boldsymbol{x},\boldsymbol{y})u_i(\boldsymbol{y})\big)\mathrm{d}s(\boldsymbol{y}) \\
&+ \int_{S^{\text{int}}_\varepsilon} \big(G_i^k(\boldsymbol{x},\boldsymbol{y})t_i(\boldsymbol{y}) - H_i^k(\boldsymbol{x},\boldsymbol{y})u_i(\boldsymbol{y})\big)\mathrm{d}s(\boldsymbol{y}) \\
&+ \int_{\Gamma_\varepsilon} \big(G_i^k(\boldsymbol{x},\boldsymbol{y})q_i(\boldsymbol{y}) - H_i^k(\boldsymbol{x},\boldsymbol{y})p_i(\boldsymbol{y})\big)\mathrm{d}s(\boldsymbol{y}) = 0,
\end{aligned} \tag{4.63}$$

and the integral in S_R is analyzed exactly as before, obtaining that it vanishes when R tends to infinity. On the contrary, the limit $\varepsilon \to 0^+$ has to be taken more carefully. If we assume that the regularity of Γ at $\boldsymbol{x}$ is at least of the $\mathcal{C}^1$-type, then both boundaries $S^{\text{ext}}_\varepsilon$ and $S^{\text{int}}_\varepsilon$ approach half-circumferences when $\varepsilon \to 0^+$. Hence, proceeding as above we obtain

$$\lim_{\varepsilon\to 0^+} \int_{S^{\text{ext}}_\varepsilon} \big(G_i^k(\boldsymbol{x},\boldsymbol{y})t_i(\boldsymbol{y}) - H_i^k(\boldsymbol{x},\boldsymbol{y})u_i(\boldsymbol{y})\big)\mathrm{d}s(\boldsymbol{y}) = -\frac{1}{2}u_k^{\text{ext}}(\boldsymbol{x}), \tag{4.64a}$$

$$\lim_{\varepsilon\to 0^+} \int_{S^{\text{int}}_\varepsilon} \big(G_i^k(\boldsymbol{x},\boldsymbol{y})t_i(\boldsymbol{y}) - H_i^k(\boldsymbol{x},\boldsymbol{y})u_i(\boldsymbol{y})\big)\mathrm{d}s(\boldsymbol{y}) = -\frac{1}{2}u_k^{\text{int}}(\boldsymbol{x}). \tag{4.64b}$$

Moreover, the boundary Γ_ε approaches Γ when ε tends to zero. Therefore, taking the limits $R \to +\infty$ and $\varepsilon \to 0^+$ in (4.63) and combining with (4.64) yields the following integral representation formula for the solution $\boldsymbol{u}$ of (4.27):

$$\frac{u_k^{\text{ext}}(\boldsymbol{x}) + u_k^{\text{int}}(\boldsymbol{x})}{2} = \int_\Gamma G_i^k(\boldsymbol{x},\boldsymbol{y})q_i(\boldsymbol{y})\mathrm{d}s(\boldsymbol{y}) - \int_\Gamma H_i^k(\boldsymbol{x},\boldsymbol{y})p_i(\boldsymbol{y})\mathrm{d}s(\boldsymbol{y}) \quad \boldsymbol{x}\in\Gamma. \tag{4.65}$$

In the case where the regularity of Γ at $\boldsymbol{x}$ is less than $\mathcal{C}^1$, that is, $\boldsymbol{x}$ is an angular point, it is possible to show by analogous techniques that left-hand side of (4.65) corresponds to a

convex combination of $\boldsymbol{u}^{\text{ext}}$ and $\boldsymbol{u}^{\text{int}}$, where the coefficients depend on the corresponding angle. For a more detailed explanation, see, e.g., Beer et al. (2008).

4.2.3 Integral equations for Dirichlet and Neumann exterior scattering

Next, we develop appropriate integral equations to solve the exterior scattering problems defined in Section 2.3. Prior to this, we define the boundary layer potentials associated with time-harmonic elasticity. These potentials permit to reexpress the integral representation formulae of the previous subsection in a more compact way.

Definition IV.1. *The integral expression defined by*

$$u_k(\boldsymbol{x}) = \mathcal{S}_i^k q_i(\boldsymbol{x}) = \int_\Gamma G_i^k(\boldsymbol{x},\boldsymbol{y}) q_i(\boldsymbol{y}) \mathrm{d}s(\boldsymbol{y}), \tag{4.66}$$

is called single layer potential, whereas the tensor $\mathcal{S}$ is called single layer integral operator. Similarly, the integral expression defined by

$$u_k(\boldsymbol{x}) = \mathcal{D}_i^k p_i(\boldsymbol{x}) = \int_\Gamma H_i^k(\boldsymbol{x},\boldsymbol{y}) p_i(\boldsymbol{y}) \mathrm{d}s(\boldsymbol{y}), \tag{4.67}$$

is called double layer potential, whereas the tensor $\mathcal{D}$ is called double layer integral operator. Both layer potentials are defined for any $\boldsymbol{x} \in \mathbb{R}^2$. When restricted to Γ, the corresponding integral operators are denoted by S and D, respectively, that is,

$$S_i^k q_i(\boldsymbol{x}) = \int_\Gamma G_i^k(\boldsymbol{x},\boldsymbol{y}) q_i(\boldsymbol{y}) \mathrm{d}s(\boldsymbol{y}) \qquad \boldsymbol{x} \in \Gamma, \tag{4.68a}$$

$$D_i^k p_i(\boldsymbol{x}) = \int_\Gamma H_i^k(\boldsymbol{x},\boldsymbol{y}) p_i(\boldsymbol{y}) \mathrm{d}s(\boldsymbol{y}) \qquad \boldsymbol{x} \in \Gamma. \tag{4.68b}$$

REMARK IV.1. *It holds that S and D are linear and continuous operators such that*

$$S : [H^{-1/2}(\Gamma)]^2 \longrightarrow [H^{1/2}(\Gamma)]^2, \tag{4.69a}$$

$$D : [H^{1/2}(\Gamma)]^2 \longrightarrow [H^{1/2}(\Gamma)]^2. \tag{4.69b}$$

By using the boundary layer potentials, the integral representation formulae (4.59) and (4.65) can be restated as

$$u_k(\boldsymbol{x}) = \mathcal{S}_i^k q_i(\boldsymbol{x}) - \mathcal{D}_i^k p_i(\boldsymbol{x}) \qquad \boldsymbol{x} \in \Omega^{\text{ext}} \cup \Omega^{\text{int}}, \tag{4.70a}$$

$$\frac{u_k^{\text{ext}}(\boldsymbol{x}) + u_k^{\text{int}}(\boldsymbol{x})}{2} = S_i^k q_i(\boldsymbol{x}) - D_i^k p_i(\boldsymbol{x}) \qquad \boldsymbol{x} \in \Gamma. \tag{4.70b}$$

In order to obtain the desired integral equations, we resort to the integral representations of the previous subsection, which were developed for expressing the solution to the transmission problem (4.27). To use these representations, we need a field of displacements $\boldsymbol{u}$ satisfying the elastic wave equation in $\Omega^{\text{ext}} \cup \Omega^{\text{int}}$, so what we do is to extend each exterior boundary-value problem to the interior domain Ω^{int}, which gives particular transmission problems. There are many ways of doing this extension, leading to obtain different integral equations in terms of only one unknown vector on Γ. We consider particular extensions for each exterior boundary-value problem, which yield the integral equations to consider in the Dirichlet and Neumann cases. Following the notation used before, $\boldsymbol{p}$ and $\boldsymbol{q}$ denote the

jumps of $\boldsymbol{u}$ and $\boldsymbol{t}$ through Γ, respectively, which were defined in (4.26). Let us begin by determining an integral equation for the Dirichlet boundary-value problem (2.39), which is rewritten in tensor notation as follows: Find $\boldsymbol{u} = (u_1, u_2) : \Omega^{\text{ext}} \to \mathbb{C}^2$ such that

$$\sigma_{ij,j}(\boldsymbol{x}) + \rho\omega^2 u_i(\boldsymbol{x}) = 0 \qquad \text{in } \Omega^{\text{ext}}, \tag{4.71a}$$

$$u_i(\boldsymbol{x}) = -u_i^{\text{inc}}(\boldsymbol{x}) \qquad \text{on } \Gamma, \tag{4.71b}$$

$$\begin{aligned} \big|\big(t_i(\boldsymbol{x}) - \mathrm{i}k_L(\lambda + 2\mu)u_i(\boldsymbol{x})\big)\hat{r}_i(\boldsymbol{x})\big| &= O(r^{-1}) \\ \big|\big(t_i(\boldsymbol{x}) - \mathrm{i}k_T\mu\, u_i(\boldsymbol{x})\big)\hat{\theta}_i(\boldsymbol{x})\big| &= O(r^{-1}) \end{aligned} \qquad \text{as } r \to +\infty. \tag{4.71c}$$

The solution $\boldsymbol{u}$ to (4.71) is extended to Ω^{int} by defining the following auxiliary problem: Find $\boldsymbol{u} : \Omega^{\text{int}} \to \mathbb{C}^2$ such that

$$\sigma_{ij,j}(\boldsymbol{x}) + \rho\omega^2 u_i(\boldsymbol{x}) = 0 \qquad \text{in } \Omega^{\text{int}}, \tag{4.72a}$$

$$u_i(\boldsymbol{x}) = -u_i^{\text{inc}}(\boldsymbol{x}) \qquad \text{on } \Gamma. \tag{4.72b}$$

This is an interior Dirichlet boundary-value problem posed in Ω^{int}. Let us determine the jumps $\boldsymbol{p}$ and $\boldsymbol{q}$ for this particular case. As both problems (4.71) and (4.72) have prescribed the same Dirichlet boundary conditions on Γ, we have that

$$p_i(\boldsymbol{x}) = u_i^{\text{ext}}(\boldsymbol{x}) - u_i^{\text{int}}(\boldsymbol{x}) = -u_i^{\text{inc}}(\boldsymbol{x}) + u_i^{\text{inc}}(\boldsymbol{x}) = 0 \qquad \boldsymbol{x} \in \Gamma, \tag{4.73}$$

that is, the jump of $\boldsymbol{u}$ through Γ is null. On the contrary, the jump of $\boldsymbol{t}$ cannot be determined a priori, so it remains as the unknown of our problem. Substitution of (4.73) in the integral representation formula (4.70b) gives the next integral equation in $\boldsymbol{q}$:

$$S_i^k q_i(\boldsymbol{x}) = -u_k^{\text{inc}}(\boldsymbol{x}) \qquad \boldsymbol{x} \in \Gamma, \tag{4.74}$$

which is known as a single layer integral equation, since it involves only the single layer potential. Replacing (4.68a), (4.74) can be reexpressed as

$$\int_\Gamma G_i^k(\boldsymbol{x}, \boldsymbol{y}) q_i(\boldsymbol{y}) \mathrm{d}s(\boldsymbol{y}) = -u_k^{\text{inc}}(\boldsymbol{x}) \qquad \boldsymbol{x} \in \Gamma. \tag{4.75}$$

REMARK IV.2. *The integral equation* (4.75) *has a unique solution on condition that* $\rho\omega^2$ *is not an eigenvalue of the interior Dirichlet boundary-value problem*

$$-\sigma_{ij,j}(\boldsymbol{x}) = \nu u_i(\boldsymbol{x}) \qquad \textit{in } \Omega^{\text{int}}, \tag{4.76a}$$

$$u_i(\boldsymbol{x}) = 0 \qquad \textit{on } \Gamma. \tag{4.76b}$$

We thus assume that the frequency ω *is such that* $\nu = \rho\omega^2$ *is not an eigenvalue of* (4.76).

Assuming that $\boldsymbol{q}$ has already been determined by solving either (4.74) or (4.75), the solution $\boldsymbol{u}$ to (4.71) can be evaluated using the integral representation formula obtained by replacing (4.73) in (4.70a), that is,

$$u_k(\boldsymbol{x}) = \mathcal{S}_i^k q_i(\boldsymbol{x}) \qquad \boldsymbol{x} \in \Omega^{\text{ext}}, \tag{4.77}$$

or else,

$$u_k(\boldsymbol{x}) = \int_\Gamma G_i^k(\boldsymbol{x}, \boldsymbol{y}) q_i(\boldsymbol{y}) \mathrm{d}s(\boldsymbol{y}) \qquad \boldsymbol{x} \in \Omega^{\text{ext}}. \tag{4.78}$$

Let us analyze now the Neumann boundary-value problem (2.42), which is rewritten in tensor notation as follows: Find $\boldsymbol{u} : \Omega^{\text{ext}} \to \mathbb{C}^2$ such that

$$\sigma_{ij,j}(\boldsymbol{x}) + \rho\omega^2 u_i(\boldsymbol{x}) = 0 \qquad \text{in } \Omega^{\text{ext}}, \tag{4.79a}$$

$$t_i(\boldsymbol{x}) = -t_i^{\text{inc}}(\boldsymbol{x}) \qquad \text{on } \Gamma, \tag{4.79b}$$

$$\begin{aligned} \left|\left(t_i(\boldsymbol{x}) - \mathrm{i}k_L(\lambda + 2\mu)u_i(\boldsymbol{x})\right)\hat{r}_i(\boldsymbol{x})\right| &= O(r^{-1}) \\ \left|\left(t_i(\boldsymbol{x}) - \mathrm{i}k_T\mu\, u_i(\boldsymbol{x})\right)\hat{\theta}_i(\boldsymbol{x})\right| &= O(r^{-1}) \end{aligned} \qquad \text{as } r \to +\infty. \tag{4.79c}$$

This time, we extend (4.79) to Ω^{int} simply by zero, that is, we pose

$$u_i(\boldsymbol{x}) = 0 \qquad \text{in } \Omega^{\text{int}}.$$

Hence, the jump $\boldsymbol{p}$ for this case is given by

$$p_i(\boldsymbol{x}) = u_i(\boldsymbol{x}) \qquad \boldsymbol{x} \in \Gamma, \tag{4.80}$$

and as the solution $\boldsymbol{u}$ has not been obtained yet, $\boldsymbol{p}$ is the unknown of our problem. On the contrary, the jump $\boldsymbol{q}$ can be determined using (4.79b):

$$q_i(\boldsymbol{x}) = t_i(\boldsymbol{x}) = -t_i^{\text{inc}}(\boldsymbol{x}) \qquad \boldsymbol{x} \in \Gamma, \tag{4.81}$$

which is a known vector, since $\boldsymbol{t}^{\text{inc}}$ is given in terms of the incident field $\boldsymbol{u}^{\text{inc}}$. Replacing (4.81) in the integral representation formula (4.70b), combining with (4.80) and rearranging, we obtain the following integral equation in $\boldsymbol{p}$:

$$D_i^k p_i(\boldsymbol{x}) + \frac{1}{2}p_k(\boldsymbol{x}) = -S_i^k t_i^{\text{inc}}(\boldsymbol{x}) \qquad \boldsymbol{x} \in \Gamma, \tag{4.82}$$

which is known as a double layer integral equation, because it involves the double layer potential. Substituting (4.68b) in (4.82), it can be reexpressed as

$$\int_\Gamma H_i^k(\boldsymbol{x},\boldsymbol{y})p_i(\boldsymbol{y})\mathrm{d}s(\boldsymbol{y}) + \frac{1}{2}p_k(\boldsymbol{x}) = -\int_\Gamma G_i^k(\boldsymbol{x},\boldsymbol{y})t_i^{\text{inc}}(\boldsymbol{y})\mathrm{d}s(\boldsymbol{y}) \qquad \boldsymbol{x} \in \Gamma. \tag{4.83}$$

REMARK IV.3. *The integral equation* (4.83) *has a unique solution on condition that* $\rho\omega^2$ *is not an eigenvalue of the interior Neumann boundary-value problem*

$$-\sigma_{ij,j}(\boldsymbol{x}) = \nu u_i(\boldsymbol{x}) \qquad \text{in } \Omega^{\text{int}}, \tag{4.84a}$$

$$\sigma_{ij}(\boldsymbol{x})n_j(\boldsymbol{x}) = 0 \qquad \text{on } \Gamma. \tag{4.84b}$$

We thus assume that the frequency ω *is such that* $\nu = \rho\omega^2$ *is not an eigenvalue of* (4.84).

Assuming that $\boldsymbol{p}$ has already been obtained by solving either (4.82) or (4.83), the solution $\boldsymbol{u}$ to (4.79) can be evaluated using the integral representation formula obtained by replacing (4.81) in (4.70a), that is,

$$u_k(\boldsymbol{x}) = -\mathcal{D}_i^k p_i(\boldsymbol{x}) - \mathcal{S}_i^k t_i^{\text{inc}}(\boldsymbol{x}) \qquad \boldsymbol{x} \in \Omega^{\text{ext}}, \tag{4.85}$$

or else,

$$u_k(\boldsymbol{x}) = -\int_\Gamma \left(H_i^k(\boldsymbol{x},\boldsymbol{y})p_i(\boldsymbol{y}) - G_i^k(\boldsymbol{x},\boldsymbol{y})t_i^{\text{inc}}(\boldsymbol{y})\right)\mathrm{d}s(\boldsymbol{y}) \qquad \boldsymbol{x} \in \Omega^{\text{ext}}. \tag{4.86}$$

4.3 Perturbed half-plane scattering

4.3.1 Generalities about the half-plane Green's function

We study hereafter the integral representations and equations for scattering in a locally perturbed half-plane. The idea of a fundamental solution is usually related to differential operators acting in the full-plane (or the full-space in three dimensions), so we deal directly with a Green's function associated with the non-perturbed half-plane $\mathbb{R}^2_+$. We consider again a source point $\boldsymbol{x}$ and a receiver point $\boldsymbol{y}$, with both of them in $\mathbb{R}^2_+$. The mentioned Green's function, denoted by G, is a second-order tensor that satisfies the elastic wave equation in $\boldsymbol{y}$ within the half-plane, with a Dirac's delta distribution centered at $\boldsymbol{x}$ as the right-hand side. We write this equation in tensor notation as

$$-\big(\mu G^k_{i,jj}(\boldsymbol{x},\boldsymbol{y}) + (\lambda+\mu) G^k_{j,ij}(\boldsymbol{x},\boldsymbol{y}) + \rho\omega^2 G^k_i(\boldsymbol{x},\boldsymbol{y})\big) = \delta_{ik}\delta_{\boldsymbol{x}}(\boldsymbol{y}) \qquad \text{in } \mathbb{R}^2_+. \quad (4.87)$$

Furthermore, G fulfills the impedance boundary conditions introduced in Section 2.4 on the infinite flat boundary $\{y_2 = 0\}$, which can be expressed in tensor notation as

$$\lambda G^k_{\ell,\ell}(\boldsymbol{x},\boldsymbol{y})\delta_{i2} + \mu\big(G^k_{i,2}(\boldsymbol{x},\boldsymbol{y}) + G^k_{2,i}(\boldsymbol{x},\boldsymbol{y})\big) + \omega Z_\infty G^k_1(\boldsymbol{x},\boldsymbol{y})\delta_{i1} = 0 \quad \text{on } \{y_2 = 0\}, \quad (4.88)$$

where we recall that $Z_\infty \in \mathbb{R}$ is the impedance of the infinite flat boundary. In addition, we assume that G satisfies adequate radiation conditions at infinity. Unlike the case of the full-plane, the half-plane Green's function is not known in explicit form, even when $Z_\infty = 0$. Nevertheless, we can assume a priori that this Green's function is decomposed as the sum of the full-plane Green's function (already determined in Section 4.2) and an additional term associated with the infinite flat boundary, which is still unknown. An analogous fact is established by Telles & Brebbia (1981) for the Green's function of the elastostatic half-plane with traction-free surface. Therefore, G is written in tensor notation as

$$G^k_i(\boldsymbol{x},\boldsymbol{y}) = [G^P]^k_i(\boldsymbol{x},\boldsymbol{y}) + [G^B]^k_i(\boldsymbol{x},\boldsymbol{y}), \quad (4.89)$$

where G^P denotes the full-plane Green's function defined in (4.23) and G^B is the additional term, which is regular as $\boldsymbol{y} \sim \boldsymbol{x}$. An accurate and effective calculation of this half-plane Green's function is performed thoroughly in Chapter VI.

4.3.2 Integral representation formulae

Next, we obtain integral representation formulae for a transmission problem defined in the half-plane with impedance boundary conditions. The procedure to deduce these formulae has several characteristics in common with that of an exterior domain, so the emphasis is placed on the main differences that arise in the deduction. One could suppose that the lack of an explicit expression for the involved Green's function appears to be a problem in obtaining the desired representation formulae. However, we will see that the hypothesis made in the previous subsection is sufficient for this purpose. Let us consider a local perturbation of the flat boundary denoted by Γ_p, which is assumed to be contained within the upper half-plane $\mathbb{R}^2_+$, as indicated in Fig. 4.4. This perturbation divides $\mathbb{R}^2_+$ into an unbounded exterior domain Ω^{ext}_+ and a bounded interior domain Ω^{int}_+. The unit normal vector on Γ_p is oriented from Ω^{ext}_+ to Ω^{int}_+. The infinite flat boundary $\{y_2 = 0\}$ is then divided into an unbounded part Γ_∞, which extends to infinity on both sides, and

a bounded part Γ^{int}, in such a way that $\partial\Omega_+^{\text{ext}} = \Gamma_\infty \cup \Gamma_p$ and $\partial\Omega_+^{\text{int}} = \Gamma^{\text{int}} \cup \Gamma_p$ (see Fig. 4.4). The integral representations will be defined on the perturbed boundary Γ_p. Let us state the transmission problem in $\mathbb{R}^2_+$. Given a vector of displacements $\boldsymbol{u} = (u_1, u_2)$ defined in $\Omega_+^{\text{ext}} \cup \Omega_+^{\text{int}}$, the stress tensor σ is defined as in (4.2) and the traction vector $\boldsymbol{t} = (t_1, t_2)$ on a regular boundary with unit normal vector $\boldsymbol{n} = (n_1, n_2)$ is defined as in (4.24). We use the same notation as before for the exterior and interior traces of $\boldsymbol{u}$ and $\boldsymbol{t}$ on Γ_p, that is,

$$u_i^{\text{ext}}(\boldsymbol{x}) = \lim_{\hat{\boldsymbol{x}} \to \boldsymbol{x}} u_i(\hat{\boldsymbol{x}})\big|_{\Omega_+^{\text{ext}}} \qquad t_i^{\text{ext}}(\boldsymbol{x}) = \lim_{\hat{\boldsymbol{x}} \to \boldsymbol{x}} t_i(\hat{\boldsymbol{x}})\big|_{\Omega_+^{\text{ext}}} \qquad \boldsymbol{x} \in \Gamma_p, \tag{4.90a}$$

$$u_i^{\text{int}}(\boldsymbol{x}) = \lim_{\hat{\boldsymbol{x}} \to \boldsymbol{x}} u_i(\hat{\boldsymbol{x}})\big|_{\Omega_+^{\text{int}}} \qquad t_i^{\text{int}}(\boldsymbol{x}) = \lim_{\hat{\boldsymbol{x}} \to \boldsymbol{x}} t_i(\hat{\boldsymbol{x}})\big|_{\Omega_+^{\text{int}}} \qquad \boldsymbol{x} \in \Gamma_p. \tag{4.90b}$$

and the jumps of $\boldsymbol{u}$ and $\boldsymbol{t}$ through Γ_p are defined as

$$[u_i](\boldsymbol{x}) = u_i^{\text{ext}}(\boldsymbol{x}) - u_i^{\text{int}}(\boldsymbol{x}), \qquad [t_i](\boldsymbol{x}) = t_i^{\text{ext}}(\boldsymbol{x}) - t_i^{\text{int}}(\boldsymbol{x}), \qquad \boldsymbol{x} \in \Gamma_p. \tag{4.91}$$

The transmission problem through Γ_p is defined as: Find $\boldsymbol{u} : \Omega_+^{\text{ext}} \cup \Omega_+^{\text{int}} \to \mathbb{C}^2$ such that

$$\sigma_{ij,j}(\boldsymbol{x}) + \rho\omega^2 u_i(\boldsymbol{x}) = 0 \qquad \text{in } \Omega_+^{\text{ext}} \cup \Omega_+^{\text{int}}, \tag{4.92a}$$

$$[u_i](\boldsymbol{x}) = p_i(\boldsymbol{x}) \qquad \text{on } \Gamma_p, \tag{4.92b}$$

$$[t_i](\boldsymbol{x}) = q_i(\boldsymbol{x}) \qquad \text{on } \Gamma_p, \tag{4.92c}$$

$$\sigma_{i2}(\boldsymbol{x}) + \omega Z_\infty u_1(\boldsymbol{x})\delta_{i1} = 0 \qquad \text{on } \{x_2 = 0\}, \tag{4.92d}$$

$$+ \text{ Outgoing radiation conditions} \qquad \text{as } r = |\boldsymbol{x}| \to +\infty, \tag{4.92e}$$

where $\boldsymbol{p} = (p_1, p_2)$ and $\boldsymbol{q} = (q_1, q_2)$ are known vector functions defined on Γ_p. The Green's function's normal derivative, denoted by H, is defined on a boundary with outward unit normal vector $\boldsymbol{n} = (n_1, n_2)$ in an analogous way to (4.30), that is,

$$H_i^k(\boldsymbol{x}, \boldsymbol{y}) = \lambda G_{\ell,\ell}^k(\boldsymbol{x}, \boldsymbol{y}) n_i(\boldsymbol{y}) + \mu\big(G_{i,j}^k(\boldsymbol{x}, \boldsymbol{y}) + G_{j,i}^k(\boldsymbol{x}, \boldsymbol{y})\big) n_j(\boldsymbol{y}), \tag{4.93}$$

where this time, G corresponds to the half-plane Green's function with impedance boundary conditions defined in the previous subsection. Replacing G from (4.89) in (4.93) yields a decomposition of the Green's function's normal derivative H as a sum of two terms. This decomposition is analogous to (4.89), and is given by

$$H_i^k(\boldsymbol{x}, \boldsymbol{y}) = [H^P]_i^k(\boldsymbol{x}, \boldsymbol{y}) + [H^B]_i^k(\boldsymbol{x}, \boldsymbol{y}), \tag{4.94}$$

where the tensor H^P corresponds to the full-plane Green's function's normal derivative, which was defined in (4.29) or (4.30). The tensor H^B denotes the normal derivative of G^B, and it is also regular as $\boldsymbol{y} \sim \boldsymbol{x}$. On the other hand, recalling that the outward unit normal

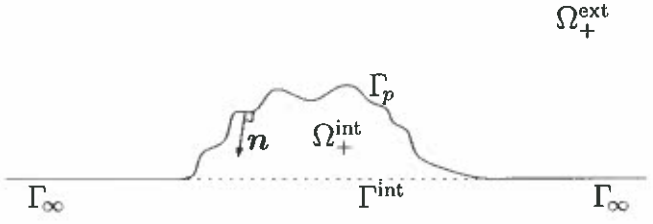

FIGURE 4.4. Exterior and interior domains in $\mathbb{R}^2_+$ separated by a boundary Γ_p.

vector on $\{y_2 = 0\}$ is given by $n_i = -\delta_{i2}$, the impedance boundary condition (4.88) can be restated in terms of H as

$$-H_i^k(\boldsymbol{x},\boldsymbol{y}) + \omega Z_\infty G_1^k(\boldsymbol{x},\boldsymbol{y})\delta_{i1} = 0 \qquad \text{on } \{y_2 = 0\}. \tag{4.95}$$

Assuming a source point $\boldsymbol{x}$ located in $\Omega_+^{\text{ext}} \cup \Omega_+^{\text{int}}$, we define an auxiliary domain, denoted by $\Omega_{R,\varepsilon,+}$, which is analogous to the domain $\Omega_{R,\varepsilon}$ introduced in Section 4.2. It corresponds to the open set $\Omega_+^{\text{ext}} \cup \Omega_+^{\text{int}}$ minus the ball B_ε of radius $\varepsilon > 0$ centered at $\boldsymbol{x}$, and truncated at infinity by the upper half-ball $B_{R,+}$ of radius $R > 0$ centered at the origin. A scheme of the domain $\Omega_{R,\varepsilon,+}$ is presented in Fig. 4.5. We pose $S_\varepsilon = \partial B_\varepsilon$ and $S_{R,+} = (\partial B_{R,+})\backslash\{y_2 = 0\}$.

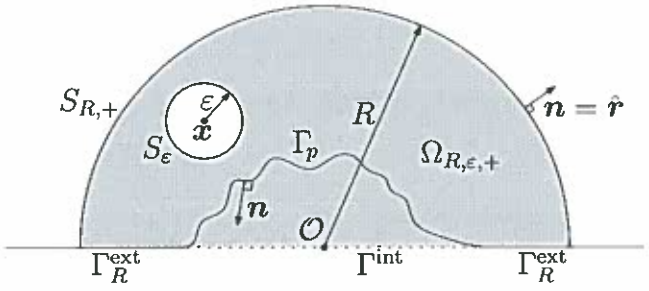

FIGURE 4.5. Truncated domain $\Omega_{R,\varepsilon,+}$ for a source point not located at Γ_p.

In addition, we define the truncated flat boundary as $\Gamma_R^{\text{ext}} = \{\boldsymbol{y} \in \Gamma_\infty \,:\, y_1 \le R\}$. The ball B_ε is assumed to be entirely contained either in Ω_+^{int} or Ω_+^{ext}, which implies that ε has to be small enough, in such a way that S_ε does not intersect with Γ_p, $S_{R,+}$ or Γ_R^{ext}. Moreover, R has to be taken sufficiently large so that $B_{R,+}$ contains $\overline{\Omega_+^{\text{int}}}$ and $\overline{B_\varepsilon}$. The domain $\Omega_{R,\varepsilon,+}$ can be mathematically defined as

$$\Omega_{R,\varepsilon,+} = \big((\Omega_+^{\text{ext}} \cup \Omega_+^{\text{int}}) \cap B_{R,+}\big)\backslash\overline{B_\varepsilon},$$

and we have that $\Omega_{R,\varepsilon,+}$ approaches $\Omega_+^{\text{ext}} \cup \Omega_+^{\text{int}}$ when the limits $R \to +\infty$ and $\varepsilon \to 0^+$ are taken. As $\boldsymbol{x} \notin \Omega_{R,\varepsilon,+}$, we deduce from (4.87) that

$$\mu G_{i,jj}^k(\boldsymbol{x},\boldsymbol{y}) + (\lambda+\mu) G_{j,ij}^k(\boldsymbol{x},\boldsymbol{y}) + \rho\omega^2 G_i^k(\boldsymbol{x},\boldsymbol{y}) = 0 \qquad \text{in } \Omega_{R,\varepsilon,+}. \tag{4.96}$$

The domain $\Omega_{R,\varepsilon,+}$ is divided into $\Omega_{R,\varepsilon,+}^{\text{ext}}$ and Ω_+^{int}, where $\Omega_{R,\varepsilon,+}^{\text{ext}} = \Omega_{R,\varepsilon,+}\backslash\overline{\Omega_+^{\text{int}}}$. Multiplying (4.96) by u_i and integrating separately in $\Omega_{R,\varepsilon,+}^{\text{ext}}$ and Ω_+^{int} yields the identities

$$\int_{\Omega_{R,\varepsilon,+}^{\text{ext}}} \big(\mu G_{i,jj}^k(\boldsymbol{x},\boldsymbol{y}) + (\lambda+\mu) G_{j,ij}^k(\boldsymbol{x},\boldsymbol{y}) + \rho\omega^2 G_i^k(\boldsymbol{x},\boldsymbol{y})\big) u_i(\boldsymbol{y}) \mathrm{d}\boldsymbol{y} = 0, \tag{4.97a}$$

$$\int_{\Omega_+^{\text{int}}} \big(\mu G_{i,jj}^k(\boldsymbol{x},\boldsymbol{y}) + (\lambda+\mu) G_{j,ij}^k(\boldsymbol{x},\boldsymbol{y}) + \rho\omega^2 G_i^k(\boldsymbol{x},\boldsymbol{y})\big) u_i(\boldsymbol{y}) \mathrm{d}\boldsymbol{y} = 0, \tag{4.97b}$$

which are treated as before, that is, they are integrated by parts twice and then expressed as boundary integrals, using (4.92a) to eliminate the remaining volume integrals. Assuming that $\overline{B_\varepsilon} \subset \Omega_{R,\varepsilon,+}^{\text{ext}}$ as in Fig. 4.5, we have that $\partial\Omega_{R,\varepsilon,+}^{\text{ext}} = \Gamma_R^{\text{ext}} \cup S_{R,+} \cup S_\varepsilon \cup \Gamma_p$ and

$\partial\Omega_+^{\text{int}} = \Gamma^{\text{int}} \cup \Gamma_p$. Therefore, (4.97a) becomes

$$\begin{aligned}
&\int_{\Gamma_R^{\text{ext}}} \big(G_i^k(\boldsymbol{x},\boldsymbol{y})t_i(\boldsymbol{y}) - H_i^k(\boldsymbol{x},\boldsymbol{y})u_i(\boldsymbol{y})\big)\mathrm{d}s(\boldsymbol{y}) \\
&+ \int_{S_{R,+}} \big(G_i^k(\boldsymbol{x},\boldsymbol{y})t_i(\boldsymbol{y}) - H_i^k(\boldsymbol{x},\boldsymbol{y})u_i(\boldsymbol{y})\big)\mathrm{d}s(\boldsymbol{y}) \\
&+ \int_{S_\varepsilon} \big(G_i^k(\boldsymbol{x},\boldsymbol{y})t_i(\boldsymbol{y}) - H_i^k(\boldsymbol{x},\boldsymbol{y})u_i(\boldsymbol{y})\big)\mathrm{d}s(\boldsymbol{y}) \\
&+ \int_{\Gamma_p} \big(G_i^k(\boldsymbol{x},\boldsymbol{y})t_i^{\text{ext}}(\boldsymbol{y}) - H_i^k(\boldsymbol{x},\boldsymbol{y})u_i^{\text{ext}}(\boldsymbol{y})\big)\mathrm{d}s(\boldsymbol{y}) = 0,
\end{aligned} \tag{4.98}$$

while (4.97b) becomes

$$\begin{aligned}
&\int_{\Gamma^{\text{int}}} \big(G_i^k(\boldsymbol{x},\boldsymbol{y})t_i(\boldsymbol{y}) - H_i^k(\boldsymbol{x},\boldsymbol{y})u_i(\boldsymbol{y})\big)\mathrm{d}s(\boldsymbol{y}) \\
&- \int_{\Gamma_p} \big(G_i^k(\boldsymbol{x},\boldsymbol{y})t_i^{\text{int}}(\boldsymbol{y}) - H_i^k(\boldsymbol{x},\boldsymbol{y})u_i^{\text{int}}(\boldsymbol{y})\big)\mathrm{d}s(\boldsymbol{y}) = 0.
\end{aligned} \tag{4.99}$$

Adding these identities and combining with (4.91), (4.92b) and (4.92c) gives

$$\begin{aligned}
&\int_{\Gamma_R^{\text{ext}}\cup\Gamma^{\text{int}}} \big(G_i^k(\boldsymbol{x},\boldsymbol{y})t_i(\boldsymbol{y}) - H_i^k(\boldsymbol{x},\boldsymbol{y})u_i(\boldsymbol{y})\big)\mathrm{d}s(\boldsymbol{y}) \\
&+ \int_{S_{R,+}} \big(G_i^k(\boldsymbol{x},\boldsymbol{y})t_i(\boldsymbol{y}) - H_i^k(\boldsymbol{x},\boldsymbol{y})u_i(\boldsymbol{y})\big)\mathrm{d}s(\boldsymbol{y}) \\
&+ \int_{S_\varepsilon} \big(G_i^k(\boldsymbol{x},\boldsymbol{y})t_i(\boldsymbol{y}) - H_i^k(\boldsymbol{x},\boldsymbol{y})u_i(\boldsymbol{y})\big)\mathrm{d}s(\boldsymbol{y}) \\
&+ \int_{\Gamma_p} \big(G_i^k(\boldsymbol{x},\boldsymbol{y})q_i(\boldsymbol{y}) - H_i^k(\boldsymbol{x},\boldsymbol{y})p_i(\boldsymbol{y})\big)\mathrm{d}s(\boldsymbol{y}) = 0.
\end{aligned} \tag{4.100}$$

If $\overline{B_\varepsilon} \subset \Omega_+^{\text{int}}$, we can resort to the same argument used in the case of an exterior domain to conclude that identity (4.100) remains valid. Hence, this identity holds for any source point $\boldsymbol{x} \in \Omega_{R,\varepsilon,+}$. Let us study separately each boundary integral on the right-hand side of (4.100). In the case of the first integral, as $\Gamma_R^{\text{ext}} \cup \Gamma^{\text{int}} \subset \{y_2 = 0\}$, we can use the impedance boundary conditions for Green's function (4.88) and for the solution (4.92d) to reexpress the term integrand. Recalling that $t_i = -\sigma_{i2}$ on $\{y_2 = 0\}$, we obtain

$$G_i^k(\boldsymbol{x},\boldsymbol{y})t_i(\boldsymbol{y}) - H_i^k(\boldsymbol{x},\boldsymbol{y})u_i(\boldsymbol{y}) = \omega Z_\infty \big(G_i^k(\boldsymbol{x},\boldsymbol{y})u_1(\boldsymbol{x}) - G_1^k(\boldsymbol{x},\boldsymbol{y})u_i(\boldsymbol{y})\big)\delta_{i1}. \tag{4.101}$$

If $i = 1$, it is clear that the term between parenthesis in (4.101) is null. On the contrary, if $i = 2$, the Kronecker's delta vanishes. Therefore, in any case it holds that

$$G_i^k(\boldsymbol{x},\boldsymbol{y})t_i(\boldsymbol{y}) - H_i^k(\boldsymbol{x},\boldsymbol{y})u_i(\boldsymbol{y}) = 0 \qquad \text{on } \{y_2 = 0\}, \tag{4.102}$$

and we conclude that for any radius R,

$$\int_{\Gamma_R^{\text{ext}}\cup\Gamma^{\text{int}}} \big(G_i^k(\boldsymbol{x},\boldsymbol{y})t_i(\boldsymbol{y}) - H_i^k(\boldsymbol{x},\boldsymbol{y})u_i(\boldsymbol{y})\big)\mathrm{d}s(\boldsymbol{y}) = 0. \tag{4.103}$$

In the case of the integral in $S_{R,+}$, since the radiation conditions (4.92e) for a half-plane with impedance boundary conditions are not known in explicit form, we make the necessary

assumptions in such a way that the following limit holds:

$$\lim_{R\to+\infty}\left|\int_{S_{R,+}}\big(G_i^k(\boldsymbol{x},\boldsymbol{y})t_i(\boldsymbol{y})-H_i^k(\boldsymbol{x},\boldsymbol{y})u_i(\boldsymbol{y})\big)\mathrm{d}s(\boldsymbol{y})\right|=0. \tag{4.104}$$

In order to analyze the integral in S_ε, we use the decompositions (4.89) and (4.94) for G and H, respectively. This integral is thus decomposed as

$$\begin{aligned}&\int_{S_\varepsilon}\big(G_i^k(\boldsymbol{x},\boldsymbol{y})t_i(\boldsymbol{y})-H_i^k(\boldsymbol{x},\boldsymbol{y})u_i(\boldsymbol{y})\big)\mathrm{d}s(\boldsymbol{y})\\&=\int_{S_\varepsilon}\big([G^P]_i^k(\boldsymbol{x},\boldsymbol{y})t_i(\boldsymbol{y})-[H^P]_i^k(\boldsymbol{x},\boldsymbol{y})u_i(\boldsymbol{y})\big)\mathrm{d}s(\boldsymbol{y})\\&+\int_{S_\varepsilon}\big([G^B]_i^k(\boldsymbol{x},\boldsymbol{y})t_i(\boldsymbol{y})-[H^B]_i^k(\boldsymbol{x},\boldsymbol{y})u_i(\boldsymbol{y})\big)\mathrm{d}s(\boldsymbol{y}).\end{aligned} \tag{4.105}$$

As the tensors G^P and H^P are the full-plane Green's function and its normal derivative, respectively, we already know from Section 4.2 that

$$\lim_{\varepsilon\to0^+}\int_{S_\varepsilon}\big([G^P]_i^k(\boldsymbol{x},\boldsymbol{y})t_i(\boldsymbol{y})-[H^P]_i^k(\boldsymbol{x},\boldsymbol{y})u_i(\boldsymbol{y})\big)\mathrm{d}s(\boldsymbol{y})=-u_k(\boldsymbol{x}), \tag{4.106}$$

and as both tensors G^B and H^B have no singular behavior as $\boldsymbol{y}\sim\boldsymbol{x}$, we have that

$$\lim_{\varepsilon\to0^+}\left|\int_{S_\varepsilon}\big([G^B]_i^k(\boldsymbol{x},\boldsymbol{y})t_i(\boldsymbol{y})-[H^B]_i^k(\boldsymbol{x},\boldsymbol{y})u_i(\boldsymbol{y})\big)\mathrm{d}s(\boldsymbol{y})\right|=0. \tag{4.107}$$

Therefore, making $\varepsilon\to0^+$ in (4.105) and combining with (4.106) and (4.107) gives

$$\lim_{\varepsilon\to0^+}\int_{S_\varepsilon}\big(G_i^k(\boldsymbol{x},\boldsymbol{y})t_i(\boldsymbol{y})-H_i^k(\boldsymbol{x},\boldsymbol{y})u_i(\boldsymbol{y})\big)\mathrm{d}s(\boldsymbol{y})=-u_k(\boldsymbol{x}). \tag{4.108}$$

Finally, taking the limits $R\to+\infty$ and $\varepsilon\to0^+$ in (4.100), combining with (4.103), (4.104) and (4.108), and rearranging, yields the desired integral representation formulae, given by

$$u_k(\boldsymbol{x})=\int_{\Gamma_p}G_i^k(\boldsymbol{x},\boldsymbol{y})q_i(\boldsymbol{y})\mathrm{d}s(\boldsymbol{y})-\int_{\Gamma_p}H_i^k(\boldsymbol{x},\boldsymbol{y})p_i(\boldsymbol{y})\mathrm{d}s(\boldsymbol{y})\qquad\boldsymbol{x}\in\Omega_+^{\mathrm{ext}}\cup\Omega_+^{\mathrm{int}}. \tag{4.109}$$

A special situation, which arises only in a half-plane, is when the source point is located on the infinite flat surface. In this case, the integral representation formula is obtained in almost the same way, except that the domain $\Omega_{R,\varepsilon,+}$ is defined without an upper half-ball of radius ε centered at $\boldsymbol{x}$ instead of a whole ball. The same analysis as above gives rise to a factor $1/2$ on the left-hand side of (4.109), so the integral representation formula becomes

$$\frac{u_k(\boldsymbol{x})}{2}=\int_{\Gamma_p}G_i^k(\boldsymbol{x},\boldsymbol{y})q_i(\boldsymbol{y})\mathrm{d}s(\boldsymbol{y})-\int_{\Gamma_p}H_i^k(\boldsymbol{x},\boldsymbol{y})p_i(\boldsymbol{y})\mathrm{d}s(\boldsymbol{y})\qquad\boldsymbol{x}\in\{x_2=0\}. \tag{4.110}$$

If the source point $\boldsymbol{x}$ is placed just on the perturbed boundary Γ_p, it is necessary to adapt the previous analysis to include this case. The domain $\Omega_{R,\varepsilon,+}$ is defined as above, with the only difference that the ball B_ε has a part contained in Ω_+^{ext} and another part contained in Ω_+^{int}, as indicated in Fig. 4.6. Its boundary S_ε is then divided into $S_\varepsilon^{\mathrm{ext}}=S_\varepsilon\cap\Omega_+^{\mathrm{ext}}$ and $S_\varepsilon^{\mathrm{int}}=S_\varepsilon\cap\Omega_+^{\mathrm{int}}$. We also define $\Gamma_{p,\varepsilon}=\Gamma_p\backslash B_\varepsilon$. We develop an identity analogous to (4.100), but this time it is necessary to consider that the domain $\Omega_{R,\varepsilon,+}$ is separated as $\Omega_{R,\varepsilon,+}=(\Omega_{R,\varepsilon,+}^{\mathrm{ext}}\backslash\overline{B_\varepsilon})\cup(\Omega_+^{\mathrm{int}}\backslash\overline{B_\varepsilon})$. Proceeding as before, two identities analogous to (4.97a) and

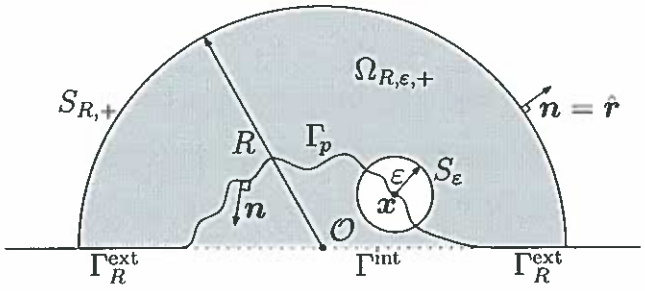

FIGURE 4.6. Truncated domain $\Omega_{R,\varepsilon,+}$ for a source point located at Γ_p.

(4.97b) are obtained, but this time the corresponding volume integrals are in $\Omega^{\text{ext}}_{R,\varepsilon,+}\backslash\overline{B_\varepsilon}$ and $\Omega^{\text{int}}_{+}\backslash\overline{B_\varepsilon}$, respectively. By means of appropriate application of two integrations by parts, these volume integrals are converted into boundary integrals, where the boundaries of the involved domains are given by $\partial(\Omega^{\text{ext}}_{R,\varepsilon,+}\backslash\overline{B_\varepsilon}) = \Gamma^{\text{ext}}_R \cup S_{R,+} \cup S^{\text{ext}}_\varepsilon \cup \Gamma_{p,\varepsilon}$ and $\partial(\Omega^{\text{int}}_{+}\backslash\overline{B_\varepsilon}) = \Gamma^{\text{int}} \cup S^{\text{int}}_\varepsilon \cup \Gamma_{p,\varepsilon}$. The resulting identities are added, giving

$$\begin{aligned}
&\int_{\Gamma_R^{\text{ext}}\cup\Gamma^{\text{int}}} \big(G_i^k(\boldsymbol{x},\boldsymbol{y})t_i(\boldsymbol{y}) - H_i^k(\boldsymbol{x},\boldsymbol{y})u_i(\boldsymbol{y})\big)\mathrm{d}s(\boldsymbol{y}) \\
&+\int_{S_{R,+}} \big(G_i^k(\boldsymbol{x},\boldsymbol{y})t_i(\boldsymbol{y}) - H_i^k(\boldsymbol{x},\boldsymbol{y})u_i(\boldsymbol{y})\big)\mathrm{d}s(\boldsymbol{y}) \\
&+\int_{S_\varepsilon^{\text{ext}}} \big(G_i^k(\boldsymbol{x},\boldsymbol{y})t_i(\boldsymbol{y}) - H_i^k(\boldsymbol{x},\boldsymbol{y})u_i(\boldsymbol{y})\big)\mathrm{d}s(\boldsymbol{y}) \\
&+\int_{S_\varepsilon^{\text{int}}} \big(G_i^k(\boldsymbol{x},\boldsymbol{y})t_i(\boldsymbol{y}) - H_i^k(\boldsymbol{x},\boldsymbol{y})u_i(\boldsymbol{y})\big)\mathrm{d}s(\boldsymbol{y}) \\
&+\int_{\Gamma_{p,\varepsilon}} \big(G_i^k(\boldsymbol{x},\boldsymbol{y})q_i(\boldsymbol{y}) - H_i^k(\boldsymbol{x},\boldsymbol{y})p_i(\boldsymbol{y})\big)\mathrm{d}s(\boldsymbol{y}) = 0.
\end{aligned} \tag{4.111}$$

We already know that the first integral is null, whereas the second one tends to zero when $R \to +\infty$. Assuming that the curve Γ_p has at least regularity of the C^1-type at $\boldsymbol{x}$, we have that $S_\varepsilon^{\text{ext}}$ and $S_\varepsilon^{\text{int}}$ approach half-circumferences, so proceeding as in the case where $\boldsymbol{x} \in \Omega^{\text{ext}}_{+} \cup \Omega^{\text{int}}_{+}$, it is possible to prove the limits

$$\lim_{\varepsilon\to 0^+} \int_{S_\varepsilon^{\text{ext}}} \big(G_i^k(\boldsymbol{x},\boldsymbol{y})t_i(\boldsymbol{y}) - H_i^k(\boldsymbol{x},\boldsymbol{y})u_i(\boldsymbol{y})\big)\mathrm{d}s(\boldsymbol{y}) = -\frac{1}{2}\,u_k^{\text{ext}}(\boldsymbol{x}), \tag{4.112a}$$

$$\lim_{\varepsilon\to 0^+} \int_{S_\varepsilon^{\text{int}}} \big(G_i^k(\boldsymbol{x},\boldsymbol{y})t_i(\boldsymbol{y}) - H_i^k(\boldsymbol{x},\boldsymbol{y})u_i(\boldsymbol{y})\big)\mathrm{d}s(\boldsymbol{y}) = -\frac{1}{2}\,u_k^{\text{int}}(\boldsymbol{x}). \tag{4.112b}$$

Consequently, taking the limits $R \to +\infty$ and $\varepsilon \to 0^+$ in (4.111), combining with (4.112) and using that $\Gamma_{p,\varepsilon}$ approaches Γ_p as ε tends to zero, we obtain the following integral representation formula for $\boldsymbol{x}$ in the perturbed boundary:

$$\frac{u_k^{\text{ext}}(\boldsymbol{x}) + u_k^{\text{int}}(\boldsymbol{x})}{2} = \int_{\Gamma_p} G_i^k(\boldsymbol{x},\boldsymbol{y})q_i(\boldsymbol{y})\mathrm{d}s(\boldsymbol{y}) - \int_{\Gamma_p} H_i^k(\boldsymbol{x},\boldsymbol{y})p_i(\boldsymbol{y})\mathrm{d}s(\boldsymbol{y}) \quad \boldsymbol{x} \in \Gamma_p. \tag{4.113}$$

As in the case of an exterior domain, if $\boldsymbol{x}$ corresponds to an angular point of Γ_p, then the coefficients multiplying $\boldsymbol{u}^{\text{ext}}$ and $\boldsymbol{u}^{\text{int}}$ at the left-hand side of (4.113) are different from $1/2$. These coefficients, whose sum has to be equal to 1, depend on the respective angle.

4.3.3 Integral equation for impedance half-plane scattering

Let us obtain now the integral equation that allows us to solve the impedance scattering problem in the perturbed half-plane defined in Section 2.4. As in the case of an exterior domain, we define the boundary layer potentials for the perturbed half-plane. This time, they correspond to integrals on the perturbed part of the boundary.

Definition IV.2. *The integral expression given by*

$$u_k(\boldsymbol{x}) = \mathcal{S}_i^k q_i(\boldsymbol{x}) = \int_{\Gamma_p} G_i^k(\boldsymbol{x},\boldsymbol{y}) q_i(\boldsymbol{y}) \mathrm{d}s(\boldsymbol{y}), \tag{4.114}$$

is called single layer potential, and the tensor $\mathcal{S}$ is called single layer integral operator. Similarly, the integral expression given by

$$u_k(\boldsymbol{x}) = \mathcal{D}_i^k p_i(\boldsymbol{x}) = \int_{\Gamma_p} H_i^k(\boldsymbol{x},\boldsymbol{y}) p_i(\boldsymbol{y}) \mathrm{d}s(\boldsymbol{y}), \tag{4.115}$$

is called double layer potential, and the tensor $\mathcal{D}$ is called double layer integral operator. Both layer potentials are defined for any $\boldsymbol{x} \in \mathbb{R}^2_+$. When restricted to Γ_p, the resulting integral operators are denoted by S and D, respectively, that is,

$$S_i^k q_i(\boldsymbol{x}) = \int_{\Gamma_p} G_i^k(\boldsymbol{x},\boldsymbol{y}) q_i(\boldsymbol{y}) \mathrm{d}s(\boldsymbol{y}), \qquad \boldsymbol{x} \in \Gamma_p, \tag{4.116a}$$

$$D_i^k p_i(\boldsymbol{x}) = \int_{\Gamma_p} H_i^k(\boldsymbol{x},\boldsymbol{y}) p_i(\boldsymbol{y}) \mathrm{d}s(\boldsymbol{y}), \qquad \boldsymbol{x} \in \Gamma_p. \tag{4.116b}$$

The integral representation formulae (4.109) and (4.113) are then expressed in terms of the boundary layer potentials as follows

$$u_k(\boldsymbol{x}) = \mathcal{S}_i^k q_i(\boldsymbol{x}) - \mathcal{D}_i^k p_i(\boldsymbol{x}) \qquad \boldsymbol{x} \in \Omega_+^{\text{ext}} \cup \Omega_+^{\text{int}}, \tag{4.117a}$$

$$\frac{u_k^{\text{ext}}(\boldsymbol{x}) + u_k^{\text{int}}(\boldsymbol{x})}{2} = S_i^k q_i(\boldsymbol{x}) - D_i^k p_i(\boldsymbol{x}) \qquad \boldsymbol{x} \in \Gamma_p. \tag{4.117b}$$

The integral equation is developed from the integral representation formula (4.113) (or (4.117b)), which expresses the exterior and interior traces of the solution to the transmission problem (4.92) in terms of boundary integrals on Γ_p. In order to use this formula for expressing the solution to the impedance boundary-value problem (2.61), it is necessary to extend properly this problem to the interior domain. Problem (2.61) is written in tensor notation as follows: Find $\boldsymbol{u} = (u_1, u_2) : \Omega_+^{\text{ext}} \longrightarrow \mathbb{R}^2_+$ such that

$$\sigma_{ij,j}(\boldsymbol{x}) + \rho\omega^2 u_i(\boldsymbol{x}) = 0 \qquad \text{in } \Omega_+^{\text{ext}}, \tag{4.118a}$$

$$-t_i(\boldsymbol{x}) + \omega Z_p(\boldsymbol{x}) u_\tau(\boldsymbol{x}) \tau_i(\boldsymbol{x}) = f_i(\boldsymbol{x}) \qquad \text{on } \Gamma_p, \tag{4.118b}$$

$$\sigma_{i2}(\boldsymbol{x}) + \omega Z_\infty u_1(\boldsymbol{x}) \delta_{i1} = 0 \qquad \text{on } \Gamma_\infty, \tag{4.118c}$$

$$+ \text{ Outgoing radiation conditions} \qquad \text{as } r = |\boldsymbol{x}| \to +\infty, \tag{4.118d}$$

where $\boldsymbol{\tau} = (\tau_1, \tau_2)$ corresponds to the unit tangent vector defined on Γ_p and the scalar u_τ denotes the tangent component of $\boldsymbol{u}$ on Γ_p, defined as $u_\tau = u_j \tau_j$. The right-hand side $\boldsymbol{f} = (f_1, f_2)$ of (4.118b) was defined in (2.62), and it can be written in tensor notation as

$$f_i(\boldsymbol{x}) = t_i^{\text{inc}}(\boldsymbol{x}) + t_i^{\text{ref}}(\boldsymbol{x}) - \omega Z_p(\boldsymbol{x})\big(u_\tau^{\text{inc}}(\boldsymbol{x}) + u_\tau^{\text{ref}}(\boldsymbol{x})\big)\tau_i(\boldsymbol{x}), \tag{4.119}$$

where $u_\tau^{\text{inc}} = u_j^{\text{inc}} \tau_j$ and $u_\tau^{\text{ref}} = u_j^{\text{ref}} \tau_j$ denote the tangent components on Γ_p of the incident field $\boldsymbol{u}^{\text{inc}} = (u_1^{\text{inc}}, u_2^{\text{inc}})$ and the reflected field $\boldsymbol{u}^{\text{ref}} = (u_1^{\text{ref}}, u_2^{\text{ref}})$, respectively. The traction vectors $\boldsymbol{t}^{\text{inc}} = (t_1^{\text{inc}}, t_2^{\text{inc}})$ and $\boldsymbol{t}^{\text{ref}} = (t_1^{\text{ref}}, t_2^{\text{ref}})$ can be directly defined in terms of $\boldsymbol{u}^{\text{inc}}$ and $\boldsymbol{u}^{\text{ref}}$, respectively, as follows:

$$t_i^{\text{inc}}(\boldsymbol{x}) = \lambda u_{\ell,\ell}^{\text{inc}}(\boldsymbol{x}) n_i(\boldsymbol{x}) + \mu\big(u_{i,j}^{\text{inc}}(\boldsymbol{x}) + u_{j,i}^{\text{inc}}(\boldsymbol{x})\big) n_j(\boldsymbol{x}), \tag{4.120a}$$

$$t_i^{\text{ref}}(\boldsymbol{x}) = \lambda u_{\ell,\ell}^{\text{ref}}(\boldsymbol{x}) n_i(\boldsymbol{x}) + \mu\big(u_{i,j}^{\text{ref}}(\boldsymbol{x}) + u_{j,i}^{\text{ref}}(\boldsymbol{x})\big) n_j(\boldsymbol{x}). \tag{4.120b}$$

Problem (4.118) is extended to the interior domain by zero, that is, we pose

$$u_i(\boldsymbol{x}) = 0 \qquad \boldsymbol{x} \in \Omega_+^{\text{int}}. \tag{4.121}$$

The jump of $\boldsymbol{u}$ through Γ_p, denoted by $\boldsymbol{p}$ is thus given by

$$p_i(\boldsymbol{x}) = u_i(\boldsymbol{x}) \qquad \boldsymbol{x} \in \Gamma_p, \tag{4.122}$$

which corresponds to the unknown of this problem. On the other hand, the jump of $\boldsymbol{t}$ through Γ_p, denoted by $\boldsymbol{q}$, is given by

$$q_i(\boldsymbol{x}) = t_i(\boldsymbol{x}) \qquad \boldsymbol{x} \in \Gamma_p,$$

and combining with the impedance boundary condition (4.118b), it can be restated as

$$q_i(\boldsymbol{x}) = \omega Z_p(\boldsymbol{x}) u_\tau(\boldsymbol{x}) \tau_i(\boldsymbol{x}) - f_i(\boldsymbol{x}) \qquad \boldsymbol{x} \in \Gamma_p. \tag{4.123}$$

Substituting (4.122) in the integral representation formula (4.117b) yields the identity

$$\frac{1}{2} u_k(\boldsymbol{x}) = \omega S_i^k(Z_p u_\tau \tau_i)(\boldsymbol{x}) - D_i^k p_i(\boldsymbol{x}) - S_i^k f_i(\boldsymbol{x}) \qquad \boldsymbol{x} \in \Gamma_p, \tag{4.124}$$

which actually corresponds to an integral equation in $\boldsymbol{p}$. In fact, combining with (4.122) and rearranging, we obtain that (4.124) can be reexpressed as

$$D_i^k p_i(\boldsymbol{x}) + \frac{1}{2} p_k(\boldsymbol{x}) - \omega S_i^k(Z_p p_\tau \tau_i)(\boldsymbol{x}) = -S_i^k f_i(\boldsymbol{x}) \qquad \boldsymbol{x} \in \Gamma_p. \tag{4.125}$$

This kind of equation is called mixed potential integral equation, because it involves both the single and the double layer potential. Notice that the single layer potential appears in a non-standard form, because it is applied to the tangent part of the vector $\boldsymbol{p}$ multiplied by a known scalar function Z_p. Replacing (4.116a) and (4.116b), we obtain that (4.125) can be reexpressed in terms of boundary integrals as follows:

$$\begin{aligned} &\int_{\Gamma_p} H_i^k(\boldsymbol{x}, \boldsymbol{y}) p_i(\boldsymbol{y}) \mathrm{d}s(\boldsymbol{y}) + \frac{1}{2} p_k(\boldsymbol{x}) \\ &\quad - \omega \int_{\Gamma_p} Z_p(\boldsymbol{y}) G_i^k(\boldsymbol{x}, \boldsymbol{y}) \tau_i(\boldsymbol{y}) \tau_j(\boldsymbol{y}) p_j(\boldsymbol{y}) \mathrm{d}s(\boldsymbol{y}) = -\int_{\Gamma_p} G_i^k(\boldsymbol{x}, \boldsymbol{y}) f_i(\boldsymbol{y}) \mathrm{d}s(\boldsymbol{y}), \end{aligned} \tag{4.126}$$

where the tangent component p_τ was made explicit in order to better handle the integral equation. Let us suppose that $\boldsymbol{p}$ has been already determined by solving either (4.125)

or (4.126). Then, the solution $\boldsymbol{u}$ to the boundary-value problem (4.118) can be evaluated using the integral representation formula (4.117a). Substituting (4.123) in (4.117a) and combining with (4.122) gives

$$u_k(\boldsymbol{x}) = -\mathcal{D}_i^k p_i(\boldsymbol{x}) + \omega \mathcal{S}_i^k (Z_p p_\tau \tau_i)(\boldsymbol{x}) - \mathcal{S}_i^k f_i(\boldsymbol{x}) \qquad \boldsymbol{x} \in \Omega_+^{\text{ext}}, \tag{4.127}$$

or else,

$$\begin{aligned} u_k(\boldsymbol{x}) = -\int_{\Gamma_p} \big(H_i^k(\boldsymbol{x},\boldsymbol{y}) p_i(\boldsymbol{y}) - \omega Z_p(\boldsymbol{y}) G_i^k(\boldsymbol{x},\boldsymbol{y}) \tau_i(\boldsymbol{y}) p_\tau(\boldsymbol{y})\big) \mathrm{d}s(\boldsymbol{y}) \\ - \int_{\Gamma_p} G_i^k(\boldsymbol{x},\boldsymbol{y}) f_i(\boldsymbol{y}) \mathrm{d}s(\boldsymbol{y}) \qquad \boldsymbol{x} \in \Omega_+^{\text{ext}}. \end{aligned} \tag{4.128}$$

If we desire to evaluate $\boldsymbol{u}$ on the infinite flat boundary $\{x_2 = 0\}$, we infer from (4.113) that it is instead necessary to use the following formula

$$\begin{aligned} \frac{u_k(\boldsymbol{x})}{2} = -\int_{\Gamma_p} \big(H_i^k(\boldsymbol{x},\boldsymbol{y}) p_i(\boldsymbol{y}) - \omega Z_p(\boldsymbol{y}) G_i^k(\boldsymbol{x},\boldsymbol{y}) \tau_i(\boldsymbol{y}) p_\tau(\boldsymbol{y})\big) \mathrm{d}s(\boldsymbol{y}) \\ - \int_{\Gamma_p} G_i^k(\boldsymbol{x},\boldsymbol{y}) f_i(\boldsymbol{y}) \mathrm{d}s(\boldsymbol{y}) \qquad \boldsymbol{x} \in \{x_2 = 0\}. \end{aligned} \tag{4.129}$$

V. BOUNDARY ELEMENT METHODS (BEM) FOR SCATTERING PROBLEMS

5.1 Introduction

This chapter is devoted to describing a procedure based upon boundary element methods to solve numerically the integral equations developed in Chapter IV, including the equations that solve exterior scattering, introduced in Section 4.2, and the equation that solves scattering in the locally perturbed half-plane, introduced in Section 4.3. We develop adequate variational formulations for each one of these boundary integral equations. In all cases, the numerical discretization is based on resorting to a particular Galerkin scheme on the variational formulations. The boundary of the obstacle or local perturbation is approximated by a discrete curve consisting of rectilinear segments, and piecewise constant functions on these segments are used to approximate the solution of each integral equation. Such a numerical procedure corresponds to a particular case of the well-known boundary element method (BEM), where Lagrange finite elements of the $\mathbb{P}_0$-type are used on the boundary. Some useful books on boundary element methods that include application to static or dynamic elasticity are, e.g., Manolis & Beskos (1988), Bonnet (1995), Linkov (2002), Steinbach (2007) and Beer et al. (2008). The numerical discretization of each integral equation gives rise to linear systems of equations, where the coefficients of the respective matrices contain double integrals that represent elemental interactions between each pair of segments. We carefully perform the boundary element calculations, that is, the computation of these elemental integrals, which contain the Green's function and its normal derivative. As both of these tensors have singularities, there are some cases where it is not possible to calculate the integrals in a numerical way, so we use a semi-analytical integration method based upon the work by Bendali & Devys (1996). Otherwise, the integrals are computed numerically by two-points quadrature formulae.

5.2 Dirichlet and Neumann exterior scattering

5.2.1 Variational formulations

In order to solve the integral equations obtained in Section 4.2, they are converted into their variational or weak formulation. Basically, the integral equation is first multiplied by a certain test function, and then it is integrated over the boundary under study. The test functions are taken in the same function space as the solution of the equation. Let us begin by the single layer integral equation (4.74) that solves the exterior scattering with Dirichlet boundary conditions. If we consider the trace of $\boldsymbol{u}^{\text{inc}}$ on Γ to lie in $[H^{1/2}(\Gamma)]^2$, as the single layer operator takes its values also in $[H^{1/2}(\Gamma)]^2$ (see (4.69a)), we have that (4.74) holds in the same function space, that is,

$$S_i^k q_i = -u_k^{\text{inc}} \qquad \text{in } [H^{1/2}(\Gamma)]^2. \tag{5.1}$$

As the domain of the single layer operator corresponds to $[H^{-1/2}(\Gamma)]^2$ (see (4.69a)), we infer that the solution $\boldsymbol{q} = (q_1, q_2)$ of (5.1) has to be searched in this function space. The

test functions of the variational formulation, denoted generically by $\boldsymbol{q}^t = (q_1^t, q_2^t)$, are thus taken in $[H^{-1/2}(\Gamma)]^2$. Therefore, we apply on both sides of (5.1) a product of duality (between $H^{-1/2}(\Gamma)$ and $H^{1/2}(\Gamma)$) by an arbitrary test function. The resulting variational formulation is: Find $\boldsymbol{q} = (q_1, q_2) \in [H^{-1/2}(\Gamma)]^2$ such that

$$\langle q_k^t, S_i^k q_i \rangle = -\langle q_k^t, u_k^{\text{inc}} \rangle, \qquad \forall \boldsymbol{q}^t = (q_1^t, q_2^t) \in [H^{-1/2}(\Gamma)]^2. \tag{5.2}$$

This theoretical form of the variational formulation is not very useful in numerical applications, so what we do is to restate it in a more explicit and convenient way by formally expressing the products of duality as integrals on Γ. In addition, the single layer potential is also written as an integral on Γ using its definition given in (4.66). Hence, (5.2) is restated as: Find $\boldsymbol{q} = (q_1, q_2) \in [H^{-1/2}(\Gamma)]^2$ such that

$$\begin{aligned} &\int_\Gamma \int_\Gamma G_i^k(\boldsymbol{x}, \boldsymbol{y}) q_i(\boldsymbol{y}) \overline{q_k^t(\boldsymbol{x})} \mathrm{d}s(\boldsymbol{y}) \mathrm{d}s(\boldsymbol{x}) \\ &\qquad = -\int_\Gamma u_k^{\text{inc}}(\boldsymbol{x}) \overline{q_k^t(\boldsymbol{x})} \mathrm{d}s(\boldsymbol{x}) \qquad \forall \boldsymbol{q}^t = (q_1^t, q_2^t) \in [H^{-1/2}(\Gamma)]^2. \end{aligned} \tag{5.3}$$

We now obtain the variational formulation of the double layer integral equation (4.82) that solves the exterior scattering with Neumann boundary conditions. As both layer operators take their values in $[H^{1/2}(\Gamma)]^2$, it is straightforward to see that (5.4) holds in the same function space, that is,

$$D_i^k p_i + \frac{1}{2} p_k = -S_i^k t_i^{\text{inc}} \qquad \text{in } [H^{1/2}(\Gamma)]^2. \tag{5.4}$$

As the domain of the double layer operator is $H^{1/2}(\Gamma)$ (see (4.69b)), then the solution $\boldsymbol{p} = (p_1, p_2)$ of (5.4) has to be taken in $[H^{1/2}(\Gamma)]^2$, and so do the test functions, denoted by $\boldsymbol{p}^t = (p_1^t, p_2^t)$. We thus apply on both sides of (5.4) a $L^2(\Gamma)$-product by a test function, leading to the next variational formulation: Find $\boldsymbol{p} = (p_1, p_2) \in [H^{1/2}(\Gamma)]^2$ such that

$$(D_i^k p_i, p_k^t)_{0,\Gamma} + \frac{1}{2} (p_k, p_k^t)_{0,\Gamma} = -(S_i^k t_i^{\text{inc}}, p_k^t)_{0,\Gamma}, \qquad \forall \boldsymbol{p}^t = (p_1^t, p_2^t) \in [H^{1/2}(\Gamma)]^2. \tag{5.5}$$

Making explicit the $L^2(\Gamma)$-products and using the definitions of the single and double layer operators in terms of integrals on Γ, given respectively in (4.66) and (4.67), we obtain that (5.5) can be reexpressed as follows: Find $\boldsymbol{p} = (p_1, p_2) \in [H^{1/2}(\Gamma)]^2$ such that

$$\begin{aligned} &\int_\Gamma \int_\Gamma H_i^k(\boldsymbol{x}, \boldsymbol{y}) p_i(\boldsymbol{y}) \overline{p_k^t(\boldsymbol{x})} \mathrm{d}s(\boldsymbol{y}) \mathrm{d}s(\boldsymbol{x}) + \frac{1}{2} \int_\Gamma p_k(\boldsymbol{x}) \overline{p_k^t(\boldsymbol{x})} \mathrm{d}s(\boldsymbol{x}) \\ &\quad = -\int_\Gamma \int_\Gamma G_i^k(\boldsymbol{x}, \boldsymbol{y}) t_i^{\text{inc}}(\boldsymbol{y}) \overline{p_k^t(\boldsymbol{x})} \mathrm{d}s(\boldsymbol{y}) \mathrm{d}s(\boldsymbol{x}), \qquad \forall \boldsymbol{p}^t = (p_1^t, p_2^t) \in [H^{1/2}(\Gamma)]^2. \end{aligned} \tag{5.6}$$

5.2.2 Numerical discretization

We now develop a numerical discretization for (5.3) and (5.6) by means of the boundary element method (BEM). The boundary Γ is approximated by a discrete curve Γ^h (see Fig. 5.1), composed by N_h rectilinear segments T_m (the boundary elements), sequentially ordered in counterclockwise direction for $m = 1, \ldots, N_h$. The segments T_m are such that their lengths are less or equal than $h > 0$, that is, $|T_m| \leq h$ for all $m = 1, \ldots, N_h$. In addition, we suppose that all the endpoints of the segments are located on the non-discrete

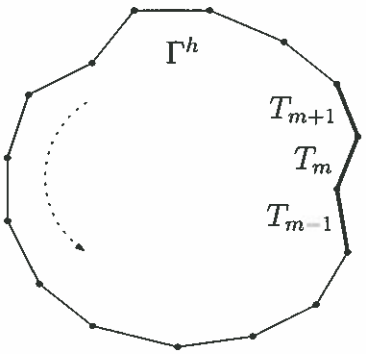

FIGURE 5.1. Discrete curve Γ^h approximating Γ.

boundary Γ. The curve Γ^h is thus described as:

$$\Gamma^h = \bigcup_{m=0}^{N_h} \overline{T_m}.$$

We define the space V^h of piecewise constant functions in Γ^h by

$$V^h = \left\{ q_h : \Gamma^h \to \mathbb{C} \ : \ q_h|_{T_m} = q^m, \ \forall m = 1, \ldots, N_h, \ \forall q^1, \ldots, q^{N_h} \in \mathbb{C} \right\}.$$

This space has finite dimension N_h. The canonical basis of V^h is composed by the functions χ_m shown in Fig. 5.2 and defined for $m = 1, \ldots, N_h$ as

$$\chi_m(\boldsymbol{x}) = \begin{cases} 1 & \text{if } \boldsymbol{x} \in T_m, \\ 0 & \text{if } \boldsymbol{x} \notin T_m. \end{cases} \tag{5.7}$$

It is straightforward to verify that the functions $\{\chi_m\}_{m=0}^{N_h}$ constitute an orthogonal set in $L^2(\Gamma^h)$ such that

$$\int_{\Gamma^h} \chi_n(\boldsymbol{x}) \chi_m(\boldsymbol{x}) \mathrm{d}s(\boldsymbol{x}) = \begin{cases} |T_n| & \text{if } m = n, \\ 0 & \text{if } m \neq n. \end{cases} \tag{5.8}$$

In virtue of the discretization, any function $q_h \in V^h$ can be expressed as a linear combination of the basis functions, that is

$$q_h(\boldsymbol{x}) = \sum_{m=1}^{N_h} q^m \chi_m(\boldsymbol{x}) \qquad \boldsymbol{x} \in \Gamma^h, \tag{5.9}$$

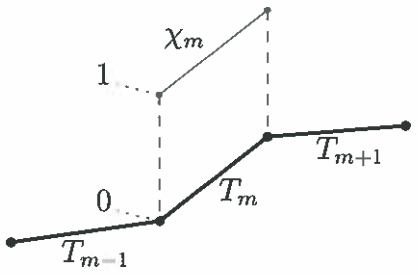

FIGURE 5.2. Piecewise basis function χ_m.

where for $m = 1, \ldots, N_h$, $q^m = q_h|_{T_m} \in \mathbb{C}$. Let us discretize the variational formulation given in (5.3), for which we approximate the associated function space $[H^{-1/2}(\Gamma)]^2$ by $[V^h]^2$. Such an approximation is called conformal, since $V^h \subset H^{-1/2}(\Gamma)$. Notice that the discrete space $[V^h]^2$ has dimension $2N_h$. The basis of this space is constructed from the functions χ_m defined in (5.7). We denote the $2N_h$ vector basis functions of $[V^h]^2$ by $\boldsymbol{\psi}_m^\ell = (\psi_{m1}^\ell, \psi_{m2}^\ell)$, where $\ell = 1, 2$ and $m = 1, \ldots, N_h$. These functions are defined as

$$\psi_{mk}^\ell(\boldsymbol{x}) = \delta_{k\ell}\, \chi_m(\boldsymbol{x}), \qquad \boldsymbol{x} \in \Gamma^h. \tag{5.10}$$

We then seek a discrete solution of (5.3), namely $\boldsymbol{q}_h = (q_{h1}, q_{h2})$ in $[V^h]^2$, satisfying the following discrete variational formulation: Find $\boldsymbol{q}_h \in [V^h]^2$ such that

$$\begin{aligned} &\int_{\Gamma^h}\int_{\Gamma^h} G_i^k(\boldsymbol{x}, \boldsymbol{y}) q_{hi}(\boldsymbol{y}) \overline{q_{hk}^t(\boldsymbol{x})} \mathrm{d}s(\boldsymbol{y}) \mathrm{d}s(\boldsymbol{x}) \\ &\qquad = -\int_{\Gamma^h} u_k^{\mathrm{inc}}(\boldsymbol{x}) \overline{q_{hk}^t(\boldsymbol{x})} \mathrm{d}s(\boldsymbol{x}) \qquad \forall \boldsymbol{q}_h^t = (q_{h1}^t, q_{h2}^t) \in [V^h]^2. \end{aligned} \tag{5.11}$$

As the components of $\boldsymbol{q}_h$ are elements of V^h, they are written in the form (5.9), that is,

$$q_{hi}(\boldsymbol{y}) = \sum_{m=1}^{N_h} q_i^m \chi_m(\boldsymbol{y}) \qquad \boldsymbol{y} \in \Gamma^h, \tag{5.12}$$

where the $2N_h$ complex coefficients $\{(q_1^m, q_2^m)\}_{m=1}^{N_h}$ are unknown. Moreover, we take the test functions $\boldsymbol{q}_h^t$ in (5.11) as the vector basis functions $\boldsymbol{\psi}_n^\ell$ defined in (5.10). Hence, substituting (5.10) and (5.12) in (5.11) and rearranging yields

$$\begin{aligned} &\sum_{m=1}^{N_h} \int_{\Gamma^h}\int_{\Gamma^h} G_i^\ell(\boldsymbol{x}, \boldsymbol{y}) \chi_m(\boldsymbol{y}) \chi_n(\boldsymbol{x}) \mathrm{d}s(\boldsymbol{y}) \mathrm{d}s(\boldsymbol{x})\, q_i^m \\ &\qquad = -\int_{\Gamma^h} u_\ell^{\mathrm{inc}}(\boldsymbol{x}) \chi_n(\boldsymbol{x}) \mathrm{d}s(\boldsymbol{x}) \qquad \forall n = 1, \ldots, N_h, \end{aligned} \tag{5.13}$$

and using the definition (5.7) of functions χ_n to reexpress the boundary integrals, we restate (5.13) for each $n = 1, \ldots, N_h$ as

$$\sum_{m=1}^{N_h} \int_{T_n}\int_{T_m} G_i^\ell(\boldsymbol{x}, \boldsymbol{y}) \mathrm{d}s(\boldsymbol{y}) \mathrm{d}s(\boldsymbol{x})\, q_i^m = -\int_{T_n} u_\ell^{\mathrm{inc}}(\boldsymbol{x}) \mathrm{d}s(\boldsymbol{x}). \tag{5.14}$$

This constitutes a system of linear equations of size $2N_h$, which we can write by blocks as

$$\begin{bmatrix} S_1^1 & S_2^1 \\ S_1^2 & S_2^2 \end{bmatrix} \begin{bmatrix} \boldsymbol{q}_1 \\ \boldsymbol{q}_2 \end{bmatrix} = \begin{bmatrix} \boldsymbol{b}^1 \\ \boldsymbol{b}^2 \end{bmatrix}, \tag{5.15}$$

where for $k, i = 1, 2$, the blocks S_i^k are matrices of size N_h, defined by components as

$$\left[S_i^k\right]_{nm} = \int_{T_n}\int_{T_m} G_i^k(\boldsymbol{x}, \boldsymbol{y}) \mathrm{d}s(\boldsymbol{y}) \mathrm{d}s(\boldsymbol{x}), \qquad n, m = 1, \ldots, N_h, \tag{5.16}$$

and $\boldsymbol{q}_1, \boldsymbol{q}_2$ are unknown vectors, both of length N_h, defined as

$$\boldsymbol{q}_i = \left(q_i^1, \ldots, q_i^{N_h}\right), \qquad i = 1, 2. \tag{5.17}$$

The vectors $\boldsymbol{b}^1, \boldsymbol{b}^2$ on the right-hand side, also of length N_h, correspond to the integrals

$$\left[\boldsymbol{b}^k\right]_n = -\int_{T_n} u_k^{\text{inc}}(\boldsymbol{x})\mathrm{d}s(\boldsymbol{x}), \qquad k = 1, 2. \tag{5.18}$$

Hence, determining a solution to (5.11) is reduced to calculating the blocks and vectors defined in (5.16) and (5.18), respectively, and then solving the system given in (5.15), which yields the solution vector defined in (5.17). We now discretize the variational formulation given in (5.6). For the sake of simplicity, the function space $[H^{1/2}(\Gamma)]^2$ is also approximated by $[V^h]^2$. However, this approximation is not conformal, since $V^h \not\subset H^{1/2}(\Gamma)$. We already know that the basis of $[V^h]^2$ is constituted by the vector functions $\boldsymbol{\psi}_m^\ell$ given in (5.10). The discrete solution of (5.6), denoted by $\boldsymbol{p}_h = (p_{h1}, p_{h2})$ in $[V^h]^2$, is searched as a solution to the next discretized variational formulation: Find $\boldsymbol{p}_h \in [V^h]^2$ such that

$$\begin{aligned}
&\int_{\Gamma^h}\int_{\Gamma^h} H_i^k(\boldsymbol{x},\boldsymbol{y}) p_{hi}(\boldsymbol{y})\overline{p_{hk}^t(\boldsymbol{x})}\mathrm{d}s(\boldsymbol{y})\mathrm{d}s(\boldsymbol{x}) + \frac{1}{2}\int_{\Gamma^h} p_{hk}(\boldsymbol{x})\overline{p_{hk}^t(\boldsymbol{x})}\mathrm{d}s(\boldsymbol{x}) \\
&= -\int_{\Gamma^h}\int_{\Gamma^h} G_i^k(\boldsymbol{x},\boldsymbol{y}) t_i^{\text{inc}}(\boldsymbol{y})\overline{p_{hk}^t(\boldsymbol{x})}\mathrm{d}s(\boldsymbol{y})\mathrm{d}s(\boldsymbol{x}), \qquad \forall \boldsymbol{p}_h^t = (p_{h1}^t, p_{h2}^t) \in [V^h]^2.
\end{aligned} \tag{5.19}$$

Expressing the components of the solution $\boldsymbol{p}_h$ in the form (5.9) yields

$$p_{hi}(\boldsymbol{y}) = \sum_{m=1}^{N_h} p_i^m \chi_m(\boldsymbol{y}) \qquad \boldsymbol{y} \in \Gamma^h, \tag{5.20}$$

for unknown coefficients $\{(p_1^m, p_2^m)\}_{m=1}^{N_h}$. On the other hand, we take the test functions $\boldsymbol{p}_h^t$ in (5.19) as the vector basis functions $\boldsymbol{\psi}_n^\ell$ defined in (5.10). In addition, the components of the vector $\boldsymbol{t}^{\text{inc}}$ on Γ^h are also written in the form (5.9), giving

$$t_i^{\text{inc}}(\boldsymbol{y}) = \sum_{m=1}^{N_h} t_i^m \chi_m(\boldsymbol{y}) \qquad \boldsymbol{y} \in \Gamma^h, \tag{5.21}$$

where the complex coefficients $\{(t_1^m, t_2^m)\}_{m=1}^{N_h}$ can be computed in an approximated way as

$$t_i^m = \frac{1}{|T_m|}\int_{T_m} t_i^{\text{inc}}(\boldsymbol{x})\mathrm{d}s(\boldsymbol{x}). \tag{5.22}$$

Therefore, replacing (5.10), (5.20) and (5.21) in (5.19) and rearranging gives

$$\begin{aligned}
&\sum_{m=1}^{N_h}\int_{\Gamma^h}\int_{\Gamma^h} H_i^\ell(\boldsymbol{x},\boldsymbol{y})\chi_m(\boldsymbol{y})\chi_n(\boldsymbol{x})\mathrm{d}s(\boldsymbol{y})\mathrm{d}s(\boldsymbol{x})\, p_i^m \\
&+ \frac{1}{2}\sum_{m=1}^{N_h}\int_{\Gamma^h}\chi_m(\boldsymbol{x})\chi_n(\boldsymbol{x})\mathrm{d}s(\boldsymbol{x})\, p_\ell^m \\
&= -\sum_{m=1}^{N_h}\int_{\Gamma^h}\int_{\Gamma^h} G_i^\ell(\boldsymbol{x},\boldsymbol{y})\chi_m(\boldsymbol{y})\chi_n(\boldsymbol{x})\mathrm{d}s(\boldsymbol{y})\mathrm{d}s(\boldsymbol{x})\, t_i^m, \qquad \forall n = 1, \ldots, N_h,
\end{aligned} \tag{5.23}$$

and using (5.7) to reexpress the boundary integrals and combining with (5.8), it is possible to restate (5.23) as

$$\sum_{m=1}^{N_h} \int_{T_n}\int_{T_m} H_i^\ell(\boldsymbol{x},\boldsymbol{y})\mathrm{d}s(\boldsymbol{y})\mathrm{d}s(\boldsymbol{x})\, p_i^m + \frac{1}{2}|T_n|\, p_\ell^n = -\sum_{m=1}^{N_h} \int_{T_n}\int_{T_m} G_i^\ell(\boldsymbol{x},\boldsymbol{y})\mathrm{d}s(\boldsymbol{y})\mathrm{d}s(\boldsymbol{x})\, t_i^m \qquad \forall n = 1,\ldots,N_h. \tag{5.24}$$

This corresponds to a system of linear equations of size $2N_h$, which we write by blocks as

$$\begin{bmatrix} D_1^1 + \frac{1}{2}W_T & D_2^1 \\ D_1^2 & D_2^2 + \frac{1}{2}W_T \end{bmatrix} \begin{bmatrix} \boldsymbol{p}_1 \\ \boldsymbol{p}_2 \end{bmatrix} = \begin{bmatrix} \boldsymbol{v}^1 \\ \boldsymbol{v}^2 \end{bmatrix}, \tag{5.25}$$

where for $k, i = 1, 2$, the blocks D_i^k are matrices of size N_h, defined by components as

$$\left[D_i^k\right]_{nm} = \int_{T_n}\int_{T_m} H_i^k(\boldsymbol{x},\boldsymbol{y})\mathrm{d}s(\boldsymbol{y})\mathrm{d}s(\boldsymbol{x}), \qquad n, m = 1,\ldots,N_h, \tag{5.26}$$

and W_T is the diagonal matrix defined as

$$W_T = \mathrm{diag}\left(|T_1|, |T_2|, \ldots, |T_{N_h}|\right). \tag{5.27}$$

The unknown vectors $\boldsymbol{p}_1, \boldsymbol{p}_2$, both of length N_h, are defined as

$$\boldsymbol{p}_i = \left(p_i^1, \ldots, p_i^{N_h}\right), \qquad i = 1, 2, \tag{5.28}$$

and the right-hand side of the system corresponds to

$$\begin{bmatrix} \boldsymbol{v}^1 \\ \boldsymbol{v}^2 \end{bmatrix} = -\begin{bmatrix} S_1^1 & S_2^1 \\ S_1^2 & S_2^2 \end{bmatrix} \begin{bmatrix} \boldsymbol{t}_1 \\ \boldsymbol{t}_2 \end{bmatrix}, \tag{5.29}$$

where the blocks S_i^k are given in (5.16) and the vectors $\boldsymbol{t}_1, \boldsymbol{t}_2$ are defined as

$$\boldsymbol{t}_i = \left(t_i^1, \ldots, t_i^{N_h}\right), \qquad i = 1, 2. \tag{5.30}$$

Therefore, the problem of solving (5.19) is reduced to calculating the matrices defined in (5.26) and (5.27), the vectors defined in (5.29) and (5.30), and then solving the system given in (5.25). This yields the solution vector defined in (5.28).

5.3 Impedance scattering in the perturbed half-plane

5.3.1 Variational formulation

We next determine the variational form of the integral equation obtained in Section 4.3, which allows its numerical resolution. This equation, given in (4.125), solves the scattering in a perturbed half-plane with impedance boundary conditions. For the sake of simplicity and by analogy with the case of Neumann boundary conditions, we assume that this equation holds in $[H^{1/2}(\Gamma_p)]^2$, that is,

$$D_i^k p_i + \frac{1}{2} p_k - \omega S_i^k(Z_p p_\tau \tau_i) = -S_i^k f_i \qquad \text{in } [H^{1/2}(\Gamma_p)]^2. \tag{5.31}$$

We thus seek the solution $\boldsymbol{p} = (p_1, p_2)$ to (5.31) in $[H^{1/2}(\Gamma_p)]^2$, and the test functions, denoted by $\boldsymbol{p}^t = (p_1^t, p_2^t)$ are taken in the same function space. Applying on both sides of

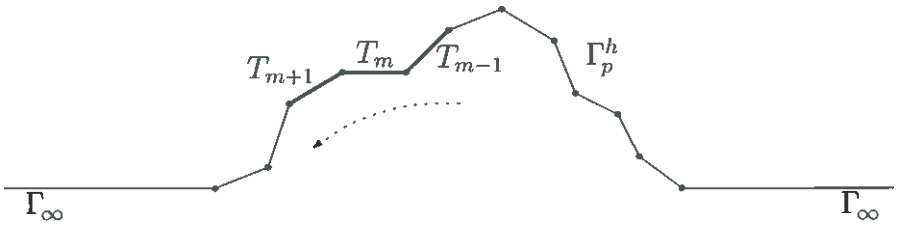

FIGURE 5.3. Discrete curve Γ_p^h approximating Γ_p.

(5.31) a $L^2(\Gamma_p)$-product by a generic test function, we obtain the next variational formulation: Find $\boldsymbol{p} = (p_1, p_2) \in [H^{1/2}(\Gamma_p)]^2$ such that

$$\begin{aligned} &\big(D_i^k p_i, p_k^t\big)_{0,\Gamma_p} + \frac{1}{2}\big(p_k, p_k^t\big)_{0,\Gamma_p} \\ &\quad - \omega\big(S_i^k(Z_p p_\tau \tau_i), p_k^t\big)_{0,\Gamma_p} = -\big(S_i^k f_i p_k^t\big)_{0,\Gamma_p} \qquad \forall \boldsymbol{p}^t = (p_1^t, p_2^t) \in [H^{1/2}(\Gamma_p)]^2. \end{aligned} \tag{5.32}$$

In order to deal with a more convenient expression of this variational formulation, the $L^2(\Gamma_p)$-products are made explicit and the single and double layer operators are written in terms of integrals, according to their definitions given in (4.114) and (4.115), respectively. The resulting variational formulation is: Find $\boldsymbol{p} = (p_1, p_2) \in [H^{1/2}(\Gamma_p)]^2$ such that

$$\begin{aligned} &\int_{\Gamma_p}\int_{\Gamma_p} H_i^k(\boldsymbol{x}, \boldsymbol{y}) p_i(\boldsymbol{y}) \overline{p_k^t(\boldsymbol{x})} \mathrm{d}s(\boldsymbol{y}) \mathrm{d}s(\boldsymbol{x}) + \frac{1}{2}\int_{\Gamma_p} p_k(\boldsymbol{x}) \overline{p_k^t(\boldsymbol{x})} \mathrm{d}s(\boldsymbol{x}) \\ &\quad - \omega \int_{\Gamma_p}\int_{\Gamma_p} Z_p(\boldsymbol{y}) G_i^k(\boldsymbol{x}, \boldsymbol{y}) \tau_i(\boldsymbol{y}) \tau_j(\boldsymbol{y}) p_j(\boldsymbol{y}) \overline{p_k^t(\boldsymbol{x})} \mathrm{d}s(\boldsymbol{y}) \mathrm{d}s(\boldsymbol{x}) \\ &\quad = \int_{\Gamma_p}\int_{\Gamma_p} G_i^k(\boldsymbol{x}, \boldsymbol{y}) f_i(\boldsymbol{y}) \overline{p_k^t(\boldsymbol{x})} \mathrm{d}s(\boldsymbol{y}) \mathrm{d}s(\boldsymbol{x}) \qquad \forall \boldsymbol{p}^t = (p_1^t, p_2^t) \in [H^{1/2}(\Gamma_p)]^2. \end{aligned} \tag{5.33}$$

5.3.2 Numerical discretization

Next, we study the numerical discretization of (5.33) by means of the boundary element method. The procedure is almost analogous to that developed in Section 5.2. The perturbed boundary Γ_p is approximated by a discrete curve Γ_p^h (see Fig. 5.3), composed by N_h rectilinear segments denoted by $\{T_m\}_{m=1}^{N_h}$, which are sequentially ordered from right to left for $m = 1, \ldots, N_h$. Given $h > 0$, these segments satisfy $|T_m| \leq h$, and their endpoints are placed just on the non-discrete curve Γ_p. Hence, the discrete curve Γ_p^h is described as

$$\Gamma_p^h = \bigcup_{m=0}^{N_h} \overline{T_m}.$$

The space V_p^h of piecewise constant functions in Γ^h is defined by

$$V_p^h = \big\{q_h : \Gamma_p^h \to \mathbb{C} \,:\, q_h|_{T_m} = q^m,\ \forall m = 1, \ldots, N_h,\ \forall q^1, \ldots, q^{N_h} \in \mathbb{C}\big\}.$$

The basis for this discrete space of dimension N_h is the same as before, that is, it consists of the functions $\{\chi_m\}_{m=1}^{N_h}$ illustrated in Fig. 5.2 and defined for $m = 1, \ldots, N_h$ as

$$\chi_m(\boldsymbol{x}) = \begin{cases} 1 & \text{if } \boldsymbol{x} \in T_m, \\ 0 & \text{if } \boldsymbol{x} \notin T_m. \end{cases} \tag{5.34}$$

These functions are an orthogonal set in $L^2(\Gamma_p^h)$ such that

$$\int_{\Gamma_p^h} \chi_n(\boldsymbol{x})\chi_m(\boldsymbol{x})\mathrm{d}s(\boldsymbol{x}) = \begin{cases} |T_n| & \text{if } m = n, \\ 0 & \text{if } m \neq n. \end{cases} \tag{5.35}$$

Consequently, any function $p_h \in V_p^h$ is expressed as a linear combination of the basis functions, that is,

$$p_h(\boldsymbol{x}) = \sum_{m=1}^{N_h} p^m \chi_m(\boldsymbol{x}) \qquad \boldsymbol{x} \in \Gamma_p^h, \tag{5.36}$$

where for each $m = 1, \ldots N_h$, $p^m \in \mathbb{C}$ corresponds to the constant value taken by the function p_h at the segment T_m. In order to discretize the variational formulation given in (5.33), we consider a non-conformal approach, where the function space $[H^{1/2}(\Gamma_p)]^2$ is approximated by $[V_p^h]^2$. The basis of this space consists of the $2N_h$ vector functions denoted by $\boldsymbol{\psi}_m^\ell = (\psi_{m1}^\ell, \psi_{m2}^\ell)$ for $\ell = 1, 2$ and $m = 1, \ldots N_h$, which are defined in terms of the functions χ_m in analogous way as above, that is,

$$\psi_{mk}^\ell(\boldsymbol{x}) = \delta_{k\ell}\chi_m(\boldsymbol{x}), \qquad \boldsymbol{x} \in \Gamma_p^h. \tag{5.37}$$

We thus seek an approximated solution of (5.33), denoted by $\boldsymbol{p}_h = (p_{h1}, p_{h2}) \in [V_p^h]^2$. This solution satisfies a discrete variational formulation obtained directly from (5.33) and expressed as: Find $\boldsymbol{p}_h \in [V_p^h]^2$ such that

$$\begin{aligned} &\int_{\Gamma_p^h}\int_{\Gamma_p^h} H_i^k(\boldsymbol{x},\boldsymbol{y})p_{hi}(\boldsymbol{y})\overline{p_{hk}^t(\boldsymbol{x})}\mathrm{d}s(\boldsymbol{y})\mathrm{d}s(\boldsymbol{x}) + \frac{1}{2}\int_{\Gamma_p^h} p_{hk}(\boldsymbol{x})\overline{p_{hk}^t(\boldsymbol{x})}\mathrm{d}s(\boldsymbol{x}) \\ &\quad - \omega\int_{\Gamma_p^h}\int_{\Gamma_p^h} Z_p(\boldsymbol{y})G_i^k(\boldsymbol{x},\boldsymbol{y})\tau_i(\boldsymbol{y})\tau_j(\boldsymbol{y})p_{hj}(\boldsymbol{y})\overline{p_{hk}^t(\boldsymbol{x})}\mathrm{d}s(\boldsymbol{y})\mathrm{d}s(\boldsymbol{x}) \\ &\quad = \int_{\Gamma_p^h}\int_{\Gamma_p^h} G_i^k(\boldsymbol{x},\boldsymbol{y})f_i(\boldsymbol{y})\overline{p_{hk}^t(\boldsymbol{x})}\mathrm{d}s(\boldsymbol{y})\mathrm{d}s(\boldsymbol{x}) \qquad \forall \boldsymbol{p}_h^t = (p_{h1}^t, p_{h2}^t) \in [V_p^h]^2. \end{aligned} \tag{5.38}$$

Since both components of the solution to (5.38) belong to the discrete space V_p^h, they are expressed in the form (5.36), that is,

$$p_{hi}(\boldsymbol{y}) = \sum_{m=1}^{N_h} p_i^m \chi_m(\boldsymbol{y}) \qquad \boldsymbol{y} \in \Gamma_p^h, \tag{5.39}$$

where $\{(p_1^m, p_2^m)\}_{m=1}^{N_h}$ are unknown coefficients. Furthermore, the components of the function $\boldsymbol{f} = (f_1, f_2)$ evaluated on Γ_p^h are also expressed in the form (5.36):

$$f_i(\boldsymbol{y}) = \sum_{m=1}^{N_h} f_i^m \chi_m(\boldsymbol{y}) \qquad \boldsymbol{y} \in \Gamma_p^h, \tag{5.40}$$

where $\{(f_1^m, f_2^m)\}_{m=1}^{N_h}$ are complex coefficients, approximately calculated as

$$f_i^m = \frac{1}{|T_m|} \int_{T_m} f_i(\boldsymbol{x}) \mathrm{d}s(\boldsymbol{x}). \tag{5.41}$$

As done before, the test functions $\boldsymbol{p}_h^t$ in (5.38) are taken as the basis functions $\boldsymbol{\psi}_n^\ell$ defined in (5.37). Therefore, replacing (5.39) and (5.40) in (5.38) gives

$$\begin{aligned}
&\sum_{m=1}^{N_h} \int_{\Gamma_p^h} \int_{\Gamma_p^h} H_i^\ell(\boldsymbol{x}, \boldsymbol{y}) \chi_m(\boldsymbol{y}) \chi_n(\boldsymbol{x}) \mathrm{d}s(\boldsymbol{y}) \mathrm{d}s(\boldsymbol{x})\, p_i^m \\
&+ \frac{1}{2} \sum_{m=1}^{N_h} \int_{\Gamma_p^h} \chi_m(\boldsymbol{x}) \chi_n(\boldsymbol{x}) \mathrm{d}s(\boldsymbol{x})\, p_\ell^m \\
&\quad - \omega \sum_{m=1}^{N_h} \int_{\Gamma_p^h} \int_{\Gamma_p^h} Z_p(\boldsymbol{y}) G_i^\ell(\boldsymbol{x}, \boldsymbol{y}) \tau_i(\boldsymbol{y}) \tau_j(\boldsymbol{y}) \chi_m(\boldsymbol{y}) \chi_n(\boldsymbol{x}) \mathrm{d}s(\boldsymbol{y}) \mathrm{d}s(\boldsymbol{x})\, p_j^m \\
&\quad = \sum_{m=1}^{N_h} \int_{\Gamma_p^h} \int_{\Gamma_p^h} G_i^\ell(\boldsymbol{x}, \boldsymbol{y}) \chi_m(\boldsymbol{y}) \chi_n(\boldsymbol{x}) \mathrm{d}s(\boldsymbol{y}) \mathrm{d}s(\boldsymbol{x})\, f_i^m \qquad \forall n = 1, \ldots, N_h,
\end{aligned} \tag{5.42}$$

and using (5.34) to reexpress the boundary integrals and combining with the orthogonality relation (5.35), we obtain that (5.42) is restated as

$$\begin{aligned}
&\sum_{m=1}^{N_h} \int_{T_n} \int_{T_m} H_i^\ell(\boldsymbol{x}, \boldsymbol{y}) \mathrm{d}s(\boldsymbol{y}) \mathrm{d}s(\boldsymbol{x})\, p_i^m + \frac{1}{2} |T_n|\, p_\ell^n \\
&\quad - \omega \sum_{m=1}^{N_h} \int_{T_n} \int_{T_m} Z_p(\boldsymbol{y}) G_i^\ell(\boldsymbol{x}, \boldsymbol{y}) \tau_i(\boldsymbol{y}) \tau_j(\boldsymbol{y}) \mathrm{d}s(\boldsymbol{y}) \mathrm{d}s(\boldsymbol{x})\, p_j^m \\
&\quad = \sum_{m=1}^{N_h} \int_{T_n} \int_{T_m} G_i^\ell(\boldsymbol{x}, \boldsymbol{y}) \mathrm{d}s(\boldsymbol{y}) \mathrm{d}s(\boldsymbol{x})\, f_i^m \qquad \forall n = 1, \ldots, N_h.
\end{aligned} \tag{5.43}$$

Moreover, notice that the tangent vectors are constant on each segment. Hence, the tangent vector associated with the segment T_m is denoted by $\boldsymbol{\tau}^m = (\tau_1^m, \tau_2^m)$. In addition, and for the sake of simplicity, the impedance Z_p is assumed to be piecewise constant. We thus restate (5.43) as

$$\begin{aligned}
&\sum_{m=1}^{N_h} \int_{T_n} \int_{T_m} H_i^\ell(\boldsymbol{x}, \boldsymbol{y}) \mathrm{d}s(\boldsymbol{y}) \mathrm{d}s(\boldsymbol{x})\, p_i^m + \frac{1}{2} |T_n|\, p_\ell^n \\
&\quad - \omega \sum_{m=1}^{N_h} Z_p^m \int_{T_n} \int_{T_m} G_i^\ell(\boldsymbol{x}, \boldsymbol{y}) \mathrm{d}s(\boldsymbol{y}) \mathrm{d}s(\boldsymbol{x})\, \tau_i^m \tau_j^m p_j^m \\
&\quad = \sum_{m=1}^{N_h} \int_{T_n} \int_{T_m} G_i^\ell(\boldsymbol{x}, \boldsymbol{y}) \mathrm{d}s(\boldsymbol{y}) \mathrm{d}s(\boldsymbol{x})\, f_i^m \qquad \forall n = 1, \ldots, N_h.
\end{aligned} \tag{5.44}$$

where $Z_p^m \in \mathbb{R}$ corresponds to the value that Z_p takes on the segment T_m. Identity (5.44) corresponds to a system of linear equations of size $2N_h$, which is written by blocks as

$$\begin{bmatrix} D_1^1 + \frac{1}{2}W_T + W_Z\mathcal{T}_1S_\tau^1 & D_2^1 + W_Z\mathcal{T}_2S_\tau^1 \\ D_1^2 + W_Z\mathcal{T}_1S_\tau^2 & D_2^2 + \frac{1}{2}W_T + W_Z\mathcal{T}_2S_\tau^2 \end{bmatrix} \begin{bmatrix} \boldsymbol{p}_1 \\ \boldsymbol{p}_2 \end{bmatrix} = \begin{bmatrix} \boldsymbol{v}^1 \\ \boldsymbol{v}^2 \end{bmatrix}, \tag{5.45}$$

where for $k, i = 1, 2$, the matrices D_i^k are defined by components as

$$\left[D_i^k\right]_{nm} = \int_{T_n}\int_{T_m} H_i^k(\boldsymbol{x}, \boldsymbol{y})\mathrm{d}s(\boldsymbol{y})\mathrm{d}s(\boldsymbol{x}), \qquad n, m = 1, \ldots, N_h, \tag{5.46}$$

and W_T and W_Z correspond to the diagonal matrices

$$W_T = \operatorname{diag}\left(|T_1|, |T_2|, \ldots, |T_{N_h}|\right), \qquad W_Z = \operatorname{diag}\left(Z_p^1, Z_p^2, \ldots, Z_p^{N_h}\right). \tag{5.47}$$

The terms $\mathcal{T}_1$ and $\mathcal{T}_2$ are also diagonal matrices, defined by

$$\mathcal{T}_i = \operatorname{diag}\left(\tau_1^i, \tau_2^i, \ldots, \tau_{N_h}^i\right), \qquad i = 1, 2, \tag{5.48}$$

and the matrices S_τ^1 and S_τ^2 are given in tensor notation by

$$S_\tau^k = \mathcal{T}_i S_i^k \qquad k = 1, 2 \tag{5.49}$$

where for $k, i = 1, 2$, the matrices S_i^k are defined by components as

$$\left[S_i^k\right]_{nm} = \int_{T_n}\int_{T_m} G_i^k(\boldsymbol{x}, \boldsymbol{y})\mathrm{d}s(\boldsymbol{y})\mathrm{d}s(\boldsymbol{x}), \qquad n, m = 1, \ldots, N_h. \tag{5.50}$$

The unknown vectors $\boldsymbol{p}_1, \boldsymbol{p}_2$ are defined as

$$\boldsymbol{p}_i = \left(p_i^1, \ldots, p_i^{N_h}\right), \qquad i = 1, 2, \tag{5.51}$$

and the right-hand side of the system is

$$\begin{bmatrix} \boldsymbol{v}^1 \\ \boldsymbol{v}^2 \end{bmatrix} = -\begin{bmatrix} S_1^1 & S_2^1 \\ S_1^2 & S_2^2 \end{bmatrix} \begin{bmatrix} \boldsymbol{f}_1 \\ \boldsymbol{f}_2 \end{bmatrix}. \tag{5.52}$$

Therefore, the problem of determining a solution to (5.38) is reduced to that of computing the matrices and vectors defined in (5.46), (5.47), (5.48), (5.49), (5.50) and (5.52), and then solving the linear system given in (5.45), which yields the solution vector defined in (5.51).

5.4 Boundary element calculations

5.4.1 Geometry

The boundary element calculations build the matrices of the linear systems (5.15), (5.25) and (5.45), which result from the discretization of different integral equations. We concentrate our attention mainly on computing numerically the elements of the blocks defined in (5.16), (5.26), (5.46) and (5.50). The main difficulty here lies in integrating the singularities of the Green's function and its normal derivative. On the other hand, the regular terms are numerically integrated by a quadrature formula. Therefore, the procedure does not change substantially if instead of dealing with the full-plane Green's function, we consider the half-plane Green's function, since the singular part remains invariant and only

regular terms are added. Let us consider a discrete curve composed by N_h rectilinear segments, which corresponds to either the closed curve Γ^h illustrated in Fig. 5.1 or the open curve Γ_p^h illustrated in Fig. 5.3, both oriented as indicated before, that is, in counterclockwise direction. We deal with the elemental interactions between two generic segments T_n and T_m, for $n, m = 1, \ldots, N_h$. For the sake of simplicity, we make a change of notation, and these segments are denoted by $K = T_n$ and $L = T_m$. In addition, the following notation is used from now on:

- h_K denotes the length of segment K.
- h_L denotes the length of segment L.
- $\boldsymbol{x}^p$, $\boldsymbol{x}^n$ denote the endpoints of segment K, agreeing with the curve orientation.
- $\boldsymbol{y}^p$, $\boldsymbol{y}^n$ denote the endpoints of segment L, agreeing with the curve orientation.
- $\boldsymbol{x}$ denotes a variable point on segment K.
- $\boldsymbol{y}$ denotes a variable point on segment L.

Fig. 5.4 shows the geometrical location of both segments and the points defined above, with respect to an origin $\mathcal{O}$. Notice that the length of segments K and L can be obtained as

$$h_K = |\boldsymbol{x}^n - \boldsymbol{x}^p|, \qquad h_L = |\boldsymbol{y}^n - \boldsymbol{y}^p|. \tag{5.53}$$

The unit tangent vector of segment L, denoted by $\boldsymbol{\tau} = (\tau_1, \tau_2)$ is calculated as

$$\boldsymbol{\tau} = \frac{\boldsymbol{y}^n - \boldsymbol{y}^p}{h_L}, \tag{5.54}$$

and the unit normal vector on L, denoted by $\boldsymbol{n} = (n_1, n_2)$, is obtained from $\boldsymbol{\tau}$ as follows:

$$(n_1, n_2) = (-\tau_2, \tau_1). \tag{5.55}$$

Notice that the vectors $\boldsymbol{\tau}$ and $\boldsymbol{n}$ are such that $\boldsymbol{\tau} \times \boldsymbol{n} = \hat{\boldsymbol{e}}_1 \times \hat{\boldsymbol{e}}_2$, as indicated in Fig. 5.5. For the elemental interactions between a point $\boldsymbol{x}$ on K and another point $\boldsymbol{y}$ on L, the following notation is also used:

- $\boldsymbol{r}$ denotes the vector pointing from $\boldsymbol{x}$ towards $\boldsymbol{y}$.
- r denotes the distance between $\boldsymbol{x}$ and $\boldsymbol{y}$.

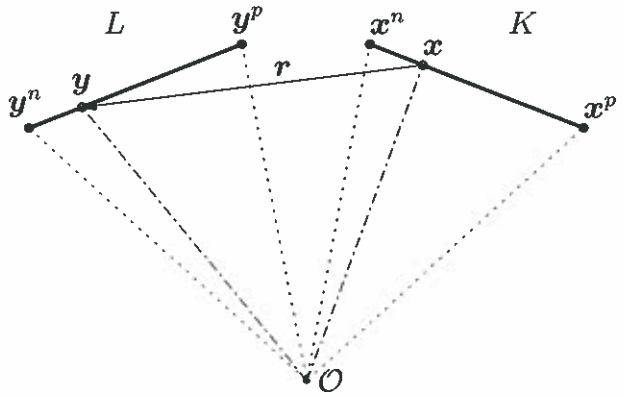

FIGURE 5.4. Geometry of segments K and L.

FIGURE 5.5. Geometry of segment L, unit tangent vector τ and unit normal vector n.

These values are given by

$$r = y - x, \tag{5.56}$$

$$r = |r| = |y - x|. \tag{5.57}$$

Furthermore, for the calculation of singular integrals, where the point x is regarded as a parameter, the following notation is also used (see. Fig. 5.6):

- r^p, r^n denote the vectors pointing from x towards the endpoints of segment L.
- r^p, r^n denote the distances between x and the endpoints of segment L.
- θ_p, θ_n denote the angles formed by the vectors r^p, r^n and the horizontal axis.
- θ_L denotes the signed angle formed by the vectors r^p and r^n.

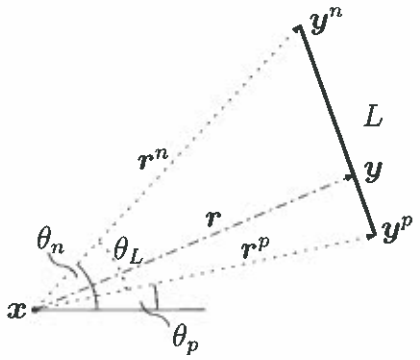

FIGURE 5.6. Geometry of segment L with x considered as a parameter.

The vectors r^p, r^n and distances r^p, r^n can be obtained as

$$r^p = y^p - x, \qquad r^n = y^n - x, \tag{5.58}$$

$$r^p = |r^p| = |y^p - x|, \qquad r^n = |r^n| = |y^n - x|, \tag{5.59}$$

and the angles θ_p, θ_n are defined as

$$\theta_p = \arctan\left(r_2^p / r_1^p\right), \qquad -\pi < \theta_p \leq \pi, \tag{5.60}$$

$$\theta_n = \arctan\left(r_2^n / r_1^n\right), \qquad -\pi < \theta_n \leq \pi. \tag{5.61}$$

On the other hand, the angle θ_L, which lies between $-\pi$ and π, is considered positive if L is counterclockwise oriented with respect to x, and negative if L is clockwise oriented with respect to x. In most of cases, θ_L can be simply obtained as the difference between θ_n and

θ_p. However, if the segment L crosses the left horizontal semiaxis, this difference will be larger in absolute value than π and a correction term of $\pm 2\pi$ is necessary. Taking all this into account, the exact definition of the signed angle θ_L is

$$\theta_L = \begin{cases} \theta_n - \theta_p + 2\pi & \text{if } \pi/2 < \theta_p \leq \pi \text{ and } -\pi \leq \theta_n < -\pi/2, \\ \theta_n - \theta_p - 2\pi & \text{if } -\pi \leq \theta_p < -\pi/2 \text{ and } \pi/2 < \theta_n \leq \pi, \\ \theta_n - \theta_p & \text{in any other case.} \end{cases} \tag{5.62}$$

5.4.2 Boundary element integrals

The boundary element integrals are the basic integrals on segments K and L that are needed in order to perform the boundary element calculations. These integrals are

$$IS_i^k = \int_K \int_L G_i^k(\boldsymbol{x}, \boldsymbol{y}) \mathrm{d}s(\boldsymbol{y}) \mathrm{d}s(\boldsymbol{x}) \qquad 1 \leq k, i \leq 2, \tag{5.63a}$$

$$ID_i^k = \int_K \int_L H_i^k(\boldsymbol{x}, \boldsymbol{y}) \mathrm{d}s(\boldsymbol{y}) \mathrm{d}s(\boldsymbol{x}) \qquad 1 \leq k, i \leq 2, \tag{5.63b}$$

where the second-order tensors G and H are the full-plane (or half-plane) Green's function and its normal derivative. Let us recall that both tensors have singularities at $\boldsymbol{y} = \boldsymbol{x}$. When the segments K and L are far away from each other, these singularities are irrelevant and the integrals (5.63a) and (5.63b) can be numerically approximated by quadrature formulae. Nevertheless, when K and L are close together, and specially if they coincide, the singularities of G and H play a central role and the integrals (5.63) cannot be computed numerically. We use instead a semi-analytical integration method, which is based upon the work done by Bendali & Devys (1996). The integrals (5.63) are decomposed as

$$IS_i^k = \int_K IG_i^k(\boldsymbol{x}) \mathrm{d}s(\boldsymbol{x}), \tag{5.64a}$$

$$ID_i^k = \int_K IH_i^k(\boldsymbol{x}) \mathrm{d}s(\boldsymbol{x}), \tag{5.64b}$$

where IG_i^k and IH_i^k correspond to the internal integrals in $\boldsymbol{y}$, that is,

$$IG_i^k(\boldsymbol{x}) = \int_L G_i^k(\boldsymbol{x}, \boldsymbol{y}) \mathrm{d}s(\boldsymbol{y}), \tag{5.65a}$$

$$IH_i^k(\boldsymbol{x}) = \int_L H_i^k(\boldsymbol{x}, \boldsymbol{y}) \mathrm{d}s(\boldsymbol{y}). \tag{5.65b}$$

This decomposition permits computing the integrals (5.63) in two steps. Firstly, we compute the internal integrals (5.65) as functions of $\boldsymbol{x}$. To do so, the singular parts of the Green's function G and its normal derivative H are isolated and integrated by analytical techniques, whereas the remaining regular parts are integrated numerically. After that, the resulting expressions are replaced in (5.64), and the external integrals are then computed numerically by quadrature formulae.

5.4.3 Numerical integration of the non-singular integrals

The numerical integration of the non-singular integrals is performed by means of a two-point Gauss quadrature formula (see, e.g., Abramowitz & Stegun 1970). For this, we

define the next points on segments K and L:

$$\boldsymbol{x}^1 = t_2\,\boldsymbol{x}^p + t_1\,\boldsymbol{x}^n, \qquad \boldsymbol{x}^2 = t_1\,\boldsymbol{x}^p + t_2\,\boldsymbol{x}^n, \tag{5.66a}$$

$$\boldsymbol{y}^1 = t_2\,\boldsymbol{y}^p + t_1\,\boldsymbol{y}^n, \qquad \boldsymbol{y}^2 = t_1\,\boldsymbol{y}^p + t_2\,\boldsymbol{y}^n, \tag{5.66b}$$

where

$$t_1 = \frac{1}{2}\left(1 - \frac{1}{\sqrt{3}}\right), \qquad t_2 = \frac{1}{2}\left(1 + \frac{1}{\sqrt{3}}\right). \tag{5.67}$$

Given two functions $\varphi(\cdot) : K \to \mathbb{C}$ and $\psi(\cdot) : L \to \mathbb{C}$, the formulae to approximate their integrals on K and L are given respectively by

$$\int_K \varphi(\boldsymbol{x})\mathrm{d}s(\boldsymbol{x}) \approx \frac{h_K}{2}\big(\varphi(\boldsymbol{x}^1) + \varphi(\boldsymbol{x}^2)\big), \tag{5.68a}$$

$$\int_L \psi(\boldsymbol{y})\mathrm{d}s(\boldsymbol{y}) \approx \frac{h_L}{2}\big(\psi(\boldsymbol{y}^1) + \psi(\boldsymbol{y}^2)\big). \tag{5.68b}$$

It is not difficult to extend the Gauss quadrature formula to a function of two variables $\Phi(\cdot,\cdot) : K \times L \to \mathbb{C}$, using for this formulae (5.68a) and (5.68b). The new formula is given by

$$\begin{aligned}\int_K \int_L \Phi(\boldsymbol{x},\boldsymbol{y})\mathrm{d}s(\boldsymbol{y})\mathrm{d}s(\boldsymbol{s}) \\ \approx \frac{h_K h_L}{4}\Big(\Phi(\boldsymbol{x}^1,\boldsymbol{y}^1) + \Phi(\boldsymbol{x}^1,\boldsymbol{y}^2) + \Phi(\boldsymbol{x}^2,\boldsymbol{y}^1) + \Phi(\boldsymbol{x}^2,\boldsymbol{y}^2)\Big).\end{aligned} \tag{5.69}$$

The points where the non-singular integrals have to be evaluated in order to perform the numerical integration are illustrated in Fig. 5.7.

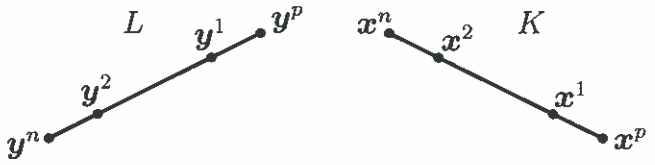

FIGURE 5.7. Evaluation points for the numerical integration.

5.4.4 Analytical integration of the singular integrals

We now develop the integration of the singular part of integrals (5.65). This integration is analytically performed in $\boldsymbol{y}$ for $\boldsymbol{x}$ constant, and as said above, the external integrals in $\boldsymbol{x}$ can be subsequently calculated by employing the quadrature formula (5.68a). We begin by calculating the singular part of (5.65a), which involves the Green's function G. In order to perform the integration, it is necessary to previously isolate the singularity of G. From (4.16) and (4.23), we recall that the full-plane Green's function is written in function of $r = |\boldsymbol{y} - \boldsymbol{x}|$ as

$$G_i^k(r) = \frac{\mathrm{i}}{4\mu}\big(A(r)\delta_{ik} + B(r)r_{,i}r_{,k}\big), \tag{5.70}$$

where the functions $A(\cdot)$ and $B(\cdot)$ were defined in (4.17). Using the expressions of Hankel functions for small argument given in (B.16), it is possible to approximate these functions for r small. We obtain that

$$A(r) \sim \frac{\mathrm{i}(1+\beta^2)}{\pi} \ln r, \qquad B(r) \sim -\frac{\mathrm{i}(1+\beta^2)}{\pi} \qquad \text{as } r \sim 0, \tag{5.71}$$

that is, we have that A has a logarithmic singularity, while B is actually bounded near the origin. We thus substitute (5.71) in (5.70), and the Green's function is reexpressed in a general way as

$$G_i^k(r) = -\frac{1+\beta^2}{4\pi\mu} \ln r \, \delta_{ik} + [G^R]_i^k(r), \tag{5.72}$$

where the tensor G^R contains only regular terms in r. This tensor can be determined explicitly using expressions (B.16). If we are dealing with the half-plane Green's function, it is further necessary to add to (5.72) the regular tensor G^B that appears in (4.89). The singular part of the integral (5.65a) then corresponds to

$$[IG^S]_i^k(\boldsymbol{x}) = -\frac{1+\beta^2}{4\pi\mu} \int_L \ln r \, \mathrm{d}s(\boldsymbol{y}) \delta_{ik}, \tag{5.73}$$

and we need to calculate only one singular integral, which is scalar and it is given by

$$IA(\boldsymbol{x}) = \int_L \ln r \, \mathrm{d}s(\boldsymbol{y}). \tag{5.74}$$

The calculation of this integral is based on taking a scalar function $w = w(r)$ that is bounded near zero and is such that

$$\triangle w(r) = \frac{1}{r} \frac{\mathrm{d}}{\mathrm{d}r} \Big(r \frac{\mathrm{d}w}{\mathrm{d}r}(r) \Big) = \ln r, \tag{5.75}$$

and we consider on the segment L the local basis constituted by the pair of mutually orthogonal unit vectors $(\boldsymbol{\tau}, \boldsymbol{n})$ defined respectively in (5.54) and (5.55). In order to simplify the analysis, we assume the origin to be placed at $\boldsymbol{x}$. As this is a fixed point, we do not lose generality with this assumption. In that case, we have that $\boldsymbol{r} = \boldsymbol{y} - \boldsymbol{x}$ lies on L. Let us allow $\boldsymbol{r}$ to come out of L, by expressing it in terms of two parameters s and t as

$$\boldsymbol{r} = \boldsymbol{r}^p + s\boldsymbol{\tau} + t\boldsymbol{n}. \tag{5.76}$$

If we set $t = 0$ and we take $0 \leq s \leq h_L$, then (5.76) corresponds to a parametrization of L. Replacing (5.75) in (5.74) and resorting to the fact that the Laplacian is invariant under a change of orthonormal basis, we can write

$$IA(\boldsymbol{x}) = \int_L \Big(\frac{\partial^2 w}{\partial s^2} + \frac{\partial^2 w}{\partial t^2} \Big) \mathrm{d}s(\boldsymbol{y}), \tag{5.77}$$

and after further calculation,

$$IA(\boldsymbol{x}) = \frac{\partial w}{\partial s}\Big|_{s=h_L} - \frac{\partial w}{\partial s}\Big|_{s=0} + \int_L \frac{\partial^2 w}{\partial t^2} \mathrm{d}s(\boldsymbol{y}). \tag{5.78}$$

On the other hand, it can be obtained from (5.75) that

$$\nabla w = \frac{\mathrm{d}w}{\mathrm{d}r} \frac{\boldsymbol{r}}{r} = \frac{1}{2} \Big(\ln r - \frac{1}{2} \Big) \boldsymbol{r}. \tag{5.79}$$

This relation permits us to easily compute the derivatives of w with respect to s and t:

$$\frac{\partial w}{\partial s} = \nabla w \cdot \boldsymbol{\tau} = \frac{1}{2}\Big(\ln r - \frac{1}{2}\Big)\boldsymbol{r} \cdot \boldsymbol{\tau}, \tag{5.80a}$$

$$\frac{\partial w}{\partial t} = \nabla w \cdot \boldsymbol{n} = \frac{1}{2}\Big(\ln r - \frac{1}{2}\Big)\boldsymbol{r} \cdot \boldsymbol{n}, \tag{5.80b}$$

and also the second derivative of w with respect to t, which is calculated from (5.80b):

$$\frac{\partial^2 w}{\partial t^2} = \frac{1}{2}\boldsymbol{r} \cdot \boldsymbol{n}\frac{\partial}{\partial t}\ln r + \frac{1}{2}\Big(\ln r - \frac{1}{2}\Big)\frac{\partial}{\partial t}\boldsymbol{r} \cdot \boldsymbol{n}. \tag{5.81}$$

From (5.76) we obtain

$$\boldsymbol{r} \cdot \boldsymbol{n} = \boldsymbol{r}^p \cdot \boldsymbol{n} + t, \tag{5.82}$$

which implies that

$$\frac{\partial}{\partial t}\boldsymbol{r} \cdot \boldsymbol{n} = 1. \tag{5.83}$$

Furthermore, it holds that

$$\frac{\partial}{\partial t}\ln r = \nabla \ln r \cdot \boldsymbol{n} = \frac{\boldsymbol{r} \cdot \boldsymbol{n}}{r^2}, \tag{5.84}$$

and substituting (5.83) and (5.84) in (5.81) yields

$$\frac{\partial^2 w}{\partial t^2} = \frac{1}{2}\Big(\frac{\boldsymbol{r} \cdot \boldsymbol{n}}{r}\Big)^2 + \frac{1}{2}\Big(\ln r - \frac{1}{2}\Big). \tag{5.85}$$

Thus, combining (5.78) with (5.80a) and (5.85) leads to the following relation for $IA(\boldsymbol{x})$:

$$\begin{aligned} IA(\boldsymbol{x}) = {} & \frac{1}{2}\Big(\ln r^n - \frac{1}{2}\Big)\boldsymbol{r}^n \cdot \boldsymbol{\tau} - \frac{1}{2}\Big(\ln r^p - \frac{1}{2}\Big)\boldsymbol{r}^p \cdot \boldsymbol{\tau} \\ & + \frac{1}{2}\int_L \Big(\frac{\boldsymbol{r} \cdot \boldsymbol{n}}{r}\Big)^2 \mathrm{d}s(\boldsymbol{y}) + \frac{1}{2}IA(\boldsymbol{x}) - \frac{1}{4}h_L, \end{aligned} \tag{5.86}$$

and after rearranging terms and combining with (5.54) and (5.82), we obtain

$$IA(\boldsymbol{x}) = \boldsymbol{r}^n \cdot \boldsymbol{\tau}\,\ln r^n - \boldsymbol{r}^p \cdot \boldsymbol{\tau}\,\ln r^p - h_L + IF(\boldsymbol{x}), \tag{5.87}$$

where

$$IF(\boldsymbol{x}) = \int_L \Big(\frac{\boldsymbol{r}^p \cdot \boldsymbol{n}}{r}\Big)^2 \mathrm{d}s(\boldsymbol{y}). \tag{5.88}$$

Let us compute this integral. It should be observed that if $\boldsymbol{x} \in L$, then $\boldsymbol{r}^p$ is parallel to $\boldsymbol{\tau}$ and orthogonal to $\boldsymbol{n}$, and consequently, $IF(\boldsymbol{x})$ vanishes. Otherwise, we consider a different parametrization of L, which uses an angular variable θ. Setting t to zero in (5.76) yields the parametrization of L in function of s:

$$\boldsymbol{r}(s) = \boldsymbol{r}^p + s\boldsymbol{\tau} \qquad 0 \le s \le h_L, \tag{5.89}$$

and the angle formed by $\boldsymbol{r}(s)$ and the horizontal axis, denoted by θ, is defined by

$$\tan\theta = \frac{r_2^p + s\tau_2}{r_1^p + s\tau_1}, \tag{5.90}$$

from which it is possible to obtain s as a function of θ

$$s = -\frac{r_2^p \cos\theta - r_1^p \sin\theta}{\tau_2 \cos\theta - \tau_1 \sin\theta}. \tag{5.91}$$

Then, replacing (5.91) in (5.89), using (5.55) and expanding yields the desired parametrization of L in terms of the angle θ:

$$\boldsymbol{r}(\theta) = \frac{\boldsymbol{r}^p \cdot \boldsymbol{n}}{\hat{\boldsymbol{r}}(\theta) \cdot \boldsymbol{n}}\, \hat{\boldsymbol{r}}(\theta) \qquad \theta_p \leq \theta \leq \theta_n, \tag{5.92}$$

where $\hat{\boldsymbol{r}}(\theta) = (\cos\theta, \sin\theta)$. The integral IF is calculated as a non-oriented line integral:

$$IF(\boldsymbol{x}) = \int_{\theta_p}^{\theta_n} \left(\frac{\boldsymbol{r}^p \cdot \boldsymbol{n}}{|\boldsymbol{r}(\theta)|}\right)^2 |\boldsymbol{r}'(\theta)|\, \operatorname{sign}\theta_L \, \mathrm{d}\theta, \tag{5.93}$$

where the sign of θ_L has been added to the integral, in order to make it independent from the orientation of L. Substituting (5.92) in (5.93) and expanding gives

$$IF(\boldsymbol{x}) = \operatorname{sign}\,\theta_L \int_{\theta_p}^{\theta_n} |\boldsymbol{r}^p \cdot \boldsymbol{n}| \mathrm{d}\theta = \left|\boldsymbol{r}^p \cdot \boldsymbol{n}\right| |\theta_L|. \tag{5.94}$$

Moreover, it is not difficult to show by geometrical arguments that the terms $\boldsymbol{r}^p \cdot \boldsymbol{n}$ and θ_L have always opposite signs. Therefore, it holds that

$$IF(\boldsymbol{x}) = -\boldsymbol{r}^p \cdot \boldsymbol{n}\, \theta_L, \tag{5.95}$$

and substituting (5.95) in (5.87), we obtain an exact expression for the integral $IA(\boldsymbol{x})$:

$$IA(\boldsymbol{x}) = \boldsymbol{r}^n \cdot \boldsymbol{\tau}\, \ln r^n - \boldsymbol{r}^p \cdot \boldsymbol{\tau}\, \ln r^p - h_L - \boldsymbol{r}^p \cdot \boldsymbol{n}\, \theta_L. \tag{5.96}$$

Finally, substitution of (5.96) in (5.73) yields the singular integral IG^S:

$$[IG^S]_i^k(\boldsymbol{x}) = -\frac{1+\beta^2}{4\pi\mu}\big(\boldsymbol{r}^n \cdot \boldsymbol{\tau}\, \ln r^n - \boldsymbol{r}^p \cdot \boldsymbol{\tau}\, \ln r^p - h_L - \boldsymbol{r}^p \cdot \boldsymbol{n}\, \theta_L\big)\delta_{ik}. \tag{5.97}$$

Let us compute now the singular part of (5.65b), which involves the Green's function's normal derivative H. As done for the other integral, we start by isolating the singularity of H. We obtain from (4.18) and (4.29) that H is written in function of r as

$$H_i^k(r) = \frac{\mathrm{i}}{4}\big(\big(D(r)\delta_{ik} + 2C(r)r_{,i}r_{,k}\big)r_{,\ell}n_\ell + D(r)r_{,i}n_k + E(r)r_{,k}n_i\big), \tag{5.98}$$

where the functions $C(\cdot)$, $D(\cdot)$ and $E(\cdot)$ were defined in (4.19). In order to approximate these functions for r small, we resort to expressions (B.16), obtaining that

$$C(r) \sim \frac{2\mathrm{i}(1-\beta^2)}{\pi r}, \qquad D(r) \sim \frac{2\mathrm{i}\beta^2}{\pi r}, \qquad E(r) \sim -\frac{2\mathrm{i}\beta^2}{\pi r}, \qquad \text{as } r \sim 0, \tag{5.99}$$

that is, these three functions behave as $1/r$ near the origin. Replacing (5.99) in (5.98), it is possible to reexpress the Green's function normal derivative in a general form as

$$H_i^k(r) = -\frac{1}{2\pi r}\big(\big(\beta^2\delta_{ik} + 2(1-\beta^2)r_{,i}r_{,k}\big)r_{,\ell}n_\ell + \beta^2(r_{,i}n_k - r_{,k}n_i)\big) + [H^R]_i^k(r), \tag{5.100}$$

where the tensor H^R is regular in r, and it can be determined explicitly from expressions (B.16). Analogously as before, if we are dealing with the half-plane, it is necessary to add to (5.100) the regular tensor H^B that appears in (4.94). The singular part of the integral (5.65b) is thus given by

$$[IH^S]_i^k(\boldsymbol{x}) = -\frac{1}{2\pi}\int_L \Big(\big(\beta^2\delta_{ik} + 2(1-\beta^2)r_{,i}r_{,k}\big)\frac{r_{,\ell}n_\ell}{r} + \beta^2\,\frac{r_{,i}n_k - r_{,k}n_i}{r}\Big)\mathrm{d}s(\boldsymbol{y}), \tag{5.101}$$

and expressing the integrand directly in terms of matrices, (5.101) can be restated as

$$[IH^S](\boldsymbol{x}) = -\frac{1}{2\pi}\int_L \Big(\big(I + (1-\beta^2)M(r)\big)\frac{\boldsymbol{r}\cdot\boldsymbol{n}}{r^2} + \beta^2 Q\frac{\boldsymbol{r}\cdot\boldsymbol{\tau}}{r^2}\Big)\mathrm{d}s(\boldsymbol{y}), \tag{5.102}$$

where the matrices $M(r)$ and Q are given by

$$M(r) = \begin{bmatrix} r_{,1}^2 - r_{,2}^2 & 2r_{,1}r_{,2} \\ 2r_{,1}r_{,2} & -(r_{,1}^2 - r_{,2}^2) \end{bmatrix}, \qquad Q = \begin{bmatrix} 0 & -1 \\ 1 & 0 \end{bmatrix}. \tag{5.103}$$

Notice that $M(r)$ is a symmetric matrix, whereas Q is a skew-symmetric matrix. This leads to identify a symmetric part and a skew-symmetric part in the integrand of (5.102). In order to integrate the symmetric part, we need to compute the following singular integrals:

$$IB_0(\boldsymbol{x}) = \int_L \frac{\boldsymbol{r}\cdot\boldsymbol{n}}{r^2}\,\mathrm{d}s(\boldsymbol{y}), \tag{5.104a}$$

$$IB_1(\boldsymbol{x}) = \int_L \frac{\boldsymbol{r}\cdot\boldsymbol{n}}{r^2}\big(r_{,1}^2 - r_{,2}^2\big)\mathrm{d}s(\boldsymbol{y}), \tag{5.104b}$$

$$IB_2(\boldsymbol{x}) = 2\int_L \frac{\boldsymbol{r}\cdot\boldsymbol{n}}{r^2}\, r_{,1}r_{,2}\,\mathrm{d}s(\boldsymbol{y}). \tag{5.104c}$$

The integral IB_0 can be straightforwardly obtained from the calculations already made. We deduce from (5.82) that $\boldsymbol{r}\cdot\boldsymbol{n} = \boldsymbol{r}^p\cdot\boldsymbol{n}$, so if $\boldsymbol{x}\in L$, then $\boldsymbol{r}^p\cdot\boldsymbol{n} = 0$ and $IB_0(\boldsymbol{x})$ vanishes. Otherwise, we obtain from (5.88) and (5.104a) that

$$IB_0(\boldsymbol{x}) = \frac{1}{\boldsymbol{r}^p\cdot\boldsymbol{n}}\, IF(\boldsymbol{x}), \tag{5.105}$$

and combining with (5.95) gives

$$IB_0(\boldsymbol{x}) = -\theta_L. \tag{5.106}$$

On the other hand, the integrals IB_1 and IB_2 are calculated as non-oriented line integrals using the parametrization $\boldsymbol{r} = \boldsymbol{r}(\theta)$ given in (5.92). By definition, we have

$$IB_1(\boldsymbol{x}) = \int_{\theta_p}^{\theta_n} \frac{\boldsymbol{r}^p\cdot\boldsymbol{n}}{|\boldsymbol{r}(\theta)|^4}\big(r_1(\theta)^2 - r_2(\theta)^2\big)|\boldsymbol{r}'(\theta)|\,\mathrm{sign}\,\theta_L\,\mathrm{d}\theta, \tag{5.107a}$$

$$IB_2(\boldsymbol{x}) = 2\int_{\theta_p}^{\theta_n} \frac{\boldsymbol{r}^p\cdot\boldsymbol{n}}{|\boldsymbol{r}(\theta)|^4}\, r_1(\theta)r_2(\theta)\,|\boldsymbol{r}'(\theta)|\,\mathrm{sign}\,\theta_L\,\mathrm{d}\theta, \tag{5.107b}$$

and replacing (5.92) gives

$$IB_1(\boldsymbol{x}) = \mathrm{sign}\,\theta_L\,\mathrm{sign}(\boldsymbol{r}^p\cdot\boldsymbol{n})\int_{\theta_p}^{\theta_n}\cos 2\theta\,\mathrm{d}\theta, \tag{5.108a}$$

$$IB_2(\boldsymbol{x}) = \mathrm{sign}\,\theta_L\,\mathrm{sign}(\boldsymbol{r}^p\cdot\boldsymbol{n})\int_{\theta_p}^{\theta_n}\sin 2\theta\,\mathrm{d}\theta. \tag{5.108b}$$

It is worthwhile to recall that the signs of θ_L and $\boldsymbol{r}^p\cdot\boldsymbol{n}$ are opposite, so their product is always equals to -1. Computing the integrals in (5.108), we obtain

$$IB_1(\boldsymbol{x}) = -(\sin\theta_n\cos\theta_n - \sin\theta_p\cos\theta_p), \tag{5.109a}$$

$$IB_2(\boldsymbol{x}) = -(\sin^2\theta_n - \sin^2\theta_p). \tag{5.109b}$$

Let us integrate now the skew-symmetric part, for which it is necessary to compute the next singular integral

$$IC(\boldsymbol{x}) = \int_L \frac{\boldsymbol{r}\cdot\boldsymbol{\tau}}{r^2}\,\mathrm{d}s(\boldsymbol{y}). \tag{5.110}$$

To do so, we resort to decomposition (5.76) and we use the relation

$$\frac{\partial}{\partial s}\ln r = \nabla \ln r\cdot\boldsymbol{\tau} = \frac{\boldsymbol{r}\cdot\boldsymbol{\tau}}{r^2}, \tag{5.111}$$

and $IC(\boldsymbol{x})$ is simply calculated as

$$IC(\boldsymbol{x}) = \int_L \frac{\partial}{\partial s}\ln r\,\mathrm{d}s(\boldsymbol{y}) = \ln(r^n) - \ln(r^p), \tag{5.112}$$

that is,

$$IC(\boldsymbol{x}) = \ln\left(\frac{r^n}{r^p}\right). \tag{5.113}$$

Combining (5.102) with (5.104) and (5.110), we obtain that the components of IH^S are expressed in terms of the integrals IB_0, IB_1, IB_2 and IC as

$$[IH^S]^1_1(\boldsymbol{x}) = -\frac{1}{2\pi}\big(IB_0(\boldsymbol{x}) + (1-\beta^2)IB_1(\boldsymbol{x})\big), \tag{5.114a}$$

$$[IH^S]^1_2(\boldsymbol{x}) = -\frac{1}{2\pi}\big(IB_2(\boldsymbol{x}) - \beta^2 IC(\boldsymbol{x})\big), \tag{5.114b}$$

$$[IH^S]^2_1(\boldsymbol{x}) = -\frac{1}{2\pi}\big(IB_2(\boldsymbol{x}) + \beta^2 IC(\boldsymbol{x})\big), \tag{5.114c}$$

$$[IH^S]^2_2(\boldsymbol{x}) = -\frac{1}{2\pi}\big(IB_0(\boldsymbol{x}) - (1-\beta^2)IB_1(\boldsymbol{x})\big), \tag{5.114d}$$

and substituting (5.106), (5.109a), (5.109b), and (5.113) in (5.114) gives

$$[IH^S]^1_1(\boldsymbol{x}) = \frac{1}{2\pi}\Big(\theta_L + (1-\beta^2)\big(\sin\theta_n\cos\theta_n - \sin\theta_p\cos\theta_p\big)\Big), \tag{5.115a}$$

$$[IH^S]^1_2(\boldsymbol{x}) = \frac{1}{2\pi}\Big((1-\beta^2)\big(\sin^2\theta_n - \sin^2\theta_p\big) + \beta^2\ln\left(\frac{r^n}{r^p}\right)\Big), \tag{5.115b}$$

$$[IH^S]^2_1(\boldsymbol{x}) = \frac{1}{2\pi}\Big((1-\beta^2)\big(\sin^2\theta_n - \sin^2\theta_p\big) - \beta^2\ln\left(\frac{r^n}{r^p}\right)\Big), \tag{5.115c}$$

$$[IH^S]^2_2(\boldsymbol{x}) = \frac{1}{2\pi}\Big(\theta_L - (1-\beta^2)\big(\sin\theta_n\cos\theta_n - \sin\theta_p\cos\theta_p\big)\Big). \tag{5.115d}$$

Hence, we have that (5.97) and (5.115) correspond to explicit expressions of the singular integrals IG^S and IH^S, respectively. They only depend on $\boldsymbol{x}\in K$, the parameters of segment L and physical constants, so they can be directly evaluated and used to compute the external integrals in $\boldsymbol{x}$ by formula (5.68a).

VI. NUMERICAL CALCULATION OF THE HALF-PLANE GREEN'S FUNCTION

6.1 Introduction

This chapter is devoted to calculate thoroughly the half-plane Green's function with impedance boundary conditions previously introduced in Section 4.3. The calculations performed herein are presented, in an abbreviated version, by Durán, Godoy & Nédélec (2006), and in a more detailed version, by Durán, Godoy & Nédélec (2010). The calculation method resorted to is strongly based upon the works by Durán, Muga & Nédélec (2005*a*), Durán, Muga & Nédélec (2006) and Durán, Hein & Nédélec (2007), where the half-plane Green's function of the Helmholtz's equation with impedance boundary conditions was theoretically determined and numerically calculated. A partial Fourier transform in the horizontal sense is applied to the impedance boundary-value problem, and the spectral Green's function (that is, transferred to the Fourier domain) is expressed as a sum of two terms, where the first one can be analytically inverted, yielding the full-plane Green's function mentioned in Section 4.2, and the second term is inverted by an analytical/numerical method. For this, it is separated as a sum of three parts, where two of them contain singularities in the spectral variable (pseudo-poles and poles) and can be analytically inverted, and the remaining term is regular, decreasing at infinity, and its inverse transform is numerically approximated via a backward fast Fourier transform (IFFT) algorithm. The part of the pseudo-poles is intimately related to the image of the source point, which lies in the lower half-plane, whereas the part of the poles has special significance, since each pair of real poles has associated the existence of a surface wave. We obtain the Rayleigh wave (or secular) equation, which will be studied in the next chapter. The calculation of the Green's function's normal derivative is also presented. In the case of the analytical terms, that is, the full-plane term and the parts of the pseudo-poles and poles, the normal derivative is calculated analytically, while the regular part's normal derivative is calculated numerically via IFFT. The derivatives of this part in the horizontal sense are computed in the Fourier domain, whereas its vertical derivatives can be directly calculated in the space domain.

6.2 Spectral Green's function

Let us consider a fixed source point $\boldsymbol{x}$ and a variable receiver point $\boldsymbol{y}$, with $\boldsymbol{x},\ \boldsymbol{y} \in \mathbb{R}^2_+$. The half-plane Green's function G is expressed through its column vectors, denoted by $\boldsymbol{g}^k = \boldsymbol{g}^k(\boldsymbol{x}, \boldsymbol{y})$ for $k = 1, 2$. We have already stated that this Green's function has to satisfy the elastic wave equation (4.87) and the impedance boundary conditions (4.88), which are respectively expressed in vector notation as

$$\operatorname{div} \sigma(\boldsymbol{g}^k(\boldsymbol{x}, \boldsymbol{y})) + \rho\omega^2 \boldsymbol{g}^k(\boldsymbol{x}, \boldsymbol{y}) = -\delta_{\boldsymbol{x}}(\boldsymbol{y})\hat{\boldsymbol{e}}_k \qquad \text{in } \mathbb{R}^2_+, \tag{6.1a}$$

$$-\sigma(\boldsymbol{g}^k(\boldsymbol{x}, \boldsymbol{y}))\hat{\boldsymbol{e}}_2 + \omega Z_\infty\, g_1^k(\boldsymbol{x}, \boldsymbol{y})\hat{\boldsymbol{e}}_1 = \boldsymbol{0} \qquad \text{on } \{y_2 = 0\}, \tag{6.1b}$$

$$+ \text{ Outgoing radiation conditions} \qquad \text{as } r = |\boldsymbol{y}| \to +\infty, \tag{6.1c}$$

where the divergence operator and all the derivatives involved in the stress tensor σ are taken with respect to the components of $\boldsymbol{y}$. Moreover, the radiation conditions are added to this problem, and as done before, they are expressed in words. Therefore, in order to determine the desired Green's function, it is necessary to solve the problem (6.1). To do so, we apply a partial Fourier transform in the horizontal variable y_1, which is defined as

$$\widehat{\boldsymbol{g}}^k(\xi, y_2) = \int_{-\infty}^{+\infty} \boldsymbol{g}^k(y_1, y_2)\, e^{-\mathrm{i}\xi(y_1 - x_1)} \mathrm{d}y_1, \tag{6.2a}$$

$$\boldsymbol{g}^k(y_1, y_2) = \frac{1}{2\pi} \int_{-\infty}^{+\infty} \widehat{\boldsymbol{g}}^k(\xi, y_2)\, e^{\mathrm{i}\xi(y_1 - x_1)} \mathrm{d}\xi, \tag{6.2b}$$

where for the sake of simplicity, the dependence of $\boldsymbol{g}^k$ on the source point $\boldsymbol{x}$ is not explicitly written for the time being. Application of this Fourier transform on (6.1a) and (6.1b), both for $j = 1$ and $j = 2$, yields

$$\begin{aligned} C_{22} \frac{\partial^2 \widehat{G}}{\partial y_2^2}(\xi, y_2) + \mathrm{i}\xi(C_{12} + C_{21}) \frac{\partial \widehat{G}}{\partial y_2}(\xi, y_2) \\ -(\xi^2 C_{11} - \rho\omega^2 I)\widehat{G}(\xi, y_2) = -\delta_{x_2}(y_2)\, I, \end{aligned} \tag{6.3a}$$

$$C_{22} \frac{\partial \widehat{G}}{\partial y_2}(\xi, 0) + (\mathrm{i}\xi C_{21} + \omega Z_\infty I_1)\, \widehat{G}(\xi, 0) = 0, \tag{6.3b}$$

which corresponds to a matrix ODE's system for the Fourier transform of the Green's function, denoted by $\widehat{G}$ and called the spectral Green's function. The matrices C_{jl} are defined by

$$C_{jl} = \begin{bmatrix} c_{1j1l} & c_{1j2l} \\ c_{2j1l} & c_{2j2l} \end{bmatrix}, \qquad 1 \leq j, l \leq 2, \tag{6.4}$$

where the coefficients c_{ijkl} are given by

$$c_{ijkl} = \begin{cases} \lambda + 2\mu & \text{if } i = j = k = l, \\ \lambda & \text{if } i = j \text{ and } k = l \neq i, \\ \mu & \text{if } i = k \text{ and } j = l \neq i, \\ \mu & \text{if } i = l \text{ and } j = k \neq i, \\ 0 & \text{in any other case,} \end{cases} \tag{6.5}$$

and $I_1 = \hat{\boldsymbol{e}}_1 \hat{\boldsymbol{e}}_1^T$. Analogously as established in Section 4.3, we attempt to express $\widehat{G}$ as a sum of two terms:

$$\widehat{G}(\xi, y_2) = \widehat{G}^P(\xi, y_2) + \widehat{G}^B(\xi, y_2), \tag{6.6}$$

where $\widehat{G}^P$ is a term associated with the full-plane and $\widehat{G}^B$ is an additional term that takes into account the infinite flat surface and the boundary condition specified. The latter is simply called the boundary term. In order to calculate the solution to (6.3), we start by solving the homogeneous equation of (6.3a) separately on regions $\{0 \leq y_2 \leq x_2\}$ and $\{y_2 \geq x_2\}$. After that, suitable transmission conditions are imposed at $y_2 = x_2$. Notice that if the right-hand side of (6.3a) is zero, then the differential equation becomes the same for both columns of $\widehat{G}$, so the homogeneous equation can be written in vector form as

$$C_{22}\, \boldsymbol{r}''(y_2) + \mathrm{i}\xi(C_{12} + C_{21})\, \boldsymbol{r}'(y_2) - (\xi^2 C_{11} - \rho\omega^2 I)\, \boldsymbol{r}(y_2) = \boldsymbol{0}, \tag{6.7}$$

where the Fourier variable ξ is assumed to be a parameter. Any solution to (6.7) can be expressed as a linear combination of terms of the form

$$\boldsymbol{r}(y_2) = \boldsymbol{w}\, e^{-\mathrm{i}\zeta y_2}, \tag{6.8}$$

where $\zeta \in \mathbb{C}$ is a scalar and $\boldsymbol{w} \in \mathbb{C}^2$ is a vector, which are unknowns and not depending on $\boldsymbol{x}$. Substituting (6.8) in (6.7) and expanding, leads to the characteristic equation

$$A(\xi, \zeta)\, \boldsymbol{w} = \boldsymbol{0}, \tag{6.9}$$

where

$$A(\xi, \zeta) = \xi^2 C_{11} - \zeta\xi\,(C_{21} + C_{12}) + \zeta^2 C_{22} - \rho\omega^2 I. \tag{6.10}$$

Therefore, the pairs $(\zeta, \boldsymbol{w})$ in (6.8) are the non-trivial solutions of the characteristic equation (6.9). In particular, the scalars ζ have to be such that A is singular, that is,

$$\det A(\xi, \zeta) = 0. \tag{6.11}$$

Replacing (6.10) in (6.11) and expanding, leads to a polynomial equation for ζ:

$$\big(\zeta^2 + (\xi^2 - k_L^2)\big)\big(\zeta^2 + (\xi^2 - k_T^2)\big) = 0, \tag{6.12}$$

where k_L and k_T are the wave numbers defined in (2.21). This equation has four independent solutions given by

$$\zeta_L^+ = \mathrm{i}\sqrt{\xi^2 - k_L^2}, \qquad \zeta_T^+ = \mathrm{i}\sqrt{\xi^2 - k_T^2}, \tag{6.13a}$$

$$\zeta_L^- = -\mathrm{i}\sqrt{\xi^2 - k_L^2}, \qquad \zeta_T^- = -\mathrm{i}\sqrt{\xi^2 - k_L^2}, \tag{6.13b}$$

Even though $\xi \in \mathbb{R}$, the square roots are complex maps, so an exact meaning has to be given to them. We pose

$$\sqrt{\xi^2 - k_L^2} = \sqrt{\xi - k_L}\sqrt{\xi + k_L}, \qquad \sqrt{\xi^2 - k_T^2} = \sqrt{\xi - k_T}\sqrt{\xi + k_T},$$

and we consider particular branches in the complex plane to define each root, as indicated in Fig. 6.1. The exact definition is

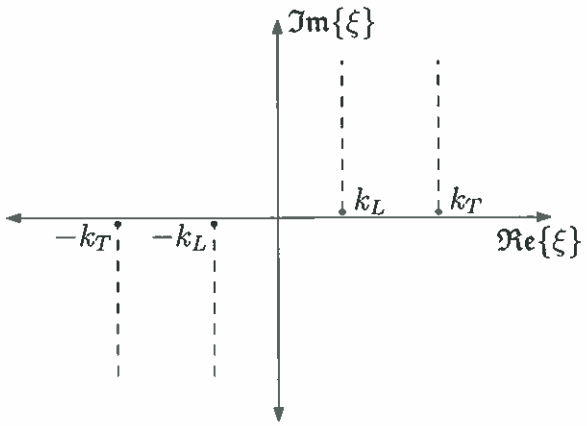

FIGURE 6.1. Domain of complex maps $\sqrt{\xi^2 - k_L^2}$ and $\sqrt{\xi^2 - k_T^2}$.

$$\sqrt{\xi^2 - k_\alpha^2} = -\mathrm{i}k_\alpha \exp\left(\int_0^\xi \frac{u}{u^2 - \xi^2}\, \mathrm{d}u \right) \qquad \alpha = L, T, \tag{6.14}$$

and then the square roots $\sqrt{\xi^2 - k_L^2}$ and $\sqrt{\xi^2 - k_T^2}$ have always non negative real part for $\xi \in \mathbb{R}$ (see Durán, Muga & Nédélec 2005*a*, 2006). The vectors $\boldsymbol{w}$ are computed by substituting the respective values ζ in (6.9). We obtain

$$\boldsymbol{w}_L^+ = \begin{bmatrix} \mathrm{i}\xi \\ \sqrt{\xi^2 - k_L^2} \end{bmatrix}, \qquad \boldsymbol{w}_T^+ = \begin{bmatrix} \sqrt{\xi^2 - k_T^2} \\ -\mathrm{i}\xi \end{bmatrix}, \tag{6.15a}$$

$$\boldsymbol{w}_L^- = \begin{bmatrix} -\mathrm{i}\xi \\ \sqrt{\xi^2 - k_L^2} \end{bmatrix}, \qquad \boldsymbol{w}_T^- = \begin{bmatrix} \sqrt{\xi^2 - k_T^2} \\ \mathrm{i}\xi \end{bmatrix}, \tag{6.15b}$$

and the general solution of (6.7) can be expressed as a linear combination:

$$\boldsymbol{r}(y_2) = \alpha_L^+ e^{-\mathrm{i}\zeta_L^+ y_2}\, \boldsymbol{w}_L^+ + \alpha_T^+ e^{-\mathrm{i}\zeta_T^+ y_2}\, \boldsymbol{w}_T^+ + \alpha_L^- e^{-\mathrm{i}\zeta_L^- y_2}\, \boldsymbol{w}_L^- + \alpha_T^- e^{-\mathrm{i}\zeta_T^- y_2}\, \boldsymbol{w}_T^-, \tag{6.16}$$

for general complex coefficients α_L^+, α_T^+, α_L^- and α_T^-. Moreover, $\boldsymbol{r}$ has to verify a boundary condition at $y_2 = 0$, which can be easily obtained from (6.3b):

$$C_{22}\, \boldsymbol{r}'(0) + (\mathrm{i}\xi C_{21} + \omega Z_\infty I_1)\, \boldsymbol{r}(0) = \boldsymbol{0}. \tag{6.17}$$

Replacing $\boldsymbol{r}$ from (6.16) in (6.17) gives the identity

$$\alpha_L^+ \boldsymbol{v}_L^+ + \alpha_T^+ \boldsymbol{v}_T^+ + \alpha_L^- \boldsymbol{v}_L^- + \alpha_T^- \boldsymbol{v}_T^- = \boldsymbol{0}, \tag{6.18}$$

where the vectors $\boldsymbol{v}$ are obtained from the vectors $\boldsymbol{w}$ by means of the relation

$$\boldsymbol{v}_\alpha^\pm = (\zeta_\alpha^\pm C_{22} - \xi C_{21} + \mathrm{i}\omega Z_\infty I_1)\boldsymbol{w}_\alpha^\pm \qquad \alpha = L, T. \tag{6.19}$$

Substituting (6.13) and (6.15) in (6.19) yields

$$\boldsymbol{v}_L^+ = \begin{bmatrix} -\xi\left(2\mu\sqrt{\xi^2 - k_L^2} + \omega Z_\infty\right) \\ \mathrm{i}\mu\left(2\xi^2 - k_T^2\right) \end{bmatrix}, \tag{6.20a}$$

$$\boldsymbol{v}_L^- = \begin{bmatrix} -\xi\left(2\mu\sqrt{\xi^2 - k_L^2} - \omega Z_\infty\right) \\ -\mathrm{i}\mu\left(2\xi^2 - k_T^2\right) \end{bmatrix}, \tag{6.20b}$$

$$\boldsymbol{v}_T^+ = \begin{bmatrix} \mathrm{i}\mu\left(2\xi^2 - k_T^2\right) + \mathrm{i}\omega Z_\infty \sqrt{\xi^2 - k_T^2} \\ 2\mu\xi\sqrt{\xi^2 - k_T^2} \end{bmatrix}, \tag{6.20c}$$

$$\boldsymbol{v}_T^- = \begin{bmatrix} -\mathrm{i}\mu\left(2\xi^2 - k_T^2\right) + \mathrm{i}\omega Z_\infty \sqrt{\xi^2 - k_T^2} \\ 2\mu\xi\sqrt{\xi^2 - k_T^2} \end{bmatrix}. \tag{6.20d}$$

As each column of $\widehat{G}$ is expressed in the form (6.16), we use a concise notation to write it directly. For this, we define the matrices

$$W_+ = \left[\boldsymbol{w}_L^+ \middle| \boldsymbol{w}_T^+\right], \qquad W_- = \left[\boldsymbol{w}_L^- \middle| \boldsymbol{w}_T^-\right], \tag{6.21}$$

which fulfill the properties

$$W_\pm^{-1} = -\frac{1}{\det W_\pm} W_\pm, \qquad \det W_+ = \det W_-. \tag{6.22}$$

Additionally, we define the diagonal matrix

$$D(y_2) = \mathrm{diag}\left(e^{\sqrt{\xi^2 - k_L^2}\, y_2},\ e^{\sqrt{\xi^2 - k_T^2}\, y_2}\right), \tag{6.23}$$

which satisfies

$$D(y_2) = \operatorname{diag}\left(e^{-i\zeta_L^+ y_2},\, e^{-i\zeta_T^+ y_2}\right), \tag{6.24a}$$

$$D(-y_2) = \operatorname{diag}\left(e^{-i\zeta_L^- y_2},\, e^{-i\zeta_T^- y_2}\right). \tag{6.24b}$$

The spectral Green's function $\widehat{G}$ is then expressed as

$$\widehat{G}(s, y_2) = \begin{cases} W_+ D(y_2) A_+ + W_- D(-y_2) A_- & \text{if } 0 \le y_2 \le x_2, \\ W_+ D(y_2) B_+ + W_- D(-y_2) B_- & \text{if } y_2 \ge x_2, \end{cases} \tag{6.25}$$

where A_+, A_-, B_+ and B_- are unknown matrices depending on ξ and x_2. These matrices are determined by imposing the radiation conditions when y_2 tends to infinity, the transmissions conditions at $y_2 = x_2$ and the boundary condition at $y_2 = 0$ given by (6.18). Let us begin by analyzing the case when $y_2 \to +\infty$. If $|\xi| > k_L$, then $\sqrt{\xi^2 - k_L^2}$ is real, positive and the functions $e^{\sqrt{\xi^2 - k_L^2} y_2}$ and $e^{-\sqrt{\xi^2 - k_L^2} y_2}$ are exponentially increasing and decreasing in y_2, respectively. On the contrary, if $|\xi| < k_L$, then $\sqrt{\xi^2 - k_L^2}$ is purely imaginary and both the above exponential functions behave oscillatorily in y_2. Indeed, it can be easily verified that in accordance with our definition of complex square roots, the imaginary part of $\sqrt{\xi^2 - k_L^2}$ is negative. Consequently, $e^{\sqrt{\xi^2 - k_L^2} y_2}$ contains waves that travel in the $-y_2$ sense, that is, incoming terms, whereas $e^{-\sqrt{\xi^2 - k_L^2} y_2}$ contains waves that travel in the $+y_2$ sense, that is, outgoing terms. The analysis for the functions $\sqrt{\xi^2 - k_T^2}$, $e^{\sqrt{\xi^2 - k_T^2} y_2}$ and $e^{-\sqrt{\xi^2 - k_T^2} y_2}$ is completely analogous. We want to eliminate any exponentially increasing term in y_2, because it has no physical meaning, and all the incoming terms, in order to fulfill the radiation conditions at infinity. It is easy to observe that all these undesired behaviors occur in the matrix $D(y_2)$ (see (6.23) and (6.25)), therefore, it is natural to set

$$B_+ = 0, \tag{6.26}$$

and then we only keep the terms that behave as desired, which are contained within the matrix $D(-y_2)$. Let us study now the transmission conditions at $y_2 = x_2$. We assume $\widehat{G}$ to be continuous at $y_2 = x_2$, that is,

$$W_- D(-x_2) B_- = W_+ D(x_2) A_+ + W_- D(-x_2) A_-. \tag{6.27}$$

However, $\widehat{G}$ is not differentiable at this point, and its first derivative has a jump given by

$$\left[\frac{\partial \widehat{G}}{\partial y_2}\right](\xi, x_2) = \lim_{y_2 \to x_2^+} \frac{\partial \widehat{G}}{\partial y_2}(\xi, y_2) - \lim_{y_2 \to x_2^-} \frac{\partial \widehat{G}}{\partial y_2}(\xi, y_2). \tag{6.28}$$

Computing the derivatives from (6.25), replacing (6.21) and combining with (6.27) and (2.21) yields

$$\left[\frac{\partial \widehat{G}}{\partial y_2}\right](\xi, x_2) = -\frac{2\rho\omega}{\det W_+} C_{22}^{-1} N W_+ D(x_2) A_+, \tag{6.29}$$

where

$$N = \operatorname{diag}\left(\sqrt{\xi^2 - k_L^2},\, \sqrt{\xi^2 - k_T^2}\right), \tag{6.30}$$

and the second derivative of $\widehat{G}$ in the sense of distributions corresponds to a Dirac mass centered at x_2 and multiplied by the jump of the derivative of $\widehat{G}$ at $y_2 = x_2$. Substituting $\widehat{G}$

from (6.25) in (6.3a) and combining with (6.22), (6.27) and (6.29) gives A_+:

$$A_+ = -\frac{1}{2\rho\omega} D(-x_2) W_+ N^{-1}. \tag{6.31}$$

Notice that at the moment, we have the solution to (6.3a) (taking into account the right-hand side). Finally, the boundary condition at $y_2 = 0$ given by (6.18) is imposed to each column of $\widehat{G}$, obtaining:

$$V_+ A_+ + V_- A_- = 0, \tag{6.32}$$

where the matrices V_+ and V_- are defined from the vectors $\boldsymbol{v}_{L^+}$, $\boldsymbol{v}_{L^-}$, $\boldsymbol{v}_{T^+}$ and $\boldsymbol{v}_{T^-}$ as follows:

$$V_+ = \left[\boldsymbol{v}_{L^+} \middle| \boldsymbol{v}_{T^+}\right], \qquad V_- = \left[\boldsymbol{v}_{L^-} \middle| \boldsymbol{v}_{T^-}\right]. \tag{6.33}$$

Then, replacing (6.31) in (6.32), we determine A_-:

$$A_- = \frac{1}{2\rho\omega} V_-^{-1} V_+ D(-x_2) W_+ N^{-1}, \tag{6.34}$$

and substituting (6.31) and (6.34) in (6.27) gives B_-:

$$B_- = -\frac{1}{2\rho\omega}\left(D(x_2) W_- - V_-^{-1} V_+ D(-x_2) W_+\right) N^{-1}. \tag{6.35}$$

After that, replacing (6.26), (6.31), (6.34) and (6.35) in (6.25), the terms of the sum in (6.6) can be determined. The full-plane term $\widehat{G}^P$ is given by

$$\widehat{G}^P(s, y_2) = \begin{cases} -\dfrac{1}{2\rho\omega} W_+ D(y_2 - x_2) W_+ N^{-1} & \text{if } 0 \le y_2 \le x_2, \\ -\dfrac{1}{2\rho\omega} W_- D(x_2 - y_2) W_- N^{-1} & \text{if } y_2 \ge x_2, \end{cases} \tag{6.36}$$

and the boundary term $\widehat{G}^B$ is given by

$$\widehat{G}^B(\xi, y_2) = \frac{1}{2\rho\omega} W_- D(-y_2) V_-^{-1} V_+ D(-x_2) W_+ N^{-1}. \tag{6.37}$$

Replacing (6.21), (6.23) and (6.30) in (6.36) yields $\widehat{G}^P$, which is a symmetric matrix whose components are

$$\widehat{G}^P_{11}(\xi, y_2) = \frac{1}{2\rho\omega^2}\left(\frac{\xi^2 e^{-\sqrt{\xi^2 - k_L^2}|y_2 - x_2|}}{\sqrt{\xi^2 - k_L^2}} - \sqrt{\xi^2 - k_T^2}\, e^{-\sqrt{\xi^2 - k_T^2}|y_2 - x_2|}\right), \tag{6.38a}$$

$$\widehat{G}^P_{12}(\xi, y_2) = \frac{\mathrm{i}\xi}{2\rho\omega^2} \operatorname{sign}(y_2 - x_2)\left(e^{-\sqrt{\xi^2 - k_L^2}|y_2 - x_2|} - e^{-\sqrt{\xi^2 - k_T^2}|y_2 - x_2|}\right), \tag{6.38b}$$

$$\widehat{G}^P_{22}(\xi, y_2) = -\frac{1}{2\rho\omega^2}\left(\sqrt{\xi^2 - k_L^2}\, e^{-\sqrt{\xi^2 - k_L^2}|y_2 - x_2|} - \frac{\xi^2 e^{-\sqrt{\xi^2 - k_T^2}|y_2 - x_2|}}{\sqrt{\xi^2 - k_T^2}}\right). \tag{6.38c}$$

On the other hand, substituting (6.21), (6.33), (6.23) and (6.30) in (6.37), we obtain the components of $\widehat{G}^B$:

$$\begin{aligned}
\widehat{G}^B_{11}(\xi,y_2) = -\frac{1}{2\rho\omega^2}\Bigg(&\Big(\big(2\xi^2-k_T^2\big)^2+4\xi^2\sqrt{\xi^2-k_L^2}\sqrt{\xi^2-k_T^2}\\
&+\frac{\omega}{\mu}Z_\infty k_T^2\sqrt{\xi^2-k_T^2}\Big)\frac{\xi^2 e^{-\sqrt{\xi^2-k_L^2}(y_2+x_2)}}{\sqrt{\xi^2-k_L^2}}+\Big(\big(2\xi^2-k_T^2\big)^2\\
&+4\xi^2\sqrt{\xi^2-k_L^2}\sqrt{\xi^2-k_T^2}-\tfrac{\omega}{\mu}Z_\infty k_T^2\sqrt{\xi^2-k_T^2}\Big)\\
&\times\sqrt{\xi^2-k_T^2}\,e^{-\sqrt{\xi^2-k_T^2}(y_2+x_2)}-4\xi^2\big(2\xi^2-k_T^2\big)\sqrt{\xi^2-k_T^2}\\
&\times\Big(e^{-\left(\sqrt{\xi^2-k_L^2}y_2+\sqrt{\xi^2-k_T^2}x_2\right)}+e^{-\left(\sqrt{\xi^2-k_T^2}y_2+\sqrt{\xi^2-k_L^2}x_2\right)}\Big)\Bigg)\\
&\Big/\Big(\big(2\xi^2-k_T^2\big)^2-4\xi^2\sqrt{\xi^2-k_L^2}\sqrt{\xi^2-k_T^2}+\tfrac{\omega}{\mu}Z_\infty k_T^2\sqrt{\xi^2-k_T^2}\Big),
\end{aligned}\tag{6.39a}$$

$$\begin{aligned}
\widehat{G}^B_{12}(\xi,y_2) = -\frac{\mathrm{i}\xi}{2\rho\omega^2}\Bigg(&\Big(\big(2\xi^2-k_T^2\big)^2+4\xi^2\sqrt{\xi^2-k_L^2}\sqrt{\xi^2-k_T^2}\\
&+\frac{\omega}{\mu}Z_\infty k_T^2\sqrt{\xi^2-k_T^2}\Big)e^{-\sqrt{\xi^2-k_L^2}(y_2+x_2)}+\Big(\big(2\xi^2-k_T^2\big)^2\\
&+4\xi^2\sqrt{\xi^2-k_L^2}\sqrt{\xi^2-k_T^2}-\tfrac{\omega}{\mu}Z_\infty k_T^2\sqrt{\xi^2-k_T^2}\Big)e^{-\sqrt{\xi^2-k_T^2}(y_2+x_2)}\\
&-4\big(2\xi^2-k_T^2\big)\Big(\sqrt{\xi^2-k_L^2}\sqrt{\xi^2-k_T^2}\,e^{-\left(\sqrt{\xi^2-k_L^2}y_2+\sqrt{\xi^2-k_T^2}x_2\right)}\\
&+\xi^2 e^{-\left(\sqrt{\xi^2-k_T^2}y_2+\sqrt{\xi^2-k_L^2}x_2\right)}\Big)\Bigg)\\
&\Big/\Big(\big(2\xi^2-k_T^2\big)^2-4\xi^2\sqrt{\xi^2-k_L^2}\sqrt{\xi^2-k_T^2}+\tfrac{\omega}{\mu}Z_\infty k_T^2\sqrt{\xi^2-k_T^2}\Big),
\end{aligned}\tag{6.39b}$$

$$\begin{aligned}
\widehat{G}^B_{21}(\xi,y_2) = \frac{\mathrm{i}\xi}{2\rho\omega^2}\Bigg(&\Big(\big(2\xi^2-k_T^2\big)^2+4\xi^2\sqrt{\xi^2-k_L^2}\sqrt{\xi^2-k_T^2}\\
&+\frac{\omega}{\mu}Z_\infty k_T^2\sqrt{\xi^2-k_T^2}\Big)e^{-\sqrt{\xi^2-k_L^2}(y_2+x_2)}+\Big(\big(2\xi^2-k_T^2\big)^2\\
&+4\xi^2\sqrt{\xi^2-k_L^2}\sqrt{\xi^2-k_T^2}-\tfrac{\omega}{\mu}Z_\infty k_T^2\sqrt{\xi^2-k_T^2}\Big)e^{-\sqrt{\xi^2-k_T^2}(y_2+x_2)}\\
&-4\big(2\xi^2-k_T^2\big)\Big(\xi^2 e^{-\left(\sqrt{\xi^2-k_L^2}y_2+\sqrt{\xi^2-k_T^2}x_2\right)}\\
&+\sqrt{\xi^2-k_L^2}\sqrt{\xi^2-k_T^2}\,e^{-\left(\sqrt{\xi^2-k_T^2}y_2+\sqrt{\xi^2-k_L^2}x_2\right)}\Big)\Bigg)\\
&\Big/\Big(\big(2\xi^2-k_T^2\big)^2-4\xi^2\sqrt{\xi^2-k_L^2}\sqrt{\xi^2-k_T^2}+\tfrac{\omega}{\mu}Z_\infty k_T^2\sqrt{\xi^2-k_T^2}\Big),
\end{aligned}\tag{6.39c}$$

$$
\begin{aligned}
\widehat{G}^B_{22}(\xi, y_2) = -\frac{1}{2\rho\omega^2}\Bigg(& \Big(\big(2\xi^2 - k_T^2\big)^2 + 4\xi^2\sqrt{\xi^2 - k_L^2}\sqrt{\xi^2 - k_T^2} \\
& + \frac{\omega}{\mu} Z_\infty k_T^2 \sqrt{\xi^2 - k_T^2} \Big) \sqrt{\xi^2 - k_L^2}\, e^{-\sqrt{\xi^2 - k_L^2}(y_2 + x_2)} \\
& + \Big(\big(2\xi^2 - k_T^2\big)^2 + 4\xi^2\sqrt{\xi^2 - k_L^2}\sqrt{\xi^2 - k_T^2} - \tfrac{\omega}{\mu} Z_\infty k_T^2 \sqrt{\xi^2 - k_T^2} \Big) \\
& \times \frac{\xi^2 e^{-\sqrt{\xi^2 - k_T^2}(y_2 + x_2)}}{\sqrt{\xi^2 - k_T^2}} - 4\xi^2\big(2\xi^2 - k_T^2\big)\sqrt{\xi^2 - k_L^2} \\
& \times \Big(e^{-\left(\sqrt{\xi^2 - k_L^2} y_2 + \sqrt{\xi^2 - k_T^2} x_2\right)} + e^{-\left(\sqrt{\xi^2 - k_T^2} y_2 + \sqrt{\xi^2 - k_L^2} x_2\right)} \Big) \Bigg) \\
& \Big/ \Big(\big(2\xi^2 - k_T^2\big)^2 - 4\xi^2\sqrt{\xi^2 - k_L^2}\sqrt{\xi^2 - k_T^2} + \tfrac{\omega}{\mu} Z_\infty k_T^2 \sqrt{\xi^2 - k_T^2} \Big),
\end{aligned}
\tag{6.39d}
$$

The Green's function G is then determined as the inverse Fourier transform of the spectral Green's function $\widehat{G}$, that is,

$$
G(\boldsymbol{x}, \boldsymbol{y}) = \frac{1}{2\pi} \int_{-\infty}^{+\infty} \widehat{G}(\xi, y_2)\, e^{\mathrm{i}\xi(y_1 - x_1)} \mathrm{d}\xi. \tag{6.40}
$$

For this, we use the decomposition (6.6) of $\widehat{G}$, that is, the Green's function is calculated as

$$
G(\boldsymbol{x}, \boldsymbol{y}) = \frac{1}{2\pi} \int_{-\infty}^{+\infty} \widehat{G}^P(\xi, y_2)\, e^{\mathrm{i}\xi(y_1 - x_1)} \mathrm{d}\xi + \frac{1}{2\pi} \int_{-\infty}^{+\infty} \widehat{G}^B(\xi, y_2)\, e^{\mathrm{i}\xi(y_1 - x_1)} \mathrm{d}\xi, \tag{6.41}
$$

where the components of the terms $\widehat{G}^P$ and $\widehat{G}^B$ are given in (6.38) and (6.39), respectively. The integrals on the right-hand side of (6.41) are calculated separately in the next section.

6.3 Effective calculation of Green's function

6.3.1 The full-plane term

Next, we compute the term G^P of Green's function, defined as the inverse Fourier transform

$$
G^P(\boldsymbol{x}, \boldsymbol{y}) = \frac{1}{2\pi} \int_{-\infty}^{+\infty} \widehat{G}^P(\xi, y_2)\, e^{\mathrm{i}\xi(y_1 - x_1)} \mathrm{d}\xi. \tag{6.42}
$$

For this, we observe from (6.38) that it suffices to compute the inverse Fourier transforms of the functions $\widehat{\phi}_1$, $\widehat{\phi}_2$ and $\widehat{\phi}_3$ defined by

$$
\widehat{\phi}_1(\xi, y_2) = \frac{\xi^2 e^{-\sqrt{\xi^2 - k_\alpha^2}\,|y_2 - x_2|}}{\sqrt{\xi^2 - k_\alpha^2}}, \tag{6.43a}
$$

$$
\widehat{\phi}_2(\xi, y_2) = \sqrt{\xi^2 - k_\alpha^2}\, e^{-\sqrt{\xi^2 - k_\alpha^2}\,|y_2 - x_2|}, \tag{6.43b}
$$

$$
\widehat{\phi}_3(\xi, y_2) = \mathrm{i}\xi\, \mathrm{sign}(y_2 - x_2)\, e^{-\sqrt{\xi^2 - k_\alpha^2}\,|y_2 - x_2|}, \tag{6.43c}
$$

where $\alpha = L, T$. Their inverse Fourier transforms, denoted respectively by ϕ_1, ϕ_2 and ϕ_3, are computed by employing integral formulae (B.20) and recurrence formulae (B.12) for

the Hankel functions, giving

$$\phi_1(y_1,y_2) = \frac{\mathrm{i}k_\alpha^2}{2}\left(\frac{1}{k_\alpha r}H_1^{(1)}(k_\alpha r) - H_2^{(1)}(k_\alpha r)\frac{(y_1-x_1)^2}{r^2}\right), \tag{6.44a}$$

$$\phi_2(y_1,y_2) = -\frac{\mathrm{i}k_\alpha^2}{2}\left(\frac{1}{k_\alpha r}H_1^{(1)}(k_\alpha r) - H_2^{(1)}(k_\alpha r)\frac{(y_2-x_2)^2}{r^2}\right), \tag{6.44b}$$

$$\phi_3(y_1,y_2) = -\frac{\mathrm{i}k_\alpha^2}{2}H_2^{(1)}(k_\alpha r)\frac{(y_1-x_1)(y_2-x_2)}{r^2}, \tag{6.44c}$$

where as usual, $r = |\boldsymbol{y}-\boldsymbol{x}|$. Using formulae (6.44) with α substituted by L or T as appropriate, we compute the inverse Fourier transforms of expressions (6.38), giving

$$G_{11}^P(\boldsymbol{x},\boldsymbol{y}) = \frac{\mathrm{i}}{4\mu}\left(A(r) + B(r)\frac{(y_1-x_1)^2}{r^2}\right), \tag{6.45a}$$

$$G_{12}^P(\boldsymbol{x},\boldsymbol{y}) = G_{21}^P(\boldsymbol{x},\boldsymbol{y}) = \frac{\mathrm{i}}{4\mu}B(r)\frac{(y_1-x_1)(y_2-x_2)}{r^2}, \tag{6.45b}$$

$$G_{22}^P(\boldsymbol{x},\boldsymbol{y}) = \frac{\mathrm{i}}{4\mu}\left(A(r) + B(r)\frac{(y_2-x_2)^2}{r^2}\right). \tag{6.45c}$$

where $A(\cdot)$ and $B(\cdot)$ are the functions defined in (4.17). As the derivatives of r are given by the formula $r_{,i} = (y_i - x_i)/r$, the term G^P given in (6.45) coincides with that defined, e.g., in (5.70). Consequently, G^P is actually the full-plane Green's function, which agrees with that stated in Section 4.3, that is, the half-plane Green's function we are currently calculating is decomposed as indicated in (4.89). If we want to compute G^P for $y_2 = x_2$, a difficulty is encountered: The functions $\widehat{\phi}_1$, $\widehat{\phi}_2$ and $\widehat{\phi}_3$ are no longer exponentially decreasing in ξ and formulae (B.20) are not directly applicable. Hence, what we do in that case is to perform the calculations assuming $y_2 = x_2 + \varepsilon$ for ε small, and after that we make $\varepsilon \to 0$ in (6.45), which is actually equivalent to simply evaluating G^P at $y_2 = x_2$.

6.3.2 Decomposition of the boundary term

We are now interested in calculating the term G^B of the Green's function, defined as the inverse Fourier transform

$$G^B(\boldsymbol{x},\boldsymbol{y}) = \frac{1}{2\pi}\int_{-\infty}^{+\infty}\widehat{G}^B(\xi,y_2)\,e^{\mathrm{i}\xi(y_1-x_1)}\mathrm{d}\xi. \tag{6.46}$$

This term requires special attention, because $\widehat{G}^B$ has singularities (pseudo-poles and poles) that make difficult the calculation of its inverse Fourier transform. For that reason, these singularities are previously removed by subtracting certain suitable terms, whose inverse transforms are analytically calculable. The advantage of this approach is that the remaining term is regular and its inverse Fourier transform can be numerically approximated. This procedure thus decomposes the term $\widehat{G}^B$ into a sum of three parts:

$$\widehat{G}^B(\xi,y_2) = \widehat{G}^{B,\mathrm{psp}}(\xi,y_2) + \widehat{G}^{B,\mathrm{pol}}(\xi,y_2) + \widehat{G}^{B,\mathrm{reg}}(\xi,y_2), \tag{6.47}$$

where $\widehat{G}^{B,\mathrm{reg}}$ is the regular part, $\widehat{G}^{B,\mathrm{psp}}$ is the part of the pseudo-poles and $\widehat{G}^{B,\mathrm{pol}}$ is the part of the poles. Their inverse Fourier transforms are denoted by $G^{B,\mathrm{reg}}$, $G^{B,\mathrm{psp}}$ and $G^{B,\mathrm{pol}}$,

respectively. This yields a decomposition for the term G^B as a sum of three parts:

$$G^B(\boldsymbol{x},\boldsymbol{y}) = G^{B,\mathrm{psp}}(\boldsymbol{x},\boldsymbol{y}) + G^{B,\mathrm{pol}}(\boldsymbol{x},\boldsymbol{y}) + G^{B,\mathrm{reg}}(\boldsymbol{x},\boldsymbol{y}), \tag{6.48}$$

Each one of these parts are calculated separately, as described in the following subsections.

6.3.3 The part of the pseudo-poles

Singularities known as pseudo-poles (or half-order poles) are present in the diagonal components $\widehat{G}^B_{11}$ and $\widehat{G}^B_{22}$, given respectively in (6.39a) and (6.39d), due to the factors $1/\sqrt{\xi^2-k_L^2}$ and $1/\sqrt{\xi^2-k_T^2}$, respectively. Specifically, $\widehat{G}^B_{11}$ has pseudo-poles at $\xi = \pm k_L$, whereas $\widehat{G}^B_{22}$ has pseudo-poles at $\xi = \pm k_T$. This kind of singularity in the spectral Green's function is closely related to the image point of each $\boldsymbol{x} \in \mathbb{R}^2_+$, which is defined as $\overline{\boldsymbol{x}} = (x_1, -x_2)$ and lies in the lower half-plane. By analogy with the Helmholtz equation (cf. Durán et al. 2007), the pseudo-poles are removed from the boundary term by adding the (spectral) full-plane Green's function associated with the image point $\overline{\boldsymbol{x}}$. Hence, the term $\widehat{G}^{B,\mathrm{psp}}$ of the decomposition (6.47) corresponds to the symmetric matrix whose components are given by

$$\widehat{G}^{B,\mathrm{psp}}_{11}(\xi,y_2) = -\frac{1}{2\rho\omega^2}\left(\frac{\xi^2 e^{-\sqrt{\xi^2-k_L^2}(y_2+x_2)}}{\sqrt{\xi^2-k_L^2}} - \sqrt{\xi^2-k_T^2}\, e^{-\sqrt{\xi^2-k_T^2}(y_2+x_2)}\right), \tag{6.49a}$$

$$\widehat{G}^{B,\mathrm{psp}}_{12}(\xi,y_2) = -\frac{\mathrm{i}\xi}{2\rho\omega^2}\left(e^{-\sqrt{\xi^2-k_L^2}(y_2+x_2)} - e^{-\sqrt{\xi^2-k_T^2}(y_2+x_2)}\right), \tag{6.49b}$$

$$\widehat{G}^{B,\mathrm{psp}}_{22}(\xi,y_2) = \frac{1}{2\rho\omega^2}\left(\sqrt{\xi^2-k_L^2}\, e^{-\sqrt{\xi^2-k_L^2}(y_2+x_2)} - \frac{\xi^2 e^{-\sqrt{\xi^2-k_T^2}(y_2+x_2)}}{\sqrt{\xi^2-k_T^2}}\right). \tag{6.49c}$$

Although the off-diagonal terms $\widehat{G}^B_{12}$ and $\widehat{G}^B_{21}$, given respectively in (6.39b) and (6.39b), do not have pseudo-poles, the term $\widehat{G}^{B,\mathrm{psp}}_{12}$ defined in (6.49b) is subtracted anyway, because it allows to deal with simpler expressions. The term obtained after extracting the pseudo-poles from the boundary term is called the pseudo-regular term, denoted by $\widehat{G}^{B,\mathrm{psr}}$ and defined as

$$\widehat{G}^{B,\mathrm{psr}}(\xi,y_2) = \widehat{G}^{B}(\xi,y_2) - \widehat{G}^{B,\mathrm{psp}}(\xi,y_2). \tag{6.50}$$

Therefore, replacing (6.39) and (6.49) in (6.50), we obtain that $\widehat{G}^{B,\mathrm{psr}}$ can be expressed as

$$\begin{aligned}\widehat{G}^{B,\mathrm{psr}}(\xi,y_2) = &-\frac{1}{\rho\omega^2}\,\Psi(\xi,y_2)\\ &\Big/\left(\left(2\xi^2-k_T^2\right)^2 - 4\xi^2\sqrt{\xi^2-k_L^2}\sqrt{\xi^2-k_T^2} + \tfrac{\omega}{\mu}Z_\infty k_T^2\sqrt{\xi^2-k_T^2}\right),\end{aligned} \tag{6.51}$$

where Ψ corresponds to a regular matrix in ξ. Its components are

$$\begin{aligned}\Psi_{11}(\xi,y_2) = &\sqrt{\xi^2-k_T^2}\left(2\xi^2 e^{-\sqrt{\xi^2-k_L^2}y_2} - \left(2\xi^2-k_T^2\right)e^{-\sqrt{\xi^2-k_T^2}y_2}\right)\\ &\times\left(2\xi^2 e^{-\sqrt{\xi^2-k_L^2}x_2} - \left(2\xi^2-k_T^2\right)e^{-\sqrt{\xi^2-k_T^2}x_2}\right),\end{aligned} \tag{6.52a}$$

$$\begin{aligned}\Psi_{12}(\xi,y_2) = &\mathrm{i}\xi\left(2\sqrt{\xi^2-k_L^2}\sqrt{\xi^2-k_T^2}\, e^{-\sqrt{\xi^2-k_L^2}y_2} - \left(2\xi^2-k_T^2\right)e^{-\sqrt{\xi^2-k_T^2}y_2}\right)\\ &\times\left(2\xi^2 e^{-\sqrt{\xi^2-k_L^2}x_2} - \left(2\xi^2-k_T^2\right)e^{-\sqrt{\xi^2-k_T^2}x_2}\right),\end{aligned} \tag{6.52b}$$

$$\begin{aligned}\Psi_{21}(\xi,y_2) = -\mathrm{i}\xi\Big(&\big(2\xi^2-k_T^2\big)e^{-\sqrt{\xi^2-k_L^2}y_2} - 2\sqrt{\xi^2-k_L^2}\sqrt{\xi^2-k_T^2}\,e^{-\sqrt{\xi^2-k_T^2}y_2}\Big)\\ &\times\Big(\big(2\xi^2-k_T^2\big)e^{-\sqrt{\xi^2-k_L^2}x_2} - 2\xi^2 e^{-\sqrt{\xi^2-k_T^2}x_2}\Big)\\ &-\mathrm{i}\tfrac{\omega}{\mu}Z_\infty k_T^2\,\xi\sqrt{\xi^2-k_T^2}\Big(e^{-\left(\sqrt{\xi^2-k_L^2}y_2+\sqrt{\xi^2-k_T^2}x_2\right)}\\ &-e^{-\left(\sqrt{\xi^2-k_T^2}y_2+\sqrt{\xi^2-k_L^2}x_2\right)}\Big),\end{aligned} \tag{6.52c}$$

$$\begin{aligned}\Psi_{22}(\xi,y_2) = &\sqrt{\xi^2-k_L^2}\Big(\big(2\xi^2-k_T^2\big)e^{-\sqrt{\xi^2-k_L^2}y_2} - 2\xi^2 e^{-\sqrt{\xi^2-k_T^2}y_2}\Big)\\ &\times\Big(\big(2\xi^2-k_T^2\big)e^{-\sqrt{\xi^2-k_L^2}x_2} - 2\xi^2 e^{-\sqrt{\xi^2-k_T^2}x_2}\Big)\\ &+\tfrac{\omega}{\mu}Z_\infty k_T^2\Big(\sqrt{\xi^2-k_L^2}\sqrt{\xi^2-k_T^2}\,e^{-\left(\sqrt{\xi^2-k_L^2}y_2+\sqrt{\xi^2-k_T^2}x_2\right)}\\ &-\xi^2 e^{-\left(\sqrt{\xi^2-k_T^2}y_2+\sqrt{\xi^2-k_L^2}x_2\right)}\Big).\end{aligned} \tag{6.52d}$$

These functions do not have any singularity. Moreover, it is straightforward to verify that the components Ψ_{11} and Ψ_{22} are even functions in ξ, while the components Ψ_{21} and Ψ_{12} are odd functions in ξ. On the other hand, the inverse Fourier transform of the term $\widehat{G}^{B,\mathrm{psp}}$ given in (6.49) is computed analogously to the full-plane term, giving the components

$$G_{11}^{B,\mathrm{psp}}(\boldsymbol{x},\boldsymbol{y}) = -\frac{\mathrm{i}}{4\mu}\left(A(\overline{r}) + B(\overline{r})\,\frac{(y_1-x_1)^2}{\overline{r}^{\,2}}\right), \tag{6.53a}$$

$$G_{12}^{B,\mathrm{psp}}(\boldsymbol{x},\boldsymbol{y}) = G_{21}^{B,\mathrm{psp}}(\boldsymbol{x},\boldsymbol{y}) = -\frac{\mathrm{i}}{4\mu}\,B(\overline{r})\,\frac{(y_1-x_1)(y_2+x_2)}{\overline{r}^{\,2}}, \tag{6.53b}$$

$$G_{22}^{B,\mathrm{psp}}(\boldsymbol{x},\boldsymbol{y}) = -\frac{\mathrm{i}}{4\mu}\left(A(\overline{r}) + B(\overline{r})\,\frac{(y_2+x_2)^2}{\overline{r}^{\,2}}\right), \tag{6.53c}$$

where $\overline{r}$ denotes the distance between $\boldsymbol{y}$ and the image point $\overline{\boldsymbol{x}}$, that is,

$$\overline{r} = \sqrt{(y_1-x_1)^2+(y_2+x_2)^2}. \tag{6.54}$$

6.3.4 The part of the poles

The poles of the spectral Green's function are extracted from the pseudo-regular term $\widehat{G}^{B,\mathrm{psr}}$, which is given in (6.51) and it has no pseudo-poles. As the matrix function $\Psi(\xi,y_2)$ is regular in ξ, all the poles come from the denominator in (6.51). These poles are located at those values of ξ such that this denominator vanishes, that is, they are solutions of the equation

$$\big(2\xi^2-k_T^2\big)^2 - 4\xi^2\sqrt{\xi^2-k_L^2}\sqrt{\xi^2-k_T^2} + \tfrac{\omega}{\mu}Z_\infty k_T^2\sqrt{\xi^2-k_T^2} = 0. \tag{6.55}$$

This equation is known as the Rayleigh wave equation, or secular equation. The solutions of this equation cannot, in general, be determined analytically. However, as the dependence on ξ is through ξ^2, it is possible to establish a priori that they correspond to pairs symmetrically located with respect to the origin in the complex plane. Moreover, as we will see in the next chapter, a pair of real solutions gives rise to a surface wave propagating through the infinite flat surface. In other words, there is a correspondence between real poles of

the spectral Green's function and surface waves. In order to solve (6.55), it is necessary to employ numerical procedures, and this matter is discussed in the next chapter. For the time being, what we do is to take two solutions of (6.55), namely $\xi = \hat{k}$ and $\xi = -\hat{k}$, with $\mathfrak{Re}\{\hat{k}\} > 0$, and we assume that $\widehat{G}^{B,\mathrm{psr}}$ has two simple poles at these locations. The poles are extracted by subtracting a simple term from $\widehat{G}^{B,\mathrm{psr}}$, which behaves in the same way at the neighborhood of each pole and is regular elsewhere. We are referring to the term $\widehat{G}^{B,\mathrm{pol}}$ of the decomposition (6.47), which is written as

$$\widehat{G}^{B,\mathrm{pol}}(\xi, y_2) = -\frac{1}{\rho\omega^2}\left(\frac{1}{\xi - \hat{k}}\, C^{+}(\hat{k}, y_2) + \frac{1}{\xi + \hat{k}}\, C^{-}(\hat{k}, y_2)\right), \tag{6.56}$$

where $C^{+}(\hat{k}, y_2)$ and $C^{-}(\hat{k}, y_2)$ are the residue matrices associated with the poles at $\xi = \hat{k}$ and $\xi = -\hat{k}$, respectively. These matrices correspond to the limits

$$C^{+}(\hat{k}, y_2) = -\rho\omega^2 \lim_{\xi \to +\hat{k}} (\xi - \hat{k})\, \widehat{G}^{B,\mathrm{psr}}(\xi, y_2), \tag{6.57a}$$

$$C^{-}(\hat{k}, y_2) = -\rho\omega^2 \lim_{\xi \to -\hat{k}} (\xi + \hat{k})\, \widehat{G}^{B,\mathrm{psr}}(\xi, y_2). \tag{6.57b}$$

Combining with (6.51) yields

$$C^{+}(\hat{k}, y_2) = \lim_{\xi \to +\hat{k}} \frac{(\xi - \hat{k})\, \Psi(\xi, y_2)}{\left(2\xi^2 - k_T^2\right)^2 - 4\xi^2\sqrt{\xi^2 - k_L^2}\sqrt{\xi^2 - k_T^2} + \frac{\omega}{\mu} Z_\infty k_T^2 \sqrt{\xi^2 - k_T^2}}, \tag{6.58a}$$

$$C^{-}(\hat{k}, y_2) = \lim_{\xi \to -\hat{k}} \frac{(\xi + \hat{k})\, \Psi(\xi, y_2)}{\left(2\xi^2 - k_T^2\right)^2 - 4\xi^2\sqrt{\xi^2 - k_L^2}\sqrt{\xi^2 - k_T^2} + \frac{\omega}{\mu} Z_\infty k_T^2 \sqrt{\xi^2 - k_T^2}}. \tag{6.58b}$$

Because of the evenness or oddness of each component of $\Psi(s, y_2)$ (see (6.52)), it is direct to verify that the following symmetries hold:

$$\begin{aligned} C_{11}^{+}(\hat{k}, y_2) &= -C_{11}^{-}(\hat{k}, y_2), & C_{12}^{+}(\hat{k}, y_2) &= C_{12}^{-}(\hat{k}, y_2), \\ C_{21}^{+}(\hat{k}, y_2) &= C_{21}^{-}(\hat{k}, y_2), & C_{22}^{+}(\hat{k}, y_2) &= -C_{22}^{-}(\hat{k}, y_2). \end{aligned} \tag{6.59}$$

Hence, in order to simplify the notation, we put $c_{i\ell}(\hat{k}, y_2) = C_{i\ell}^{+}(\hat{k}, y_2)$, where $1 \leq i, \ell \leq 2$. The matrices $C^{+}(\hat{k}, y_2)$ and $C^{-}(\hat{k}, y_2)$ are thus expressed as follows:

$$C_{+}(\hat{k}, y_2) = \begin{bmatrix} c_{11}(\hat{k}, y_2) & c_{12}(\hat{k}, y_2) \\ c_{21}(\hat{k}, y_2) & c_{22}(\hat{k}, y_2) \end{bmatrix}, \tag{6.60a}$$

$$C_{-}(\hat{k}, y_2) = \begin{bmatrix} -c_{11}(\hat{k}, y_2) & c_{12}(\hat{k}, y_2) \\ c_{21}(\hat{k}, y_2) & -c_{22}(\hat{k}, y_2) \end{bmatrix}, \tag{6.60b}$$

where the coefficients $c_{i\ell}(\hat{k}, y_2)$ can be computed by employing L'Hôpital's rule, giving

$$c_{i\ell}(\hat{k}, y_2) = \frac{\Psi_{i\ell}(\hat{k}, y_2)}{\frac{\mathrm{d}}{\mathrm{d}\xi}\left[\left(2\xi^2 - k_T^2\right)^2 - 4\xi^2\sqrt{\xi^2 - k_L^2}\sqrt{\xi^2 - k_T^2} + \frac{\omega}{\mu} Z_\infty k_T^2 \sqrt{\xi^2 - k_T^2}\right]\Big|_{\xi = \hat{k}}}. \tag{6.61}$$

The inverse Fourier transform of the term $\widehat{G}^{B,\mathrm{pol}}$ given in (6.56) is analytically computed. In order to determine the diagonal terms of $G^{B,\mathrm{pol}}$, it is necessary to calculate the inverse

transform

$$F_-(y_1) = \frac{1}{2\pi}\int_{-\infty}^{+\infty}\left(\frac{1}{\xi-\hat{k}} - \frac{1}{\xi+\hat{k}}\right)e^{\mathrm{i}\xi(y_1-x_1)}\mathrm{d}\xi. \tag{6.62}$$

Let us assume that $\hat{k}$ is real. In that case, the computation of the integral in (6.62) must be carefully done, because the functions $1/(\xi-\hat{k})$ and $1/(\xi+\hat{k})$ are not integrable in $\mathbb{R}$, at least in the classical sense. In order to overcome this difficulty, we resort to the limiting absorption principle. First, the pole at $\xi = \hat{k}$ is regarded as the limit

$$\hat{k} = \lim_{\varepsilon\to 0^+}\hat{k}^\varepsilon = \lim_{\varepsilon\to 0^+}\left(\hat{k}+\mathrm{i}\varepsilon\right), \tag{6.63}$$

and the calculation is made assuming that the poles are placed at $\xi = \pm\hat{k}^\varepsilon$, where $\varepsilon > 0$ is fixed. This procedure takes out both poles from the real axis and the inverse Fourier transform becomes correctly defined in the classical sense. Notice that the pole at $\xi = \hat{k}$ is displaced towards the upper complex half-plane, whereas the pole at $\xi = -\hat{k}$ is displaced towards the lower complex half-plane. This particular choice of sign for the imaginary part of each pole gives the solution having the right physical sense, that is, outgoing waves (for a more detailed explanation, see Durán et al. 2007). Once the inverse transform has been computed, we take the limit $\varepsilon \to 0^+$ in the obtained expression. Let us define the function $f_\varepsilon = f_\varepsilon(\xi)$ as the integrand of (6.62) with $\hat{k}$ replaced by $\hat{k}^\varepsilon$, that is,

$$f_\varepsilon(\xi) = \left(\frac{1}{\xi-\hat{k}^\varepsilon} - \frac{1}{\xi+\hat{k}^\varepsilon}\right)e^{\mathrm{i}\xi(y_1-x_1)}. \tag{6.64}$$

This function has two complex simple poles at $\xi = \hat{k}^\varepsilon$ and at $\xi = -\hat{k}^\varepsilon$. The integral in (6.62) is computed by application of Cauchy's residues theorem. This calculation is separately performed for the cases $y_1 - x_1 \geq 0$ and $y_1 - x_1 \leq 0$, dealing with different clockwise-oriented contours in the complex plane for each case. These contours are shown in Fig. 6.2, where $R > |\hat{k}^\varepsilon|$ is a parameter destined to tend to infinity. When $y_1 - x_1 \geq 0$, we integrate along the upper contour, which consists of two parts, namely the straight line I_R^+ and the upper semicircle S_R^+ (see Fig. 6.2 a)). Notice that only the pole at $\xi = \hat{k}^\varepsilon$ lies

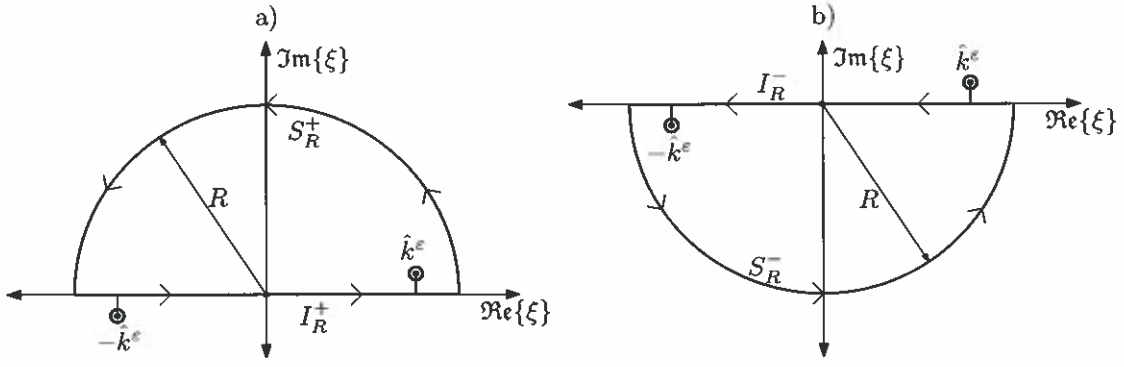

FIGURE 6.2. Contours in the complex plane for cases a) $y_1 - x_1 \geq 0$, b) $y_1 - x_1 \leq 0$.

inside this contour, so it follows from the residues theorem that

$$\int_{I_R^+} f_\varepsilon(\xi)\mathrm{d}\xi + \int_{S_R^+} f_\varepsilon(\xi)\mathrm{d}\xi = 2\pi\mathrm{i}\operatorname*{Res}_{\xi=\hat{k}^\varepsilon} f_\varepsilon(\xi). \tag{6.65}$$

As the contour is clockwise oriented, it is immediate that

$$\lim_{R\to+\infty}\int_{I_R^+} f_\varepsilon(\xi) = \int_{-\infty}^{+\infty}\left(\frac{1}{\xi-\hat{k}^\varepsilon} - \frac{1}{\xi+\hat{k}^\varepsilon}\right) e^{\mathrm{i}\xi(y_1-x_1)}\mathrm{d}\xi. \tag{6.66}$$

Moreover, it is not difficult to prove the estimation

$$\left|\int_{S_R^+} f_\varepsilon(\xi)\mathrm{d}\xi\right| \leq \frac{2R|\hat{k}^\varepsilon|}{R^2-|\hat{k}^\varepsilon|^2}\int_0^\pi e^{-R\sin\theta(y_1-x_1)}\mathrm{d}\theta, \tag{6.67}$$

and as $y_1 - x_1 \geq 0$, it follows from (6.67) that

$$\lim_{R\to+\infty}\left|\int_{S_R^+} f_\varepsilon(\xi)\mathrm{d}\xi\right| = 0. \tag{6.68}$$

On the other hand, the residue of f_ε associated with the pole at $\xi = \hat{k}^\varepsilon$ is computed as

$$\operatorname*{Res}_{\xi=\hat{k}^\varepsilon} f_\varepsilon(\xi) = \lim_{\xi\to\hat{k}^\varepsilon}\left(\xi-\hat{k}^\varepsilon\right) f_\varepsilon(\xi), \tag{6.69}$$

and combining with (6.64) gives

$$\operatorname*{Res}_{\xi=\hat{k}^\varepsilon} f_\varepsilon(\xi) = \lim_{\xi\to\hat{k}^\varepsilon}\left(1-\frac{\xi-\hat{k}^\varepsilon}{\xi+\hat{k}^\varepsilon}\right) e^{\mathrm{i}\xi(y_1-x_1)} = e^{\mathrm{i}\hat{k}^\varepsilon(y_1-x_1)}. \tag{6.70}$$

Consequently, taking the limit $R \longrightarrow +\infty$ in (6.65) and replacing (6.66), (6.68) and (6.70) leads to the identity

$$\int_{-\infty}^{+\infty}\left(\frac{1}{\xi-\hat{k}^\varepsilon} - \frac{1}{\xi+\hat{k}^\varepsilon}\right) e^{\mathrm{i}\xi(y_1-x_1)}\mathrm{d}\xi = 2\pi\mathrm{i}\, e^{\mathrm{i}\hat{k}^\varepsilon(y_1-x_1)}, \tag{6.71}$$

which is valid when $y_1 - x_1 \geq 0$. When $y_1 - x_1 \leq 0$, we integrate along the lower contour, which consists of the straight line I_R^- and the lower semicircle S_R^- (see Fig. 6.2 b)). The procedure is analogous to the previous case, but this time it is necessary to take into account that this contour only encircles the pole at $\xi = -\hat{k}^\varepsilon$. We finally obtain the identity

$$\int_{-\infty}^{+\infty}\left(\frac{1}{\xi-\hat{k}^\varepsilon} - \frac{1}{\xi+\hat{k}^\varepsilon}\right) e^{\mathrm{i}\xi(y_1-x_1)}\mathrm{d}\xi = 2\pi\mathrm{i}\, e^{-\mathrm{i}\hat{k}^\varepsilon(y_1-x_1)}, \tag{6.72}$$

which is valid when $y_1 - x_1 \leq 0$. In the general case, both identities (6.71) and (6.72) can be expressed in a single form

$$\int_{-\infty}^{+\infty}\left(\frac{1}{\xi-\hat{k}^\varepsilon} - \frac{1}{\xi+\hat{k}^\varepsilon}\right) e^{\mathrm{i}\xi(y_1-x_1)}\mathrm{d}\xi = 2\pi\mathrm{i}\, e^{\mathrm{i}\hat{k}^\varepsilon|y_1-x_1|}. \tag{6.73}$$

Finally, taking the limit $\varepsilon \longrightarrow 0^+$ in (6.73) and replacing in (6.62), we obtain

$$F_-(y_1) = \mathrm{i}\, e^{\mathrm{i}\hat{k}|y_1-x_1|}. \tag{6.74}$$

In order to determine the off-diagonal terms of $G^{B,\mathrm{psr}}$, it is necessary to compute:

$$F_+(y_1) = \frac{1}{2\pi}\int_{-\infty}^{+\infty}\left(\frac{1}{\xi-\hat{k}}+\frac{1}{\xi+\hat{k}}\right)e^{\mathrm{i}\xi(y_1-x_1)}\mathrm{d}\xi. \tag{6.75}$$

The development for calculating this integral is completely analogous to that already done for (6.62). The final result is

$$F_+(y_1) = \mathrm{i}\,\mathrm{sign}\,(y_1-x_1)\,e^{\mathrm{i}\hat{k}|y_1-x_1|}. \tag{6.76}$$

If $\hat{k}$ has a nonzero imaginary part, it is not necessary to add an imaginary part, and the inverse Fourier transform of (6.56) can be computed directly by application of the Cauchy's residues theorem, leading to the same result in function of $\hat{k}$. Then, substituting (6.74) and (6.76) in (6.56) yields the components of $G^{B,\mathrm{pol}}$:

$$G_{11}^{B,\mathrm{pol}}(\boldsymbol{x},\boldsymbol{y}) = -\frac{\mathrm{i}}{\rho\,\omega^2}\,c_{11}(\hat{k},y_2)\,e^{\mathrm{i}\hat{k}|y_1-x_1|}, \tag{6.77a}$$

$$G_{12}^{B,\mathrm{pol}}(\boldsymbol{x},\boldsymbol{y}) = -\frac{\mathrm{i}}{\rho\,\omega^2}\,c_{12}(\hat{k},y_2)\,\mathrm{sign}\,(y_1-x_1)\,e^{\mathrm{i}\hat{k}|y_1-x_1|}, \tag{6.77b}$$

$$G_{21}^{B,\mathrm{pol}}(\boldsymbol{x},\boldsymbol{y}) = -\frac{\mathrm{i}}{\rho\,\omega^2}\,c_{21}(\hat{k},y_2)\,\mathrm{sign}\,(y_1-x_1)\,e^{\mathrm{i}\hat{k}|y_1-x_1|}, \tag{6.77c}$$

$$G_{22}^{B,\mathrm{pol}}(\boldsymbol{x},\boldsymbol{y}) = -\frac{\mathrm{i}}{\rho\,\omega^2}\,c_{22}(\hat{k},y_2)\,e^{\mathrm{i}\hat{k}|y_1-x_1|}. \tag{6.77d}$$

In order to make easier the subsequent numerical implementation of these expressions, we write the coefficients $c_{i\ell}$ explicitly. Computing the derivative of the denominator in (6.51) yields

$$\begin{aligned}\frac{\mathrm{d}}{\mathrm{d}\xi}\left\{\left(2\xi^2-k_T^2\right)^2-4\xi^2\sqrt{\xi^2-k_L^2}\sqrt{\xi^2-k_T^2}+\frac{\omega}{\mu}Z_\infty k_T^2\sqrt{\xi^2-k_T^2}\right\} = \\ \xi\Bigg\{8\left(2\xi^2-k_T^2-\sqrt{\xi^2-k_L^2}\sqrt{\xi^2-k_T^2}\right) \\ -4\xi^2\left(\frac{\sqrt{\xi^2-k_L^2}}{\sqrt{\xi^2-k_T^2}}+\frac{\sqrt{\xi^2-k_T^2}}{\sqrt{\xi^2-k_L^2}}\right)+\frac{\omega}{\mu}Z_\infty\frac{k_T^2}{\sqrt{\xi^2-k_T^2}}\Bigg\},\end{aligned} \tag{6.78}$$

and we define the quantities $\hat{k}_L$ and $\hat{k}_T$ as

$$\hat{k}_L = \sqrt{\hat{k}^2-k_L^2}, \qquad \hat{k}_T = \sqrt{\hat{k}^2-k_T^2}. \tag{6.79}$$

Hence, the expressions for the coefficients $c_{i\ell}$ are obtained by evaluating (6.52) and (6.78) in $\xi=\hat{k}$, combining with (6.79) and substituting in (6.61):

$$\begin{aligned}c_{11}(\hat{k},y_2) = \frac{\hat{k}_T/\hat{k}\left(2\hat{k}^2e^{-\hat{k}_Ly_2}-\left(2\hat{k}^2-k_T^2\right)e^{-\hat{k}_Ty_2}\right)}{8\left(2\hat{k}^2-k_T^2-\hat{k}_L\hat{k}_T\right)-4\hat{k}^2\left(\hat{k}_L/\hat{k}_T+\hat{k}_T/\hat{k}_L\right)+\frac{\omega}{\mu}Z_\infty k_T^2/\hat{k}_T} \\ \times\left(2\hat{k}^2e^{-\hat{k}_Lx_2}-\left(2\hat{k}^2-k_T^2\right)e^{-\hat{k}_Tx_2}\right),\end{aligned} \tag{6.80a}$$

$$c_{12}(\hat{k}, y_2) = \frac{\mathrm{i}\left(\hat{k}_L\hat{k}_T e^{-\hat{k}_L y_2} - (2\hat{k}^2 - k_T^2)e^{-\hat{k}_T y_2}\right)}{8(2\hat{k}^2 - k_T^2 - \hat{k}_L\hat{k}_T) - 4\hat{k}^2(\hat{k}_L/\hat{k}_T + \hat{k}_T/\hat{k}_L) + \frac{\omega}{\mu}Z_\infty k_T^2/\hat{k}_T} \times \left(2\hat{k}^2 e^{-\hat{k}_L x_2} - (2\hat{k}^2 - k_T^2)e^{-\hat{k}_T x_2}\right), \tag{6.80b}$$

$$c_{21}(\hat{k}, y_2) = -\frac{\mathrm{i}\left((2\hat{k}^2 - k_T^2)e^{-\hat{k}_L y_2} - 2\hat{k}_L\hat{k}_T e^{-\hat{k}_T y_2}\right)}{8(2\hat{k}^2 - k_T^2 - \hat{k}_L\hat{k}_T) - 4\hat{k}^2(\hat{k}_L/\hat{k}_T + \hat{k}_T/\hat{k}_L) + \frac{\omega}{\mu}Z_\infty k_T^2/\hat{k}_T} \times \left((2\hat{k}^2 - k_T^2)e^{-\hat{k}_L x_2} - 2\hat{k}^2 e^{-\hat{k}_T x_2}\right) \tag{6.80c}$$

$$- \frac{\mathrm{i}\frac{\omega}{\mu}Z_\infty k_T^2\hat{k}_T\left(e^{-(\hat{k}_L y_2 + \hat{k}_T x_2)} - e^{-(\hat{k}_T y_2 + \hat{k}_L x_2)}\right)}{8(2\hat{k}^2 - k_T^2 - \hat{k}_L\hat{k}_T) - 4\hat{k}^2(\hat{k}_L/\hat{k}_T + \hat{k}_T/\hat{k}_L) + \frac{\omega}{\mu}Z_\infty k_T^2/\hat{k}_T},$$

$$c_{22}(\hat{k}, y_2) = \frac{\hat{k}_L/\hat{k}\left((2\hat{k}^2 - k_T^2)e^{-\hat{k}_L y_2} - 2\hat{k}^2 e^{-\hat{k}_T y_2}\right)}{8(2\hat{k}^2 - k_T^2 - \hat{k}_L\hat{k}_T) - 4\hat{k}^2(\hat{k}_L/\hat{k}_T + \hat{k}_T/\hat{k}_L) + \frac{\omega}{\mu}Z_\infty k_T^2/\hat{k}_T} \times \left((2\hat{k}^2 - k_T^2)e^{-\hat{k}_L x_2} - 2\hat{k}^2 e^{-\hat{k}_T x_2}\right) \tag{6.80d}$$

$$+ \frac{\frac{\omega}{\mu}Z_\infty k_T^2/\hat{k}\left(\hat{k}_L\hat{k}_T e^{-(\hat{k}_L y_2 + \hat{k}_T x_2)} - \hat{k}^2 e^{-(\hat{k}_T y_2 + \hat{k}_L x_2)}\right)}{8(2\hat{k}^2 - k_T^2 - \hat{k}_L\hat{k}_T) - 4\hat{k}^2(\hat{k}_L/\hat{k}_T + \hat{k}_T/\hat{k}_L) + \frac{\omega}{\mu}Z_\infty k_T^2/\hat{k}_T}.$$

6.3.5 The regular part

Once the terms corresponding to pseudo-poles and poles have been subtracted from $\widehat{G}^B$, the following term remains:

$$\widehat{G}^{B,\mathrm{reg}}(\xi, y_2) = \widehat{G}^{B,\mathrm{psr}}(\xi, y_2) - \widehat{G}^{B,\mathrm{pol}}(\xi, y_2), \tag{6.81}$$

and the term we desire to calculate can be written as

$$G^{B,\mathrm{reg}}(\boldsymbol{x}, \boldsymbol{y}) = \frac{1}{2\pi}\int_{-\infty}^{+\infty} \widehat{G}^{B,\mathrm{reg}}(\xi, y_2)e^{\mathrm{i}\xi(y_1 - x_1)}\mathrm{d}\xi. \tag{6.82}$$

The term $\widehat{G}^{B,\mathrm{reg}}$ is regular, because all its singularities in ξ have been removed. In addition, it decreases fast at infinity in ξ, since $\widehat{G}^{B,\mathrm{psr}}$ is exponentially decreasing. The inverse Fourier transform of $\widehat{G}^{B,\mathrm{reg}}$ is thus numerically approximated by the inverse discrete Fourier transform (IDFT) and efficiently computed by an algorithm of inverse (or backward) fast Fourier transform (IFFT). To do so, we deal with the centered variable $v = y_1 - x_1$. Both the spatial and spectral domains are discretized by considering N equispaced samples v_n and ξ_m, where $n, m = 0, 1, \ldots, N-1$ and N corresponds to a power of 2 for the application of the IFFT, that is, $N = 2^M$ for some $M \in \mathbb{N}$. The discretized spatial and spectral domains are thus given respectively by

$$v_n = -v^{\max} + n\Delta v, \qquad n = 0, 1, \ldots, N-1, \tag{6.83a}$$

$$\xi_m = -\xi^{\max} + m\Delta\xi, \qquad m = 0, 1, \ldots, N-1, \tag{6.83b}$$

where $v^{\max} > 0$ and $\xi^{\max} > 0$ are the maximum values of $|v|$ and $|\xi|$, respectively, whereas Δv and $\Delta\xi$ are the steps of discretization in v and ξ, respectively. The following relations link the parameters of this discretization:

$$N\Delta v = 2v^{\max}, \tag{6.84a}$$

$$N\Delta\xi = 2\xi^{\max}, \tag{6.84b}$$

$$N\Delta v\,\Delta\xi = 2\pi, \tag{6.84c}$$

$$2v^{\max}\,\xi^{\max} = N\pi. \tag{6.84d}$$

Therefore, given a function $\phi(v)$ and its Fourier transform $\Phi(\xi)$, their discrete approximations ϕ_n and Φ_m are defined as

$$\Phi_m = \frac{v^{\max}}{N}\sum_{n=0}^{N-1}\phi_n\, e^{-\frac{2\pi i n m}{N}}, \qquad n = 0, 1, \ldots, N-1, \tag{6.85a}$$

$$\phi_n = \frac{2\xi^{\max}}{N\pi}\sum_{m=0}^{N-1}\Phi_m\, e^{\frac{2\pi i n m}{N}}, \qquad m = 0, 1, \ldots, N-1. \tag{6.85b}$$

This algorithm gives a numerical approximation of $G^{B,\mathrm{reg}}$ in a bounded region of $\mathbb{R}^2_+$, which we write in general as

$$G^{B,\mathrm{reg}}(\boldsymbol{x},\boldsymbol{y}) \approx \mathrm{IFFT}\big\{\widehat{G}^{B,\mathrm{reg}}(\xi, y_2)\big\}(y_1 - x_1). \tag{6.86}$$

6.4 Effective calculation of the Green's function's normal derivative

6.4.1 Definition and decomposition of the normal derivative

We now analyze the calculation of the normal derivative of the half-plane Green's function G determined in the previous section, which is denoted by H. A numerically evaluable expression for this normal derivative is necessary, in order to be able to implement the boundary element method developed in Chapter V. The components of H can be obtained from formula (4.30), which is given in tensor notation in terms of the derivatives of G. Expanding this formula, we obtain that the components of H are

$$\begin{aligned} H_{11}(\boldsymbol{x},\boldsymbol{y}) = {} & \left((\lambda+2\mu)\frac{\partial G_{11}}{\partial y_1}(\boldsymbol{x},\boldsymbol{y}) + \lambda\frac{\partial G_{12}}{\partial y_2}(\boldsymbol{x},\boldsymbol{y})\right) n_1(\boldsymbol{y}) \\ & + \mu\left(\frac{\partial G_{11}}{\partial y_2}(\boldsymbol{x},\boldsymbol{y}) + \frac{\partial G_{12}}{\partial y_1}(\boldsymbol{x},\boldsymbol{y})\right) n_2(\boldsymbol{y}), \end{aligned} \tag{6.87a}$$

$$\begin{aligned} H_{12}(\boldsymbol{x},\boldsymbol{y}) = {} & \mu\left(\frac{\partial G_{11}}{\partial y_2}(\boldsymbol{x},\boldsymbol{y}) + \frac{\partial G_{12}}{\partial y_1}(\boldsymbol{x},\boldsymbol{y})\right) n_1(\boldsymbol{y}) \\ & + \left(\lambda\frac{\partial G_{11}}{\partial y_1}(\boldsymbol{x},\boldsymbol{y}) + (\lambda+2\mu)\frac{\partial G_{12}}{\partial y_2}(\boldsymbol{x},\boldsymbol{y})\right) n_2(\boldsymbol{y}), \end{aligned} \tag{6.87b}$$

$$\begin{aligned} H_{21}(\boldsymbol{x},\boldsymbol{y}) = {} & \left((\lambda+2\mu)\frac{\partial G_{21}}{\partial y_1}(\boldsymbol{x},\boldsymbol{y}) + \lambda\frac{\partial G_{22}}{\partial y_2}(\boldsymbol{x},\boldsymbol{y})\right) n_1(\boldsymbol{y}) \\ & + \mu\left(\frac{\partial G_{21}}{\partial y_2}(\boldsymbol{x},\boldsymbol{y}) + \frac{\partial G_{22}}{\partial y_1}(\boldsymbol{x},\boldsymbol{y})\right) n_2(\boldsymbol{y}), \end{aligned} \tag{6.87c}$$

$$H_{22}(\boldsymbol{x},\boldsymbol{y}) = \mu\left(\frac{\partial G_{21}}{\partial y_2}(\boldsymbol{x},\boldsymbol{y}) + \frac{\partial G_{22}}{\partial y_1}(\boldsymbol{x},\boldsymbol{y})\right) n_1(\boldsymbol{y}) + \left(\lambda\frac{\partial G_{21}}{\partial y_1}(\boldsymbol{x},\boldsymbol{y}) + (\lambda+2\mu)\frac{\partial G_{22}}{\partial y_2}(\boldsymbol{x},\boldsymbol{y})\right) n_2(\boldsymbol{y}), \tag{6.87d}$$

where n_1 and n_2 are the components of the outward unit normal vector on the surface in study. On the other hand, we infer from the previous subsection that H is decomposed as

$$H(\boldsymbol{x},\boldsymbol{y}) = H^P(\boldsymbol{x},\boldsymbol{y}) + H^B(\boldsymbol{x},\boldsymbol{y}), \tag{6.88}$$

where H^P and H^B are the normal derivative of the full-plane term and the boundary term, respectively. This decomposition was also deduced in Section 4.3, and it is given in tensor notation in (4.94). In addition, the boundary term is decomposed as

$$H^B(\boldsymbol{x},\boldsymbol{y}) = H^{B,\mathrm{psp}}(\boldsymbol{x},\boldsymbol{y}) + H^{B,\mathrm{pol}}(\boldsymbol{x},\boldsymbol{y}) + H^{B,\mathrm{reg}}(\boldsymbol{x},\boldsymbol{y}), \tag{6.89}$$

where $H^{B,\mathrm{psp}}$, $H^{B,\mathrm{pol}}$ and $H^{B,\mathrm{reg}}$ denote the normal derivative of the part of the pseudo-poles $G^{B,\mathrm{psp}}$, the part of the poles $G^{B,\mathrm{pol}}$ and the regular part $G^{B,\mathrm{reg}}$, respectively. It is clear that all these terms are calculated from formulae (6.87), with G substituted by the corresponding part of Green's function. In what follows, we perform the calculations of these normal derivatives.

6.4.2 The full-plane term and the part of the pseudo-poles

The normal derivative of the full-plane term was already calculated and is given, e.g., in (5.98). We write this normal derivative explicitly by components as

$$H^P_{11}(\boldsymbol{x},\boldsymbol{y}) = \frac{\mathrm{i}}{4}\left\{\left(D(r) + 2C(r)\frac{(y_1-x_1)^2}{r^2}\right)\left(\frac{(y_1-x_1)}{r}n_1 + \frac{(y_2-x_2)}{r}n_2\right) + \big(D(r)+E(r)\big)\frac{(y_1-x_1)}{r}n_1\right\}, \tag{6.90a}$$

$$H^P_{12}(\boldsymbol{x},\boldsymbol{y}) = \frac{\mathrm{i}}{4}\left\{2C(r)\frac{(y_1-x_1)(y_2-x_2)}{r^2}\left(\frac{(y_1-x_1)}{r}n_1 + \frac{(y_2-x_2)}{r}n_2\right) + D(r)\frac{(y_2-x_2)}{r}n_1 + E(r)\frac{(y_1-x_1)}{r}n_2\right\}, \tag{6.90b}$$

$$H^P_{21}(\boldsymbol{x},\boldsymbol{y}) = \frac{\mathrm{i}}{4}\left\{2C(r)\frac{(y_1-x_1)(y_2-x_2)}{r^2}\left(\frac{(y_1-x_1)}{r}n_1 + \frac{(y_2-x_2)}{r}n_2\right) + D(r)\frac{(y_1-x_1)}{r}n_2 + E(r)\frac{(y_2-x_2)}{r}n_1\right\}, \tag{6.90c}$$

$$H^P_{22}(\boldsymbol{x},\boldsymbol{y}) = \frac{\mathrm{i}}{4}\left\{\left(D(r) + 2C(r)\frac{(y_2-x_2)^2}{r^2}\right)\left(\frac{(y_1-x_1)}{r}n_1 + \frac{(y_2-x_2)}{r}n_2\right) + \big(D(r)+E(r)\big)\frac{(y_2-x_2)}{r}n_2\right\}, \tag{6.90d}$$

Let us calculate the normal derivative of the part of the pseudo-poles. As this part corresponds to minus the full-plane term, evaluated at the image point $\overline{\boldsymbol{x}}$ defined above, this

normal derivative can be easily determined from this fact and (6.90). Its components are

$$H_{11}^{B,\mathrm{psp}}(\boldsymbol{x},\boldsymbol{y}) = -\frac{\mathrm{i}}{4}\Big\{\Big(D(\overline{r}) + 2C(\overline{r})\frac{(y_1-x_1)^2}{\overline{r}^{\,2}}\Big)\Big(\frac{(y_1-x_1)}{\overline{r}}\,n_1 + \frac{(y_2+x_2)}{\overline{r}}\,n_2\Big) + \big(D(\overline{r}) + E(\overline{r})\big)\frac{(y_1-x_1)}{\overline{r}}\,n_1\Big\}, \tag{6.91a}$$

$$H_{12}^{B,\mathrm{psp}}(\boldsymbol{x},\boldsymbol{y}) = -\frac{\mathrm{i}}{4}\Big\{2C(\overline{r})\frac{(y_1-x_1)(y_2+x_2)}{\overline{r}^{\,2}}\Big(\frac{(y_1-x_1)}{\overline{r}}\,n_1 + \frac{(y_2+x_2)}{\overline{r}}\,n_2\Big) + D(\overline{r})\,\frac{(y_2+x_2)}{\overline{r}}\,n_1 + E(\overline{r})\,\frac{(y_1-x_1)}{\overline{r}}\,n_2\Big\}, \tag{6.91b}$$

$$H_{21}^{B,\mathrm{psp}}(\boldsymbol{x},\boldsymbol{y}) = -\frac{\mathrm{i}}{4}\Big\{2C(\overline{r})\frac{(y_1-x_1)(y_2+x_2)}{\overline{r}^{\,2}}\Big(\frac{(y_1-x_1)}{\overline{r}}\,n_1 + \frac{(y_2+x_2)}{\overline{r}}\,n_2\Big) + D(\overline{r})\,\frac{(y_1-x_1)}{\overline{r}}\,n_2 + E(\overline{r})\,\frac{(y_2+x_2)}{\overline{r}}\,n_1\Big\}, \tag{6.91c}$$

$$H_{22}^{B,\mathrm{psp}}(\boldsymbol{x},\boldsymbol{y}) = -\frac{\mathrm{i}}{4}\Big\{\Big(D(\overline{r}) + 2C(\overline{r})\frac{(y_2+x_2)^2}{\overline{r}^{\,2}}\Big)\Big(\frac{(y_1-x_1)}{\overline{r}}\,n_1 + \frac{(y_2+x_2)}{\overline{r}}\,n_2\Big) + \big(D(\overline{r}) + E(\overline{r})\big)\frac{(y_2+x_2)}{\overline{r}}\,n_2\Big\}. \tag{6.91d}$$

Notice that although G^P and $G^{B,\mathrm{psp}}$ are symmetric matrices, their normal derivatives H^P and $H^{B,\mathrm{psp}}$ are not.

6.4.3 The part of the poles and the regular part

Let us compute the derivatives of part of the poles $G^{B,\mathrm{pol}}$ given in (6.77). The derivatives with respect to y_1 in the sense of distributions are

$$\frac{\partial G_{11}^{B,\mathrm{pol}}}{\partial y_1}(\boldsymbol{x},\boldsymbol{y}) = \frac{1}{\rho\,\omega^2}\,\hat{k}c_{11}(\hat{k},y_2)\,\mathrm{sign}\,(y_1-x_1)\,e^{\mathrm{i}\hat{k}|y_1-x_1|}, \tag{6.92a}$$

$$\frac{\partial G_{12}^{B,\mathrm{pol}}}{\partial y_1}(\boldsymbol{x},\boldsymbol{y}) = \frac{1}{\rho\,\omega^2}\,c_{12}(\hat{k},y_2)\big(\hat{k}e^{\mathrm{i}\hat{k}|y_1-x_1|} - 2\mathrm{i}\delta_{x_1}(y_1)\big), \tag{6.92b}$$

$$\frac{\partial G_{21}^{B,\mathrm{pol}}}{\partial y_1}(\boldsymbol{x},\boldsymbol{y}) = \frac{1}{\rho\,\omega^2}\,c_{21}(\hat{k},y_2)\big(\hat{k}e^{\mathrm{i}\hat{k}|y_1-x_1|} - 2\mathrm{i}\delta_{x_1}(y_1)\big), \tag{6.92c}$$

$$\frac{\partial G_{22}^{B,\mathrm{pol}}}{\partial y_1}(\boldsymbol{x},\boldsymbol{y}) = \frac{1}{\rho\,\omega^2}\,\hat{k}c_{22}(\hat{k},y_2)\,\mathrm{sign}\,(y_1-x_1)\,e^{\mathrm{i}\hat{k}|y_1-x_1|}, \tag{6.92d}$$

while the derivatives with respect to y_2 are

$$\frac{\partial G_{11}^{B,\mathrm{pol}}}{\partial y_2}(\boldsymbol{x},\boldsymbol{y}) = -\frac{\mathrm{i}}{\rho\,\omega^2}\,\frac{\partial c_{11}}{\partial y_2}(\hat{k},y_2)\,e^{\mathrm{i}\hat{k}|y_1-x_1|}, \tag{6.93a}$$

$$\frac{\partial G_{12}^{B,\mathrm{pol}}}{\partial y_2}(\boldsymbol{x},\boldsymbol{y}) = -\frac{\mathrm{i}}{\rho\,\omega^2}\,\frac{\partial c_{12}}{\partial y_2}(\hat{k},y_2)\,\mathrm{sign}\,(y_1-x_1)\,e^{\mathrm{i}\hat{k}|y_1-x_1|}, \tag{6.93b}$$

$$\frac{\partial G_{21}^{B,\mathrm{pol}}}{\partial y_2}(\boldsymbol{x},\boldsymbol{y}) = -\frac{\mathrm{i}}{\rho\,\omega^2}\,\frac{\partial c_{21}}{\partial y_2}(\hat{k},y_2)\,\mathrm{sign}\,(y_1-x_1)\,e^{\mathrm{i}\hat{k}|y_1-x_1|}, \tag{6.93c}$$

$$\frac{\partial G_{22}^{B,\mathrm{pol}}}{\partial y_2}(\boldsymbol{x},\boldsymbol{y}) = -\frac{\mathrm{i}}{\rho\,\omega^2}\,\frac{\partial c_{22}}{\partial y_2}(\hat{k},y_2)\,e^{\mathrm{i}\hat{k}|y_1-x_1|}, \tag{6.93d}$$

where the derivatives of the coefficients $c_{i\ell}$ are given by

$$\begin{aligned}\frac{\partial c_{11}}{\partial y_2}(\hat{k},y_2) = &-\frac{\hat{k}_T/\hat{k}\left(2\hat{k}^2\hat{k}_L e^{-\hat{k}_L y_2} - \left(2\hat{k}^2-k_T^2\right)\hat{k}_T e^{-\hat{k}_T y_2}\right)}{8\left(2\hat{k}^2-k_T^2-\hat{k}_L\hat{k}_T\right) - 4\hat{k}^2\left(\hat{k}_L/\hat{k}_T+\hat{k}_T/\hat{k}_L\right)+\frac{\omega}{\mu}Z_\infty k_T^2/\hat{k}_T} \\ &\times\left(2\hat{k}^2 e^{-\hat{k}_L x_2} - \left(2\hat{k}^2-k_T^2\right)e^{-\hat{k}_T x_2}\right),\end{aligned} \tag{6.94a}$$

$$\begin{aligned}\frac{\partial c_{12}}{\partial y_2}(\hat{k},y_2) = &-\frac{\mathrm{i}\hat{k}_T\left(\left(\hat{k}^2-k_L^2\right)e^{-\hat{k}_L y_2} - \left(2\hat{k}^2-k_T^2\right)e^{-\hat{k}_T y_2}\right)}{8\left(2\hat{k}^2-k_T^2-\hat{k}_L\hat{k}_T\right) - 4\hat{k}^2\left(\hat{k}_L/\hat{k}_T+\hat{k}_T/\hat{k}_L\right)+\frac{\omega}{\mu}Z_\infty k_T^2/\hat{k}_T} \\ &\times\left(2\hat{k}^2 e^{-\hat{k}_L x_2} - \left(2\hat{k}^2-k_T^2\right)e^{-\hat{k}_T x_2}\right),\end{aligned} \tag{6.94b}$$

$$\begin{aligned}\frac{\partial c_{21}}{\partial y_2}(\hat{k},y_2) = &\frac{\mathrm{i}\hat{k}_L\left(\left(2\hat{k}^2-k_T^2\right)e^{-\hat{k}_L y_2} - 2\left(\hat{k}^2-k_T^2\right)e^{-\hat{k}_T y_2}\right)}{8\left(2\hat{k}^2-k_T^2-\hat{k}_L\hat{k}_T\right) - 4\hat{k}^2\left(\hat{k}_L/\hat{k}_T+\hat{k}_T/\hat{k}_L\right)+\frac{\omega}{\mu}Z_\infty k_T^2/\hat{k}_T} \\ &\times\left(\left(2\hat{k}^2-k_T^2\right)e^{-\hat{k}_L x_2} - 2\hat{k}^2 e^{-\hat{k}_T x_2}\right) \\ &+\frac{\mathrm{i}\frac{\omega}{\mu}Z_\infty k_T^2\hat{k}_T\left(\hat{k}_L e^{-(\hat{k}_L y_2+\hat{k}_T x_2)} - \hat{k}_T e^{-(\hat{k}_T y_2+\hat{k}_L x_2)}\right)}{8\left(2\hat{k}^2-k_T^2-\hat{k}_L\hat{k}_T\right) - 4\hat{k}^2\left(\hat{k}_L/\hat{k}_T+\hat{k}_T/\hat{k}_L\right)+\frac{\omega}{\mu}Z_\infty k_T^2/\hat{k}_T},\end{aligned} \tag{6.94c}$$

$$\begin{aligned}\frac{\partial c_{22}}{\partial y_2}(\hat{k},y_2) = &-\frac{\hat{k}_L/\hat{k}\left(\left(2\hat{k}^2-k_T^2\right)\hat{k}_L e^{-\hat{k}_L y_2} - 2\hat{k}^2\hat{k}_T e^{-\hat{k}_T y_2}\right)}{8\left(2\hat{k}^2-k_T^2-\hat{k}_L\hat{k}_T\right) - 4\hat{k}^2\left(\hat{k}_L/\hat{k}_T+\hat{k}_T/\hat{k}_L\right)+\frac{\omega}{\mu}Z_\infty k_T^2/\hat{k}_T} \\ &\times\left(\left(2\hat{k}^2-k_T^2\right)e^{-\hat{k}_L x_2} - 2\hat{k}^2 e^{-\hat{k}_T x_2}\right) \\ &-\frac{\frac{\omega}{\mu}Z_\infty k_T^2\hat{k}_T/\hat{k}\left(\left(\hat{k}^2-k_L^2\right)e^{-(\hat{k}_L y_2+\hat{k}_T x_2)} - \hat{k}^2 e^{-(\hat{k}_T y_2+\hat{k}_L x_2)}\right)}{8\left(2\hat{k}^2-k_T^2-\hat{k}_L\hat{k}_T\right) - 4\hat{k}^2\left(\hat{k}_L/\hat{k}_T+\hat{k}_T/\hat{k}_L\right)+\frac{\omega}{\mu}Z_\infty k_T^2/\hat{k}_T}.\end{aligned} \tag{6.94d}$$

Therefore, replacing (6.92) and (6.93) in (6.87), with G substituted by $G^{B,\mathrm{pol}}$, and assuming for a moment that $y_1 \neq x_1$, we obtain that the components of $H^{B,\mathrm{pol}}$ are

$$\begin{aligned}H_{11}^{B,\mathrm{pol}}(\boldsymbol{x},\boldsymbol{y}) = \frac{1}{\rho\,\omega^2}\Bigg\{&\left((\lambda+2\mu)\hat{k}c_{11}(\hat{k},y_2) - \mathrm{i}\lambda\frac{\partial c_{12}}{\partial y_2}(\hat{k},y_2)\right)\mathrm{sign}\,(y_1-x_1)n_1 \\ &+\mu\left(\hat{k}c_{12}(\hat{k},y_2) - \mathrm{i}\frac{\partial c_{11}}{\partial y_2}(\hat{k},y_2)\right)n_2\Bigg\}\,e^{\mathrm{i}\hat{k}|y_1-x_1|},\end{aligned} \tag{6.95a}$$

$$\begin{aligned}H_{12}^{B,\mathrm{pol}}(\boldsymbol{x},\boldsymbol{y}) = \frac{1}{\rho\,\omega^2}\Bigg\{&\mu\left(\hat{k}c_{12}(\hat{k},y_2) - \mathrm{i}\frac{\partial c_{11}}{\partial y_2}(\hat{k},y_2)\right)n_1 \\ &+\left(\lambda\hat{k}c_{11}(\hat{k},y_2) - \mathrm{i}(\lambda+2\mu)\frac{\partial c_{12}}{\partial y_2}(\hat{k},y_2)\right)\mathrm{sign}\,(y_1-x_1)n_2\Bigg\}\,e^{\mathrm{i}\hat{k}|y_1-x_1|},\end{aligned} \tag{6.95b}$$

$$H_{21}^{B,\mathrm{pol}}(\boldsymbol{x},\boldsymbol{y}) = \frac{1}{\rho\,\omega^2}\Bigg\{\bigg((\lambda+2\mu)\hat{k}c_{21}(\hat{k},y_2) - \mathrm{i}\lambda\frac{\partial c_{22}}{\partial y_2}(\hat{k},y_2)\bigg)n_1 + \mu\bigg(\hat{k}c_{22}(\hat{k},y_2) - \mathrm{i}\frac{\partial c_{21}}{\partial y_2}(\hat{k},y_2)\bigg)\,\mathrm{sign}\,(y_1-x_1)n_2\Bigg\}\,e^{\mathrm{i}\hat{k}|y_1-x_1|}, \tag{6.95c}$$

$$H_{22}^{B,\mathrm{pol}}(\boldsymbol{x},\boldsymbol{y}) = \frac{1}{\rho\,\omega^2}\Bigg\{\mu\bigg(\hat{k}c_{22}(\hat{k},y_2) - \mathrm{i}\frac{\partial c_{21}}{\partial y_2}(\hat{k},y_2)\bigg)\,\mathrm{sign}\,(y_1-x_1)n_1 + \bigg(\lambda\hat{k}c_{21}(\hat{k},y_2) - \mathrm{i}(\lambda+2\mu)\frac{\partial c_{22}}{\partial y_2}(\hat{k},y_2)\bigg)n_2\Bigg\}\,e^{\mathrm{i}\hat{k}|y_1-x_1|}. \tag{6.95d}$$

In the case where $y_1 = x_1$, we will see that Dirac's delta distributions in (6.92b) and (6.92c) are actually canceled by other terms coming from the derivatives of the regular part $G^{B,\mathrm{reg}}$, so they do not need to be taken into account. In order to compute the derivatives of $G^{B,\mathrm{reg}}$, it is necessary to deal with the corresponding spectral part $\widehat{G}^{B,\mathrm{reg}}$ defined in (6.81), since $G^{B,\mathrm{reg}}$ is not known in explicit form. Using properties of the Fourier transform, the derivatives of $G^{B,\mathrm{reg}}$ with respect to y_1 can be computed as follows:

$$\frac{\partial G^{B,\mathrm{reg}}}{\partial y_1}(\boldsymbol{x},\boldsymbol{y}) = \frac{1}{2\pi}\int_{-\infty}^{+\infty}\mathrm{i}\xi\widehat{G}^{B,\mathrm{reg}}(\xi,y_2)e^{\mathrm{i}\xi(y_1-x_1)}\mathrm{d}\xi, \tag{6.96}$$

while the derivatives with respect to y_2 are computed directly inside the integral sign:

$$\frac{\partial G^{B,\mathrm{reg}}}{\partial y_2}(\boldsymbol{x},\boldsymbol{y}) = \frac{1}{2\pi}\int_{-\infty}^{+\infty}\frac{\partial\widehat{G}^{B,\mathrm{reg}}}{\partial y_2}(\xi,y_2)e^{\mathrm{i}\xi(y_1-x_1)}\mathrm{d}\xi. \tag{6.97}$$

We thus define the spectral term $\widehat{H}^{B,\mathrm{reg}}$ in an analogous way as (6.87) but in the Fourier domain, that is,

$$\widehat{H}_{11}^{B,\mathrm{reg}}(\xi,y_2) = \bigg(\mathrm{i}(\lambda+2\mu)\xi\widehat{G}_{11}^{B,\mathrm{reg}}(\xi,y_2) + \lambda\frac{\partial\widehat{G}_{12}^{B,\mathrm{reg}}}{\partial y_2}(\xi,y_2)\bigg)n_1(\boldsymbol{y}) + \mu\bigg(\frac{\partial\widehat{G}_{11}^{B,\mathrm{reg}}}{\partial y_2}(\xi,y_2) + \mathrm{i}\xi\widehat{G}_{12}^{B,\mathrm{reg}}(\xi,y_2)\bigg)n_2(\boldsymbol{y}), \tag{6.98a}$$

$$\widehat{H}_{12}^{B,\mathrm{reg}}(\xi,y_2) = \mu\bigg(\frac{\partial\widehat{G}_{11}^{B,\mathrm{reg}}}{\partial y_2}(\xi,y_2) + \mathrm{i}\xi\widehat{G}_{12}^{B,\mathrm{reg}}(\xi,y_2)\bigg)n_1(\boldsymbol{y}) + \bigg(\mathrm{i}\lambda\xi\widehat{G}_{11}^{B,\mathrm{reg}}(\xi,y_2) + (\lambda+2\mu)\frac{\partial\widehat{G}_{12}^{B,\mathrm{reg}}}{\partial y_2}(\xi,y_2)\bigg)n_2(\boldsymbol{y}), \tag{6.98b}$$

$$\widehat{H}_{21}^{B,\mathrm{reg}}(\xi,y_2) = \bigg(\mathrm{i}(\lambda+2\mu)\xi\widehat{G}_{21}^{B,\mathrm{reg}}(\xi,y_2) + \lambda\frac{\partial\widehat{G}_{22}^{B,\mathrm{reg}}}{\partial y_2}(\xi,y_2)\bigg)n_1(\boldsymbol{y}) + \mu\bigg(\frac{\partial\widehat{G}_{21}^{B,\mathrm{reg}}}{\partial y_2}(\xi,y_2) + \mathrm{i}\xi\widehat{G}_{22}^{B,\mathrm{reg}}(\xi,y_2)\bigg)n_2(\boldsymbol{y}), \tag{6.98c}$$

$$\widehat{H}_{22}^{B,\mathrm{reg}}(\xi,y_2) = \mu\bigg(\frac{\partial\widehat{G}_{21}^{B,\mathrm{reg}}}{\partial y_2}(\xi,y_2) + \mathrm{i}\xi\widehat{G}_{22}^{B,\mathrm{reg}}(\xi,y_2)\bigg)n_1(\boldsymbol{y}) + \bigg(\mathrm{i}\lambda\xi\widehat{G}_{21}^{B,\mathrm{reg}}(\xi,y_2) + (\lambda+2\mu)\frac{\partial\widehat{G}_{22}^{B,\mathrm{reg}}}{\partial y_2}(\xi,y_2)\bigg)n_2(\boldsymbol{y}). \tag{6.98d}$$

In order to evaluate $\widehat{H}^{B,\mathrm{reg}}$, the term $\widehat{G}^{B,\mathrm{reg}}$ is decomposed as in (6.81), and their derivatives with respect to y_2 are computed using the same decomposition, that is,

$$\frac{\partial \widehat{G}^{B,\mathrm{reg}}}{\partial y_2}(\xi, y_2) = \frac{\partial \widehat{G}^{B,\mathrm{psr}}}{\partial y_2}(\xi, y_2) - \frac{\partial \widehat{G}^{B,\mathrm{pol}}}{\partial y_2}(\xi, y_2), \tag{6.99}$$

where the terms $\widehat{G}^{B,\mathrm{psr}}$ and $\widehat{G}^{B,\mathrm{pol}}$ are given in (6.51) and (6.56), respectively. The derivatives of $\widehat{G}^{B,\mathrm{psr}}$ are calculated as

$$\begin{aligned}\frac{\partial \widehat{G}^{B,\mathrm{psr}}}{\partial y_2}(\xi, y_2) = -\frac{1}{\rho\omega^2}\frac{\partial \Psi}{\partial y_2}(\xi, y_2) \\ \Big/\Big(\big(2\xi^2 - k_T^2\big)^2 - 4\xi^2\sqrt{\xi^2 - k_L^2}\sqrt{\xi^2 - k_T^2} + \tfrac{\omega}{\mu} Z_\infty k_T^2 \sqrt{\xi^2 - k_T^2}\Big),\end{aligned} \tag{6.100}$$

where the derivatives of the components of the regular tensor Ψ, given in (6.52), are

$$\begin{aligned}\frac{\partial \Psi_{11}}{\partial y_2}(\xi, y_2) = -\sqrt{\xi^2 - k_T^2}\Big(2\xi^2\sqrt{\xi^2 - k_L^2}\, e^{-\sqrt{\xi^2-k_L^2}y_2} \\ - \big(2\xi^2 - k_T^2\big)\sqrt{\xi^2 - k_T^2}\, e^{-\sqrt{\xi^2-k_T^2}y_2}\Big) \\ \times \Big(2\xi^2 e^{-\sqrt{\xi^2-k_L^2}x_2} - \big(2\xi^2 - k_T^2\big)e^{-\sqrt{\xi^2-k_T^2}x_2}\Big),\end{aligned} \tag{6.101a}$$

$$\begin{aligned}\frac{\partial \Psi_{12}}{\partial y_2}(\xi, y_2) = -\mathrm{i}\xi\sqrt{\xi^2 - k_T^2}\Big(2\big(\xi^2 - k_L^2\big)e^{-\sqrt{\xi^2-k_L^2}y_2} \\ - \big(2\xi^2 - k_T^2\big)e^{-\sqrt{\xi^2-k_T^2}y_2}\Big) \\ \times \Big(2\xi^2 e^{-\sqrt{\xi^2-k_L^2}x_2} - \big(2\xi^2 - k_T^2\big)e^{-\sqrt{\xi^2-k_T^2}x_2}\Big),\end{aligned} \tag{6.101b}$$

$$\begin{aligned}\frac{\partial \Psi_{21}}{\partial y_2}(\xi, y_2) = \mathrm{i}\xi\sqrt{\xi^2 - k_L^2}\Big(\big(2\xi^2 - k_T^2\big)e^{-\sqrt{\xi^2-k_L^2}y_2} \\ - 2\big(\xi^2 - k_T^2\big)e^{-\sqrt{\xi^2-k_T^2}y_2}\Big) \\ \times \Big(\big(2\xi^2 - k_T^2\big)e^{-\sqrt{\xi^2-k_L^2}x_2} - 2\xi^2 e^{-\sqrt{\xi^2-k_T^2}x_2}\Big) \\ + \mathrm{i}\tfrac{\omega}{\mu} Z_\infty k_T^2\, \xi\sqrt{\xi^2 - k_T^2}\Big(\sqrt{\xi^2 - k_L^2}\, e^{-\left(\sqrt{\xi^2-k_L^2}y_2 + \sqrt{\xi^2-k_T^2}x_2\right)} \\ - \sqrt{\xi^2 - k_T^2}\, e^{-\left(\sqrt{\xi^2-k_T^2}y_2 + \sqrt{\xi^2-k_L^2}x_2\right)}\Big),\end{aligned} \tag{6.101c}$$

$$\begin{aligned}\frac{\partial \Psi_{22}}{\partial y_2}(\xi, y_2) = -\sqrt{\xi^2 - k_L^2}\Big(\big(2\xi^2 - k_T^2\big)\sqrt{\xi^2 - k_L^2}\, e^{-\sqrt{\xi^2-k_L^2}y_2} \\ - 2\xi^2\sqrt{\xi^2 - k_T^2}\, e^{-\sqrt{\xi^2-k_T^2}y_2}\Big) \\ \times \Big(\big(2\xi^2 - k_T^2\big)e^{-\sqrt{\xi^2-k_L^2}x_2} - 2\xi^2 e^{-\sqrt{\xi^2-k_T^2}x_2}\Big) \\ - \tfrac{\omega}{\mu} Z_\infty k_T^2\sqrt{\xi^2 - k_T^2}\Big(\big(\xi^2 - k_L^2\big)e^{-\left(\sqrt{\xi^2-k_L^2}y_2 + \sqrt{\xi^2-k_T^2}x_2\right)} \\ - \xi^2 e^{-\left(\sqrt{\xi^2-k_T^2}y_2 + \sqrt{\xi^2-k_L^2}x_2\right)}\Big).\end{aligned} \tag{6.101d}$$

The derivatives of $\widehat{G}^{B,\mathrm{pol}}$ are given by

$$\frac{\partial \widehat{G}^{B,\mathrm{pol}}}{\partial y_2}(\xi, y_2) = -\frac{1}{\rho\,\omega^2}\left(\frac{1}{\xi - \hat{k}}\,\frac{\partial C^{+}}{\partial y_2}(\hat{k}, y_2) + \frac{1}{\xi + \hat{k}}\,\frac{\partial C^{-}}{\partial y_2}(\hat{k}, y_2)\right), \tag{6.102}$$

where the derivatives of the residue matrices in (6.60) are

$$\frac{\partial C_{+}}{\partial y_2}(\hat{k}, y_2) = \begin{bmatrix} \dfrac{\partial c_{11}}{\partial y_2}(\hat{k}, y_2) & \dfrac{\partial c_{12}}{\partial y_2}(\hat{k}, y_2) \\ \dfrac{\partial c_{21}}{\partial y_2}(\hat{k}, y_2) & \dfrac{\partial c_{22}}{\partial y_2}(\hat{k}, y_2) \end{bmatrix}, \tag{6.103a}$$

$$\frac{\partial C_{-}}{\partial y_2}(\hat{k}, y_2) = \begin{bmatrix} -\dfrac{\partial c_{11}}{\partial y_2}(\hat{k}, y_2) & \dfrac{\partial c_{12}}{\partial y_2}(\hat{k}, y_2) \\ \dfrac{\partial c_{21}}{\partial y_2}(\hat{k}, y_2) & -\dfrac{\partial c_{22}}{\partial y_2}(\hat{k}, y_2) \end{bmatrix}, \tag{6.103b}$$

and the derivatives $\partial c_{i\ell}/\partial y_2$ are given in (6.94). On the other hand, let us consider the derivatives with respect to y_1 of the off-diagonal terms $\widehat{G}^{B,\mathrm{pol}}_{12}$ and $\widehat{G}^{B,\mathrm{pol}}_{21}$, which are computed in the Fourier domain by multiplying by $\mathrm{i}\xi$. From (6.56) and (6.58), these derivatives are given by

$$\mathrm{i}\xi\widehat{G}^{B,\mathrm{pol}}_{i\ell}(\xi, y_2) = -\frac{\mathrm{i}c_{i\ell}(\hat{k}, y_2)}{\rho\,\omega^2}\left(\frac{\xi}{\xi - \hat{k}} + \frac{\xi}{\xi + \hat{k}}\right), \tag{6.104}$$

where $1 \leq i \neq \ell \leq 2$. In virtue of the decomposition (6.81), these terms appear in all the components of $\widehat{H}^{B,\mathrm{reg}}$, given in (6.98). By expanding appropriately, (6.104) can be restated as

$$\mathrm{i}\xi\widehat{G}^{B,\mathrm{pol}}_{i\ell}(\xi, y_2) = -\frac{\mathrm{i}c_{i\ell}(\hat{k}, y_2)}{\rho\,\omega^2}\left(2 + \frac{\hat{k}}{\xi - \hat{k}} - \frac{\hat{k}}{\xi + \hat{k}}\right), \tag{6.105}$$

and the derivative of $G^{B,\mathrm{pol}}_{i\ell}$ with respect to y_1 is thus computed as

$$\frac{\partial G^{B,\mathrm{pol}}_{i\ell}}{\partial y_1}(\boldsymbol{x}, \boldsymbol{y}) = -\frac{\mathrm{i}c_{i\ell}(\hat{k}, y_2)}{2\pi\rho\,\omega^2}\int_{-\infty}^{+\infty}\left(2 + \frac{\hat{k}}{\xi - \hat{k}} - \frac{\hat{k}}{\xi + \hat{k}}\right)e^{\mathrm{i}\xi(y_1 - x_1)}\mathrm{d}\xi. \tag{6.106}$$

Using properties of the Fourier transform for distributions, (6.106) is rewritten as

$$\begin{aligned}\frac{\partial G^{B,\mathrm{pol}}_{i\ell}}{\partial y_1}(\boldsymbol{x}, \boldsymbol{y}) = -\frac{\mathrm{i}c_{i\ell}(\hat{k}, y_2)}{\rho\,\omega^2}\Bigg\{&2\delta_{x_1}(y_1) \\ &+ \frac{1}{2\pi}\int_{-\infty}^{+\infty}\left(\frac{\hat{k}}{\xi - \hat{k}} - \frac{\hat{k}}{\xi + \hat{k}}\right)e^{\mathrm{i}\xi(y_1 - x_1)}\mathrm{d}\xi\Bigg\}.\end{aligned} \tag{6.107}$$

The Dirac's delta distribution at the right-hand side of (6.107) cancels those appearing in (6.92b) and (6.92c). In virtue of this fact, (6.104) is restated as

$$\mathrm{i}\xi\widehat{G}^{B,\mathrm{pol}}_{i\ell}(\xi, y_2) = -\frac{\mathrm{i}\hat{k}c_{i\ell}(\hat{k}, y_2)}{\rho\,\omega^2}\left(\frac{1}{\xi - \hat{k}} - \frac{1}{\xi + \hat{k}}\right), \tag{6.108}$$

and this term is implemented as a part of $\widehat{H}^{B,\mathrm{reg}}$ in (6.98). Finally, the regular part $H^{B,\mathrm{reg}}$ is calculated numerically by employing the IFFT algorithm described in the previous section.

This yields an approximation that we write as

$$H^{B,\mathrm{reg}}(\boldsymbol{x},\boldsymbol{y}) \approx \mathrm{IFFT}\big\{\widehat{H}^{B,\mathrm{reg}}(\xi, y_2)\big\}(y_1 - x_1). \tag{6.109}$$

VII. ANALYSIS OF THE SURFACE WAVES APPEARING WITH IMPEDANCE BOUNDARY CONDITIONS

7.1 Introduction

This chapter is concerned with the study of the surface waves that arise in the half-plane with impedance boundary conditions. The Rayleigh wave equation (6.55), determined in the previous chapter as the equation that gives the poles of the spectral Green's function, is deduced by a different and simpler approach consisting in an analysis of surface waves in the non-perturbed half-plane $\mathbb{R}^2_+$. In order to simplify the subsequent analysis, this equation is expressed in terms of the slownesses $s_L = k_L/\omega$ and $s_T = k_T/\omega$, instead of k_L and k_T. The Rayleigh wave is first studied in the case of a traction-free surface, where the Rayleigh wave equation is standard. Two accurate explicit formulae for the Rayleigh slowness s_R, provided by Malischewsky (2000) and Vinh & Ogden (2004), are exhibited. In the general case of impedance boundary conditions, it is demonstrated that for all real impedance Z_∞ there is one and only one real solution to the Rayleigh wave equation in the range $s > s_T$. This solution corresponds to the Rayleigh slowness s_R, which is an increasing function of the impedance. On the other hand, it is proven that if the impedance takes a certain value, then there is an additional real solution to the Rayleigh wave equation, located within the range $s_L < s < s_T$. This solution corresponds to the slowness of an additional surface wave that appears in this particular case, whose expression is given explicitly. In addition, we prove that when the special value of the impedance mentioned above is slightly perturbed, then the additional solution becomes complex, with a strictly positive imaginary part, and thus there is no longer an additional surface wave. Finally, the Rayleigh wave equation is numerically solved by the iterative Newton-Raphson method, yielding the Rayleigh and the additional solutions as functions of the impedance. Three rocks of different type are considered as examples of elastic materials. The numerical results obtained are presented, in order to illustrate what is stated theoretically.

7.2 Deduction of the Rayleigh wave equation

Let us consider the half-plane $\mathbb{R}^2_+$ with impedance boundary conditions. We desire to find the surface waves as particular solutions to the elastic wave equation with the characteristics of a surface wave, that is, with oscillatory behavior along the infinite flat surface and exponentially decaying amplitude towards the interior of the half-plane. Such solutions have a different nature from the volume waves determined in Appendix A.2. The procedure to determine the surface waves is mainly based upon Achenbach (1973) and Harris (2001), where the usual case of traction-free surface is considered. The desired solution, denoted by $\boldsymbol{u}^{\mathrm{sur}} \neq \mathbf{0}$, satisfies the homogeneous system.

$$\operatorname{div} \sigma(\boldsymbol{u}^{\mathrm{sur}}(\boldsymbol{x})) + \rho\omega^2 \boldsymbol{u}^{\mathrm{sur}}(\boldsymbol{x}) = \mathbf{0} \qquad \text{in } \mathbb{R}^2_+, \tag{7.1a}$$

$$\sigma(\boldsymbol{u}^{\mathrm{sur}}(\boldsymbol{x}))\hat{\boldsymbol{e}}_2 + \omega Z_\infty u_1^{\mathrm{sur}}(\boldsymbol{x})\hat{\boldsymbol{e}}_1 = \mathbf{0} \qquad \text{on } \{x_2 = 0\}. \tag{7.1b}$$

The solution to (7.1a) is determined by the method exhibited in Section 2.2, that is, we seek $\boldsymbol{u}^{\mathrm{sur}}$ of the form

$$\boldsymbol{u}^{\mathrm{sur}}(\boldsymbol{x}) = \nabla\psi^{(L)}(\boldsymbol{x}) + \nabla^{\perp}\psi^{(T)}(\boldsymbol{x}), \tag{7.2}$$

where the scalar potentials $\psi^{(L)}$ and $\psi^{(T)}$ satisfy

$$\triangle\psi^{(L)}(\boldsymbol{x}) + k_L^2\,\psi^{(L)}(\boldsymbol{x}) = 0, \tag{7.3a}$$

$$\triangle\psi^{(T)}(\boldsymbol{x}) + k_T^2\,\psi^{(T)}(\boldsymbol{x}) = 0. \tag{7.3b}$$

We write $\psi^{(L)}$ and $\psi^{(T)}$ as

$$\psi^{(L)}(\boldsymbol{x}) = A^{(L)}e^{\mathrm{i}kx_1}e^{-k\gamma_L x_2}, \qquad \psi^{(T)}(\boldsymbol{x}) = A^{(T)}e^{\mathrm{i}kx_1}e^{-k\gamma_T x_2}, \tag{7.4}$$

where $A^{(L)}$, $A^{(T)}$ are arbitrary amplitudes, $k \in \mathbb{R}$ is an unknown wave number associated with the desired surface wave, and the quantities γ_L, γ_T have to be chosen in such a way that both Helmholtz equations (7.3) hold. Replacing (7.4) in (7.3), we obtain that k is related with γ_L and γ_T by means of

$$k\gamma_\alpha = \sqrt{k^2 - k_\alpha^2}, \qquad \alpha = L,\, T, \tag{7.5}$$

where the square roots are defined as the complex maps introduced in Section 6.2. The displacement field $\boldsymbol{u}^{\mathrm{sur}}$ is obtained by substitution of (7.4) in (7.2), and is given by

$$\boldsymbol{u}^{\mathrm{sur}}(x_1, x_2) = A^{(L)}\big(-\mathrm{i}\hat{\boldsymbol{e}}_1 + \gamma_L\hat{\boldsymbol{e}}_2\big)e^{\mathrm{i}kx_1}e^{-k\gamma_L x_2} + A^{(T)}\big(\gamma_T\hat{\boldsymbol{e}}_1 + \mathrm{i}\hat{\boldsymbol{e}}_2\big)e^{\mathrm{i}kx_1}e^{-k\gamma_T x_2}. \tag{7.6}$$

Replacing (7.6) in (7.1b) and expanding, we obtain that $\boldsymbol{u}^{\mathrm{sur}}$ fulfills the impedance boundary conditions if both amplitudes satisfy the homogeneous system of linear equations

$$\begin{bmatrix} \mathrm{i}\big(2\mu k\gamma_L - \omega Z_\infty\big) & -\mu k\big(1+\gamma_T^2\big) + \omega Z_\infty\gamma_T \\ -\mu k\big(1+\gamma_T^2\big) & -2\mathrm{i}\mu k\gamma_T \end{bmatrix} \begin{bmatrix} A^{(L)} \\ A^{(T)} \end{bmatrix} = \begin{bmatrix} 0 \\ 0 \end{bmatrix}. \tag{7.7}$$

Therefore, in order to obtain the nontrivial solutions of (7.7), the determinant of the matrix is set to zero, giving the identity

$$\mu k\Big(\big(1+\gamma_T^2\big)^2 - 4\gamma_L\gamma_T\Big) + \omega Z_\infty\gamma_T\big(1-\gamma_T^2\big) = 0. \tag{7.8}$$

Substituting γ_L, γ_T from (7.5) and rearranging, we obtain the equation

$$\big(2k^2 - k_T^2\big)^2 - 4k^2\sqrt{k^2-k_L^2}\sqrt{k^2-k_T^2} + \tfrac{\omega}{\mu}Z_\infty k_T^2\sqrt{k^2-k_T^2} = 0, \tag{7.9}$$

which coincides with the Rayleigh wave equation determined in Section 6.3. This equation can be also expressed in terms of the slowness $s = k/\omega$ (reciprocal of velocity) as

$$\big(2s^2 - s_T^2\big)^2 - 4s^2\sqrt{s^2-s_L^2}\sqrt{s^2-s_T^2} + \tfrac{1}{\mu}Z_\infty s_T^2\sqrt{s^2-s_T^2} = 0, \tag{7.10}$$

where $s_L = k_L/\omega$ and $s_T = k_T/\omega$ are the slownesses of the longitudinal and transverse waves, respectively. These quantities can be expressed in a more explicit way as

$$s_L = \sqrt{\frac{\rho}{\lambda+2\mu}}, \qquad s_T = \sqrt{\frac{\rho}{\mu}}. \tag{7.11}$$

The advantage of expressing the Rayleigh wave equation in the form (7.10) is that it does not depend on ω. Given any solution to (7.10), the associated solution to (7.9) is simply obtained by multiplying it by ω, so it suffices to deal with (7.10). In what follows, we study,

from an analytical and numerical point of view, the nature of the solutions of (7.10), which also yield the poles of the spectral Green's function determined in Section 6.2.

7.3 The Rayleigh wave

7.3.1 Case of traction-free boundary conditions

The Rayleigh wave equation for the traction-free case is obtained by setting $Z_\infty = 0$ in (7.10). This equation is classic, and can be found, e.g., in Achenbach (1973), Graff (1991), or Harris (2001). It is given by

$$\left(2s^2 - s_T^2\right)^2 - 4s^2\sqrt{s^2 - s_L^2}\sqrt{s^2 - s_T^2} = 0. \tag{7.12}$$

In this case, it is well-known that there appears a surface wave globally known as the Rayleigh wave. Its slowness, denoted by s_R, corresponds to a real solution of (7.12) that satisfies $s_R > s_T$. A proof of existence and uniqueness of this solution is provided by Nkemzi (1997), together with a formula for the Rayleigh slowness derived using Cauchy integrals. Nevertheless, the most widely used approach to determine s_R consists in transforming (7.12) into a cubic equation in s^2. The Rayleigh slowness is then expressed employing Cardan's formulae for the roots of the cubic equation. However, it is not clear a priori which of these roots gives s_R, especially when all of them are real. Hence, it is necessary to perform a careful analysis of the roots, in order to correctly determine s_R. An explicit formula for s_R, introduced by Malischewsky (2000), is given by

$$s_R^2 = \frac{3}{2}\, s_T^2\left(4 - \sqrt[3]{h(\beta^2) + 17 - 45\beta^2} + d\sqrt[3]{d(h(\beta^2) - (17 - 45\beta^2))}\right)^{-1}, \tag{7.13}$$

where

$$h(\beta^2) = 3\sqrt{33 - 186\beta^2 + 321\beta^4 - 192\beta^6}, \qquad d = \operatorname{sign}(-\beta^2 + 1/6) \tag{7.14}$$

Another explicit formula, provided more recently by Vinh & Ogden (2004), is given by

$$s_R^2 = \frac{s_T^2}{4(1 - \beta^2)}\left(2 - \frac{4}{3}\beta^2 + \sqrt[3]{R + \sqrt{D}} + \sqrt[3]{R - \sqrt{D}}\right), \tag{7.15}$$

where

$$R = 2\left(27 - 90\beta^2 + 99\beta^4 - 32\beta^6\right)/27, \tag{7.16a}$$

$$D = 4\left(1 - \beta^2\right)^2\left(11 - 62\beta^2 + 107\beta^4 - 64\beta^6\right)/27. \tag{7.16b}$$

7.3.2 Case of impedance boundary conditions

Let us consider now the case of an arbitrary surface impedance $Z_\infty \in \mathbb{R}$. We start by establishing the existence and uniqueness of the Rayleigh slowness by means of the following proposition.

PROPOSITION VII.1. *For each impedance $Z_\infty \in \mathbb{R}$, the Rayleigh equation* (7.10) *has one and only one real solution within the range $s > s_T$. This solution is called the Rayleigh slowness.*

PROOF. Using the fact that (7.10) is linear in the impedance, we can easily work out its value in terms of s, obtaining a function $Z_\infty = Z_\infty(s)$, defined as

$$Z_\infty(s) = -\frac{\mu}{s_T^2}\frac{\left(2s^2 - s_T^2\right)^2 - 4s^2\sqrt{s^2 - s_L^2}\sqrt{s^2 - s_T^2}}{\sqrt{s^2 - s_T^2}}. \tag{7.17}$$

As $s > s_T > s_L$, both square roots are real, and thus this function takes real values. In what follows, we aim to demonstrate that $Z_\infty : (s_T, +\infty) \to \mathbb{R}$ is actually a bijection. We begin by proving that it is onto $\mathbb{R}$. It is clear that Z_∞ is continuous at any $s > s_T$ and

$$\lim_{s \to s_T} Z_\infty(s) = -\infty. \tag{7.18}$$

On the other hand, using Taylor approximations it is straightforward to obtain asymptotic expressions for the square roots as $s \to +\infty$:

$$\sqrt{s^2 - s_\alpha^2} \approx s - \frac{s_\alpha^2}{2s} \qquad \alpha = L, T, \tag{7.19}$$

which is employed to approximate $Z_\infty(s)$ for large values of s:

$$Z_\infty(s) \approx 2\mu\left(1 - \beta^2\right)s, \tag{7.20}$$

and then,

$$\lim_{s \to +\infty} Z_\infty(s) = +\infty. \tag{7.21}$$

Consequently, as Z_∞ is a continuous function in $(s_T, +\infty)$ that satisfies (7.18) and (7.21), we deduce that it is onto $\mathbb{R}$. Let us prove now that Z_∞ is injective. For this, we study the sign of its derivative, which can be expressed as

$$\begin{aligned} Z'_\infty(s) = \frac{\mu s}{s_T^2\sqrt{s^2 - s_T^2}}\Bigg\{ & \frac{\left(2s^2 - s_T^2\right)^2 - 4s^2\sqrt{s^2 - s_L^2}\sqrt{s^2 - s_T^2}}{s^2 - s_T^2} \\ & + 8\left(\frac{s^2}{2}\left(\frac{\sqrt{s^2 - s_L^2}}{\sqrt{s^2 - s_T^2}} + \frac{\sqrt{s^2 - s_T^2}}{\sqrt{s^2 - s_L^2}}\right) + \sqrt{s^2 - s_L^2}\sqrt{s^2 - s_T^2} - \left(2s^2 - s_T^2\right)\right)\Bigg\}. \end{aligned} \tag{7.22}$$

Using the standard inequality $a/b + b/a \geq 2$, valid for any pair of real numbers a and b, it is immediate that

$$\frac{\sqrt{s^2 - s_L^2}}{\sqrt{s^2 - s_T^2}} + \frac{\sqrt{s^2 - s_T^2}}{\sqrt{s^2 - s_L^2}} \geq 2, \tag{7.23}$$

which replaced in (7.22) leads to determine a lower bound for Z'_∞:

$$\begin{aligned} Z'_\infty(s) \geq \frac{\mu s}{s_T^2\sqrt{s^2 - s_T^2}}\Bigg\{ & \frac{\left(2s^2 - s_T^2\right)^2 - 4s^2\sqrt{s^2 - s_L^2}\sqrt{s^2 - s_T^2}}{s^2 - s_T^2} \\ & + 8\left(\sqrt{s^2 - s_L^2}\sqrt{s^2 - s_T^2} - \left(s^2 - s_T^2\right)\right)\Bigg\}. \end{aligned} \tag{7.24}$$

Expanding and regrouping terms, it is possible to restate (7.24) as

$$Z'_\infty(s) \geq \frac{\mu s\left(4\left(s^2 - 2s_T^2\right)\sqrt{s^2 - s_T^2}\left(\sqrt{s^2 - s_L^2} - \sqrt{s^2 - s_T^2}\right) + s_T^4\right)}{s_T^2\left(s^2 - s_T^2\right)^{3/2}}. \tag{7.25}$$

In addition, as $s_L < s_T$, it holds that

$$\sqrt{s^2 - s_L^2} - \sqrt{s^2 - s_T^2} > 0, \tag{7.26}$$

and substituting this in (7.25) yields

$$Z'_\infty(s) > 0, \tag{7.27}$$

which implies that Z_∞ is strictly increasing and thus it is an injective function. We conclude that $Z_\infty : (s_T, +\infty) \to \mathbb{R}$ is a bijective function, and so is its inverse. Therefore, each impedance $Z_\infty \in \mathbb{R}$ has associated one and only one real number in the range $s > s_T$ that is solution to (7.10). This solution corresponds to the Rayleigh slowness, denoted by $s_R = s_R(Z_\infty)$. □

REMARK VII.1. *Notice that proposition VII.1 includes the particular case $Z_\infty = 0$. We have thus provided a proof of existence and uniqueness of the Rayleigh wave in the well-known case of a traction-free surface.*

REMARK VII.2. *From the proof of proposition VII.1, we infer that the Rayleigh slowness s_R is a strictly increasing function of the impedance Z_∞, such that it approaches s_T as $Z_\infty \to -\infty$ (cf. (7.18)) and it increases linearly as $Z_\infty \to +\infty$ (cf. (7.20)). In particular, the larger the impedance, the slower the Rayleigh wave propagates along the surface.*

Unfortunately, in the general case there is no explicit formula for s_R in terms of the other involved variables. Nevertheless, it is quite easy to compute s_R numerically by employing an iterative root-finding algorithm such as the Newton-Raphson method. Indeed, the above analysis provides some basic ideas about where s_R has to be searched, which can be used to select a suitable starting point for the iterations. Hence, the convergence of the method should be achieved within a reasonable number of iterations, with more than acceptable accuracy.

7.4 Additional surface wave appearing in a particular case

We are now interested in studying possible surface waves that could appear within the range $s_L < s < s_T$. In the general case $Z_\infty \in \mathbb{R}$, it is not a simple matter to determine analytically from the Rayleigh equation (7.10) whether such surface waves exist or not, owing to difficulties inherent to the equation. Therefore, what we do is to solve numerically (7.10) within this range using the iterative method mentioned above, and the obtained results, presented in the next section, will give an answer to this problem. Nevertheless, there is a particular value of the impedance for which a solution to (7.10) can be analytically determined. This fact is established in the next proposition.

PROPOSITION VII.2. *If the impedance takes the value $Z_\infty = Z_\infty^* \equiv 2\mu\sqrt{s_T^2/2 - s_L^2}$, then the Rayleigh equation (7.10) has one real solution in the range $s_L < s < s_T$. This solution is given by $s = s^* \equiv s_T/\sqrt{2}$.*

PROOF. Let us assume that $s_L < s < s_T$. In that case, according to the definition of the complex square roots, we have that

$$\sqrt{s^2 - s_T^2} = -\mathrm{i}\sqrt{s_T^2 - s^2}, \tag{7.28}$$

and replacing this in (7.10) yields

$$\left(s_T^2 - 2s^2\right)^2 - \mathrm{i}\left(4s^2\sqrt{s^2 - s_L^2} - \tfrac{1}{\mu}\, s_T^2 Z_\infty\right)\sqrt{s_T^2 - s^2} = 0. \tag{7.29}$$

This is a complex identity such that the first term on its left-hand side is real, while the second term is purely imaginary. Applying real part to (7.29) gives the equation

$$\left(s_T^2 - 2s^2\right)^2 = 0, \tag{7.30}$$

which is easily solved, yielding the desired slowness:

$$s = s^* = \frac{s_T}{\sqrt{2}}. \tag{7.31}$$

Substituting this value in (7.29) and rearranging gives the equation

$$\frac{s_T^3}{\sqrt{2}}\left(2\sqrt{\frac{s_T^2}{2} - s_L^2} - \frac{1}{\mu}Z_\infty\right) = 0, \tag{7.32}$$

which holds if and only if

$$Z_\infty = Z_\infty^* = 2\mu\sqrt{\frac{s_T^2}{2} - s_L^2}, \tag{7.33}$$

that is, this is the only value of Z_∞ for which the slowness s^* given in (7.31) is a solution to (7.29) and vice versa. In addition, we have from (7.11) that

$$\frac{s_T^2}{2} - s_L^2 = \frac{\rho\lambda}{2\mu(\lambda + 2\mu)} > 0. \tag{7.34}$$

This relation implies that the impedance value given in (7.33) is real and positive. Finally, we conclude from (7.11) and (7.34) that s^* satisfies $s_L < s^* < s_T$. □

REMARK VII.3. *Proposition VII.2 establishes that there is a certain value of the impedance for which an additional surface wave appears. This surface wave is faster than the transverse wave and slower than the longitudinal wave.*

An explicit expression for the field of displacements produced by this additional surface wave can be determined by substituting (7.31) and (7.33) in (7.6) and combining with (7.7). This expression corresponds, up to a multiplicative constant, to

$$\boldsymbol{u}^{\mathrm{sur}}(x_1, x_2) = \left(\rho\omega\hat{\mathbf{e}}_1 + \mathrm{i}k^* Z_\infty^* \hat{\mathbf{e}}_2\right) e^{\mathrm{i}k^* x_1}\, e^{-\frac{\omega Z_\infty^*}{2\mu} x_2}, \tag{7.35}$$

where k^* is the associated wave number, defined as $k^* = \omega s^*$, or equivalently

$$k^* = \frac{k_T}{\sqrt{2}}, \tag{7.36}$$

As $s = s^*$ is a real solution of (7.10) that only exists when $Z_\infty = Z_\infty^*$, a natural question that arises is how this solution is affected if the value of Z_∞^* is slightly perturbed. A precise answer to this question is provided in the next proposition.

PROPOSITION VII.3. *Let us assume a perturbed value of the impedance*

$$Z_\infty = Z_\infty^*(1+\varepsilon), \tag{7.37}$$

where ε is a real parameter satisfying $|\varepsilon| << 1$. Then the Rayleigh equation (7.10) has a complex solution s satisfying $s_L \leq \mathfrak{Re}\{s\} \leq s_T$. This solution can be approximated as

$$s = s^*\big(1 + a\,\varepsilon + (b + \mathrm{i}c)\varepsilon^2\big) + o(\varepsilon^3), \tag{7.38}$$

where a, b and c are real numbers, with $c > 0$.

PROOF. In order to simplify the analysis, we deal with s^2 instead of s. Given the parameter ε, we desire to determine (approximately) another parameter $\eta = \eta(\varepsilon) \in \mathbb{C}$ such that the solution s to (7.10) can be written as

$$s^2 = s^{*2}(1+\eta). \tag{7.39}$$

Notice that if $\varepsilon = 0$, then $Z_\infty = Z_\infty^*$ and consequently $s = s^*$. We thus infer that η must satisfy $\eta(0) = 0$. Replacing (7.37) and (7.39) in (7.10), approximating the square roots by employing second-order Taylor polynomials in η (around $\eta = 0$), and combining with (7.31) and (7.33), we obtain that η satisfies the quadratic equation:

$$\Big(1 - \frac{1}{2}q + \frac{1}{4}q^2 - \frac{1}{4}\varepsilon + 2\mathrm{i}\sqrt{q}\Big)\eta^2 - \big(2 + q + \varepsilon\big)\eta + 2\varepsilon = 0, \tag{7.40}$$

where $q = 1/(1-2\beta^2)$. The quadratic equation (7.40) has two solutions, but only one of them vanishes when $\varepsilon = 0$. We thus choose this solution, which is given by

$$\eta(\varepsilon) = \frac{2 + q + \varepsilon - \big((2+q)^2 - 2(2 - 3q + q^2 + 8\mathrm{i}\sqrt{q})\varepsilon + 3\varepsilon^2\big)^{1/2}}{2 - q + \frac{1}{2}q^2 - \frac{1}{2}\varepsilon + 4\mathrm{i}\sqrt{q}}. \tag{7.41}$$

As we want to study the behavior of η for small ε, we approximate (7.41) by a second-order Taylor expansion, obtaining

$$\eta(\varepsilon) = \frac{2}{2+q}\,\varepsilon - \frac{(4-q)q - 8\mathrm{i}\sqrt{q}}{(2+q)^3}\,\varepsilon^2 + o(\varepsilon^3). \tag{7.42}$$

Hence, replacing in (7.39), we obtain an approximate expression for the solution s:

$$s \approx s^*\left(1 + \frac{2}{2+q}\,\varepsilon - \frac{(4-q)q - 8\mathrm{i}\sqrt{q}}{(2+q)^3}\,\varepsilon^2\right)^{1/2}. \tag{7.43}$$

and employing another second-order Taylor expansion to approximate the square root, we finally obtain

$$s = s^*\left(1 + \frac{1}{2+q}\,\varepsilon + \frac{2 + 5q - q^2 + 8\mathrm{i}\sqrt{q}}{2(2+q)^3}\,\varepsilon^2\right) + o(\varepsilon^3). \tag{7.44}$$

This expression coincides with (7.38), with

$$a = \frac{1}{2+q}, \qquad b = \frac{2 + 5q - q^2}{2(2+q)^3}, \qquad c = \frac{4\sqrt{q}}{(2+q)^3}. \tag{7.45}$$

It is clear that a, b and c are real numbers and $c > 0$, which concludes the proof. □

REMARK VII.4. *In virtue of proposition VII.3, if the impedance is perturbed around* $Z_\infty = Z_\infty^*$, *then the solution* $s = s^*$ *becomes a complex number with strictly positive imaginary part. Therefore, substituting* Z_∞^* *and* s^* *by their perturbed values in* (7.35), *we obtain that this expression is no longer a physical solution of the boundary-value problem* (7.1), *since it is exponentially increasing as* $x_1 \to -\infty$.

7.5 Numerical results

In this section, the Rayleigh slowness and the additional solution to (7.10) are numerically computed for different values of the surface impedance Z_∞. We consider three examples of elastic material, namely diabase (volcanic rock), limestone (sedimentary rock) and gneiss (metamorphic rock). A detailed description of these rocks and their characteristics can be found in Stacey & Page (1986). Table 7.1 shows their approximate physical and elastic properties, namely the density ρ, the Young's modulus E and the Poisson's ratio ν. The Lamé's constants λ and μ can be obtained in terms of E and ν through the usual

Material	ρ [Kg/m^3]	E [GPa]	ν
Diabase	2700	90	0.20
Limestone	2400	70	0.30
Gneiss	2800	60	0.24

TABLE 7.1. Density, Young's modulus and Poisson's ratio of the materials considered.

formulae

$$\lambda = \frac{\nu E}{(1+\nu)(1-2\nu)}, \qquad \mu = \frac{E}{2(1+\nu)}. \tag{7.46}$$

The numerical values of the Lamé's constants of each material, computed by means of these formulae, are shown in Table 7.2, whereas the values of the longitudinal and the transverse slownesses obtained from (7.11) are shown in Table 7.3. On the other hand, we take an impedance Z_∞ varying from a minimum value $Z_\infty^{\min} = -20$ [MPa s/m] to a maximum value $Z_\infty^{\max} = 20$ [MPa s/m]. The Rayleigh slowness is calculated by solving iteratively

Material	λ [GPa]	μ [GPa]
Diabase	25.000	37.500
Limestone	40.385	26.923
Gneiss	22.333	24.194

TABLE 7.2. Lamé's constants of the materials considered.

the Rayleigh equation (7.10), using for this the Newton-Raphson algorithm with a starting point for the iterations located at the region $s > s_T$, as mentioned in Section 7.3. The results

Material	$s_L \times 10^{-4}$[s/m]	$s_T \times 10^{-4}$[s/m]
Diabase	1.6432	2.6833
Limestone	1.5959	2.9857
Gneiss	1.9898	3.4020

TABLE 7.3. Longitudinal and transverse slownesses of the materials considered.

are presented in Fig. 7.1, where we confirm what was stated by proposition VII.1: The Rayleigh slowness s_R is an increasing function of the impedance Z_∞, which approaches asymptotically s_T as Z_∞ decreases to $-\infty$ and tends to a straight line as Z_∞ increases to $+\infty$. The additional solution to 7.1 is also computed by means of the Newton-Raphson algorithm, but this time the starting point is located within the region $s_L < s < s_T$. We have found that this solution does not exist for all values of Z_∞. In particular, it is not present

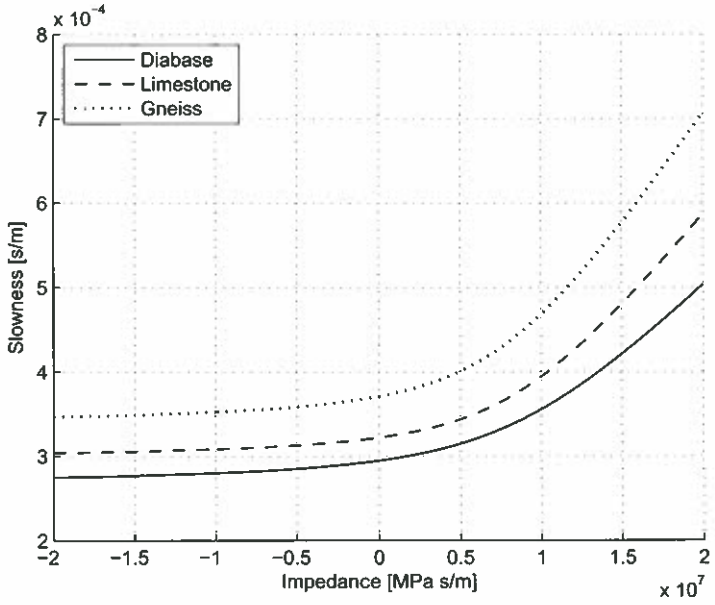

FIGURE 7.1. Rayleigh slownesses in function of the impedance.

for Z_∞ negative, so the results are presented only for $Z_\infty \geq 0$. Figs. 7.2 and 7.3 show the real and the imaginary part of the additional solution in function of the impedance. Fig. 7.3 puts in evidence, for each elastic material considered, the existence of a particular value of Z_∞ such that the imaginary part of the solution vanishes. This is the value $Z_\infty = Z_\infty^*$ established by proposition VII.2, for which the additional solution becomes real and is given by the slowness $s = s^*$. In addition, Fig. 7.3 confirms that if we perturb Z_∞ around Z_∞^*, then a strictly positive imaginary part appears in the additional solution, as stated by proposition VII.3. The numerical values of the constants Z_∞^* and s^* associated with each material are shown in Table 7.4.

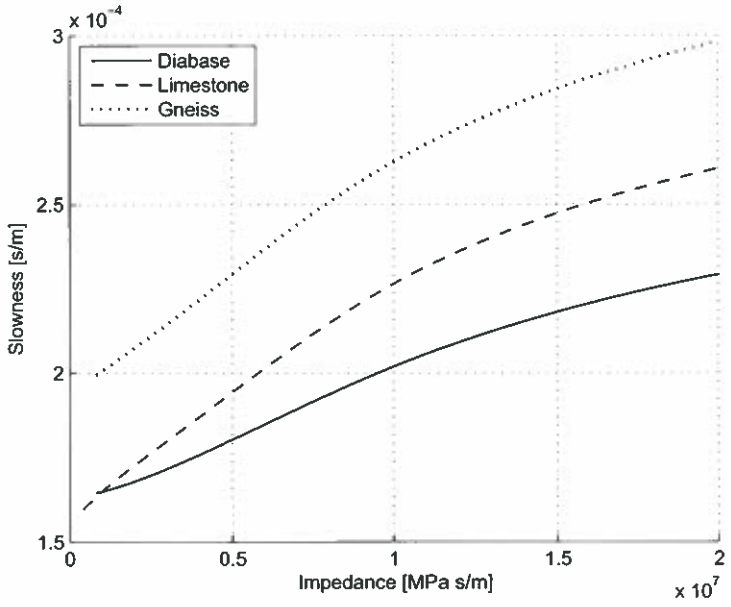

FIGURE 7.2. Real part of the additional slownesses in function of the impedance.

Material	Z^*_∞ [MPa s/m]	$s^* \times 10^{-4}$[s/m]
Diabase	7.1151	1.8974
Limestone	7.4421	2.1112
Gneiss	6.5410	2.4055

TABLE 7.4. Impedance Z^*_∞ and slowness s^* of the materials considered.

REMARK VII.5. *It should be noticed from proposition VII.3 and Fig. 7.3 that there is an important range of values of Z_∞ for which the imaginary part of the additional solution is close to zero, especially when Z_∞ is near Z^*_∞. Consequently, if the impedance lies in this range, then the spectral Green's function obtained in Section 6.2 has a pair of poles located close to the real axis. When calculating its inverse Fourier transform by the method detailed in Section 6.3, it is natural to wonder whether such poles must be extracted or not. It can be argued that, strictly speaking, these poles are complex, so they generate no real singularities in the variable s and it should be possible to compute the* IFFT *directly, that is, without extracting them. Nevertheless, such an approach would yield inaccurate results, since the proximity of these poles to the real axis produces abrupt variations in the spectral Green's function that should be taken into account in computing its inverse Fourier transform. Therefore, for the sake of accuracy, these* quasi-real *poles need to be extracted in many cases.*

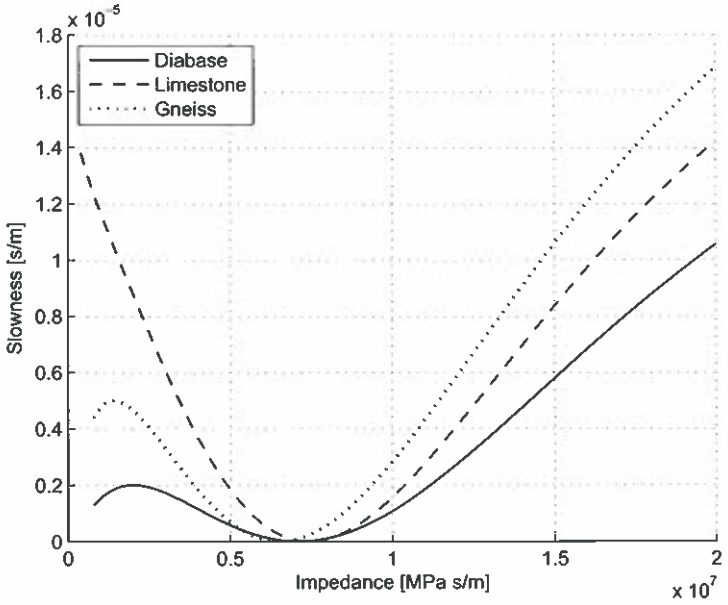

FIGURE 7.3. Imaginary part of the additional slownesses in function of the impedance.

VIII. VALIDATION OF THE NUMERICAL PROCEDURES FOR ELASTIC WAVES IN UNBOUNDED MEDIA

8.1 Introduction

In this chapter we validate the numerical procedures developed throughout this work to solve elastodynamic problems in unbounded media. In the case of exterior domains, we present some results of scattering by a circular obstacle, obtained by evaluation of the analytical solutions calculated in Section 3.2. Horizontal incident waves are assumed, either longitudinal or transverse, and results for a rigid body and a cavity are included. The two procedures proposed to solve numerically this problem, based respectively upon DtN map/finite element methods (cf. Section 3.3) and boundary element methods (cf. Section 5.2) are simultaneously validated. For this, the problem of scattering by a circle is solved by using both procedures, considering for this different sizes of discretization. The solutions obtained are then compared with the analytical solution, which is employed as a benchmark problem. The relative errors obtained are presented in log-log graphs and tables. In the case of locally perturbed half-planes, we present numerical results of the half-plane Green's function, calculated by the method developed in Chapter VI. Each one of the four components is evaluated in a rectangle and depicted graphically. The boundary element methods for locally perturbed half-planes, developed in Section 5.3 are also validated. This time, the lack of an analytical solution forces one to devise another type of benchmark problem. For this, a particular boundary-value problem is stated on the half-plane perturbed by an embedded obstacle. The solution to this problem is the Green's function with source point fixed within the obstacle. This boundary-value problem is solved numerically by BEM and the solution obtained is compared with the Green's function. The comparison is performed on the boundary, for different sizes of discretization, and the relative errors obtained are shown in log-log graphs and tables. Finally, some numerical results of scattering in the locally perturbed half-plane are presented. The perturbation assumed corresponds to a half-circle with its center lying just on the flat surface.

8.2 Methods for exterior domains

8.2.1 Results of exterior scattering by a circle

Next, we consider a circular obstacle of radius $a = 100$ [m] embedded in an infinite elastic media. This obstacle could correspond to either a rigid body or a cavity. The elastic parameters of limestone, given in Tables 7.1 and 7.2, are assumed. We only deal with horizontal incident waves, either purely longitudinal or purely transverse. Two angular frequencies are assumed, namely $\omega_1 = 2\pi \times 16$ [Rad/s] and $\omega_2 = 2\pi \times 32$ [Rad/s]. The total field (incident + scattered) determined analytically in Section 3.2 is evaluated in a square domain of side 600 [m] with the circle placed at its center. For this, the expressions given as series in polar coordinates are truncated at $N_t = 30$ and converted into cartesian coordinates. The results of horizontal and vertical displacements are presented separately.

The case of a rigid circular body is depicted in Figs. 8.1 and 8.2, for a longitudinal incident wave and ω_1, ω_2, respectively, and in Figs. 8.3 and 8.4 for a transverse incident wave and ω_1, ω_2, respectively. Similarly, the case of a circular cavity is depicted in Figs. 8.5 and 8.6, for a longitudinal incident wave and ω_1, ω_2, respectively, and in Figs. 8.7 and 8.8 for a transverse incident wave and ω_1, ω_2, respectively.

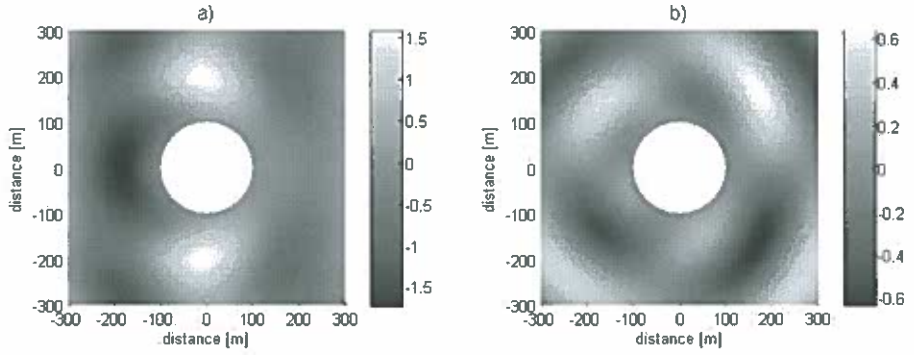

FIGURE 8.1. Total field for a rigid body, a longitudinal incident wave and $\omega = \omega_1$. a) Horizontal displacement. b) Vertical displacement.

8.2.2 Validation of the DtN map and the boundary element methods

In order to validate the DtN map calculated in Section 3.3, we implement finite element methods based upon the variational formulation given in (3.66). In addition, we implement the boundary element methods developed in Section 5.2, also in order to validate them. For this, a circle of radius $a = 100$ [m] (a rigid body or a cavity) and the elastic parameters of limestone are again assumed. We consider an external circle of radius $R = 300$ [m], which is used as the artificial boundary where the exact boundary conditions obtained in terms of the DtN map are imposed. The infinite series in expressions (3.75) and (3.76) are truncated at $N_t = 30$. Horizontal incident waves (longitudinal or transverse) with angular frequency $\omega_1 = 2\pi \times 16$ [Rad/s] are assumed. The annular region lying between both circles is discretized by using triangular meshes of different sizes. Their parameters are given in Table 8.1, namely the mesh size h, the number of triangles, the number of nodes, and the number of segments lying on the inner circle. We then state finite elements of the P1-type on these meshes. The restriction of each mesh to the obstacle corresponds to a discrete curve constituted by rectilinear segments, which are employed as boundary elements. Once the integral equation has been solved numerically, the solution is evaluated at the entire mesh by means of corresponding integral representation formula. The benchmark problem is none other than the analytical solution for the exterior of the circle evaluated at the nodes of each mesh. In this way, both numerical solutions can be directly compared with the analytical one. The relative errors in L^2-norm are computed numerically in each mesh and then plotted as log-log graphs. The errors of the numerical solutions for a rigid body are

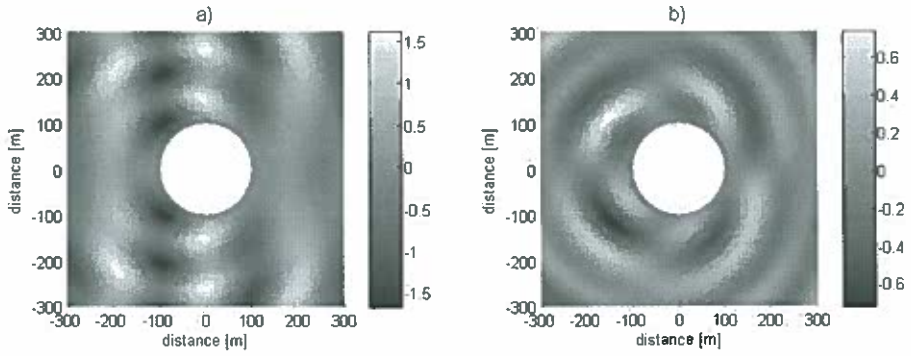

FIGURE 8.2. Total field for a rigid body, a longitudinal incident wave and $\omega = \omega_2$. a) Horizontal displacement. b) Vertical displacement.

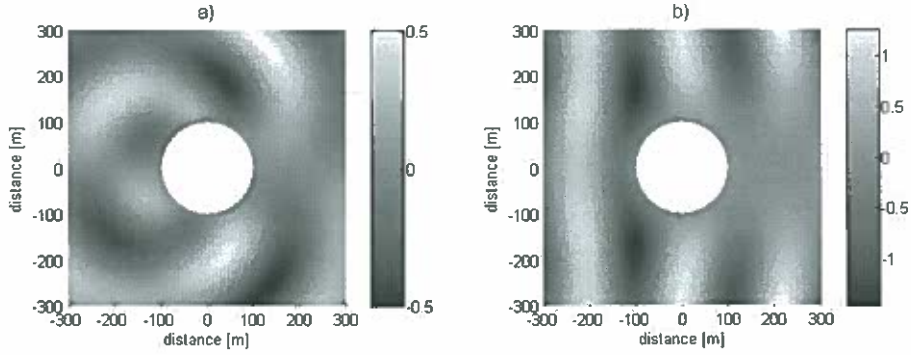

FIGURE 8.3. Total field for a rigid body, a transverse incident wave and $\omega = \omega_1$. a) Horizontal displacement. b) Vertical displacement.

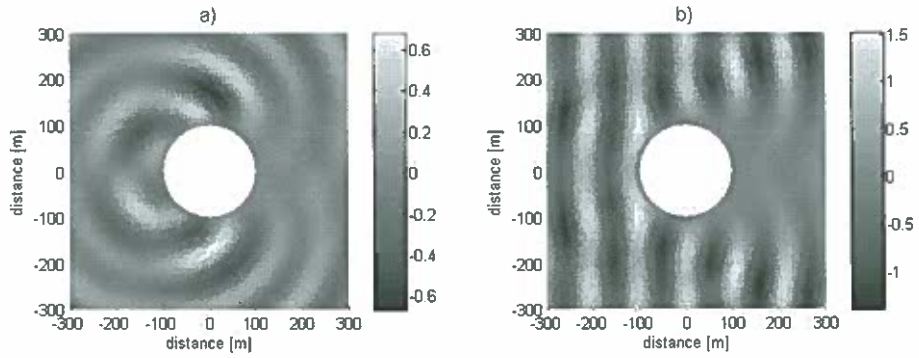

FIGURE 8.4. Total field for a rigid body, a transverse incident wave and $\omega = \omega_2$. a) Horizontal displacement. b) Vertical displacement.

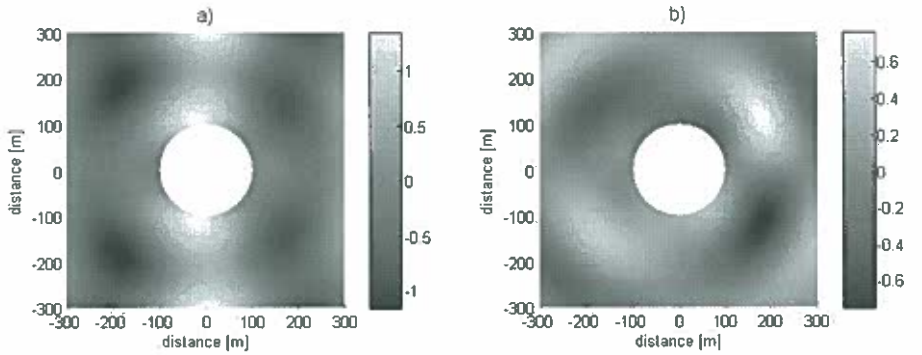

FIGURE 8.5. Total field for a cavity, a longitudinal incident wave and $\omega = \omega_1$.
a) Horizontal displacement. b) Vertical displacement.

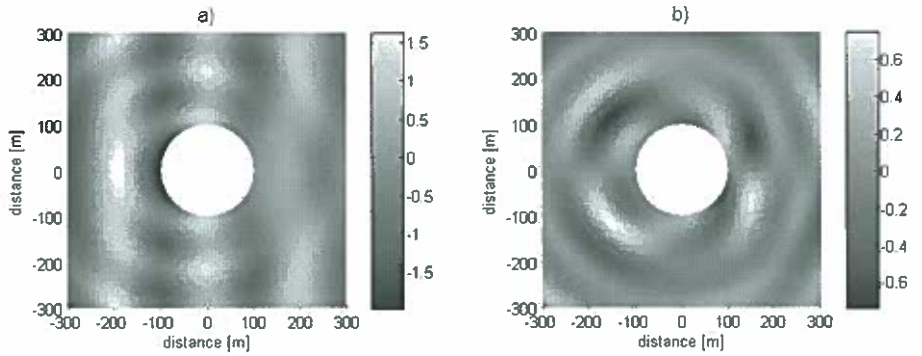

FIGURE 8.6. Total field for a cavity, a longitudinal incident wave and $\omega = \omega_2$.
a) Horizontal displacement. b) Vertical displacement.

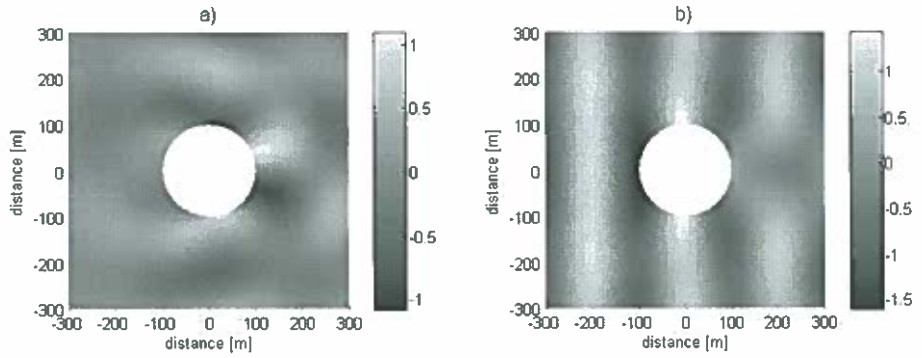

FIGURE 8.7. Total field for a cavity, a transverse incident wave and $\omega = \omega_1$.
a) Horizontal displacement. b) Vertical displacement.

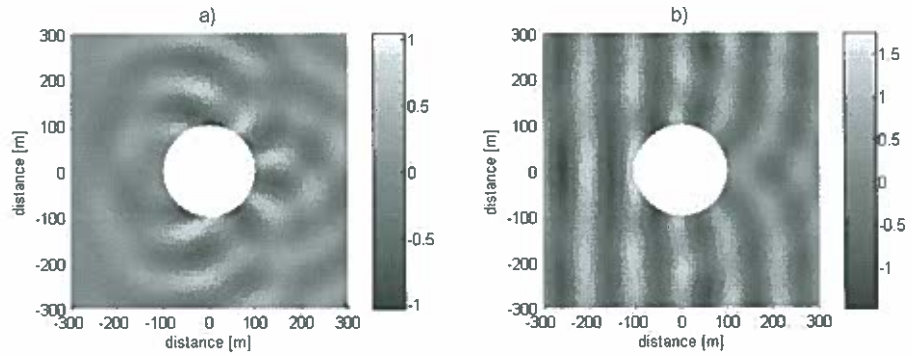

FIGURE 8.8. Total field for a cavity, a transverse incident wave and $\omega = \omega_2$. a) Horizontal displacement. b) Vertical displacement.

Mesh	h	Number of triangles	Number of nodes	Number of segments
1	14.0000	4526	2355	48
2	12.7533	5224	2712	52
3	11.6176	6276	3248	56
4	10.5830	7558	3899	60
5	9.6406	9356	4810	68
6	8.7821	11160	5724	72
7	8.0000	13400	6858	80

TABLE 8.1. Parameters of the triangular meshes considered.

shown in Figs. 8.9 and 8.10, for a longitudinal incident wave (case 1) and a transverse incident wave (case 2). Likewise, the errors of the numerical solutions for a cavity are shown in Figs. 8.11 and 8.12, for a longitudinal incident wave (case 3) and a transverse incident wave (case 4). From these figures, we observe that the relative error decreases if the mesh size is reduced, as should be expected. Moreover, the relation between the logarithm of the error and the logarithm of the mesh size is approximately linear. On the other hand, the relative errors obtained with the DtN/finite elements approach are larger than those obtained with boundary element methods. Therefore, the latter appears to be more accurate than the former, when both approaches are implemented in the same mesh. The numerical values of the percentage relative errors are presented in Table 8.2 for the DtN/finite element approach and in Table 8.3 for boundary element methods. Cases 1, 2, 3 and 4 are included.

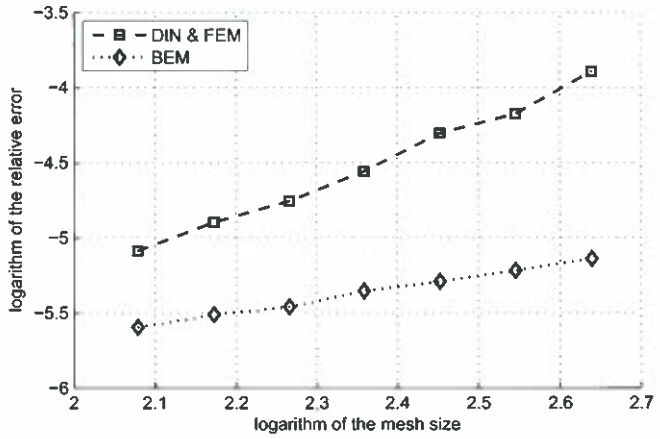

FIGURE 8.9. Relative error for a rigid body and a longitudinal incident wave.

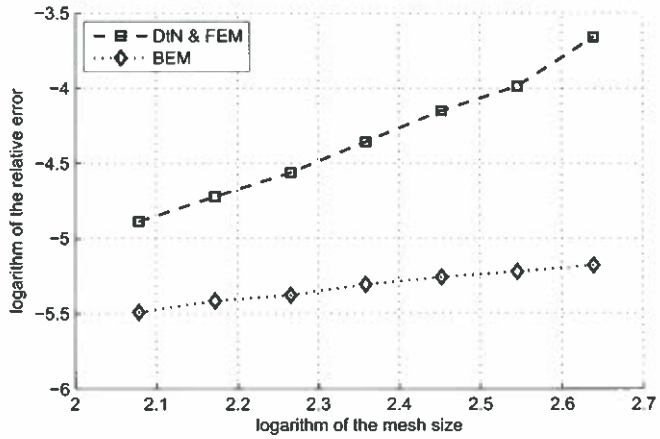

FIGURE 8.10. Relative error for a rigid body and a transverse incident wave.

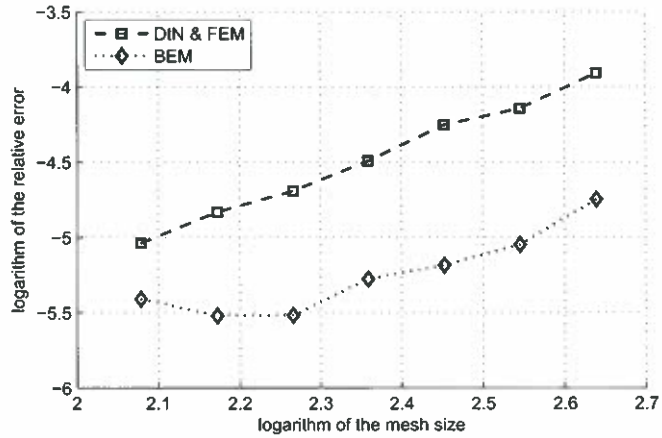

FIGURE 8.11. Relative error for a cavity and a longitudinal incident wave.

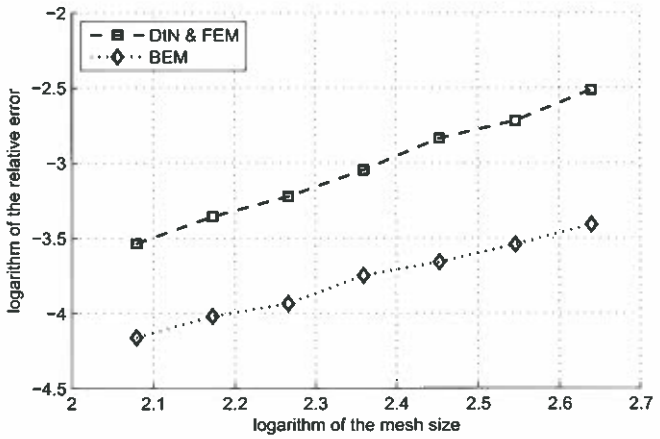

FIGURE 8.12. Relative error for a cavity and a transverse incident wave.

Mesh	% Rel. error Case 1	% Rel. error Case 2	% Rel. error Case 3	% Rel. error Case 4
1	2.0273	2.5683	2.0090	8.0921
2	1.5305	1.8491	1.5895	6.5951
3	1.3455	1.5732	1.4256	5.8696
4	1.0447	1.2796	1.1217	4.7538
5	0.8574	1.0436	0.9195	3.9843
6	0.7440	0.8897	0.7993	3.4853
7	0.6159	0.7538	0.6501	2.9104

TABLE 8.2. Percentage relative errors for the DtN/FEM approach.

Mesh	% Rel. error Case 1	% Rel. error Case 2	% Rel. error Case 3	% Rel. error Case 4
1	0.5837	0.5626	0.8690	3.3023
2	0.5398	0.5399	0.6430	2.8970
3	0.5025	0.5208	0.5610	2.5763
4	0.4716	0.4961	0.5121	2.3574
5	0.4246	0.4621	0.4024	1.9530
6	0.4031	0.4444	0.4013	1.7956
7	0.3708	0.4123	0.4483	1.5576

TABLE 8.3. Percentage relative errors for the BEM approach.

8.3 Methods for locally perturbed half-planes

8.3.1 Results of the half-plane Green's function

Next, we present some numerical results of the half-plane Green's function calculated by the procedure described in Chapter VI. We consider an elastic half-plane with the constants of limestone, a source point placed at $\boldsymbol{x} = (x_1, x_2) = (0, 50\ [\mathrm{m}])$ and the angular frequencies $\omega_1 = 2\pi \times 16$ [Rad/s] and $\omega_2 = 2\pi \times 32$ [Rad/s]. Two values of impedance are considered, namely $Z_\infty = 0$ (traction-free surface) and $Z_\infty = Z_\infty^*$. The numerical value of the latter is given in Table 7.4. The computation of the IFFT is performed by employing $N = 2^{14}$ samples distributed uniformly between -2×10^4 [m] and 2×10^4 [m]. The Green's function is evaluated at receiver points $\boldsymbol{y} = (y_1, y_2)$ such that $-400\ [\mathrm{m}] \leq y_1 \leq 400\ [\mathrm{m}]$ and $0 \leq y_2 \leq 400$ [m]. The results for $Z_\infty = 0$ are depicted in Figs. 8.13 (real part) and 8.14 (imaginary part) for $\omega = \omega_1$, and in Figs 8.15 (real part) and 8.16 (imaginary part) for $\omega = \omega_2$. In this case, only the Rayleigh pole is extracted from the spectral Green's function. Likewise, the results for $Z_\infty = Z_\infty^*$ are depicted in Figs. 8.17 (real part) and 8.18 (imaginary part) for $\omega = \omega_1$, and Figs. 8.19 (real part) and 8.20 (imaginary part) for $\omega = \omega_2$. Both the Rayleigh and the additional pole are extracted in this case.

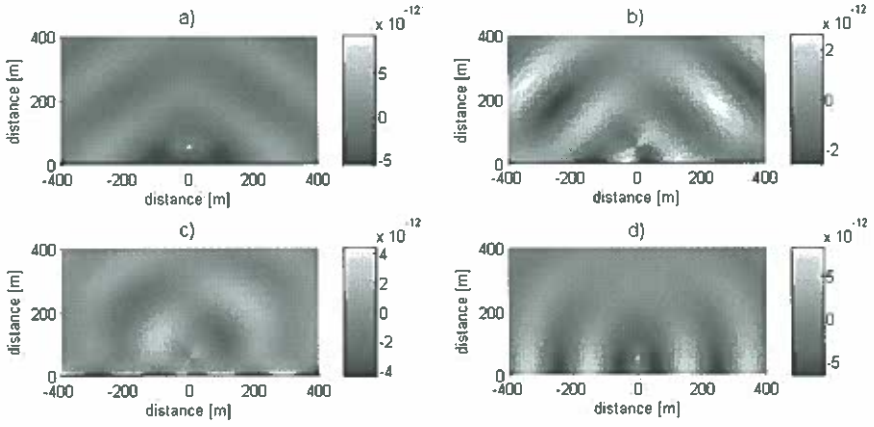

FIGURE 8.13. Real part of the half-plane Green's function for $Z_\infty = 0$ and $\omega = \omega_1$. a) $G_1^1(\boldsymbol{x}, \boldsymbol{y})$. b) $G_2^1(\boldsymbol{x}, \boldsymbol{y})$. c) $G_1^2(\boldsymbol{x}, \boldsymbol{y})$. d) $G_2^2(\boldsymbol{x}, \boldsymbol{y})$.

8.3.2 Validation of boundary element methods

We now validate the boundary element methods to solve time-harmonic elastodynamics problems in a locally perturbed half-plane. As in this case there is no analytical solution, an alternative benchmark problem needs to be used in order to perform the validation. For this, let us consider a perturbation of the half-plane consisting in an embedded obstacle. As was done in Chapter IV, we denote by Ω_+^{ext} the perturbed half-plane, by Ω_+^{int} the interior of the obstacle and by Γ_p the boundary of the obstacle. In addition, let $\boldsymbol{b}$ be any point within the obstacle. We then establish the following boundary-value problem in this perturbed

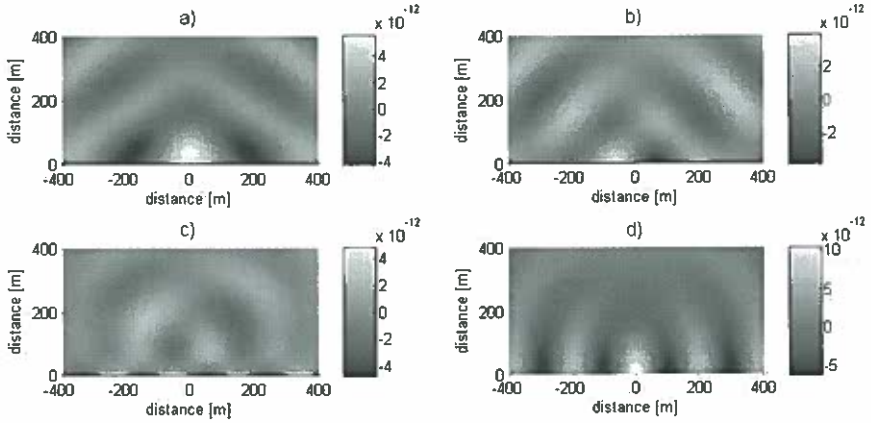

FIGURE 8.14. Imaginary part of the half-plane Green's function for $Z_\infty = 0$ and $\omega = \omega_1$. a) $G_1^1(x, y)$. b) $G_2^1(x, y)$. c) $G_1^2(x, y)$. d) $G_2^2(x, y)$.

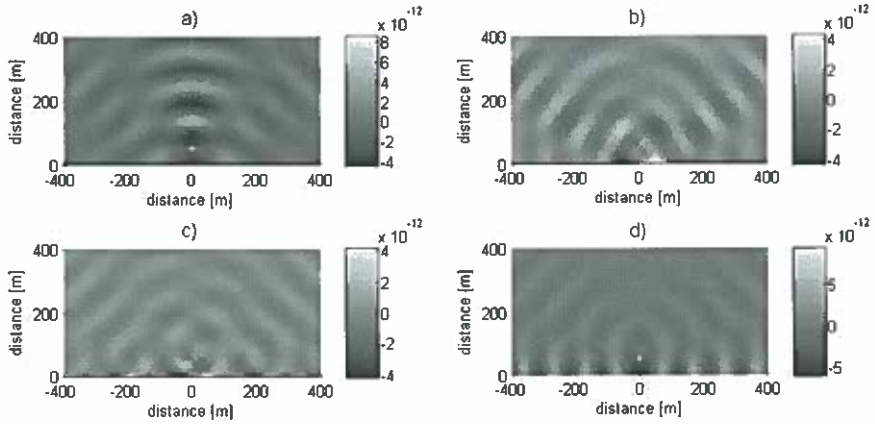

FIGURE 8.15. Real part of the half-plane Green's function for $Z_\infty = 0$ and $\omega = \omega_2$. a) $G_1^1(x, y)$. b) $G_2^1(x, y)$. c) $G_1^2(x, y)$. d) $G_2^2(x, y)$.

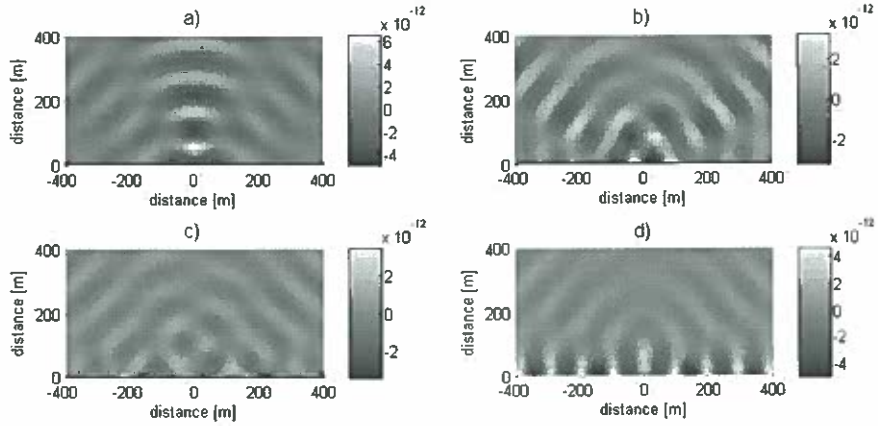

FIGURE 8.16. Imaginary part of the half-plane Green's function for $Z_\infty = 0$ and $\omega = \omega_2$. a) $G_1^1(x, y)$. b) $G_2^1(x, y)$. c) $G_1^2(x, y)$. d) $G_2^2(x, y)$.

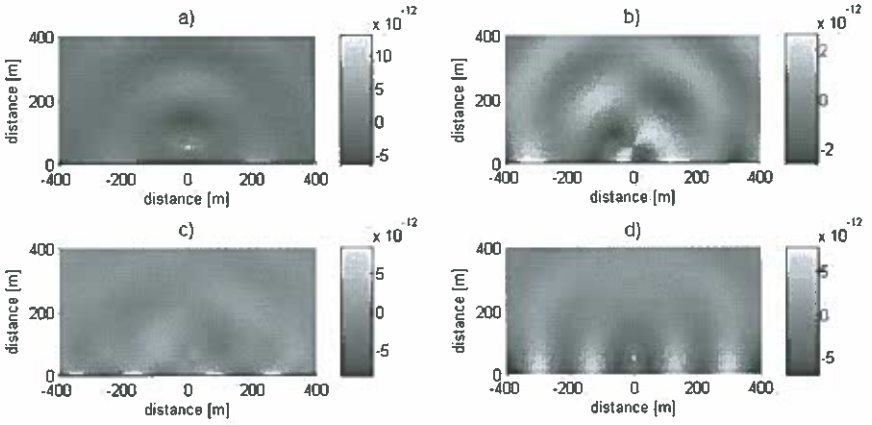

FIGURE 8.17. Real part of the half-plane Green's function for $Z_\infty = Z_\infty^*$ and $\omega = \omega_1$. a) $G_1^1(x, y)$. b) $G_2^1(x, y)$. c) $G_1^2(x, y)$. d) $G_2^2(x, y)$.

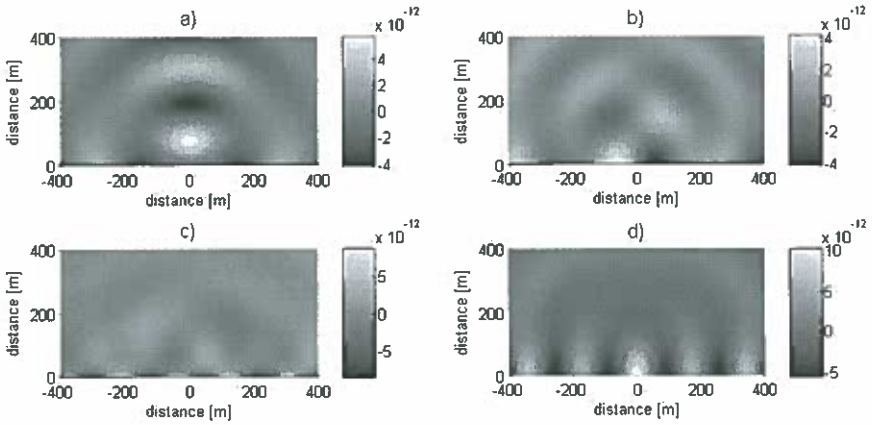

FIGURE 8.18. Imaginary part of the half-plane Green's function for $Z_\infty = Z_\infty^*$ and $\omega = \omega_1$. a) $G_1^1(x, y)$. b) $G_2^1(x, y)$. c) $G_1^2(x, y)$. d) $G_2^2(x, y)$.

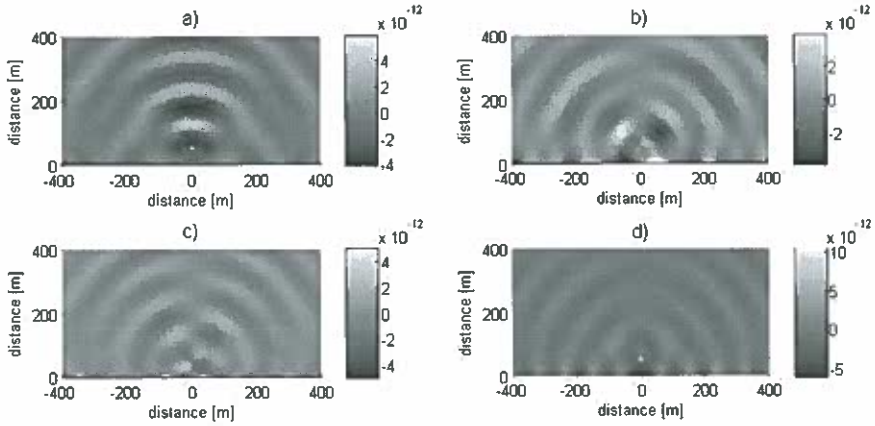

FIGURE 8.19. Real part of the half-plane Green's function for $Z_\infty = Z_\infty^*$ and $\omega = \omega_2$. a) $G_1^1(x, y)$. b) $G_2^1(x, y)$. c) $G_1^2(x, y)$. d) $G_2^2(x, y)$.

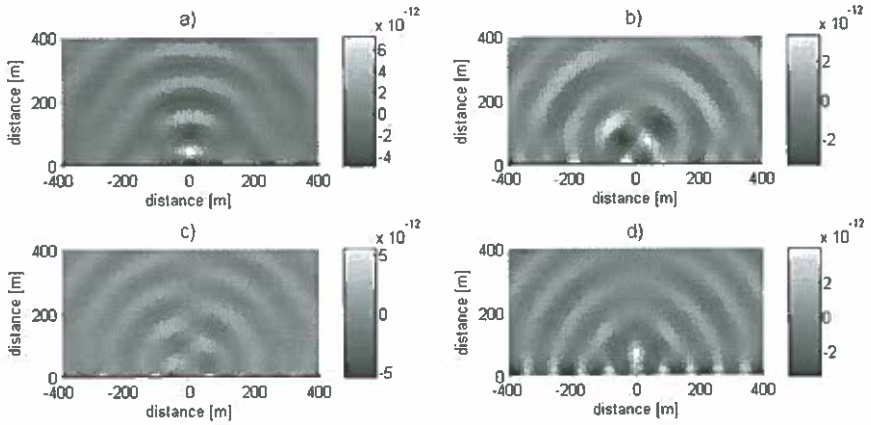

FIGURE 8.20. Imaginary part of the half-plane Green's function for $Z_\infty = Z_\infty^*$ and $\omega = \omega_2$. a) $G_1^1(\boldsymbol{x}, \boldsymbol{y})$. b) $G_2^1(\boldsymbol{x}, \boldsymbol{y})$. c) $G_1^2(\boldsymbol{x}, \boldsymbol{y})$. d) $G_2^2(\boldsymbol{x}, \boldsymbol{y})$.

half-plane: Find $\boldsymbol{u} = (u_1, u_2) : \Omega_+^{\text{ext}} \to \mathbb{C}^2$ such that

$$\sigma_{ij,j}(\boldsymbol{x}) + \rho\omega^2 u_i(\boldsymbol{x}) = 0 \qquad \text{in } \Omega_+^{\text{ext}}, \tag{8.1a}$$

$$-\sigma_{ij}(\boldsymbol{x})n_j + \omega Z_p(\boldsymbol{x})u_j(\boldsymbol{x})\tau_j\tau_i = f_i^k(\boldsymbol{x}) \qquad \text{on } \Gamma_p, \tag{8.1b}$$

$$\sigma_{i2}(\boldsymbol{x}) + \omega Z_\infty u_1(\boldsymbol{x})\delta_{i1} = 0 \qquad \text{on } \Gamma_\infty, \tag{8.1c}$$

$$+ \text{ Outgoing radiation conditions} \qquad \text{as } r = |\boldsymbol{x}| \to +\infty, \tag{8.1d}$$

where for each $k = 1, 2$, the function $\boldsymbol{f}^k = (f_1, f_2)$ is defined as

$$f_i^k(\boldsymbol{x}) = -H_i^k(\boldsymbol{b}, \boldsymbol{x}) + \omega Z_p(\boldsymbol{x})G_j^k(\boldsymbol{b}, \boldsymbol{x})\tau_j\tau_i, \tag{8.2}$$

and G_i^k and H_i^k denote the half-plane Green's function and its normal derivative, written in tensor notation. It is easy to see that the solution to (8.1) is given by

$$u_i(\boldsymbol{x}) = G_i^k(\boldsymbol{b}, \boldsymbol{x}), \qquad \boldsymbol{x} \in \Omega_+^{\text{ext}}. \tag{8.3}$$

As $\boldsymbol{b} \notin \Omega_+^{\text{ext}}$, this function is well defined for all $\boldsymbol{x} \in \Omega_+^{\text{ext}}$ and satisfies the elastic wave equation with zero right-hand side (8.1a). In addition, the impedance boundary condition on the obstacle (8.1b) is automatically satisfied by the appropriate choice of the right-hand side (8.2). Furthermore, the impedance boundary condition on the infinite flat surface (8.1c) and the radiation conditions at infinity (8.1d) hold since the half-plane Green's function fulfills both properties. On the other hand, the boundary-value problem (8.1) can be numerically solved by boundary element methods on Γ_p. The boundary integral equation for this problem is given in (4.126), and its solution corresponds to the displacement of the boundary Γ_p, which can be compared with the theoretical solution (8.3). This procedure of validation is implemented numerically, for which we consider a circular obstacle with a radius of 50 [m] and a center located at 100 [m] from the flat surface. The point $\boldsymbol{b}$ is placed exactly at the center of the circle. The parameters of limestone are assumed and the angular frequency is fixed at $\omega_1 = 2\pi \times 16$ [Rad/s]. The circumference is then partitioned into segments of equal length, which are used as boundary elements for the numerical solution of (8.1). In addition, the half-plane Green's function is calculated at the middle

point of these segments, in order to evaluate the theoretical solution (8.3) at the circumference. In this way, it is possible to compare both solutions of (8.1). Different numbers of segments are considered, giving rise to partitions of variable size. Table 8.4 presents the parameters of these partitions, namely the segment size h and the number of segments.

Partition	h	Number of segments
1	15.6434	20
2	12.0537	26
3	9.2268	34
4	7.1339	44
5	5.4139	58
6	4.1325	76
7	3.1411	100

TABLE 8.4. Parameters of the partitions considered.

The values of impedance assumed on the circle and the flat surface are $Z_\infty = Z_p = 0$ and $Z_\infty = Z_p = Z_\infty^*$, and the parameters for implementing the IFFT are the same as above. The variables measured on the circle are the norms of the displacement vectors produced by horizontal and vertical application of the Dirac's delta distribution at b. This is equivalent to consider $k = 1$ and $k = 2$ in (8.2), respectively. The relative errors in L^2-norm between the theoretical and the numerical solution are computed in each partition and then plotted as log-log graphs. Figs. 8.21 and 8.22 show the numerical values of the percentage relative errors for the cases $Z_\infty = 0$ and $Z_\infty = Z_\infty^*$, respectively. From these graphs we observe

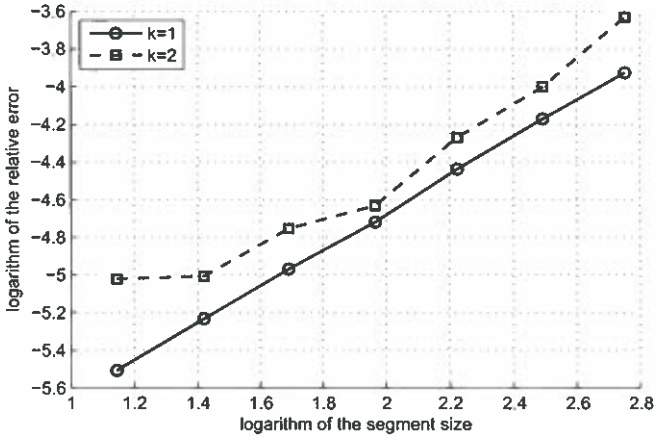

FIGURE 8.21. Relative errors for $Z_\infty = 0$.

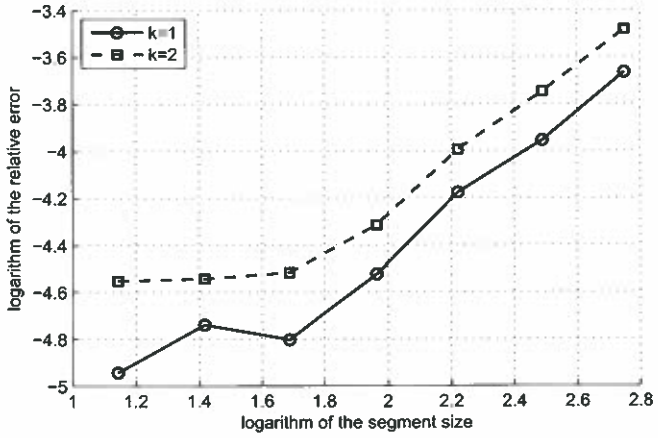

FIGURE 8.22. Relative error for $Z_\infty = Z_\infty^*$.

that the relative error decreases as the segment size is reduced. The numerical values of these errors are presented in Table 8.5.

Partition	% Rel. Error $Z_\infty = 0$ $k = 1$	% Rel. Error $Z_\infty = 0$ $k = 2$	% Rel. Error $Z_\infty = Z_\infty^*$ $k = 1$	% Rel. Error $Z_\infty = Z_\infty^*$ $k = 2$
1	1.9671	2.6450	2.5570	3.0675
2	1.5405	1.8259	1.9153	2.3570
3	1.1799	1.3963	1.5356	1.8446
4	0.8903	0.9726	1.0843	1.3383
5	0.6933	0.8597	0.8200	1.0918
6	0.5330	0.6679	0.8739	1.0627
7	0.4055	0.6588	0.7133	1.0535

TABLE 8.5. Percentage relative errors for the BEM approach.

8.3.3 Numerical results of scattering by a half-circle

In what follows, we consider a half-plane perturbed by a half-circle of radius 100 [m] placed on its surface. The scattered field by this semi-circle is calculated numerically by BEM, assuming again the constants of limestone. Incident waves with an angle of 60° are considered, either purely longitudinal or purely transverse, with angular frequencies $\omega_1 = 2\pi \times 16$ [Rad/s] and $\omega_2 = 2\pi \times 32$ [Rad/s]. The parameters associated with the computation of the IFFT are the same as before. The values of impedance considered are $Z_\infty = 0$ and $Z_\infty = Z_\infty^*$. The real part of the total field (incident+reflected+scattered) is evaluated in a rectangle of width 800 [m] and height 400 [m], with the center of the half-circle located at 200 [m] from the left side. We separate into horizontal and vertical displacements. The results for the case $Z_\infty = 0$ are depicted in Figs. 8.23 and 8.24, for a longitudinal incident

wave and ω_1, ω_2, respectively, and in Figs. 8.25 and 8.26 for a transverse incident wave and ω_1, ω_2, respectively. Likewise, the results for the case $Z_\infty = Z_\infty^*$ are depicted in Figs. 8.27 and 8.28, for a longitudinal incident wave and ω_1, ω_2, respectively, and in Figs. 8.29 and 8.30 for a transverse incident wave and ω_1, ω_2, respectively.

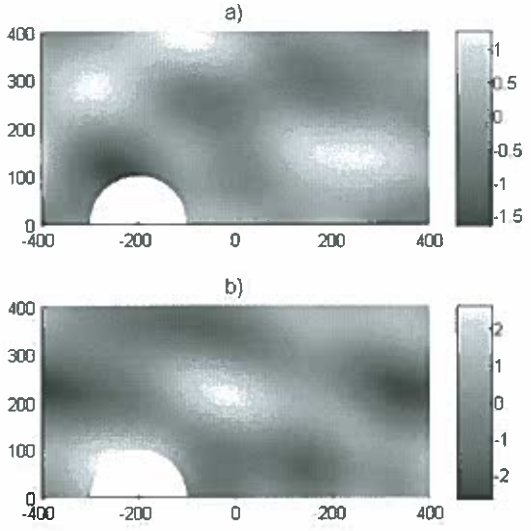

FIGURE 8.23. Total field for $Z_\infty = 0$, a longitudinal incident wave and $\omega = \omega_1$. a) Horizontal displacement. b) Vertical displacement.

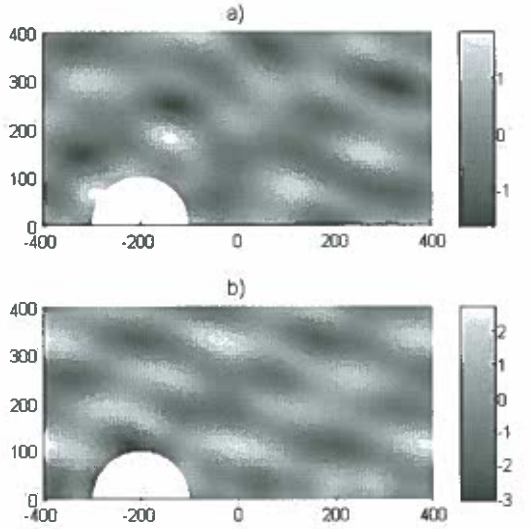

FIGURE 8.24. Total field for $Z_\infty = 0$, a longitudinal incident wave and $\omega = \omega_2$. a) Horizontal displacement. b) Vertical displacement.

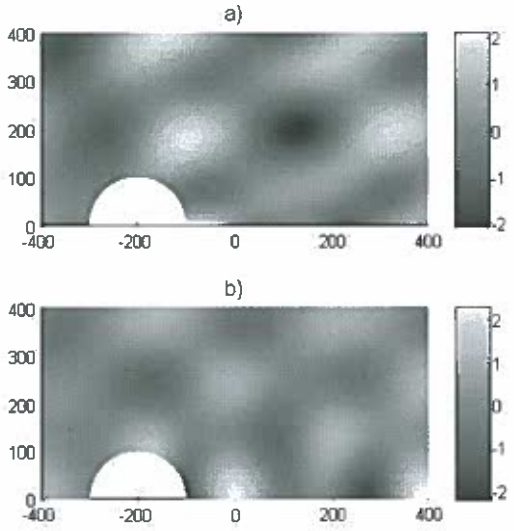

FIGURE 8.25. Total field for $Z_\infty = 0$, a transverse incident wave and $\omega = \omega_1$. a) Horizontal displacement. b) Vertical displacement.

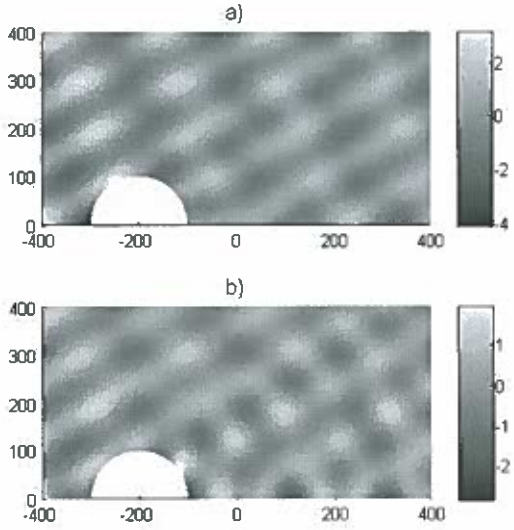

FIGURE 8.26. Total field for $Z_\infty = 0$, a transverse incident wave and $\omega = \omega_2$. a) Horizontal displacement. b) Vertical displacement.

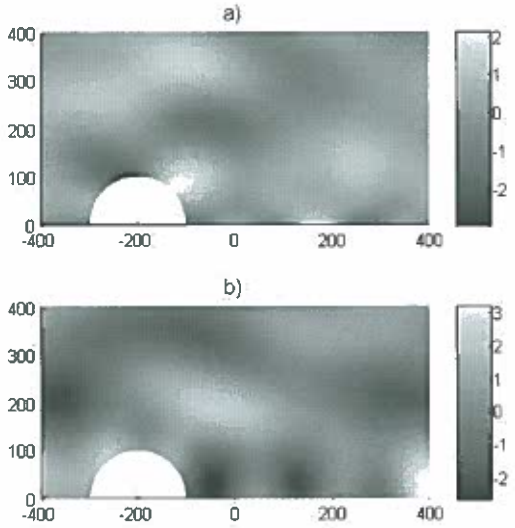

FIGURE 8.27. Total field for $Z_\infty = Z_\infty^*$, a longitudinal incident wave and $\omega = \omega_1$. a) Horizontal displacement. b) Vertical displacement.

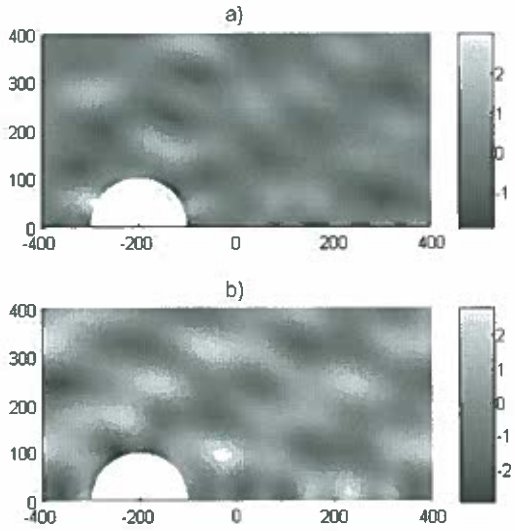

FIGURE 8.28. Total field for $Z_\infty = Z_\infty^*$, a longitudinal incident wave and $\omega = \omega_2$. a) Horizontal displacement. b) Vertical displacement.

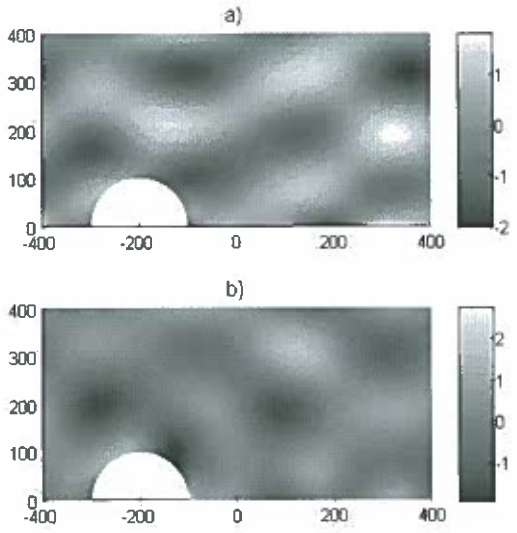

FIGURE 8.29. Total field for $Z_\infty = Z_\infty^*$, a transverse incident wave and $\omega = \omega_1$. a) Horizontal displacement. b) Vertical displacement.

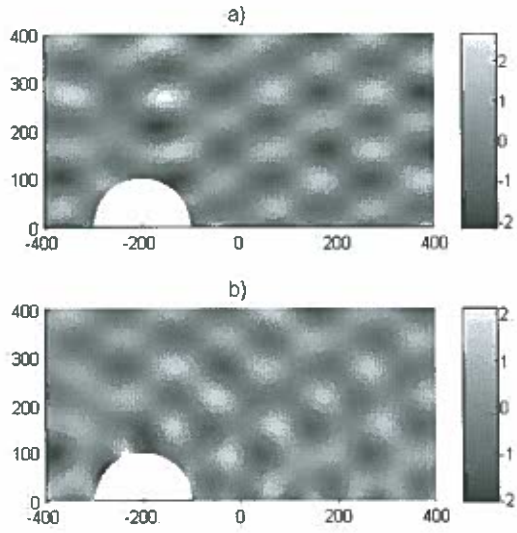

FIGURE 8.30. Total field for $Z_\infty = Z_\infty^*$, a transverse incident wave and $\omega = \omega_2$. a) Horizontal displacement. b) Vertical displacement.

REFERENCES

Abboud, T. & Terrasse, I. (2006), Modélisation des phénomènes de propagation d'ondes, Technical report, Éditions de l'École Polytechnique.

Abramowitz, M. & Stegun, I. A. (1970), *Handbook of Mathematical Functions*, Dover Publications, New York.

Achenbach, J. D. (1973), *Wave Propagation in Elastic Solids*, Vol. 16 of *North-Holland Series in Applied Mathematics and Mechanics*, Elsevier Science.

Aki, K. & Richards, P. G. (2002), *Quantitative Seismology*, 2nd edn, University Science Books.

Ammari, H. (2008), *An Introduction to Mathematics of Emerging Biomedical Imaging*, Vol. 62 of *Mathématiques et Applications*, Springer-Verlag, Berlin.

Antes, H. (1985), 'Boundary element procedure for transient wave propagation in two-dimensional isotropic elastic media', *Finite Elements in Analysis and Design* **1**(4), 313–322.

Arias, I. & Achenbach, J. D. (2004), 'Rayleigh wave correction for the BEM analysis of two-dimensional elastodynamic problems in a half-space', *International Journal for Numerical Methods in Engineering* **60**(13), 2131–2146.

Bateman, H. (1954), *Tables of Integral Transformations, Volume I*, McGraw-Hill Book Company.

Beer, G., Smith, I. & Duenser, C. (2008), *The Boundary Element Method with Programming - For Scientists and Engineers*, Springer-Verlag, New York.

Bell, W. W. (1968), *Special Functions for Scientists and Engineers*, Dover Publications, New York.

Bendali, A. & Devys, C. (1996), Calcul numérique du rayonnement de cornets électromagnétiques dont l'ouverture est partiellement remplie par un diélectrique, Technical report, CERFACS, Toulouse.

Bonnet, M. (1995), *Boundary Integral Equation Methods for Solids and Fluids*, John Wiley & Sons, Chichester.

Brebbia, C. A. & Domínguez, J. (1989), *Boundary Elements - An Introductory Course*, McGraw-Hill, New York.

Buchen, P. W. (1978), 'The elastodynamic Green's tensor for the 2D half-space', *Journal of the Australian Mathematical Society, Series B - Applied Mathematics* **20**(4), 385–400.

Chandler-Wilde, S. N. (1997), 'The impedance boundary value problem for the Helmholtz equation in a half-plane', *Mathematical Methods in the Applied Sciences* **20**(10), 813–840.

Chandler-Wilde, S. N. & Peplow, A. (2005), 'A boundary integral equation formulation for the Helmholtz equation in a locally perturbed half-plane', *ZAMM - Journal of Applied Mathematics and Mechanics* **85**(2), 79–88.

Chapman, C. (2004), *Fundamentals of Seismic Wave Propagation*, Cambridge University Press.

Chen, Z. & Dravinski, M. (2007*a*), 'Numerical evaluation of harmonic Green's functions for triclinic half-space with embedded sources - Part I: A 2D model', *International Journal for Numerical Methods in Engineering* **69**(2), 347–366.

Chen, Z. & Dravinski, M. (2007*b*), 'Numerical evaluation of harmonic Green's functions for triclinic half-space with embedded sources - Part II: A 3D model', *International Journal for Numerical Methods in Engineering* **69**(2), 367–389.

Ciarlet, P. G. (1978), *The Finite Element Method for Elliptic Problems*, Vol. 4 of *Studies in Mathematics and Its Applications*, North Holland Publishing Company, Amsterdam.

Dravinski, M. & Zheng, T. (2000), 'Numerical evaluation of three-dimensional time-harmonic Green's function for a nonisotropic full-space', *Wave Motion* **32**(2), 141–151.

Dumir, P. C. & Mehta, A. K. (1987), 'Boundary element solution for elastic orthotropic half-plane problems', *Computers & Structures* **26**(3).

Durán, M., Godoy, E. & Nédélec, J.-C. (2006), 'Computing Green's function of elasticity in a half-plane with impedance boundary condition', *Comptes Rendus Mécanique* **334**(12), 725–731.

Durán, M., Godoy, E. & Nédélec, J.-C. (2010), 'Theoretical aspects and numerical computation of the time-harmonic Green's function for an isotropic elastic half-plane with an impedance boundary condition', *ESAIM: Mathematical Modelling and Numerical Analysis* . Published online February 23, 2010.

Durán, M., Hein, R. & Nédélec, J.-C. (2007), 'Computing numerically the Green's function of the half-plane Helmholtz operator with impedance boundary conditions', *Numerische Mathematik* **107**(2), 295–314.

Durán, M., Muga, I. & Nédélec, J.-C. (2005*a*), 'The Helmholtz equation with impedance in a half-plane', *Comptes Rendus Mathématique* **340**(7), 483–488.

Durán, M., Muga, I. & Nédélec, J.-C. (2005*b*), 'The Helmholtz equation with impedance in a half-space', *Comptes Rendus Mathématique* **341**(9), 561–566.

Durán, M., Muga, I. & Nédélec, J.-C. (2006), 'The Helmholtz equation in a locally perturbed half-plane with passive boundary', *IMA Journal of Applied Mathematics* **71**(6), 853–876.

Durán, M., Muga, I. & Nédélec, J.-C. (2009*a*), 'The Helmholtz equation in a locally perturbed half-space with non-absorbing boundary', *Archive for Rational Mechanics and Analysis* **191**(1), 143–172.

Durán, M., Muga, I. & Nédélec, J.-C. (2009*b*), 'Radiation condition and uniqueness for the outgoing elastic wave in a half-plane with free boundary', *Comptes Rendus Mathématique* **347**(21-22), 1321–1324.

Durán, M. & Nédélec, J.-C. (2000), 'Un problème spectral issu d'un couplage élasto-acoustique', *ESAIM: Mathematical Modelling and Numerical Analysis* **34**(4), 835–857.

Gächter, G. K. & Grote, M. J. (2003), 'Dirichlet-to-Neumann map for three-dimensional elastic waves', *Wave Motion* **37**(3), 293–311.

Gaitanaros, A. P. & Karabalis, D. L. (1987), 'Dynamic analysis of 3-D flexible embedded foundations by a frequency domain BEM-FEM', *Earthquake Engineering & Structural Dynamics* **16**(5), 653–674.

García-Huidobro, J. C. (2009), Aspectos teóricos y numéricos de la elasticidad en un semiespacio aplicada al estudio de las tensiones inducidas por la actividad minera, Master's thesis, Pontificia Universidad Católica de Chile.

Givoli, D. & Keller, J. B. (1990), 'Non-reflecting boundary conditions for elastic waves', *Wave Motion* **12**(3), 261–279.

Givoli, D. & Vigdergauz, S. (1993), 'Artificial boundary conditions for 2D problems in geophysics', *Computer Methods in Applied Mechanics and Engineering* **110**(1-2), 87–101.

Graff, K. F. (1991), *Wave Motion in Elastic Solids*, Dover Publications, New York.

Grote, M. J. & Keller, J. B. (2000), 'Exact nonreflecting boundary condition for elastic waves', *SIAM Journal on Applied Mathematics* **60**(3), 803–819.

Han, H., Bao, W. & Wang, T. (1997), 'Numerical simulation for the problem of infinite elastic foundation', *Computer Methods in Applied Mechanics and Engineering* **147**(3-4), 369–385.

Han, H. & Wu, X. (1992), 'The approximation of the exact boundary conditions at an artificial boundary for linear elastic equations and its application', *Mathematics of Computation* **59**(199), 21–37.

Harari, I. & Haham, S. (1998), 'Improved finite element methods for elastic waves', *Computer Methods in Applied Mechanics and Engineering* **166**(1-2), 143–164.

Harari, I. & Shohet, Z. (1998), 'On non-reflecting boundary conditions in unbounded elastic solids', *Computer Methods in Applied Mechanics and Engineering* **163**(1-4), 123–139.

Harris, J. G. (2001), *Linear Elastic Waves*, Cambridge Texts in Applied Mathematics, Cambridge University Press.

Helms, L. L. (1969), *Introduction to Potential Theory*, Vol. 22 of *Pure and Applied Mathematics*, John Wiley & Sons.

Huang, Y.-Y. & Yin, L.-F. (1987), 'A direct method for deriving fundamental solution of half-plane problem', *Applied Mathematics and Mechanics (English Edition)* **8**(12), 1181–1190.

Ihlenburg, F. (1998), *Finite Element Analysis of Acoustic Scattering*, Vol. 132 of *Applied Mathematical Sciences*, Springer-Verlag, New York.

Johnson, L. R. (1974), 'Green function's for Lamb's problem', *Geophysical Journal of the Royal Astronomical Society* **37**(1), 99–131.

Karabalis, D. L. & Beskos, D. E. (1985), 'Dynamic response of 3-D flexible foundations by time domain BEM and FEM', *International Journal of Soil Dynamics and Earthquake Engineering* **4**(2), 91–101.

Karabalis, D. L. & Beskos, D. E. (1986), 'Dynamic response of 3-D embedded foundations by the boundary element method', *Computer Methods in Applied Mechanics and Engineering* **56**(1), 91–119.

Katsikadelis, J. T. (2002), *Boundary Elements - Theory and Applications*, Elsevier Science.

Kupradze, V. D. (1965), *Potential Methods in the Theory of Elasticity*, Israel Program for Scientific Translations, Jerusalem.

Lamb, H. (1904), 'On the propagation of tremors over the surface of an elastic solid', *Philosophical Transactions of the Royal Society of London - Series A: Mathematical and Physical Sciences* **203**, 1–42.

Lenoir, M. (2005), Équations intégrales et problèmes de diffraction, Technical report, ENSTA, UMA.

Linkov, A. M. (2002), *Boundary Integral Equations in Elasticity Theory*, Solid Mechanics and Its Applications, Kluwer Academic Publishers, Dordrecht, Boston.

Liu, G. R. & Lam, K. Y. (1996), 'Two-dimensional time-harmonic elastodynamic Green's functions for anisotropic media', *International Journal of Engineering Science* **34**(11), 1327–1338.

Malischewsky, P. G. (2000), 'Comment to "A new formula for the velocity of Rayleigh waves" by D. Nkemzi [Wave Motion 26 (1997) 199-205]', *Wave Motion* **31**(1), 93–96.

Manolis, G. D. & Beskos, D. E. (1988), *Boundary Element Methods in Elastodynamics*, Unwin Hyman, London and Boston.

Martin, P. A. (1990), 'On the scattering of elastic waves by an elastic inclusion in two dimensions', *Quarterly Journal of Mechanics and Applied Mathematics* **43**(3), 275–291.

Martin, P. A. (1992), 'Boundary integral equations for the scattering of elastic waves by elastic inclusions with thin interface layers', *Journal of Nondestructive Evaluation* **11**(3-4), 167–174.

Nédélec, J.-C. (2001), *Acoustic and Electromagnetic Equations. Integral Representations for Harmonic Problems*, Vol. 144 of *Applied Mathematical Sciences*, Springer-Verlag, Berlin.

Niwa, Y., Hirose, S. & Kitahara, M. (1986), 'Application of the boundary integral equation (BIE) method to transient response analysis of inclusions in a half space', *Wave Motion* **8**(1), 77–91.

Nkemzi, D. (1997), 'A new formula for the velocity of Rayleigh waves', *Wave Motion* **26**(2), 199–205.

Okada, Y. (1992), 'Internal deformation due to shear and tensile faults in a half-space', *Bulletin of the Seismological Society of America* **82**(2), 1018–1040.

Pan, L., Rizzo, F. J. & Martin, P. A. (1998), 'Some efficient boundary integral strategies for time-harmonic wave problems in an elastic halfspace', *Computer Methods in Applied Mechanics and Engineering* **164**(1-2), 207–221.

Peplow, A. & Chandler-Wilde, S. N. (1999), 'Noise propagation from a cutting of arbitrary cross-section and impedance', *Journal of Sound and Vibration* **223**(3), 355–378.

Perrey-Debain, E., Trevelyan, J. & Bettess, P. (2003), 'P-wave and S-wave decomposition in boundary integral equation for plane elastodynamic problems', *Communications in Numerical Methods in Engineering* **19**(12), 945–958.

Pujol, J. (2003), *Elastic Wave Propagation and Generation in Seismology*, Cambridge University Press.

Rajapakse, R. K. N. D. & Wang, Y. (1990), 'Elastodynamic Green's functions of orthotropic half plane', *Journal of Engineering Mechanics* **117**(3), 588–604.

Raviart, P. A. & Thomas, J. M. (1983), *Introduction à l'Analyse Numérique des Équations aux Dérivées Partielles*, Masson, Paris.

Reinoso, E., Wrobel, L. C. & Power, H. (1997), 'Three-dimensional scattering of seismic waves from topographical structures', *Soil Dynamics and Earthquake Engineering* **16**(1), 41–61.

Richter, C. & Schmid, G. (1999), 'A Green's function time-domain boundary element method for the elastodynamic half-plane', *International Journal for Numerical Methods in Engineering* **46**(5), 627–648.

Rizzo, F. J. (1967), 'An integral equation approach to boundary value problems of classical elastostatics', *Quarterly of Applied Mathematics* **25**(1), 83–95.

Rizzo, F. J., Shippy, D. J. & Rezayat, M. (1985), 'A boundary integral equation method for radiation and scattering of elastic waves in three dimensions', *International Journal for Numerical Methods in Engineering* **21**(1), 115–129.

Sánchez-Sesma, F. J. & Luzón, F. (1995), 'Seismic response of three-dimensional alluvial valleys for incident P, S, and Rayleigh waves', *Bulletin of the Seismological Society of America* **85**(1), 269–284.

Savage, W. Z. (2004), 'An exact solution for effects of topography on free Rayleigh waves', *Bulletin of the Seismological Society of America* **94**(5), 1706–1727.

Shibahara, M. & Taniguchi, Y. (1983), 'Application of the integral equation method to the elastodynamic boundary-value problems', *Bulletin of JSME* **26**(222), 2054–2059.

Stacey, T. R. & Page, C. H. (1986), *Practical Handbook for Underground Rock Mechanics*, Vol. 12 of *Series on Rock and Soil Mechanics*, Trans Tech Publications, Germany.

Steinbach, O. (2007), *Numerical Approximation Methods for Elliptic Boundary Value Problems: Finite and Boundary Elements*, Springer-Verlag, New York.

Tadeu, A., Kausel, E. & Vrettos, C. (1996), 'Scattering of waves by subterranean structures via the boundary element method', *Soil Dynamics and Earthquake Engineering* **15**(6), 387–397.

Telles, J. C. F. & Brebbia, C. A. (1981), 'Boundary element solution for half-plane problems', *International Journal of Solids and Structures* **17**(12), 1149–1158.

Triantafyllidis, T. (1991), '3-D time domain BEM using half-space Green's functions', *Engineering Analysis with Boundary Elements* **8**(3), 115–124.

Vinh, P. C. & Ogden, R. W. (2004), 'On formulas for the Rayleigh wave speed', *Wave Motion* **39**(3), 191–197.

Von Estorff, O. & Kausel, E. (1989), 'Coupling of boundary and finite elements for soil-structure interaction problems', *Earthquake Engineering & Structural Dynamics* **18**(7), 1065–1075.

Wang, C.-Y. & Achenbach, J. D. (1994), 'Elastodynamic fundamental solutions for anisotropic solids', *Geophysical Journal International* **118**(2), 384–392.

Zheng, T. & Dravinski, M. (2000), 'Scattering of elastic waves by a 3D anisotropic basin', *Earthquake Engineering & Structural Dynamics* **29**(4), 419–439.

Zienkiewicz, O. C. (2000), *The Finite Element Method*, 5th edn, McGraw-Hill, Oxford.

APPENDIX

A. PLANE WAVES

A.1 Plane waves in the full-plane

In this appendix we obtain explicit expressions in terms of plane waves for an incident field $\boldsymbol{u}^{\text{inc}}$ satisfying the elastic wave equation in the full-plane:

$$\operatorname{div}\sigma(\boldsymbol{u}^{\text{inc}}(\boldsymbol{x})) + \rho\omega^2\boldsymbol{u}^{\text{inc}}(\boldsymbol{x}) = \boldsymbol{0} \qquad \text{in } \mathbb{R}^2. \tag{A.1}$$

The solutions to (A.1) are determined by using the procedure introduced in Section 2.2. We seek $\boldsymbol{u}^{\text{inc}}$ of the form

$$\boldsymbol{u}^{\text{inc}}(\boldsymbol{x}) = \nabla\psi^{(L)}(\boldsymbol{x}) + \nabla^{\perp}\psi^{(T)}(\boldsymbol{x}), \tag{A.2}$$

with potentials $\psi^{(L)}$ and $\psi^{(T)}$ satisfying

$$\triangle\psi^{(L)}(\boldsymbol{x}) + k_L^2\,\psi^{(L)}(\boldsymbol{x}) = 0, \tag{A.3a}$$

$$\triangle\psi^{(T)}(\boldsymbol{x}) + k_T^2\,\psi^{(T)}(\boldsymbol{x}) = 0. \tag{A.3b}$$

The direction of propagation of the plane waves is defined by the angle α_0, measured downwards with respect to the horizontal. The standard plane wave solutions to the Helmholtz equations (A.3a) and (A.3b) propagating in this direction are

$$\psi^{(L)}(\boldsymbol{x}) = a^{(L)}e^{\mathrm{i}k_L\hat{\boldsymbol{p}}_0\cdot\boldsymbol{x}}, \tag{A.4a}$$

$$\psi^{(T)}(\boldsymbol{x}) = a^{(T)}e^{\mathrm{i}k_T\hat{\boldsymbol{p}}_0\cdot\boldsymbol{x}}, \tag{A.4b}$$

where $a^{(L)}$, $a^{(T)}$ are generic multiplicative constants and $\hat{\boldsymbol{p}}_0$ is a unit vector in the direction of propagation of the wave, given by

$$\hat{\boldsymbol{p}}_0 = \cos\alpha_0\,\hat{\boldsymbol{e}}_1 - \sin\alpha_0\,\hat{\boldsymbol{e}}_2. \tag{A.5}$$

Computing the gradient of $\psi^{(L)}$ and the orthogonal gradient of $\psi^{(T)}$ yields

$$\nabla\psi^{(L)}(\boldsymbol{x}) = \mathrm{i}a^{(L)}k_L\,\hat{\boldsymbol{p}}_0\,e^{\mathrm{i}k_L\hat{\boldsymbol{p}}_0\cdot\boldsymbol{x}}, \tag{A.6a}$$

$$\nabla^{\perp}\psi^{(T)}(\boldsymbol{x}) = \mathrm{i}a^{(T)}k_T\,\hat{\boldsymbol{p}}_0^{\perp}e^{\mathrm{i}k_T\hat{\boldsymbol{p}}_0\cdot\boldsymbol{x}}, \tag{A.6b}$$

where $\hat{\boldsymbol{p}}_0^{\perp}$ is a unit vector orthogonal to $\hat{\boldsymbol{p}}_0$, given by

$$\hat{\boldsymbol{p}}_0^{\perp} = \sin\alpha_0\,\hat{\boldsymbol{e}}_1 + \cos\alpha_0\,\hat{\boldsymbol{e}}_2. \tag{A.7}$$

Substitution of (A.6a) and (A.6b) in (A.2) yields the next expression for $\boldsymbol{u}^{\text{inc}}$:

$$\boldsymbol{u}^{\text{inc}}(\boldsymbol{x}) = A^{(L)}\hat{\boldsymbol{p}}_0e^{\mathrm{i}k_L\hat{\boldsymbol{p}}_0\cdot\boldsymbol{x}} + A^{(T)}\hat{\boldsymbol{p}}_0^{\perp}e^{\mathrm{i}k_T\hat{\boldsymbol{p}}_0\cdot\boldsymbol{x}}, \tag{A.8}$$

where $A^{(L)}$ and $A^{(T)}$ are arbitrary amplitudes that absorb any other multiplicative constants. We have expressed the incident field $\boldsymbol{u}^{\text{inc}}$ as a sum of two terms. The first one defines a longitudinal plane wave, where the polarization vector (the one that multiplies the exponential function) is parallel to the direction of propagation of the wave. The second term defines a transverse plane wave, where the polarization vector is perpendicular to the direction of propagation of the wave. It should be observed that as the amplitudes are arbitrary, it is possible to obtain pure longitudinal or transverse waves by setting $A^{(T)}$ and $A^{(L)}$ to

zero, respectively. We actually consider the elementary cases $(A^{(L)}, A^{(T)}) = (1, 0)$ and $(A^{(L)}, A^{(T)}) = (0, 1)$. The incident fields associated with these cases, denoted respectively by $\boldsymbol{u}^{\mathrm{inc}(L)}$ and $\boldsymbol{u}^{\mathrm{inc}(L)}$, are given by.

$$\boldsymbol{u}^{\mathrm{inc}(L)}(\boldsymbol{x}) = \hat{\boldsymbol{p}}_0 e^{ik_L \hat{\boldsymbol{p}}_0 \cdot \boldsymbol{x}}, \tag{A.9a}$$

$$\boldsymbol{u}^{\mathrm{inc}(T)}(\boldsymbol{x}) = \hat{\boldsymbol{p}}_0^{\perp} e^{ik_T \hat{\boldsymbol{p}}_0 \cdot \boldsymbol{x}}. \tag{A.9b}$$

In addition, it is possible to express these fields in a more explicit way by replacing (A.5) and (A.7) in (A.9a):

$$\boldsymbol{u}^{\mathrm{inc}(L)}(x_1, x_2) = (\cos\alpha_0\, \hat{\boldsymbol{e}}_1 - \sin\alpha_0\, \hat{\boldsymbol{e}}_2) e^{ik_L(\cos\alpha_0 x_1 - \sin\alpha_0 x_2)}, \tag{A.10a}$$

$$\boldsymbol{u}^{\mathrm{inc}(T)}(x_1, x_2) = (\sin\alpha_0\, \hat{\boldsymbol{e}}_1 + \cos\alpha_0\, \hat{\boldsymbol{e}}_2) e^{ik_T(\cos\alpha_0 x_1 - \sin\alpha_0 x_2)}. \tag{A.10b}$$

A.2 Plane waves in the half-plane

In this appendix we deal with the non-perturbed half-plane $\mathbb{R}^2_+$ with impedance boundary conditions (cf. Section 2.4). Let us suppose that an incident field $\boldsymbol{u}^{\mathrm{inc}}$ encounters the infinite flat boundary $\{x_2 = 0\}$. For the sake of simplicity, we assume this field to consist of pure longitudinal or transverse plane waves. The analytical expressions for these two cases are given in (A.9a) (or (A.10a)) and in (A.9b) (or (A.10b)), respectively. Notice that the angle of incidence α_0 must be strictly positive, in order to have an incident field that comes from the interior of $\mathbb{R}^2_+$. Our aim is to determine an explicit expression for the reflected field $\boldsymbol{u}^{\mathrm{ref}}$. For this, we mainly follow Harris (2001), where the case of a half-plane with traction-free boundary conditions is treated. The reflected field satisfies the elastic wave equation in $\mathbb{R}^2_+$ and consists in general of a longitudinal and a transverse wave. In addition, the sum $\boldsymbol{u}^{\mathrm{inc}} + \boldsymbol{u}^{\mathrm{ref}}$ fulfills the impedance boundary conditions (2.52) on $\{x_2 = 0\}$. Consequently, $\boldsymbol{u}^{\mathrm{ref}}$ is a solution of the system:

$$\operatorname{div}\sigma(\boldsymbol{u}^{\mathrm{ref}}(\boldsymbol{x})) + \rho\omega^2 \boldsymbol{u}^{\mathrm{ref}}(\boldsymbol{x}) = \boldsymbol{0} \qquad \text{in } \mathbb{R}^2_+, \tag{A.11a}$$

$$\sigma(\boldsymbol{u}^{\mathrm{ref}}(\boldsymbol{x}))\hat{\boldsymbol{e}}_2 + \omega Z_\infty u_1^{\mathrm{ref}}(\boldsymbol{x})\hat{\boldsymbol{e}}_1 = \boldsymbol{f}(\boldsymbol{x}) \qquad \text{on } \{x_2 = 0\}. \tag{A.11b}$$

where the right-hand side of (A.11b) is given by

$$\boldsymbol{f}(\boldsymbol{x}) = -\sigma(\boldsymbol{u}^{\mathrm{inc}}(\boldsymbol{x}))\hat{\boldsymbol{e}}_2 - \omega Z_\infty u_1^{\mathrm{inc}}(\boldsymbol{x})\hat{\boldsymbol{e}}_1. \tag{A.12}$$

We first assume a longitudinal incident field, that is,

$$\boldsymbol{u}^{\mathrm{inc}}(\boldsymbol{x}) = \hat{\boldsymbol{p}}_0\, e^{ik_L \hat{\boldsymbol{p}}_0 \cdot \boldsymbol{x}}, \tag{A.13}$$

where the vector $\hat{\boldsymbol{p}}_0$ is given in terms of α_0 in (A.5). The reflected field $\boldsymbol{u}^{\mathrm{ref}}$ is given by

$$\boldsymbol{u}^{\mathrm{ref}}(\boldsymbol{x}) = R^{(L)}\boldsymbol{u}^{\mathrm{ref}(L)}(\boldsymbol{x}) + R^{(T)}\boldsymbol{u}^{\mathrm{ref}(T)}(\boldsymbol{x}), \tag{A.14}$$

where $R^{(L)}$, $R^{(T)}$ are reflection coefficients. The reflected longitudinal wave $\boldsymbol{u}^{\mathrm{ref}(L)}$ is written as

$$\boldsymbol{u}^{\mathrm{ref}(L)} = \hat{\boldsymbol{p}}_1\, e^{ik_L \hat{\boldsymbol{p}}_1 \cdot \boldsymbol{x}}, \tag{A.15}$$

where $\hat{\boldsymbol{p}}_1$ is a unit vector defining the direction of propagation, given in function of the angle of reflection α_1 by

$$\hat{\boldsymbol{p}}_1 = \cos\alpha_1\,\hat{\boldsymbol{e}}_1 + \sin\alpha_1\,\hat{\boldsymbol{e}}_2. \tag{A.16}$$

The reflected transverse wave $\boldsymbol{u}^{\mathrm{ref}(T)}$ is expressed as

$$\boldsymbol{u}^{\mathrm{ref}(T)}(\boldsymbol{x}) = \hat{\boldsymbol{p}}_2^{\perp}\, e^{\mathrm{i}k_T\hat{\boldsymbol{p}}_2\cdot\boldsymbol{x}}, \tag{A.17}$$

where $\hat{\boldsymbol{p}}_2$ and $\hat{\boldsymbol{p}}_2^{\perp}$ are mutually orthogonal unit vectors defining the directions of propagation and polarization, respectively. These vectors are given in function of the angle of reflection α_2 by

$$\hat{\boldsymbol{p}}_2 = \cos\alpha_2\,\hat{\boldsymbol{e}}_1 + \sin\alpha_2\,\hat{\boldsymbol{e}}_2, \tag{A.18}$$

$$\hat{\boldsymbol{p}}_2^{\perp} = -\sin\alpha_2\,\hat{\boldsymbol{e}}_1 + \cos\alpha_2\,\hat{\boldsymbol{e}}_2. \tag{A.19}$$

Both angles of reflection α_1 and α_2 are measured upwards with respect to the horizontal. Replacing (A.15) and (A.17) gives an explicit expression for the reflected field:

$$\boldsymbol{u}^{\mathrm{ref}}(\boldsymbol{x}) = R^{(L)}\hat{\boldsymbol{p}}_1\, e^{\mathrm{i}k_L\hat{\boldsymbol{p}}_1\cdot\boldsymbol{x}} + R^{(T)}\hat{\boldsymbol{p}}_2^{\perp}\, e^{\mathrm{i}k_T\hat{\boldsymbol{p}}_2\cdot\boldsymbol{x}}, \tag{A.20}$$

where the reflection coefficients $R^{(L)}$ and $R^{(T)}$ are still unknown. It is straightforward to verify that $\boldsymbol{u}^{\mathrm{ref}}$ defined in (A.20) satisfies the elastic wave equation (A.11a). On the other hand, substituting (A.13) and (A.20) in (A.11b) and combining with (A.12) yields the relation

$$\boldsymbol{a}_1 R^{(L)}\, e^{\mathrm{i}k_L\cos\alpha_1 x_1} + \boldsymbol{a}_2 R^{(T)}\, e^{\mathrm{i}k_T\cos\alpha_2 x_1} = \boldsymbol{b}\, e^{\mathrm{i}k_L\cos\alpha_0 x_1}, \tag{A.21}$$

where

$$\boldsymbol{a}_1 = (\mathrm{i}k_L\mu\sin 2\alpha_1 + \omega Z_\infty\cos\alpha_1)\,\hat{\boldsymbol{e}}_1 + \mathrm{i}k_L(\lambda + 2\mu\sin^2\alpha_1)\,\hat{\boldsymbol{e}}_2, \tag{A.22a}$$

$$\boldsymbol{a}_2 = (\mathrm{i}k_T\mu\cos 2\alpha_2 - \omega Z_\infty\sin\alpha_2)\,\hat{\boldsymbol{e}}_1 + \mathrm{i}k_T\mu\sin 2\alpha_2\,\hat{\boldsymbol{e}}_2, \tag{A.22b}$$

$$\boldsymbol{b} = (\mathrm{i}k_L\mu\sin 2\alpha_0 - \omega Z_\infty\cos\alpha_0)\,\hat{\boldsymbol{e}}_1 - \mathrm{i}k_L(\lambda + 2\mu\sin^2\alpha_0)\,\hat{\boldsymbol{e}}_2. \tag{A.22c}$$

Relation (A.21) holds for all $x_1 \in \mathbb{R}$ only if the angles α_0, α_1 and α_2 satisfy

$$\alpha_0 = \alpha_1, \tag{A.23a}$$

$$k_L\cos\alpha_0 = k_T\cos\alpha_2. \tag{A.23b}$$

These two identities are known as phase-matching conditions. They allow us to determine exactly the angles of reflection α_1 and α_2 in function of the angle of incidence α_0. Assuming that these conditions hold, (A.21) is simply expressed as

$$\boldsymbol{a}_1 R^{(L)} + \boldsymbol{a}_2 R^{(T)} = \boldsymbol{b}, \tag{A.24}$$

and this relation corresponds to a 2×2 system of linear equations for $R^{(L)}$ and $R^{(T)}$. The coefficients of the respective matrix can be straightforwardly obtained by replacing (A.22a), (A.22b) and (A.22c) in (A.24). By rearranging appropriately the equations, using standard trigonometric identities and combining with (A.23), this linear system can be restated as follows:

$$\begin{aligned}(\beta\sin 2\alpha_0 - \mathrm{i}\gamma Z_\infty\cos\alpha_0)R^{(L)} \\ +(\cos 2\alpha_2 + \mathrm{i}\gamma Z_\infty\sin\alpha_2)R^{(T)} &= \beta\sin 2\alpha_0 + \mathrm{i}\gamma Z_\infty\cos\alpha_0,\end{aligned} \tag{A.25}$$

$$\cos 2\alpha_2 R^{(L)} - \beta \sin 2\alpha_2 R^{(T)} = -\cos 2\alpha_2, \tag{A.26}$$

where

$$\beta = \frac{k_L}{k_T}, \qquad \gamma = \frac{1}{\sqrt{\rho\mu}}. \tag{A.27}$$

Solving (A.2) and combining with (A.23b) yields the next expressions for $R^{(L)}$ and $R^{(T)}$:

$$R^{(L)} = \frac{\Theta_-(\alpha_0) + \mathrm{i}\gamma Z_\infty \sin\alpha_2}{\Theta_+(\alpha_0) - \mathrm{i}\gamma Z_\infty \sin\alpha_2}, \tag{A.28a}$$

$$R^{(T)} = \frac{2\beta \sin 2\alpha_0 \cos 2\alpha_2}{\Theta_+(\alpha_0) - \mathrm{i}\gamma Z_\infty \sin\alpha_2}, \tag{A.28b}$$

where

$$\Theta_\pm(\alpha_0) = \beta^2 \sin 2\alpha_0 \sin 2\alpha_2 \pm \cos^2 2\alpha_2. \tag{A.29}$$

Notice that the dependence of this function on α_2 is not made explicit, because α_2 is given in function of α_0 in (A.23b). In the case of a traction-free boundary, the reflection coefficients are (cf. Harris 2001):

$$R^{(L)} = \frac{\Theta_-(\alpha_0)}{\Theta_+(\alpha_0)}, \qquad R^{(T)} = \frac{2\beta \sin 2\alpha_0 \cos 2\alpha_2}{\Theta_+(\alpha_0)}. \tag{A.30}$$

Let us assume now a transverse incident field, that is,

$$\boldsymbol{u}^{\mathrm{inc}}(\boldsymbol{x}) = \hat{\boldsymbol{p}}_0^{\perp} e^{\mathrm{i}k_T \hat{\boldsymbol{p}}_0 \cdot \boldsymbol{x}}. \tag{A.31}$$

The reflected field is

$$\boldsymbol{u}^{\mathrm{ref}}(\boldsymbol{x}) = R^{(L)} \hat{\boldsymbol{p}}_1 \, e^{\mathrm{i}k_L \hat{\boldsymbol{p}}_1 \cdot \boldsymbol{x}} + R^{(T)} \hat{\boldsymbol{p}}_2^{\perp} \, e^{\mathrm{i}k_T \hat{\boldsymbol{p}}_2 \cdot \boldsymbol{x}}, \tag{A.32}$$

where this time the reflection coefficients are different. Proceeding analogously as above, we obtain the phase-matching conditions

$$k_T \cos\alpha_0 = k_L \cos\alpha_1, \tag{A.33a}$$

$$\alpha_0 = \alpha_2, \tag{A.33b}$$

and the following expressions for the coefficients $R^{(L)}$ and $R^{(T)}$:

$$R^{(L)} = -\frac{\beta \sin 4\alpha_0}{\Theta_+(\alpha_0) - \mathrm{i}\gamma Z_\infty \sin\alpha_0}, \tag{A.34a}$$

$$R^{(T)} = \frac{\Theta_-(\alpha_0) - \mathrm{i}\gamma Z_\infty \sin\alpha_0}{\Theta_+(\alpha_0) - \mathrm{i}\gamma Z_\infty \sin\alpha_0}, \tag{A.34b}$$

where

$$\Theta_\pm(\alpha_0) = \beta^2 \sin 2\alpha_0 \sin 2\alpha_1 \pm \cos^2 2\alpha_0. \tag{A.35}$$

In the traction-free case, the reflection coefficients are (cf. Harris 2001):

$$R^{(L)} = -\frac{\beta \sin 4\alpha_0}{\Theta_+(\alpha_0)}, \qquad R^{(T)} = \frac{\Theta_-(\alpha_0)}{\Theta_+(\alpha_0)}. \tag{A.36}$$

The reflected field is thus obtained by replacing in (A.17) the reflection coefficients $R^{(L)}$ and $R^{(T)}$, given either in (A.28) or (A.34).

B. PROPERTIES OF BESSEL AND HANKEL FUNCTIONS

In this appendix, we introduce the Bessel and Hankel function as solutions of the Bessel equation. Some useful properties of these functions are mentioned, which have been obtained from Bell (1968) and Abramowitz & Stegun (1970). In the following, $z \in \mathbb{C}$ denotes a complex variable, $\nu \in \mathbb{C}$ a complex index, and $n \in \mathbb{N}$ a nonnegative integer. The Bessel equation for a function v corresponds to the ordinary differential equation

$$z^2 \frac{\mathrm{d}^2 v}{\mathrm{d}z^2}(z) + z \frac{\mathrm{d}v}{\mathrm{d}z}(z) + (z^2 - \nu^2) v(z) = 0. \tag{B.1}$$

Two linearly independent solutions of this equation are the Bessel functions of the first kind J_ν and of the second kind Y_ν, the latter also known as Neumann or Weber function. The Hankel functions of the first kind $H_\nu^{(1)}$ and of the second kind $H_\nu^{(2)}$ are also independent solutions of the Bessel equation, and they are obtained from J_ν and Y_ν through the relations

$$H_\nu^{(1)}(z) = J_\nu(z) + \mathrm{i} Y_\nu(z), \tag{B.2a}$$

$$H_\nu^{(2)}(z) = J_\nu(z) - \mathrm{i} Y_\nu(z). \tag{B.2b}$$

The Bessel function J_ν admits the power series expansion

$$J_\nu(z) = \sum_{m=0}^{+\infty} \frac{(-1)^m}{m!\,\Gamma(\nu + m + 1)} \left(\frac{z}{2}\right)^{2m+\nu}, \tag{B.3}$$

where Γ is the Gamma function, given by

$$\Gamma(z) = \int_0^{+\infty} t^{z-1} e^{-t} \mathrm{d}t. \tag{B.4}$$

Some interesting properties of Γ are

$$\Gamma(1) = 1, \tag{B.5a}$$

$$\Gamma(z+1) = z\,\Gamma(z), \tag{B.5b}$$

$$\Gamma(z)\Gamma(1-z) = \frac{\pi}{\sin \pi z}, \qquad (z \notin \mathbb{Z}), \tag{B.5c}$$

$$\Gamma(z)\Gamma(-z) = -\frac{\pi}{z \sin \pi z}, \qquad (z \notin \mathbb{Z}), \tag{B.5d}$$

$$\Gamma(z)\Gamma\left(z + \frac{1}{2}\right) = 2^{1-2z} \sqrt{\pi}\, \Gamma(2z). \tag{B.5e}$$

When the argument is integer, some additional properties of Γ (actually deductible from (B.5)) are

$$\Gamma(n+1) = n!, \tag{B.6a}$$

$$\Gamma\left(n + \frac{1}{2}\right) = \frac{(2n)!\sqrt{\pi}}{n!\,2^{2n}}, \tag{B.6b}$$

$$\Gamma\left(-n + \frac{1}{2}\right) = \frac{(-1)^n\, n!\, 2^{2n} \sqrt{\pi}}{(2n)!}. \tag{B.6c}$$

The Bessel function Y_ν is defined from J_ν as

$$Y_\nu(z) = \frac{J_\nu(z)\cos\nu\pi - J_{-\nu}(z)}{\sin\nu\pi}, \qquad \nu \notin \mathbb{Z}, \tag{B.7a}$$

$$Y_n(z) = \lim_{\nu\to n} \frac{J_\nu(z)\cos\nu\pi - J_{-\nu}(z)}{\sin\nu\pi}, \qquad n \in \mathbb{Z} \quad . \tag{B.7b}$$

For a positive integer order n, the Bessel function J_n has thus the power series expansion

$$J_n(z) = \sum_{m=0}^{+\infty} \frac{(-1)^m}{m!\,(n+m)!}\left(\frac{z}{2}\right)^{2m+n}, \tag{B.8}$$

while the Bessel function Y_n admits the following explicit expression:

$$\begin{aligned} Y_n(z) = \frac{2}{\pi}\left(\ln\frac{z}{2} + \gamma - \frac{1}{2}\sum_{\ell=1}^{n}\frac{1}{\ell}\right)J_n(z) - \frac{1}{\pi}\sum_{m=0}^{n-1}\frac{(n-m-1)!}{m!}\left(\frac{z}{2}\right)^{2m-n} \\ - \frac{1}{\pi}\sum_{m=0}^{+\infty}\frac{(-1)^m}{m!\,(m+n)!}\left(\frac{z}{2}\right)^{2m+n}\sum_{\ell=1}^{m}\left(\frac{1}{\ell}+\frac{1}{n+\ell}\right), \end{aligned} \tag{B.9}$$

where $\gamma =$ denotes the Euler-Mascheroni's constant, given by

$$\gamma = \lim_{m\to+\infty}\left(\sum_{\ell=1}^{m}\frac{1}{\ell} - \ln m\right) \approx 0.57721566\ldots \tag{B.10}$$

In the case of a negative integer order, the Bessel functions satisfy

$$J_{-n}(z) = (-1)^n J_n(z), \tag{B.11a}$$

$$Y_{-n}(z) = (-1)^n Y_n(z). \tag{B.11b}$$

Let ζ denote J, Y, $H^{(1)}$, $H^{(2)}$, or any linear combination of these functions where the coefficients do not depend on z or ν. Then the following recurrence relations hold

$$\zeta_{\nu+1}(z) + \zeta_{\nu-1}(z) = \frac{2\nu}{z}\zeta_\nu(z), \tag{B.12a}$$

$$\zeta_{\nu+1}(z) - \zeta_{\nu-1}(z) = -2\zeta'_\nu(z). \tag{B.12b}$$

Another pair of valid recurrence relations (actually deductible from (B.12)) is

$$\zeta'_\nu(z) = \frac{n}{z}\zeta_\nu(z) - \zeta_{\nu+1}(z), \tag{B.13a}$$

$$\zeta'_\nu(z) = \zeta_{\nu-1}(z) - \frac{n}{z}\zeta_\nu(z). \tag{B.13b}$$

The asymptotic expressions for the Bessel and Hankel functions, when ν is fixed and $z \to +\infty$, are

$$J_\nu(z) = \sqrt{\frac{2}{\pi z}}\cos\left(z - (2\nu+1)\frac{\pi}{4}\right) + O(z^{-3/2}), \quad |\arg z| < \pi, \tag{B.14a}$$

$$J_\nu(z) = \sqrt{\frac{2}{\pi z}}\sin\left(z - (2\nu+1)\frac{\pi}{4}\right) + O(z^{-3/2}), \quad |\arg z| < \pi, \tag{B.14b}$$

$$H^{(1)}_\nu(z) = \sqrt{\frac{2}{\pi z}}\,e^{\mathrm{i}(z-(2\nu+1)\frac{\pi}{4})} + O(z^{-3/2}), \tag{B.14c}$$

$$H_\nu^{(2)}(z) = \sqrt{\frac{2}{\pi z}}\, e^{-\mathrm{i}(z-(2\nu+1)\frac{\pi}{4})} + O(z^{-3/2}). \tag{B.14d}$$

On the contrary, when ν is fixed and $z \to 0$, then the Bessel and Hankel functions behave like

$$J_\nu(z) \sim \frac{1}{\Gamma(\nu+1)}\left(\frac{z}{2}\right)^\nu, \qquad \nu \neq -1, -2, -3, \ldots \tag{B.15a}$$

$$Y_0(z) \sim -\mathrm{i}H_0^{(1)}(z) \sim \mathrm{i}H_0^{(2)}(z) \sim \frac{2}{\pi}\ln z. \tag{B.15b}$$

$$Y_\nu(z) \sim -\mathrm{i}H_\nu^{(1)}(z) \sim \mathrm{i}H_\nu^{(2)}(z) \sim \frac{\Gamma(\nu)}{\pi}\left(\frac{2}{z}\right)^\nu, \qquad \mathfrak{Re}\{\nu\} > 0. \tag{B.15c}$$

In the case of the Hankel functions of the first kind of order 0 and 1, the following explicit expressions hold (cf. Bonnet 1995):

$$H_0^{(1)}(z) = 1 + \frac{2\mathrm{i}}{\pi}\left(\gamma + \ln\frac{z}{2}\right) + z^2\sum_{n=0}^{+\infty} a_n^0(z)\left(\frac{z}{2}\right)^{2n}, \tag{B.16a}$$

$$H_1^{(1)}(z) = -\frac{2\mathrm{i}}{\pi z} + \frac{\mathrm{i}z}{\pi}\left(\gamma - \frac{1}{2} + \ln\frac{z}{2}\right) + \frac{z}{2} + \frac{z^3}{2}\sum_{n=0}^{+\infty} a_n^1(z)\left(\frac{z}{2}\right)^{2n}, \tag{B.16b}$$

where

$$a_n^0(z) = \frac{1}{4}\left[1 + \frac{2\mathrm{i}}{\pi}\left(\gamma + \ln\frac{z}{2} - \sum_{\ell=1}^{n+1}\frac{1}{\ell}\right)\right]\frac{(-1)^{n+1}}{(n+1)!^2}, \tag{B.17a}$$

$$a_n^1(z) = \frac{1}{4}\left[1 + \frac{2\mathrm{i}}{\pi}\left(\gamma + \ln\frac{z}{2} - \sum_{\ell=1}^{n+1}\frac{1}{\ell} - \frac{1}{2(n+2)}\right)\right]\frac{(-1)^{n+1}}{(n+1)!(n+2)!}. \tag{B.17b}$$

In addition, we exhibit some integral formulae obtained from Bateman (1954). For this, we define the modified Bessel function K_ν as

$$K_\nu(z) = \frac{\pi}{2}\,\mathrm{i}^{\nu+1}H_\nu^{(1)}(\mathrm{i}z), \tag{B.18}$$

which is a solution of the modified Bessel equation

$$z^2\frac{\mathrm{d}^2v}{\mathrm{d}z^2}(z) + z\frac{\mathrm{d}v}{\mathrm{d}z}(z) - (z^2+\nu^2)v(z) = 0. \tag{B.19}$$

The mentioned integral formulae are

$$\int_0^{+\infty} \frac{e^{-b\sqrt{\xi^2+a^2}}}{\sqrt{\xi^2+a^2}}\cos(c\xi)\mathrm{d}\xi = K_0\big(a\sqrt{b^2+c^2}\big), \tag{B.20a}$$

$$\int_0^{+\infty} e^{-b\sqrt{\xi^2+a^2}}\cos(c\xi)\mathrm{d}\xi = \frac{ab}{\sqrt{b^2+c^2}}K_1\big(a\sqrt{b^2+c^2}\big), \tag{B.20b}$$

$$\int_0^{+\infty} \frac{\xi\, e^{-b\sqrt{\xi^2+a^2}}}{\sqrt{\xi^2+a^2}}\sin(c\xi)\mathrm{d}\xi = \frac{ac}{\sqrt{b^2+c^2}}K_1\big(a\sqrt{b^2+c^2}\big), \tag{B.20c}$$

$$\int_0^{+\infty} \xi\, e^{-b\sqrt{\xi^2+a^2}}\sin(c\xi)\mathrm{d}\xi = \frac{a^2bc}{b^2+c^2}K_2\big(a\sqrt{b^2+c^2}\big). \tag{B.20d}$$